



<https://theses.gla.ac.uk/>

Theses Digitisation:

<https://www.gla.ac.uk/myglasgow/research/enlighten/theses/digitisation/>

This is a digitised version of the original print thesis.

Copyright and moral rights for this work are retained by the author

A copy can be downloaded for personal non-commercial research or study, without prior permission or charge

This work cannot be reproduced or quoted extensively from without first obtaining permission in writing from the author

The content must not be changed in any way or sold commercially in any format or medium without the formal permission of the author

When referring to this work, full bibliographic details including the author, title, awarding institution and date of the thesis must be given

Enlighten: Theses

<https://theses.gla.ac.uk/>
research-enlighten@glasgow.ac.uk

PHARMACOLOGICAL AND PATHOLOGICAL ALTERATIONS

IN HIPPOCAMPAL FUNCTION:

AN AUTORADIOGRAPHIC ANALYSIS OF GLUTAMATERGIC

AND CHOLINERGIC TRANSMITTER SYSTEMS

Fiona M. Inglis B. Sc.

A thesis submitted for the Degree of Doctor of Philosophy
to the Faculty of Medicine, University of Glasgow

Wellcome Surgical Institute & Hugh Fraser Neuroscience Laboratories,
University of Glasgow,
Bearsden Road, Glasgow, G61 1QH.

© Fiona M. Inglis, 1992

ProQuest Number: 13815363

All rights reserved

INFORMATION TO ALL USERS

The quality of this reproduction is dependent upon the quality of the copy submitted.

In the unlikely event that the author did not send a complete manuscript and there are missing pages, these will be noted. Also, if material had to be removed, a note will indicate the deletion.



ProQuest 13815363

Published by ProQuest LLC (2018). Copyright of the Dissertation is held by the Author.

All rights reserved.

This work is protected against unauthorized copying under Title 17, United States Code
Microform Edition © ProQuest LLC.

ProQuest LLC.
789 East Eisenhower Parkway
P.O. Box 1346
Ann Arbor, MI 48106 – 1346

Thesis
9250
copy 1

GLASGOW
UNIVERSITY
LIBRARY

CONTENTS

PAGE NO:

<u>LIST OF TABLES</u>	10
<u>LIST OF FIGURES</u>	11
<u>ACKNOWLEDGEMENTS</u>	14
<u>SUMMARY</u>	16
<u>PREFACE AND DECLARATION</u>	21

CHAPTER I: INTRODUCTION

1.	THE HIPPOCAMPUS: A BRIEF HISTORICAL OVERVIEW	23
2.	ANATOMICAL ORGANISATION OF THE HIPPOCAMPUS	25
2.1.	The Trisynaptic Pathway	26
2.2.	The Septohippocampal Pathway	28
3.	GLUTAMATE AND THE HIPPOCAMPUS	30
3.1.	Glutamate as a Neurotransmitter	30
3.1.1.	Sub-types of Glutamate Receptor	30
3.1.2.	Ligand-Binding to Glutamate Receptors	33
3.1.3.	Anatomical Distribution of Glutamatergic Receptors	34
3.2.	Glutamate and Long-Term Potentiation (LTP)	35
3.2.1.	Induction of LTP	35
3.2.2.	Mechanisms of Maintenance of LTP	36
4.	ACETYLCHOLINE AND THE HIPPOCAMPUS	41
4.1.	Acetylcholine as a Neurotransmitter	41
4.1.1.	Sub-types of Acetylcholine Receptor	41
4.1.2.	Muscarinic Receptors and Second Messenger Activity	43

4.1.3.	Ligand-Binding to Muscarinic Receptors	46
4.1.4.	Anatomical Distribution of Muscarinic Receptors	48
4.532.	Acetylcholine and the Septohippocampal Pathway	49
5.	NEUROPATHOLOGY OF THE HIPPOCAMPUS	53
5.1.	Alzheimer's Disease	53
5.1.1.	Cholinergic Dysfunction in Alzheimer's Disease and the Cholinergic Hypothesis of Learning and Memory	56
5.1.2.	Glutamate and Alzheimer's Disease	58
5.1.3.	Second Messenger Systems and Alzheimer's Disease	61
5.1.4.	Animal Models of Alzheimer's Disease: Cholinergic Denervation	63
5.2.	Cerebral Ischaemia	66
5.2.1.	Glutamate Neurotoxicity and Ischaemia	66
5.2.2.	Mechanisms of Excitotoxicity	67
5.2.3.	Cytotoxicity and Calcium	69
5.2.4.	Neurochemical Alterations in Response to Cerebral Ischaemia .	71
5.2.5.	Animal Models of Cerebral Ischaemia	72
5.2.6.	Neuroprotection and Ischaemia: NMDA Antagonists	75
6.	AUTORADIOGRAPHIC IMAGING OF THE CENTRAL NERVOUS SYSTEM	78
6.1.	Deoxyglucose Autoradiography	78
6.2.	Quantitative Ligand-Binding Autoradiography	82
7.	AIMS OF THESIS	84
7.1.	Effects of Glutamatergic and Cholinergic Agents on Cerebral Glucose Utilisation	84
7.1.1.	D-CPP-ene, a Novel Competitive NMDA Antagonist	84

7.1.2.	L-679-512, a Novel Muscarinic Agonist	85
7.1.3.	9-Amino-1,2,3,4-Tetrahydroaminoacridine (THA), a Cholinesterase Inhibitor with Potential Glutamatergic Activity	86
7.2.	Functional Plasticity of the Hippocampus in Response to Lesions of the Medial Septum	87
7.2.1.	Functional Activity in the Hippocampus after Ibotenic Acid Lesions of the Medial Septum	87
7.2.2.	Alterations in Ligand-Binding to Hippocampal Cholinergic and Glutamatergic Receptors After Lesions of the Medial Septum	87
7.2.3.	Muscarinic-Mediated Phosphoinositide Hydrolysis in the Hippocampus Following Ibotenic Acid Lesions of the Medial Septum	88
7.3.	The Cerebral Metabolic Effects of Acute Subdural Haematoma in the Rat	88

CHAPTER II: METHODS

1.	QUANTITATIVE AUTORADIOGRAPHY	91
1.1.	<i>In Vivo</i> [¹⁴ C]-Deoxyglucose Autoradiography	91
1.1.1.	Theory: Mathematical Model and the Operational Equation	91
1.1.2.	Methodological Considerations	93
1.1.3.	Animals	94
1.1.4.	Surgical Preparation	94
1.1.5.	Autoradiographic Sampling and Preparation of Autoradiograms	95
1.1.6.	Liquid Scintillation Analysis	96
1.1.7.	Calculation of Local Cerebral Glucose Utilisation	96

1.1.8.	Drug Administration	96
1.1.9.	Chemicals	98
1.2.	<i>In Vitro</i> Ligand Binding Autoradiography	98
1.2.1.	Theory	98
1.2.2.	Preparation of Sections for Ligand-Binding Autoradiography	100
1.2.3.	Procedure	102
1.2.4.	Chemicals	103
1.3.	Analysis of Autoradiograms	103
1.4.	Statistical Analysis	106
2.	LESIONS OF THE CNS	107
2.1.	Stereotaxic Lesions of the Medial Septal Nucleus	107
2.1.1.	Theory: The Use of Ibotenic Acid as a Neurotoxin	107
2.1.2.	Animals	107
2.1.3.	Chemicals	107
2.1.4.	Surgical Procedure	108
2.1.5.	Quantification of the Extent of Lesion	109
2.2.	Acute Subdural Haematoma: A Rat Model of Focal Cerebral Ischaemia	110
2.2.1.	Surgical Preparation	110
2.2.2.	Experimental Routines and Drug Administration	111
2.2.3.	Quantification of Ischaemic Lesion	112

3.	BIOCHEMICAL ANALYSIS OF SECOND MESSENGER SYSTEMS IN THE HIPPOCAMPUS: ESTIMATION OF PHOSPHOINOSITIDE TURNOVER	113
3.1.	Theory: and Background to Assay	113
3.2.	Method	114
3.3.	Analysis of Results	116
3.4.	Materials	116

CHAPTER III: RESULTS

1.	EFFECTS OF GLUTAMATERGIC AND CHOLINERGIC AGENTS ON CEREBRAL GLUCOSE USE	119
1.1.	General Observations	119
1.2.	Local Cerebral Glucose Utilisation	120
1.2.1.	D-CPP-ene, a competitive NMDA antagonist	121
1.2.2.	L-679-512, a Novel Muscarinic Agonist	124
1.2.3.	9-Amino-1,2,3,4-Tetrahydroacridine (THA), a Cholinesterase Inhibitor with Potential Glutamatergic Activity	126
2.	FUNCTIONAL PLASTICITY OF THE HIPPOCAMPUS IN RESPONSE TO LESIONS OF THE MEDIAL SEPTUM	129
2.1.	Characterisation of Ibotenic Acid-Induced Lesions of the Medial Septum.	129
2.2.	Local Cerebral Glucose Utilisation Following Lesions of the Medial Septum	130
2.2.1.	Local Cerebral Glucose Utilisation Within the Hippocampus	130
2.2.2.	Cerebral Glucose Utilisation in the Hippocampus and Limbic Regions Following Lesions of the Medial Septum	131

2.3.	Muscarinic and Glutamatergic Receptor Binding in Hippocampal Regions Following Lesions of the Medial Septum	131
2.3.1.	Anatomical distribution of Muscarinic and Glutamatergic Binding Sites Within the Hippocampus and Associated Regions	131
2.3.2.	Alterations in Muscarinic and Glutamatergic Receptor Binding Within Hippocampal and Associated Regions Following Lesions of the Medial Septum	133
2.4.	Measurement of Phosphoinositide Turnover Following Lesions of the Medial Septum	135
3.	THE CEREBRAL METABOLIC EFFECTS OF ACUTE SUBDURAL HAEMATOMA IN THE RAT	138
3.1.	Effects of Acute Subdural Haematoma on Local Cerebral Glucose Utilisation	138

CHAPTER IV: DISCUSSION

1.	EFFECTS OF GLUTAMATERGIC AND CHOLINERGIC AGENTS ON CEREBRAL GLUCOSE USE	142
1.1.	The Competitive NMDA antagonist D-CPP-ene	142
1.2.	The Novel Muscarinic Agonist L-679-512	154
1.3.	9-Amino-1,2,3,4-tetrahydroacridine (THA)	161
2.	FUNCTIONAL PLASTICITY OF THE HIPPOCAMPUS IN RESPONSE TO LESIONS OF THE MEDIAL SEPTUM	165
2.1.	Glucose Utilisation and Synaptic Modification	165
2.2.	Muscarinic Receptor Plasticity and Medial Septal Lesions	169
2.3.	Glutamatergic Receptor Plasticity and Medial Septal Lesions	174

2.4.	Phosphoinositide Hydrolysis: Response to Medial Septal Lesions	185
3.	THE CEREBRAL METABOLIC EFFECTS OF ACUTE SUBDURAL HAEMATOMA IN THE RAT	188
3.1.	Functional activity and Acute Subdural Haematoma in the Rat	188
3.2.	Comment on the Application of the Deoxyglucose Method to the Ischaemic Brain	198
4.	OVERVIEW: COMMENT ON TECHNIQUES FOR ANALYSIS OF HIPPOCAMPAL FUNCTION	200

APPENDICES

APPENDIX I

THE CEREBRAL METABOLIC EFFECTS OF THE COMPETITIVE NMDA ANTAGONIST, D-CPP-ENE, IN THE RAT	205
--	-----

APPENDIX II

THE CEREBRAL METABOLIC EFFECTS OF A NOVEL MUSCARINIC AGONIST, L-679-512, IN THE RAT	213
---	-----

APPENDIX III

THE CEREBRAL METABOLIC EFFECTS OF 9-AMINO-1,2,3,4-TETRAHYDROACRIDINE (THA), A COMPOUND OF POTENTIALLY MIXED CHOLINERGIC AND GLUTAMATERGIC ACTION	221
--	-----

APPENDIX IV

LOCAL CEREBRAL GLUCOSE UTILISATION IN RESPONSE TO
LESIONS OF THE MEDIAL SEPTUM 229

APPENDIX V

QUANTITATIVE LIGAND BINDING TO GLUTAMATERGIC
AND MUSCARINIC RECEPTORS IN HIPPOCAMPAL AND
ASSOCIATED STRUCTURES FOLLOWING MEDIAL SEPTAL
LESIONS 234

APPENDIX VI

LOCAL CEREBRAL GLUCOSE UTILISATION IN RESPONSE TO
ACUTE SUBDURAL HAEMATOMA 239

REFERENCES 244

PUBLICATIONS 299

LIST OF TABLES

PAGE:

1.	COMPETITIVE NMDA ANTAGONISTS AND CEREBRAL ISCHAEMIA	76
2.	SUMMARY OF LIGANDS AND LIGAND BINDING PROTOCOLS	101
3.	BASAL AND CARBACHOL-STIMULATED [³ H]-INOSITOL PHOSPHATE ACCUMULATION AND CHAT ACTIVITY IN THE RAT HIPPOCAMPUS FOLLOWING LESIONS OF THE MEDIAL SEPTUM	136

LIST OF FIGURES

AFTER PAGE NO:

1.	Anatomy of the hippocampal formation	25
2.	Schematic diagram of the trisynaptic pathway	26
3.	Schematic representation of the NMDA receptor	31
4.	Theoretical model of deoxyglucose uptake in the brain	91
5.	The Operational equation	92
6.	General procedure for quantitative receptor autoradiography <i>in vitro</i>	102
7.	Histological analysis of acute subdural haematoma in the rat	112
8.	The phosphoinositide cycle	113
9.	Local cerebral glucose utilisation in the hippocampus following D-CPP-ene administration: Ammon's horn	121
10.	Local cerebral glucose utilisation in the hippocampus following D-CPP-ene administration: dentate gyrus, presubiculum and subiculum	121
11.	Autoradiograms of glucose utilisation in the rat brain following D-CPP-ene: hippocampus, auditory and visual regions	121
12.	Local cerebral glucose utilisation in cortical areas associated with limbic function following D-CPP-ene administration	122
13.	Local cerebral glucose utilisation in limbic structures following D-CPP-ene administration: subcortical areas	122
14.	Autoradiograms of glucose utilisation in the rat brain following D-CPP-ene: parietal cortex	122
15.	Local cerebral glucose utilisation in olfactory areas following D-CPP-ene administration	123
16.	Autoradiograms of glucose utilisation in the rat brain following D-CPP-ene: olfactory cortex	123

17.	Local cerebral glucose utilisation in visual and auditory structures following D-CPP-ene administration	123
18.	Local cerebral glucose utilisation in the hippocampus following L-679-512 administration: Ammon's horn	124
19.	Local cerebral glucose utilisation in the hippocampus following L-679-512 administration: dentate gyrus, presubiculum and subiculum	124
20.	Local cerebral glucose utilisation in limbic structures following L-679-512 administration	125
21.	Local cerebral glucose utilisation in olfactory structures following L-679-512 administration	125
22.	Local cerebral glucose utilisation following L-679-512 administration: auditory and visual structures	125
23.	Local cerebral glucose utilisation in hippocampal and limbic structures following THA administration	126
24.	Local cerebral glucose utilisation in auditory and visual structures following THA administration	126
25.	Autoradiograms of glucose utilisation in the rat brain following THA: hippocampus, auditory and visual structures	127
26.	Quantification of ibotenate lesions of the medial septum	129
27.	Histological profile of ibotenate lesions of the medial septum	129
28.	Autoradiogram of glucose utilisation in the rat hippocampus	130
29.	Local cerebral glucose utilisation in hippocampal and limbic regions following lesions of the medial septum	130
30.	Autoradiograms of ligand binding to glutamatergic and muscarinic receptors in the rat hippocampus	131
31.	[³ H]-QNB binding in the hippocampal area: CA and dentate gyrus	133
32.	[³ H]-QNB binding in the hippocampal region: subicular area, entorhinal cortex and septal area	133

33.	[³ H]-AMPA binding in the hippocampal region: CA and dentate gyrus	133
34.	[³ H]-AMPA binding in the hippocampal region: subicular area, entorhinal cortex and septal area	133
35.	[³ H]-kainate binding in the hippocampal region: CA and dentate gyrus	134
36.	[³ H]-kainate binding in the hippocampal region: subicular area, entorhinal cortex and septal area	134
37.	NMDA-displaceable [³ H]-glutamate binding in the hippocampal region: CA and dentate gyrus	134
38.	NMDA-displaceable [³ H]-glutamate binding in the hippocampal region: subicular area, entorhinal cortex and septal area	134
39.	Phosphoinositide hydrolysis following lesions of the medial septum	136
40.	Autoradiograms of glucose utilisation in the rat hippocampus following acute subdural haematoma	138
41.	Local cerebral glucose utilisation following acute subdural haematoma: hippocampal formation	139
42.	Local cerebral glucose utilisation following acute subdural haematoma: limbic, auditory and visual regions	140
43.	Competitive NMDA antagonists	143
44.	The novel muscarinic agonist L-679-512: chemical structure	155
45.	The cholinergic septohippocampal path	172
46.	Hippocampal association pathways	179

ACKNOWLEDGEMENTS

It has been the unenviable task of Professor James McCulloch to supervise my work for this thesis. His insistence upon experimental rigour, combined with his albeit daunting encouragement to follow my research interests freely, have provided me with a firm foundation from which to build my future work.

Through his untiring efforts and single-minded dedication to this Institute, Professor Murray Harper has provided facilities, a stimulating environment, and a degree of freedom which is rare among developing scientists. I am most grateful to him for allowing me the considerable privilege of working in his laboratories, and for his personal devotion to my work.

My studies have also benefitted greatly by my contacts and discussions with Miss Sue Browne, Mr. Ross Bullock, Dr. Deborah Dewar, Professor David Graham, Dr. Karen Horsburgh, Dr. Mhairi Macrae, Mr. Mark McLaughlin, Mr. Brian Ross, and Dr. Chris Wallace.

The excellent assistance of the technical staff of the biochemical laboratory is graciously acknowledged, and I would like to thank Hayley-Jane Dingwall, Lindsay Dover, Michael Dunne, Mairi Law, Margaret Roberts, Marion Steele, Joan Stewart and Margaret Stewart. Thanks are also extended to the technical help provided by Margaret Crossling, Peter Johnston, Gordon Littlejohn and Dave Love, and to the animal nurses, under supervision of Christine Stirton and Morag Findlay.

I am particularly indebted to Mr. Ross Bullock, of the Institute of Neurological Sciences, Southern General Hospital, for allowing me to work with him on his research into ischaemia, in what proved to be an exciting and rewarding endeavour.

Sincere thanks are also due to Professor David Graham, for his advice on histological techniques and analysis of lesioned material. Thanks are extended to the staff of the Department of Neuropathology, Southern

General Hospital, for the histological processing of the lesioned material presented in this thesis.

A large portion of the work which comprises this thesis was performed in Organon Laboratories, Oss, Netherlands. I would like to thank the staff of Organon, particularly my supervisors Jeroen Tonnaer and Ton van Delft, for allowing me to visit their laboratories, and for giving me access to the Ibas Densitometer and their second messenger analysis methods. My most grateful thanks is extended to Tijs de Boer, Peter Room, Jim Hagan and Frans van Huizen, Chris Verstegeen, Geert Schuiers, Ton Tielemans, and the other laboratory staff, for their help, and all the lessons in Dutch. (Heel Bedankt, en tot ziens!)

Expert secretarial assistance was provided by Mrs. Anne-Marie Colquhoun, Mrs Lyndsay Graham and Mrs. Jean Pearce. My especial thanks is deserved by Mrs. Lyndsay Graham, for typing the appendices in this thesis. The accuracy and speed with which these were typed is in itself a tribute to her abilities.

Finally, and most of all I am indebted to my family and friends for their considerable personal devotion: to my parents for their endless financial and emotional support, without which this thesis would not exist. To Katriona and Sandra for their help and patience, and to Philip for his terrible jokes. To Mike and Jane, for their ever-present help and advice, various adventures, many fine wines, and their perpetual youth. To Ross Macleod, for his immeasurable help and constant optimism, and his constant supply of tea and biscuits. To all is dedicated this thesis.

SUMMARY

The effects of pharmacological and pathological manipulation of hippocampal cholinergic and glutamatergic neurotransmitter receptor systems were examined using quantitative *in vivo* [¹⁴C]-deoxyglucose autoradiography and *in vitro* ligand binding autoradiography. In three series of rats, local cerebral glucose utilisation was assessed in 76 anatomically defined hippocampal, limbic and other structures following administration of three novel cholinergic or glutamatergic agents in order to assess the physiological changes in cerebral metabolism in response to pharmacological challenge. Secondly, to assess the plastic responses of hippocampal cholinergic and glutamatergic transmitter systems in the hippocampus to cholinergic denervation, ligand binding to N-methyl-D-aspartate (NMDA), AMPA-sensitive quisqualate, kainate and muscarinic receptors was performed in rats which had received surgery to lesion the medial septum three weeks previously. The status of cholinergic systems was further investigated using biochemical techniques to estimate muscarinic-stimulated second messenger turnover following septal lesions. Local cerebral glucose utilisation was measured in rats using the deoxyglucose technique three weeks after medial septal lesion as an index of function. Finally, the effects of acute experimental subdural haematoma, a novel ischaemic technique, on functional activity in the hippocampus and associated limbic regions were assessed using deoxyglucose autoradiography. The ability of a novel glutamate antagonist to prevent functional disturbances produced by subdural haematoma were also assessed, with a view to potential clinical treatment of ischaemia.

These studies demonstrate that manipulation of cholinergic and glutamatergic transmitter systems in the CNS may result in widespread functional alterations in the brain, and suggest that cholinergic and glutamatergic systems may interact in the plastic modifications which

accompany cholinergic denervation in the limbic system.

1. Pharmacological Effects of Cholinergic and Glutamatergic Agents on Cerebral Glucose Use

The effects on functional activity in the hippocampus and other regions of the CNS of a glutamate antagonist, a muscarinic agonist and a cholinesterase inhibitor with potential glutamatergic activity were examined using deoxyglucose autoradiography.

The novel competitive NMDA antagonist D-CPP-ene (0.3, 3 or 30mgkg⁻¹) induced widespread, heterogeneous patterns of altered glucose utilisation in the brain. These alterations were not directly related to glutamate receptor density: in the hippocampus, D-CPP-ene treatment (3mgkg⁻¹) significantly depressed glucose utilisation in the subiculum and CA4 pyramidal layer (22% and 31% relative to saline-treated controls), while other regions of the hippocampus such as the glutamate receptor-dense CA1 were not significantly affected. In cortical and subcortical regions involved with sensory processing, D-CPP-ene evoked marked depression of glucose utilisation. The most marked reduction in glucose use occurred in auditory cortex (Layer IV), which exhibited a 49% decrease relative to controls. In contrast, D-CPP-ene (30mgkg⁻¹) elicited marked increases in glucose use in olfactory regions: in the lateral olfactory tract, glucose use increased by 79% relative to control values following D-CPP-ene treatment.

The novel potent muscarinic agonist L-679-512 (3, 10 or 30 µgkg⁻¹) produced few significant alterations in glucose utilisation in 76 brain regions. In the hippocampus, L-679-512 resulted in decreased glucose utilisation in the CA1 and CA2 stratum lacunosum moleculare (11% and 14% reduction relative to controls, respectively), and the CA2 stratum oriens/pyramidale (15%). In limbic regions, glucose utilisation was

consistently reduced in the mamillary body following L-679-512 administration. L-679-512 ($30\mu\text{gkg}^{-1}$) induced decreased glucose use in olfactory regions: glucose utilisation in the entorhinal cortex was reduced by 25% relative to controls.

The cholinesterase inhibitor THA (2.5mgkg^{-1}) evoked little functional response in hippocampal or limbic regions. Glucose utilisation was increased significantly in the subiculum (17%) and anteroventral thalamic nucleus (25%), and was decreased significantly in the dorsal raphé (15%), but remained unaltered in other limbic regions. Instead, THA elicited large, highly significant increases in glucose use in visual structures such as the superior colliculus (40%) and dorsolateral geniculate body (28%), thus providing evidence for a cholinergic, rather than glutamatergic, mode of action.

2. Effect of Cholinergic Denervation on the Integrity of Muscarinic and Glutamatergic Transmission in the Hippocampus

Medial septal lesions were produced in rats using stereotaxic injection of ibotenic acid ($6\mu\text{g}$). Lesions resulted in a decrease in choline acetyltransferase activity of 25% compared to sham-operated controls. Three weeks after lesions of the medial septum, quantitative *in vitro* ligand binding autoradiography was used to estimate densities of cholinergic and glutamatergic receptors in hippocampal and limbic regions. [^3H]-QNB, [^3H]-AMPA, [^3H]-kainate and NMDA-displaceable [^3H]-glutamate were used to assess muscarinic, AMPA-sensitive quisqualate, kainate and NMDA receptors in hippocampal and limbic regions. Cerebral glucose use was measured using [^{14}C]-deoxyglucose autoradiography. There were no alterations in [^3H]-kainate and NMDA-displaceable [^3H]-glutamate binding in hippocampal and limbic regions; however, [^3H]-QNB binding was significantly reduced in the subiculum

(14%) and in the medial and lateral septum (32% and 13% respectively). [³H]-AMPA binding was also found to be reduced following septal lesions: binding was significantly reduced throughout the pyramidal region, with the most significant decrease in CA2 (18%). [³H]-AMPA binding was also reduced in the CA1 stratum radiatum and CA2 stratum lacunosum moleculare, and in the entorhinal cortex. In the septal region, a 49% reduction in [³H]-AMPA binding was observed in the medial septal nucleus. In comparison, glucose use was not altered three weeks post-lesion compared to sham-operated control values. These results provide evidence that glutamatergic receptors are modified in response to cholinergic denervation of the hippocampus.

To assess further the integrity of the cholinergic system following medial septal lesions, carbachol-stimulated accumulation of [³H]-inositol phosphate accumulation was measured in hippocampal slices three weeks following septal lesion or sham operation. No significant difference was measured between sham and lesioned groups, suggesting that muscarinic coupling to phosphoinositide metabolism is unaltered in the absence of the major cholinergic input to the hippocampus.

3. Effects of Acute Subdural Haematoma on Cerebral Glucose Use in the Rat

Cerebral glucose use in hippocampal, limbic and other structures was investigated in a novel model of ischaemia in the rat. Acute subdural haematoma was produced by injection of 0.4ml autologous blood below the dura, over the left parietal cortex, two hours prior to [¹⁴C]-deoxyglucose autoradiography. In rats which received haematoma, marked increases in glucose utilisation were measured bilaterally throughout the glutamate receptor-dense hippocampus. In the ipsilateral CA1 stratum radiatum, glucose use was increased by 142% compared to sham-operated controls, while in the dentate molecular layer, glucose use

was increased by 112%. The ischaemic cortex was almost devoid of deoxyglucose uptake, while in the bordering "penumbral" zone, deoxyglucose uptake was observed to be higher than in the surrounding non-ischaemic cortex. Acute subdural haematoma also reduced glucose utilisation in auditory and visual regions: glucose use was decreased by 48% following subdural haematoma.

In a third group of rats, pretreatment with the competitive NMDA antagonist D-CPP-ene fifteen minutes before deoxyglucose autoradiography reduced the functional disturbances associated with acute subdural haematoma. In the hippocampal CA1 and CA3 regions, D-CPP-ene pretreatment resulted in rates of glucose use significantly lower than those in the non-pretreated group. In addition, D-CPP-ene abolished the rim of increased deoxyglucose uptake surrounding the infarct, and reduced the functional deficit produced by the haematoma in auditory and visual regions. These results provide an *in vivo* perspective of the functional disturbances which accompany ischaemia, and support the glutamatergic hypothesis of ischaemia; further, these results suggest that glutamatergic antagonists may be of benefit in the clinical treatment of ischaemia.

The results presented in this thesis highlight the advantages of *in vivo* mapping of cerebral events, particularly in situations where dynamic alterations in function are likely to occur, such as acute pharmacological, or pathological challenge. Furthermore, the use of receptor autoradiography provides insights into the processes of modification following denervation, and suggest that in the hippocampus, both cholinergic and glutamatergic systems are involved in synaptic modifications which accompany cholinergic denervation.

PREFACE AND DECLARATION

This thesis presents results from studies of deoxyglucose autoradiography and ligand binding autoradiography in the rat brain. Quantitative [¹⁴C]-deoxyglucose autoradiography was used to measure the local cerebral glucose utilisation as an index of cerebral function in the conscious rat. Ligand binding techniques were used to measure receptor binding densities in vitro.

Investigations have been conducted in three broadly defined areas:

- (1) The effects of intravenous administration of cholinergic and glutamatergic agents on cerebral function in the rat.
- (2) The effects of cholinergic denervation on glutamatergic and muscarinic transmitter systems and on cerebral glucose use in the hippocampus.
- (3) The effects of a novel model of ischaemia on cerebral glucose utilisation in the hippocampus, and the ability of a glutamate antagonist with anti-ischaemic efficacy to ameliorate ischaemia-induced functional disturbances.

Results of these studies are discussed separately. In the final overview I have attempted to discuss critically the techniques, in terms of their advantages and limitations, in relation to their employment in studies of the hippocampus.

This thesis comprises my own original work and has not been presented previously as a thesis in any form.

CHAPTER I

INTRODUCTION

1. THE HIPPOCAMPUS: A BRIEF HISTORICAL OVERVIEW.

The hippocampus forms part of the temporal cortical mantle, immediately caudal to the amygdala and is so-named because of its resemblance when dissected to a seahorse lying along the inferior horn of the lateral ventricle. In the nineteenth century, the use of the Golgi technique to stain neurones revealed that in comparison to other cortical areas, the hippocampus is comprised of a striking, highly distinct laminar organisation; this provided the impetus for expanded neuroanatomical research, and consequently the hippocampus has become the most topographically defined cortical region in terms of its intrinsic neuronal circuitry and its efferent and afferent connections. In contrast, however, the precise role of the hippocampus in cerebral function remains enigmatic.

The hypothesis that the hippocampus plays a critical role in learning and memory has become accepted in recent years due to a vast body of experimental evidence that lesions of the hippocampus or its afferents result in deficits in a variety of learning and memory tasks (O'Keefe & Nadel, 1978; Squire & Zola-Morgan, 1983). In humans, destruction of hippocampal neurones is associated with cognitive deficits in diseases such as Alzheimer's Disease (Hyman et al., 1984), and certain types of amnesia (Zola-Morgan et al., 1986). Further, long-term potentiation (or LTP), an increase in synaptic efficacy in response to bursts of high frequency neuronal firing (Collingridge, 1985), has been demonstrated to occur in most hippocampal regions, and has been proposed as the synaptic component of learning: blockade of long-term potentiation by pharmacological means in rats is associated with impaired cognitive ability in behavioural learning tasks (Morris et al., 1986).

Two factors are paramount in the sustained interest in hippocampal function: firstly, the relative simplicity of neuronal circuitry has facilitated the study and analysis of long-term potentiation, and its

modulation by pharmacological manipulations or physiological stimulation of afferent structures. The hippocampus therefore provides a model upon which to challenge hypotheses of synaptic efficacy and plasticity in the analysis of learning and memory. Secondly, a number of disease states which affect memory and mnemonic processes in humans have been demonstrated to result in alterations in receptors, second messengers and cellular components within the hippocampus. Therefore, a focus of recent research has been to quantify alterations in hippocampal transduction mechanisms underlying the disease process with the aim of treating or even preventing the disruption of hippocampal function. These two separate approaches have resulted in a number of hypotheses which address the mechanisms underlying hippocampal transmission; yet neither have been able to elucidate the precise physiological actions of transmitters and receptors in the hippocampus, and the degree of involvement of individual transmitter systems in neurodegenerative diseases remains obscure.

2. ANATOMICAL ORGANISATION OF THE HIPPOCAMPUS

The anatomical organisation of the hippocampus is detailed in Figure 1. The hippocampal formation may be divided into four major areas (for review, see Swanson et al., 1987): the entorhinal area, the subicular complex, the dentate gyrus, and Ammon's horn (Cornu Ammonis or CA).

A variety of staining techniques reveal the existence of four laminae of Ammon's horn: from the superficial to deep layers, these are the stratum lacunosum moleculare (or molecular layer), the cell-sparse stratum radiatum, the stratum pyramidale (or pyramidal cell layer), and the stratum oriens which lies adjacent to the hippocampal white matter or alveus. On morphological grounds, Ammon's horn has been subdivided into distinct CA sectors (Lorente de Nó, 1934), a terminology which has wide acceptance, and which is used in the present study. Fields CA1 and CA3 are anatomically distinct: CA3 contains an additional lamina, the stratum lucidum, which represents the terminal region for dentate mossy fibres. CA1 and CA3 have different patterns of innervation, and are separated by a narrow transitional zone, CA2; the functional significance of CA2 is not clear.

The dentate gyrus consists of three laminae: the molecular layer, an underlying granular cell layer, and an infragranular layer, which corresponds to the CA4 or hilus region, and borders the CA4 stratum pyramidale. The dentate gyrus is also sub-divided into a superior and inferior blade, and on functional grounds the outer and inner portions of the molecular layer can be considered distinctly.

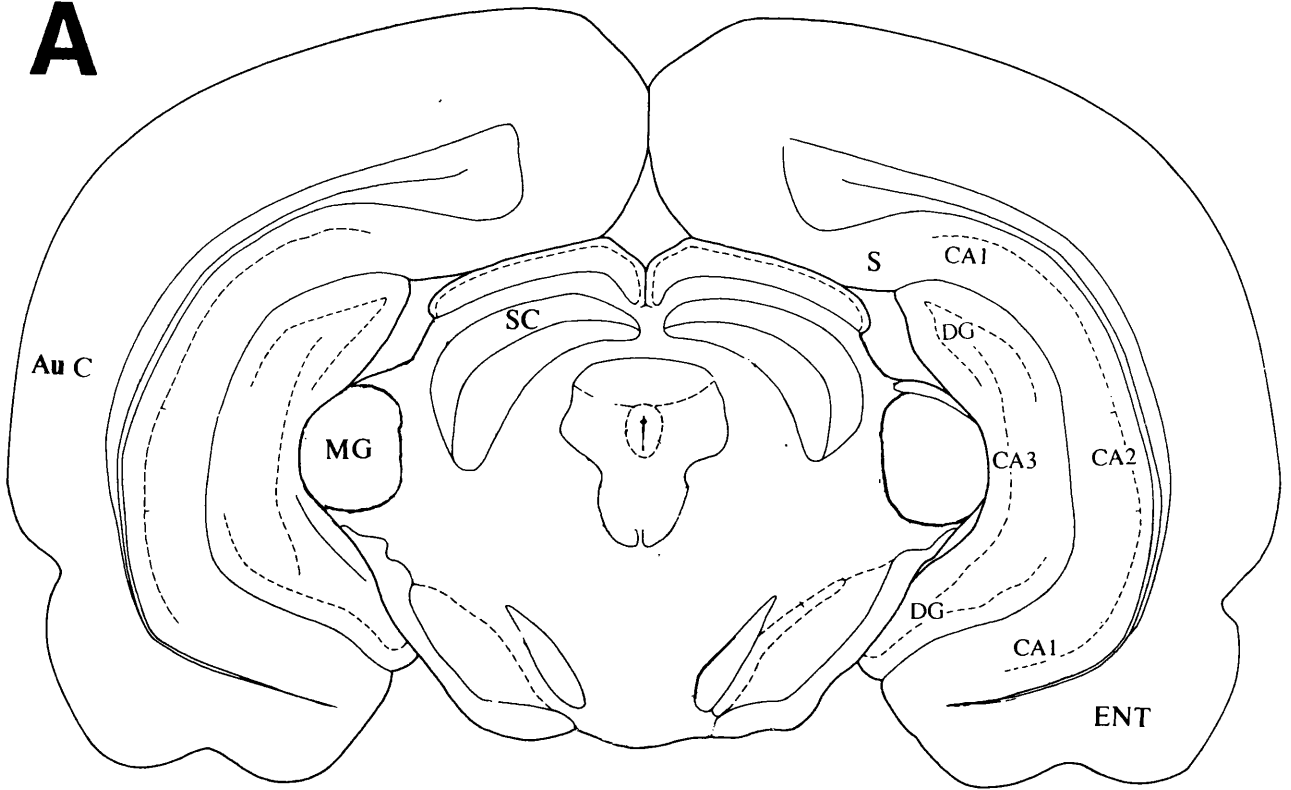
The subicular complex consists of the subiculum, parasubiculum and presubiculum. Compared to other hippocampal regions, these are less well-defined in terms of their laminar organisation, and their function within hippocampal neuronal has attracted less attention, although they receive extensive projections from sensory cortical regions, as well as a

LEGEND TO FIGURE 1

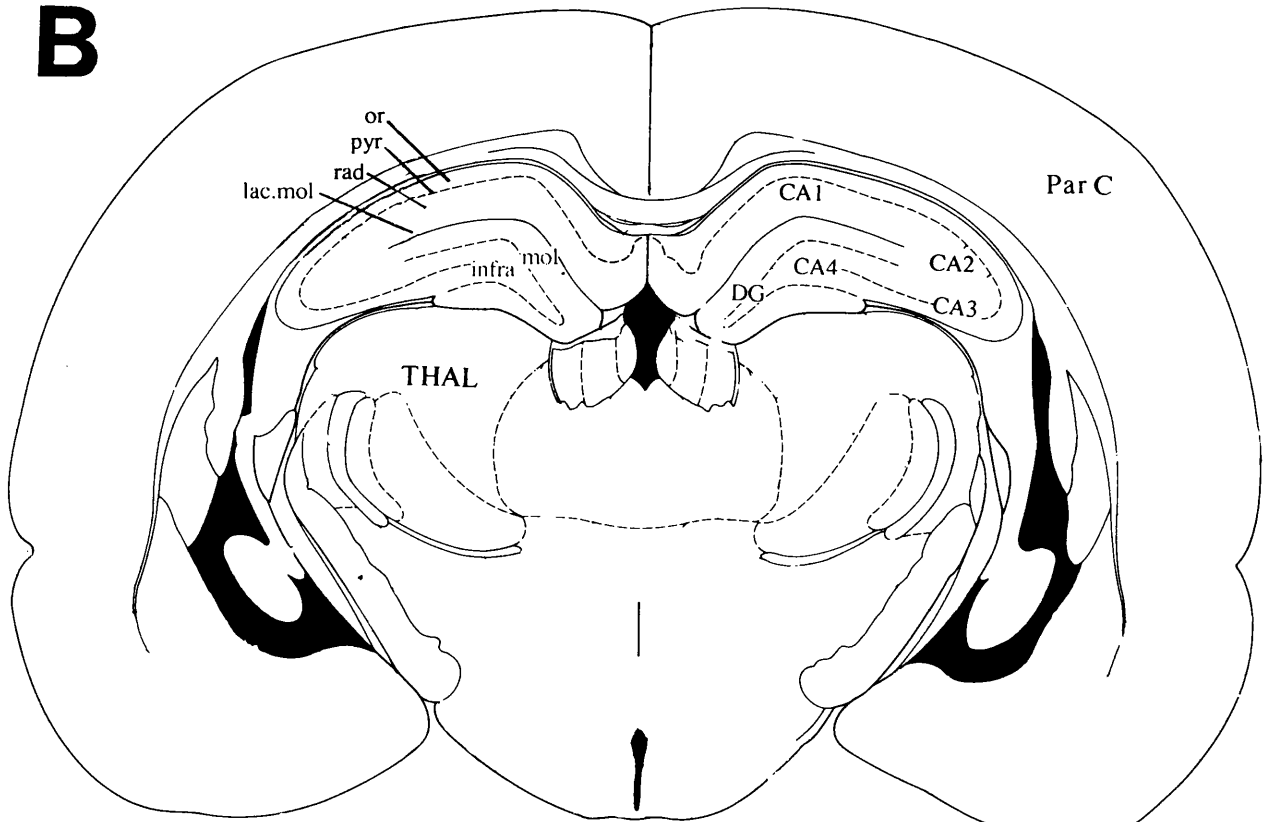
ANATOMY OF THE HIPPOCAMPAL FORMATION

Diagrammatic representation of coronal sections at the level of the ventral (A) and dorsal (B) hippocampus.

Abbreviations: or: stratum oriens; pyr: stratum pyramidale; rad: stratum radiatum; lac.mol: lacunosum moleculare; DG: dentate gyrus; mol: molecular layer; infra: infragranular region; S: subiculum; ENT: entorhinal cortex; MG: medial geniculate body; SC: superior colliculus; Au C: auditory cortex; THAL: thalamus; Par C: parietal cortex.

A

Bregma -6.04 mm

B

Bregma -3.80 mm

FIGURE 1: ANATOMY OF THE HIPPOCAMPAL FORMATION

direct input from the entorhinal and septal areas. While the presubiculum and parasubiculum have a similar architecture to that of the entorhinal cortex immediately adjacent, the subiculum represents a marked change in lamination, and is composed of a deep pyramidal layer, an intermediate cell-sparse layer which is continuous with the CA stratum radiatum, and a superficial molecular layer, continuous with that of the presubiculum and CA1 on either side. However, in contrast to the highly stratified patterns of receptor distribution and local cerebral glucose utilisation which are demonstrated in other hippocampal regions, the subicular complex has relatively homogeneous rates of glucose use and receptor binding densities, and is therefore considered homogeneous in the present study.

Finally, the entorhinal cortex can be divided immediately into lateral and medial portions on the grounds of anatomical structure and innervation: each portion contains six structurally distinct layers, while clusters of stellate cells in layer II of the lateral portion are absent in the medial portion of the entorhinal cortex, and the lateral and medial entorhinal cortices are functionally distinct in terms of their efferent hippocampal projections.

2.1. THE TRISYNAPTIC PATHWAY

The perforant pathway, perhaps the best characterised hippocampal pathway (Ramon y Cajal, 1911), originates in the entorhinal cortex, and projects to the molecular layer of the dentate gyrus to form the first synapse in the trisynaptic pathway (Figure 2). Lesions confined to the lateral entorhinal area result in degeneration of nerve terminals in the outer third of the dentate molecular layer, while lesions of the medial entorhinal area cause neurodegeneration in the middle portion of the molecular layer (Hjorth-Simonsen, 1972; Hjorth-Simonsen & Jeune,

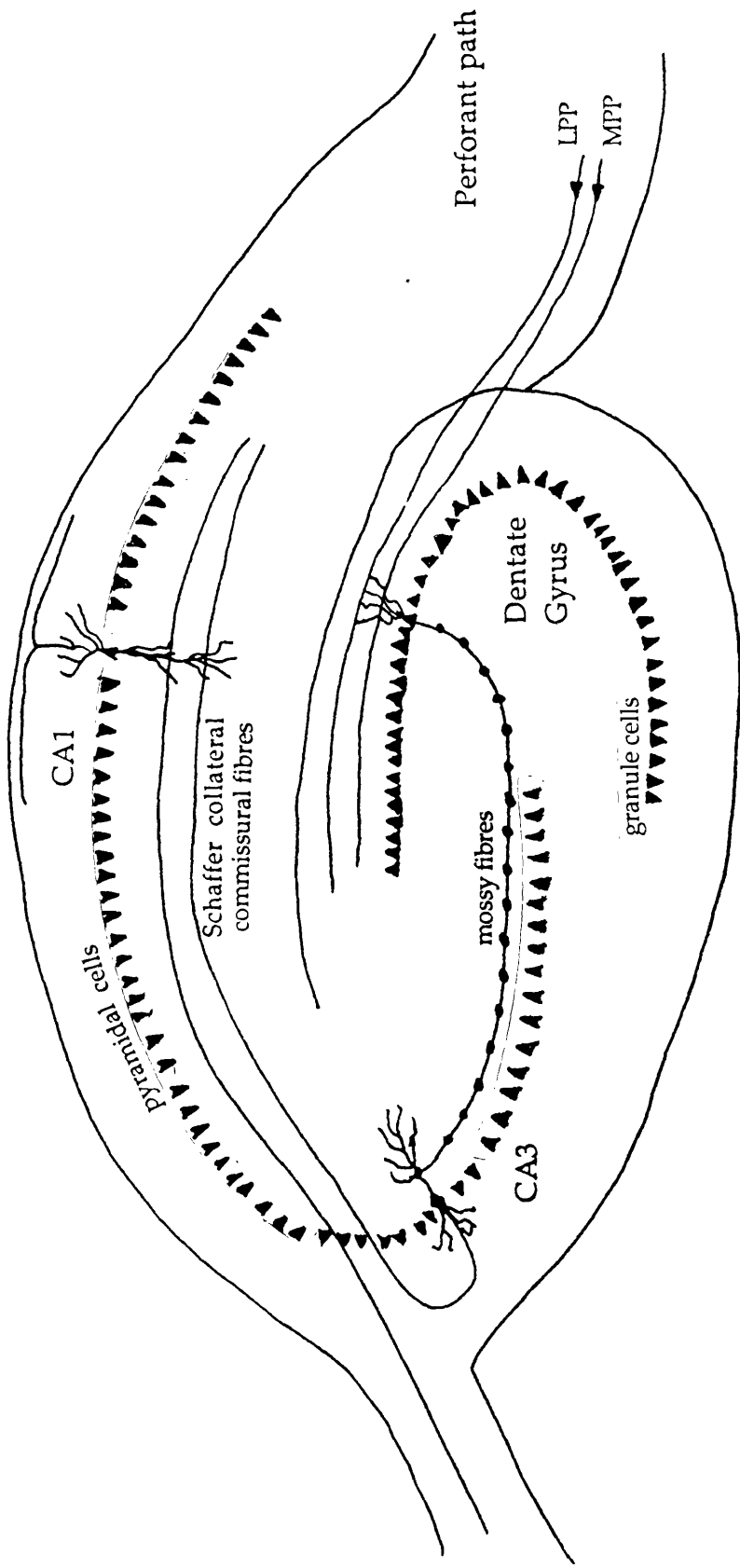


FIGURE 2: SCHEMATIC DIAGRAM OF THE GLUTAMATERGIC TRISYNAPTIC PATHWAY

1972), providing evidence for distinct lateral and medial components of the perforant path. This has been confirmed electrophysiologically (McNaughton, 1980). The perforant path fibres synapse with dendrites of granule cells in the dentate gyrus, and are thought to use glutamate as a neurotransmitter (Storm-Mathisen, 1977; Storm-Mathisen et al., 1983).

The dentate granule cells in turn give rise to apical mossy fibre projections, characterised by large boutons which synapse in the stratum lucidum on the spines of proximal dendrites of the CA3 pyramidal cells (Blackstad & Kjaerheim, 1961), to form the second connection in the trisynaptic pathway. These synapses are putatively glutamatergic (Fonnum et al., 1979; Storm-Mathisen & Iversen, 1979), and possibly act through kainate receptors, as evidenced by the high density of kainate receptor binding in the stratum lucidum (Cotman et al., 1987).

The CA3 pyramidal cells thence send out divergent Schaffer collateral fibres and commissural fibres which course through the strata radiatum and oriens, and synapse with the CA1 pyramidal dendrites in the same layers, to form the third synapse in the trisynaptic pathway. Abundant evidence suggests that these synapses are glutamatergic (for example, see Nadler et al., 1976; Fonnum & Walaas, 1978; Storm-Mathisen & Iversen, 1979; Collingridge et al., 1983), and there is a large projection from CA3 to the contralateral CA1, via the fimbria fornix (Gottlieb & Cowan, 1973).

In addition to the perforant path, the entorhinal cortex gives rise to, fibres which synapse directly in the stratum lacunosum moleculare with distal dendrites of the CA pyramidal cells. Thus the entorhinal cortex is afforded the potential for considerable control over hippocampal firing.

2.2. THE SEPTOHIPPOCAMPAL PATHWAY

The hippocampus receives its major extrinsic cholinergic input from the septal area, situated in the forebrain; in comparison to the entorhinal glutamatergic input, the cholinergic input is relatively diffuse, and appears to innervate all hippocampal fields (Lewis et al., 1967). The septal area may be sub-divided: the medial septum and the diagonal band nucleus form a continuum, although evidence suggests that these can be considered separate due to differences in innervation and neurochemistry (Amaral & Kurz, 1985; Saper, 1984; Swanson & Cowan, 1979). Both structures contain large cholinergic cell bodies, which are distinct from the smaller cells of the adjacent lateral septum. In addition to a cholinergic projection, a large proportion of cells in the medial septum are GABAergic (Köhler et al., 1984).

Although it has been demonstrated that the medial septal cholinergic input to the hippocampus innervates all regions of the hippocampal formation (Mellgren & Srebro, 1973; Nyakas et al, 1987; Swanson & Cowan, 1979), projections to the dentate gyrus are particularly dense, and synapse mainly within the dentate hilar region. In the CA region, fibres from the medial septum project to the strata oriens and radiatum of CA3, and less densely to the stratum oriens of CA1. In comparison, a diffuse septal input to the subicular complex exists. Additionally, the septum projects to the entorhinal cortex, specifically to layers II, IV and VI.

The vast majority of septal fibres reach the hippocampus via the fimbria fornix; however, two additional routes appear to exist. Firstly a projection from the diagonal band runs over the genu of the corpus callosum, and innervates the anterior cingulate and retrosplenial areas, ending in temporal regions of the subicular complex. The second projection, which accounts for approximately 10% of the cholinergic input into the hippocampus, runs ventrally through the amygdala and terminates within the temporal hippocampus (Milner & Amaral, 1984;

Gage et al., 1984).

The topography of projections from the septal region is a matter of some debate, although there is acceptance that medial septal cells innervate septal (or dorsal) regions of the hippocampus preferentially (Meibach & Siegel, 1977).

There is extensive evidence to support acetylcholine as the major transmitter in the septohippocampal pathway. Acetylcholinesterase and choline acetyltransferase (ChAT) are markedly reduced in the hippocampus following lesions of the septal area or fimbria fornix (Lewis et al., 1967; Mellgren & Srebro, 1973; Storm-Mathisen, 1970). However, the involvement of other transmitter substances within septal hippocampal afferents merits consideration: it has been reported that as much as 50% of medial septal neurones do not stain positively with antisera to ChAT (Mesulam et al., 1983). At least 30% of septohippocampal neurones stain positively with antisera to glutamic acid decarboxylase (GAD), and therefore a sizeable component of the septal hippocampal input can be presumed to be GABAergic (Köhler et al., 1984). While the role of septal cholinergic transmission has been examined in detail, the function of GABAergic septohippocampal fibres in hippocampal neuronal firing have received little attention to date, and therefore remains obscure.

3. GLUTAMATE AND THE HIPPOCAMPUS

3.1. GLUTAMATE AS A NEUROTRANSMITTER

Since Curtis and colleagues (1959) demonstrated that application of glutamate resulted in depolarisation of single neurones in the brain, and despite considerable scepticism, extensive evidence has accumulated that glutamate is an excitatory neurotransmitter in the mammalian central nervous system (CNS). Glutamate-like immunoreactivity has been located to synaptic vesicles (Ottersen & Storm-Mathisen, 1984), and the distribution of these corresponds with that of a high affinity uptake site localised immunohistochemically (Fonnum, 1984), suggesting that glutamate is stored presynaptically within specific neuronal populations. Ligand-binding studies have established that glutamatergic receptors are organised into specific, anatomically defined pathways (Cotman et al., 1987), and the existence of specific agonists and antagonists for glutamate receptors substantiates further the belief that glutamate acts as a neurotransmitter in the CNS. Recently, the use of the [^{14}C]-deoxyglucose autoradiographic technique has demonstrated that pharmacological blockade of glutamate receptors can result in cerebral metabolic alterations which are limited to discrete neuronal populations (Kurumaji et al., 1989); these studies provide evidence for the action *in vivo* of glutamate in the modulation of neuronal activity.

3.1.1. Sub-types of Glutamate Receptor

At least three distinct sub-types of glutamatergic receptor have been described (Watkins & Evans, 1981), based on their relative affinities for the glutamatergic agonists N-methyl-D-aspartate (NMDA), kainate and quisqualate. A fourth receptor sub-type, defined by binding of the antagonist L-2-aminophosphonobutyrate (L-AP4), has also been

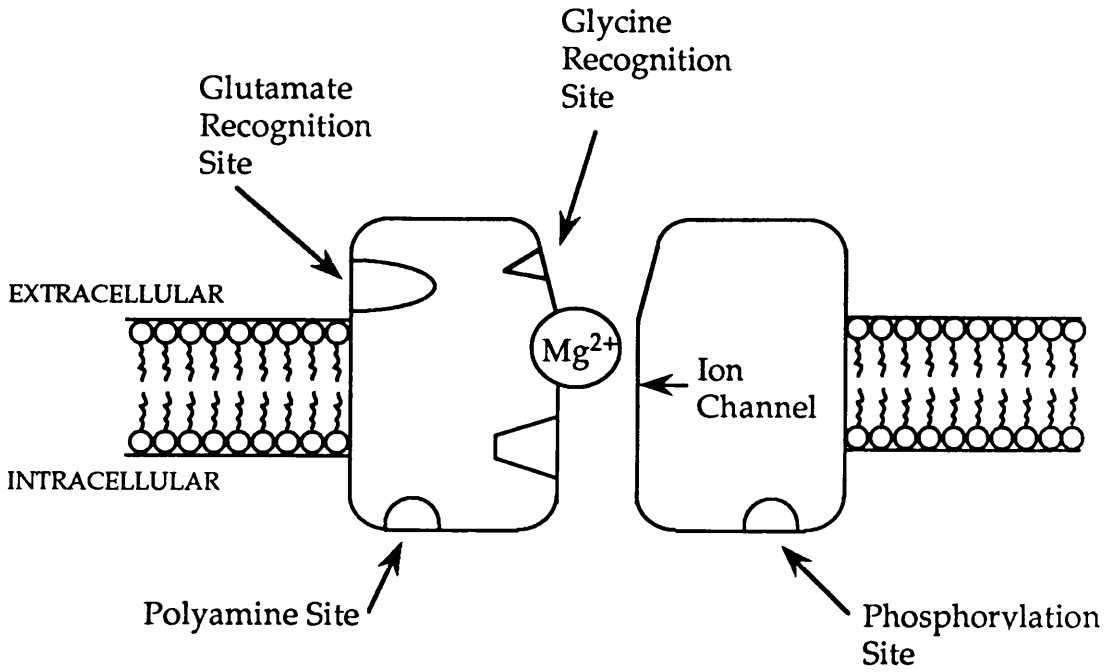
described; however, the precise physiological significance of this receptor is unclear.

NMDA Receptors

The availability of high affinity agonists and antagonists, and the use of radioligand assays have enabled the NMDA receptor to become the most clearly defined glutamatergic receptor (Figure 3). NMDA receptors were defined initially by their high affinity for the agonists NMDA, NMLA, aspartate and ibotenate. Competitive NMDA antagonists with high affinity and relatively high specificity for the NMDA binding site, such as APV and CPP, have been employed in radioligand assays to characterise further the NMDA site; these compounds have been superseded by the recent development of a number of derivatives, such as CGS 19755 and D-CPP-ene, which have much higher affinity for the NMDA site.

In addition, a number of compounds, including MK-801 (dizocilpine) and the dissociative anaesthetics, phencyclidine and ketamine, have been classified as non-competitive antagonists, and are shown to act at a functionally distinct site (Kemp et al., 1987). Antagonism of NMDA-receptor-mediated neuronal firing by these compounds is agonist- and voltage-dependent (Kemp et al., 1987), and it is suggested that these compounds bind within an ion channel associated with the NMDA receptor. Divalent ions, particularly Mg^{2+} , impose a voltage-dependent blockade on the ion channel, a phenomenon which is thought to underlie the voltage-dependency of NMDA-mediated firing: addition of physiological concentrations of Mg^{2+} to hippocampal cells in magnesium-free solutions prevent NMDA-evoked neuronal firing, unless the cell membrane is depolarised sufficiently to remove the Mg^{2+} blockade of the ion channel (Ascher & Nowack, 1987). In contrast, NMDA-mediated neuronal firing is enhanced by glycine; therefore the NMDA receptor represents a complex, multifarious component of

1. RESTING
(Channel closed):



2. ACTIVATED
(Channel open)

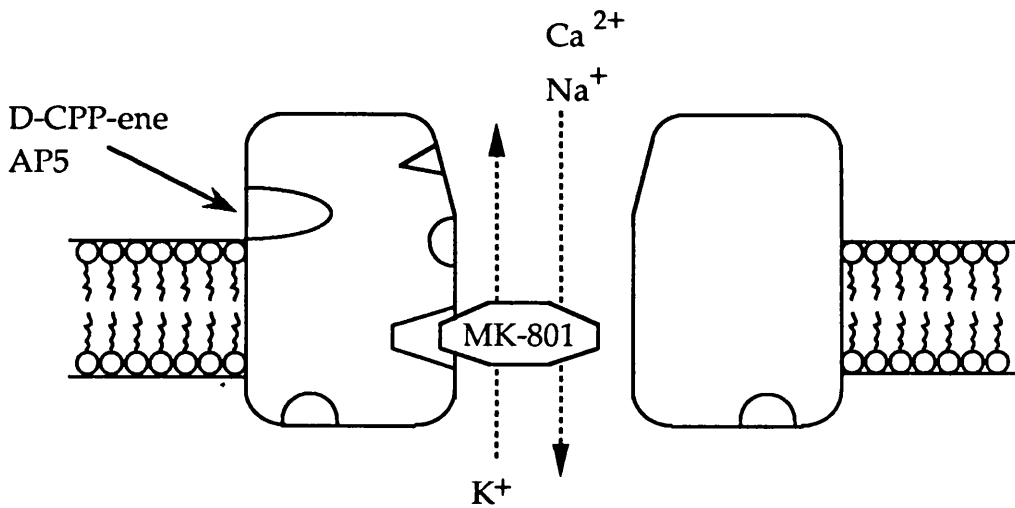


FIGURE 3: SCHEMATIC REPRESENTATION OF THE NMDA RECEPTOR

excitatory amino acidergic transmission in the hippocampus.

Quisqualate Receptors

These are activated selectively by quisqualate and L-glutamate. The high affinity agonist α -amino-3-hydroxy-5-methyl-4-isoxazole propionic acid (AMPA) activates a sub-set of quisqualate receptors, the AMPA receptor or AMPA-sensitive quisqualate receptor, associated with an ion channel. No specific antagonists exist for AMPA-sensitive quisqualate receptor. However, three compounds exist with potent antagonistic properties at non-NMDA receptors: 6,7-dinitro-quinoxaline-2,3-dione (DNQX), 6-cyano-7-nitro-quinoxaline-2,3-dione (CNQX), and 2,3-dihydro-6-nitro-7-sulphamylbenzo(f)quinoxaline (NBQX) have a high specific activity for AMPA-sensitive quisqualate receptors (Honoré et al., 1988; Sheardown et al., 1990).

Recently, a quisqualate receptor associated with activation of a G-protein and phosphoinositide hydrolysis has been described and named the metabotropic or Q_p receptor (Sugiyama et al., 1987). This quisqualate receptor is activated by ibotenate and ACPD, and is inhibited by AP4. This receptor has been deemed distinct from the AMPA-sensitive quisqualate receptor on the grounds that AMPA does not stimulate phosphoinositide hydrolysis (Schoepp & Johnson, 1988), and the antagonists GDEE and CNQX do not inhibit quisqualate-induced phosphoinositide turnover (Nicoletti et al., 1986). The precise function of the Q_p receptor is not fully understood, but it appears to be involved in synaptic plasticity associated with long-term potentiation (Collingridge & Singer, 1990).

Kainate Receptors

Kainate-induced neuronal impulses are unaffected by antagonists of the NMDA site, and show little sensitivity to the quisqualate-sensitive antagonist GDEE, suggesting that kainate receptors represent a distinct

class of glutamate receptor (McLennan & Lodge, 1979). Kainate and domoate are highly potent agonists at kainate receptors, while AMPA and glutamate are moderately affected (Davies et al., 1982).

3.1.2. Ligand-Binding to Glutamate Receptors

The "mixed agonist" property of glutamate requires the use of ligands selective for glutamatergic receptor sub-types. On the basis of electrophysiological data, the prototypic agonists NMDA, quisqualate and kainate would be considered the most appropriate candidates for radioligands. However, [^3H]-NMDA binds with low affinity and low specificity to the NMDA receptor, and has not been employed routinely as a ligand (Foster & Fagg, 1987). The NMDA antagonists [^3H]-APV and [^3H]-CPP have been used with some success as markers for the NMDA receptor (Foster & Fagg, 1987; Olverman et al., 1986); however, the high degree of non-specific binding and rapid dissociation time of these compounds has limited their use. [^3H]-L-glutamate has been shown to exhibit a high degree of specific binding to NMDA receptors under appropriate binding conditions, and with the use of NMDA as the displacer, has been employed successfully to label NMDA receptors (Monaghan & Cotman, 1985).

AMPA rather than quisqualate has been used to label quisqualate receptors, due to concern about the possibility of quisqualate binding to kainate receptors (Honoré et al., 1982). The affinity of [^3H]-AMPA for its binding site is increased by chaotropic ions (e.g. SCN^-), an observation which has facilitated the autoradiographic investigation of AMPA-sensitive quisqualate receptors (Honoré & Nielsen, 1985). More recently, the "metabotropic" (or Qp) quisqualate receptor has been proposed to exist (Sugiyama et al., 1987). To date, however, there is no convincing method for autoradiographic analysis of this receptor sub-type.

[^3H]-Kainate has been reported to bind to both high and low affinity sites (Foster & Fagg, 1984); [^3H]-kainate binding to the high affinity site

has similar distribution to the kainate-sensitive [³H]-L-glutamate binding site. It has been suggested that the low affinity site represents the AMPA-sensitive quisqualate site (Honoré & Nielsen, 1985). Kainate and AMPA-sensitive quisqualate receptors therefore show considerable overlap in their pharmacological profile, an observation which has fuelled the belief by some groups that these sub-types represent the same receptor (Jahr & Stevens, 1987; Cull-Candy & Usowicz, 1987).

3.1.3. Anatomical Distribution of Glutamatergic Receptors

Electrophysiological studies indicate that NMDA receptors are activated in conjunction with quisqualate and/or kainate receptors (Collingridge and Bliss, 1987). Thus, it is of interest to compare the anatomical distribution of these receptor sub-types.

NMDA, AMPA-sensitive quisqualate and kainate receptors are found in highest levels in the hippocampus (Cotman et al., 1987; Monaghan et al., 1983; Monaghan & Cotman, 1985). AMPA and NMDA receptors are generally co-localised in the hippocampus. NMDA-sensitive [³H]-L-glutamate binds in highest concentrations within CA1 strata radiatum and oriens; [³H]-AMPA binding is also concentrated in the strata oriens and radiatum, but has been reported to bind in higher amounts in the CA1 stratum pyramidale (Cotman et al, 1987). In contrast, [³H]-kainate binding shows a remarkably different pattern of distribution in the hippocampus; kainate receptors are confined primarily to the terminal zone of the dentate mossy fibres in the CA3 stratum lucidum, a region which displays low concentrations of AMPA and NMDA sites. In the dentate gyrus, AMPA and NMDA receptors are found in highest quantities in the dentate molecular layer; however, NMDA receptors are concentrated towards the inner portion of the molecular layer. Kainate receptors are also concentrated within the extreme inner portion of the dentate molecular layer. Therefore, each receptor sub-type is organised distinctly

within the hippocampus.

3.2. GLUTAMATE AND LONG-TERM POTENTIATION (LTP)

In the hippocampus, brief, high-frequency stimulation of the major glutamatergic afferents leads to a long-lasting enhancement in the synaptic response: this phenomenon is known as long-term potentiation (LTP). The long-lasting nature of LTP, and the involvement of the hippocampus in memory processes has led to considerable speculation that LTP represents a physiological substrate for learning and memory, and consequently, the physiological processes which contribute to the induction of LTP in the hippocampus, and their manipulation by pharmacological means, have been studied in detail.

3.2.1. Induction of LTP

Under conditions of low-frequency firing in the hippocampus, neuronal impulses are depressed by broad spectrum glutamate antagonists and by non-NMDA antagonists, suggesting that under these conditions, activation of glutamatergic receptors other than the NMDA sub-type is required for neuronal transmission. Indeed, extensive evidence suggests that NMDA receptors are inhibited under conditions of low-frequency firing by a voltage-dependent Mg^{2+} blockade (Nowak et al., 1984). It has been hypothesised that tetanic stimulation of glutamatergic afferents depolarises the cell membrane for sufficiently long to temporarily remove the Mg^{2+} blockade of NMDA channels, allowing activation of NMDA receptors and induction of LTP. Thus a single volley of neuronal impulses does not lead to NMDA receptor activation and LTP induction, since the cell membrane becomes hyperpolarised rapidly following the impulse, and the Mg^{2+} blockade is

replaced.

That NMDA receptor activation is required for the induction of LTP is well established. The competitive NMDA receptor antagonist aminophosphonovalerate (APV, AP5) has been demonstrated to prevent the induction of LTP in most regions of the hippocampus (Bliss & Lomo, 1973; Collingridge et al., 1983; Mody & Heinemann 1987; Morris et al., 1986), and application of NMDA leads to an LTP-like enhancement of neuronal firing, which is sensitive to APV (Collingridge et al., 1983).

Although NMDA receptor activation is required for LTP induction, it appears that other mechanisms are involved in its maintenance. LTP cannot be diminished post-induction by application of NMDA antagonists (Collingridge et al., 1983). However, LTP is diminished by the AMPA-sensitive quisqualate receptor antagonist, CNQX, suggesting that quisqualate receptors mediate to an extent the maintenance of LTP in the hippocampus (Davies et al., 1989).

NMDA receptors are not responsible for the induction of LTP in all hippocampal regions: APV does not prevent LTP induction in the CA3 region following stimulation of the mossy fibre inputs, a result consistent with the observation that the terminal zone of the mossy fibre inputs to CA3 contains very few NMDA receptors. It is likely that kainate receptors, which in contrast are present in this area in extremely high quantities, are involved in the induction of LTP in the mossy fibre pathway; however, this mechanism is not fully understood.

3.2.2. Mechanisms of Maintenance of LTP

Although the mechanisms which contribute to the induction of LTP are generally well understood, the processes which provide maintenance of LTP are less clearly defined. Since the discovery of LTP, the locus of change responsible for its maintenance has been in question, and remains a matter of controversy. Bliss and colleagues have demonstrated

that LTP is associated with an increased release of glutamate (Bliss et al., 1986), an effect which is prevented by APV (Errington et al, 1987), and the authors have suggested therefore that LTP is maintained by presynaptic mechanisms. In contrast, evidence for a postsynaptic mechanism has arisen from observations of slice preparations in electrophysiological conditions which allow activation of both NMDA receptors and quisqualate receptors, such as low Mg^{2+} concentrations (Muller & Lynch, 1988). When hippocampal neurones were subjected to conditions which induce LTP formation, quisqualate receptor-mediated ionic currents were potentiated to a considerably larger degree than NMDA-mediated currents, suggesting that a quisqualate receptor-linked event is involved in the maintenance of LTP. Had LTP resulted in simply an increased transmitter release, then responses to NMDA and quisqualate receptor activation might have been expected to be potentiated in parallel; thus it was suggested that quisqualate-sensitive responses in the postsynaptic neurone are modified selectively in response to LTP. Further evidence for a postsynaptic location for LTP maintenance is derived from iontophoretic experiments which demonstrated that LTP is associated with an increase in sensitivity of CA1 neurones to AMPA and quisqualate (Davies et al., 1989). The increased sensitivity was prevented if APV was present during tetanic stimulation of neurones, and thus is apparently dependent on induction of LTP through stimulation of NMDA receptors. Further, the increase in sensitivity developed slowly after induction of LTP, and reached maximum approximately one hour after induction of LTP. These observations have lead to the suggestion, therefore, that LTP may be maintained initially by presynaptic mechanisms, such as increased transmitter release, and at later times by modulation of postsynaptic events.

In addition, a number of second messenger-related events are thought to be involved in the maintenance of LTP. There is considerable evidence that Ca^{2+} enters the postsynaptic cell through NMDA channels,

and may be involved in postsynaptic events. LTP can be prevented by the injection of calcium chelators (Lynch et al., 1988), while increasing the Ca^{2+} concentration induces an LTP-like increase in synaptic transmission (Malenka et al., 1988). The effect is specific to NMDA receptors: prompting Ca^{2+} entry through voltage-gated ion channels by depolarising the cell does not induce LTP, and thus calcium entry specifically through NMDA channels would seem to be a requirement for LTP. Substantial experimental evidence exists to support a role for protein phosphorylation in LTP. Phosphorylation of protein F1 (or GAP43; B50), a substrate for protein kinase C, has been demonstrated in the dentate gyrus following LTP induction (Linden et al., 1988); this mechanism is prevented by APV. However, the precise function of protein kinase C in LTP is unclear. Incubation of hippocampal slices with phorbol ester, which activates protein kinase C, results in a synaptic facilitation which is similar to LTP (Muller et al., 1988b); however, the effect is dependent on the presence of phorbol ester, and is reversed when the slices are returned to control medium. Further, the protein kinase C inhibitor H-7 did not block the formation of LTP in response to high-frequency stimulation, suggesting that protein kinase C activation is not critical in the induction of LTP. Other authors have reported that incubation of hippocampal slices in the presence of protein kinase C inhibitors results in the formation of LTP which is short-lasting (Malinow et al., 1988), and hypothesised that protein kinase C activation may be required for the long-term maintenance, rather than the induction, of LTP. The protein kinase C inhibitor K-252-b has been demonstrated to block the prolonged maintenance of LTP and the increase in sensitivity to AMPA of CA1 neurones (Collingridge et al., 1989); these observations support the role for a slowly-developing postsynaptic mechanism of LTP maintenance. However, the actions of K-252-b on other kinases, in particular Ca^{2+} /calmodulin-dependent kinase, have not been quantified, and therefore the particular kinase involved in this response cannot be

identified with certainty.

The quisqualate metabotropic receptor has been suggested to play a role in synaptic plasticity, and has therefore received attention as a possible mediator of LTP in the hippocampus. Activation of the metabotropic receptor results in stimulation of phospholipase C and consequent production of the second messengers diacylglycerol and inositol tris-phosphate (IP_3), and therefore may be responsible for the observed phosphorylation of protein F1 following LTP. Nicoletti and colleagues (1988) provided further evidence for the involvement of the phosphoinositide system in the demonstration that stimulation of phosphoinositide hydrolysis by glutamate and ibotenate in the rat hippocampus is potentiated following spatial learning. This would support a function for a glutamate receptor linked to phosphoinositide metabolism in the alterations which accompany LTP in the hippocampus.

If a presynaptic mechanism such as increased transmitter release is responsible for maintaining LTP immediately following its induction, then it is of interest to consider how this mechanism may be initiated. It is possible that increased transmitter release is the result of the actions of glutamate at presynaptic autoreceptors; indeed, some evidence exists to suggest that glutamatergic receptors situated on the presynaptic nerve terminal do mediate increased release of glutamate from the nerve ending (Nadler et al., 1990).

Bliss and colleagues have proposed that arachidonic acid metabolites may act as second messengers in LTP; these are able to diffuse across the cell membrane, and hence may be employed as trans-synaptic messengers, produced postsynaptically when LTP is induced, and acting presynaptically to increase transmitter release. Accordingly, the lipoxygenase inhibitor nordihydroguaiaretic acid (NDGA), which prevents arachidonic acid metabolism, blocked LTP induction in the dentate gyrus, and prevented the maintenance of LTP in CA1 (Williams

& Bliss, 1988). In addition, NDGA has been shown to reduce pre-established LTP (Williams & Bliss, 1989), suggesting a direct role for arachidonic acid and its metabolites in the maintenance of LTP.

Finally, Lynch & Baudry (1984) have proposed that Ca^{2+} flux during LTP activates calpain, a protease which degrades a structural, spectrin-like protein called fodrin. The authors suggested that proteolysis induces a conformational alteration of the postsynaptic membrane, resulting in liberation of previously occluded glutamatergic receptors, allowing them to participate in the postsynaptic element of LTP. The use of such a system may explain the increased sensitivity of CA1 neurones to AMPA following induction of LTP.

The availability of pharmacological agents specific for glutamate receptor sub-types, and the relative neuroanatomical simplicity of hippocampal excitatory amino acidergic pathways, have facilitated experimental analysis of glutamatergic mechanisms in hippocampal transmission. The discovery of LTP and its implications as a substrate for learning and memory have enhanced interest in the processes directly responsible for its induction and modulation. Indeed, despite its relatively recent discovery, much more is known about the hippocampal glutamatergic system than many other transmitter systems demonstrated to modulate hippocampal transmission.

4. ACETYLCHOLINE AND THE HIPPOCAMPUS

4.1. ACETYLCHOLINE AS A NEUROTRANSMITTER

Ironically, although acetylcholine occupies a historically senior position among neurotransmitter candidates, much more information is available on the anatomical organisation of other, non-cholinergic neurones identified more recently. A major factor for this has been the lack of unequivocal methodology for identifying CNS cholinergic neurones: the precursors to acetylcholine (choline and acetate) are entrenched in many other biological pathways, and thus cannot be used to discriminate specific cholinergic sites from non-specific metabolic sites. However, in recent years, histochemical and immunoassay techniques have been used to map successfully the enzymes which catalyse the formation and subsequent breakdown of acetylcholine: these are, respectively, choline acetyltransferase and acetylcholinesterase, and their use has enabled cholinergic neurones to be identified throughout the CNS (for review see Cuello & Sofroniew, 1984).

The recent development of radiolabelled ligands specific for cholinergic receptors has facilitated more specifically the distribution of cholinergic receptors to be studied, and these techniques have led within a relatively recent time-frame to detailed anatomical analysis of cholinergic systems; however, the precise function of acetylcholine within many areas of the CNS remains obscure.

4.1.1. Sub-types of Acetylcholine Receptor

On the basis of their affinities for muscarine and nicotine, cholinergic receptors may be sub-divided into muscarinic and nicotinic receptors. These two classes of receptors have markedly different distributions and functions within the CNS. However, in view of the belief that

transmission in the septohippocampal pathway is mediated by muscarinic receptors (Cole & Nicoll, 1984b), this thesis will focus on muscarinic mechanisms of transmission only.

Muscarinic receptors have been sub-divided following rigorous pharmacological, electrophysiological and more recently molecular biological investigations. Around 1970, observations were made that muscarinic drugs affected selectively the physiological responses of some peripheral organ systems. For example, the muscarinic antagonist pirenzepine produced very few of the side effects attributed to muscarinic blockade by atropine (Ishimori & Yamagata, 1982), and Hammer and colleagues (1980) demonstrated that muscarinic receptors may be sub-divided depending on their affinity for pirenzepine. Further evidence for receptor heterogeneity has arisen from ligand-binding experiments. While the classical antagonists such as atropine, N-methylscopolamine and quinuclidinylbenzilate fail to differentiate between muscarinic receptor subpopulations, [³H]-pirenzepine binding occurs with different affinities in different tissue populations: for example, the affinity for pirenzepine in sympathetic ganglion cells has been measured to be 23-fold higher than in isolated rat ileum (Brown et al., 1980). Goyal and Rattan (1978) proposed the existence of two receptor sub-types: those which mediated inhibition in ganglionic receptors were designated M1 receptors, while those receptors which mediated smooth muscle contraction were named M2; while the precise inhibitory or excitatory role of each receptor sub-type is unclear, this nomenclature is widely accepted. Thus, M1 receptors display a high affinity, and M2 receptors display a low affinity, for the muscarinic antagonist pirenzepine. Using ligand-binding techniques, Mash and colleagues (1985) observed that M2 receptors are selectively reduced following denervation, and concluded that M1 receptors were located postsynaptically, while M2 receptors were found presynaptically, perhaps acting as autoreceptors in the control of acetylcholine release. However, other authors have not replicated these

results (see Results and Commentary, Section 2.5.2., this study).

Until recently, the molecular basis for the diversity of muscarinic receptors has been the subject of debate. Some reports have claimed that M1 and M2 binding sites are interconvertible, since muscarinic receptors lose their pirenzepine selectivity upon solubilization, indicating that membrane-related factors such as coupling to an effector system may determine the binding characteristics of muscarinic receptors (Baumgold et al., 1987). Further, it has been suggested that specific antagonists induce receptor isomerisation, resulting in an enhanced affinity for the binding site for those antagonists (Luthin & Wolfe, 1984). Recently, the existence of two separate populations of M1 receptors with high or low affinity for carbachol has been observed (Flynn et al., 1991; Freedman et al., 1988; Potter & Ferrendelli, 1989), and it has been suggested that these represent states of coupling to the regulatory G proteins. One report has correlated inhibition of phosphoinositide turnover in the striatum by selective muscarinic agonists with receptor occupancy (Monsma et al., 1988); the authors noted that inhibition of carbachol-stimulated phosphoinositide turnover by the selective M1 antagonist pirenzepine conformed to a two-site model, thus from these results it would appear that high and low affinity M1 receptors are coupled to the same second messenger system.

With the advent of cloning techniques, it has become apparent that muscarinic receptors may be sub-divided in terms of their molecular structure. In a recent review, five structurally distinct muscarinic receptors have been identified (Bonner, 1989), but it is unclear whether these are functionally heterogeneous, since there exists at present no pharmacological means for their discrimination.

4.1.2. Muscarinic Receptors and Second Messenger Activity

Other attempts to classify muscarinic receptors according to their effector systems have demonstrated a complex relationship between

receptors and transduction mechanisms. It has been suggested that the M1 receptor is coupled to phosphoinositide hydrolysis (Fisher & Bartus, 1985) through the activation of a phospholipase-specific G-protein, G_p , while the M2 receptor activates a G-protein, G_i , which leads to inhibition of adenylate cyclase activity (Onali et al., 1983). However, other reports have suggested that in the rat brain M1 and M2 receptors may be coupled to phosphoinositide turnover (Ashkenazi et al., 1987; Brown et al., 1985; Fisher & Bartus, 1985; Lazareno et al., 1985). The possibility of "cross-talk" between adenylate cyclase and phosphoinositide second messenger systems (Otte et al., 1989), and also the lack of agonists with high specificity for M1 and M2 receptors, are factors which have as yet prevented the elucidation of the precise function of M1 and M2 receptors in CNS cholinergic transmission. The evidence for muscarinic coupling to phosphoinositide metabolism and adenylate cyclase activity is reviewed below.

Phosphoinositide Metabolism

There is convincing evidence that muscarinic receptors are coupled to the phosphoinositide cycle: muscarinic agonists have been demonstrated to induce phosphoinositide hydrolysis in the brain (see Berridge et al., 1983; Fisher & Agranoff, 1987 for reviews). An apparent relationship exists between the potency of a muscarinic agonist to induce phosphoinositide hydrolysis and the density of muscarinic binding sites in different brain regions. Accordingly, phosphoinositide turnover is pronounced in the hippocampus, cortex and striatum, which contain large numbers of muscarinic receptors, while the brainstem and cerebellum yield less inositol phosphate metabolism. However, studies which employ selective agonists and antagonists reveal a more complex receptor-effector relationship. Inositol phosphate metabolism in the cortex and hippocampus is inhibited readily by low concentrations of pirenzepine, suggesting the involvement of an M1 receptor (Fisher &

Bartus, 1985; Fisher & Snider, 1987; Gil & Wolfe, 1985; Lazareno et al., 1985). In contrast, in the striatum and brainstem pirenzepine displays a moderate potency in blocking phosphoinositide metabolism, indicating that M2 receptors are involved (Fisher & Bartus, 1985; Fisher & Snider, 1987; Lazareno et al., 1985).

If the majority of muscarinic receptors coupled to phosphoinositide metabolism in the hippocampus and cortex are of the M1 sub-type, then it would be expected that M1-selective agonists should stimulate maximally phosphoinositide turnover in these areas. It has been suggested however that the intrinsic agonist activity as well as the occurrence of receptor reserve, i.e., the efficacy of receptor-effector coupling as well as receptor density determine the final cellular response to muscarinic stimulation. Fisher and colleagues (Fisher & Bartus, 1985; Fisher & Snider, 1987) reported a different regional efficacy of coupling between muscarinic receptors and phosphoinositide hydrolysis, and postulated that spare receptors may underlie the differences in efficiency of coupling. Thus in the striatum an efficient coupling is achieved by the presence of spare receptors, while in the hippocampus and cortex, the apparent paucity of receptor reserve would indicate a less efficient coupling. As a consequence, full agonists produce phosphoinositide hydrolysis in the hippocampus and cortex, while partial agonists are almost entirely ineffective (Brown et al., 1984; Fisher et al., 1983). Paradoxically, carbachol, a full agonist with apparent M2-selectivity, is highly active in the hippocampus and cortex, and is used routinely to promote phosphoinositide hydrolysis (Gonzales & Crews, 1984; Janowsky et al., 1984); the most obvious explanation is that carbachol displays some affinity for M1 receptors; however, carbachol has been used in ligand-binding experiments to differentiate between M1 and M2 receptors, although it has been suggested that under certain conditions, carbachol may bind to both M1 and M2 receptors (see Mash & Potter, 1986 for discussion). Instead, M2 receptors in the hippocampus may indeed be

linked to phosphoinositide hydrolysis in the hippocampus and cortex, and may be responsible for the efficacy of carbachol in the induction of phosphoinositide metabolism. The development of full muscarinic agonists with specific M1-selectivity would perhaps clarify the role of M1 receptors in phosphoinositide hydrolysis. At present, therefore, the relative contributions of M1 and M2 muscarinic receptor sub-types to phosphoinositide metabolism in the brain are not fully understood.

Adenylate Cyclase Activity

Muscarinic agonists have been observed to inhibit adenylate cyclase-mediated formation of cyclic AMP (cAMP). Thus, neuronal adenylate cyclase is thought to be coupled to muscarinic receptor occupation via an inhibitory G-protein (Onali et al., 1983), and cAMP levels have been observed to diminish in the presence of muscarinic agonists such as oxotremorine. Gil and Wolfe (1985) demonstrated that the inhibitory effects of muscarinic receptor activation on striatal adenylate cyclase activity were not sensitive to pirenzepine, supporting the involvement of M2 rather than M1 receptors in this response. Further, muscarinic receptor-mediated inhibition of adenylate cyclase is apparently achieved through activation of a pertussis toxin-sensitive G-protein; therefore cAMP inhibition by muscarinic agonists is reduced by treatment with pertussis toxin, while phosphoinositide hydrolysis is unaffected (Kelly et al., 1985a). Therefore, M2 receptors appear to be coupled independently to both adenylate cyclase and phosphoinositide second messenger systems.

4.1.3. Ligand-Binding to Muscarinic Receptors

The distribution of muscarinic receptors in the brain has been demonstrated convincingly with the use of ligand-binding techniques. Two ligands have been employed extensively: the tertiary compound [³H]-quinuclidinyl benzilate ([³H]-QNB; Wamsley et al., 1984), and the

quaternary compound [^3H]-N-methylscopolamine ([^3H]-NMS; Wamsley et al., 1980). These ligands do not show selectivity for M1 or M2 sub-types of muscarinic receptors. Several groups, however, have noted that [^3H]-NMS labels far fewer muscarinic receptor sites than does [^3H]-QNB in intact cells or brain homogenates, and it has been suggested that the lipophilicity of [^3H]-QNB allows it to label internalised muscarinic receptors which, because of their position in the cell membrane, are inaccessible to the positively charged [^3H]-NMS (Lee et al., 1986). However, NMS has been demonstrated to inhibit fully phosphoinositide hydrolysis, suggesting that the sub-set of muscarinic receptors detected by [^3H]-QNB probably do not contribute to the physiological response (Brown & Goldstein, 1986). Therefore [^3H]-QNB has been suggested to measure the total number of receptors within the cell, while [^3H]-NMS measures only those receptors whose occupation contributes to a cellular response.

Confirmation of different muscarinic sub-types, and detailed description of their anatomical distribution, has been hampered by the lack of radiolabelled ligands specific for sub-types of muscarinic receptors. [^3H]-Pirenzepine has been used with some success in assays to locate M1 muscarinic receptors (Tonnaer et al., 1988; Wamsley et al, 1984), while the partial agonist [^3H]-Oxotremorine-M has been used to label M2 receptors specifically (Mash et al., 1985; Spencer et al., 1986). An alternative approach has been used by Mash and colleagues in subsequent studies (Mash & Potter, 1986): muscarinic receptors were labelled with [^3H]-QNB in the presence of non-labelled pirenzepine or carbachol, in order to displace binding to M1 or M2 receptors respectively.

Recently, Regenold and colleagues (1989) used [^3H]-AF-DX 116, a novel muscarinic antagonist highly selective for M2 receptors in quantitative autoradiographic studies of the rat brain. The authors showed that differences occurred between the regional distributions of [^3H]-AF-DX 116 binding and those of [^3H]-oxotremorine-methiodide ([^3H]-OXO-M), a full

M2-selective muscarinic agonist (Spencer et al., 1986), and suggested that these discrepancies may be due to the existence of sub-types of M2 receptors. However, until more specific pharmacological agents become available, the further sub-division of muscarinic receptor sub-types by ligand-binding techniques is not possible, and their functional relevance will remain uncertain.

4.1.4. Anatomical Distribution of Muscarinic Receptors

Ligand-binding studies which employ agonists or antagonists specific for M1 or M2 sub-types of muscarinic receptors have demonstrated that these two sub-types differ markedly in their anatomical distribution (Mash & Potter, 1986; Regenold et al., 1989; Tonnaer et al., 1988).

Mash & Potter used [³H]-QNB in the presence of the M1-selective antagonist pirenzepine, or the M2-selective agonist carbachol, in order to measure M2 or M1 receptor densities respectively. The authors reported that M2 receptors are distributed in a similar manner to acetylcholinesterase, and suggested therefore that M2 binding sites represent presynaptic autoreceptors, while M1 receptors are found postsynaptically. Consequently, in the hippocampus, M2 receptors are prevalent as a sharp band in the stratum oriens throughout CA1-CA4, in agreement with the distribution of acetylcholinesterase (Mosko et al., 1973). In the dentate gyrus, M2 receptors were concentrated in the infragranular layer. [³H]-QNB binding to M1 receptors in the hippocampus was marked in the CA1 stratum radiatum and in the dentate molecular and granule cell layers. M1 binding was observed to be very low in the subiculum.

A more quantitative approach which involved histological definition of ligand-binding in distinct hippocampal regions was used by Tonnaer and colleagues (Tonnaer et al., 1988). The authors employed [³H]-QNB to measure total muscarinic receptor concentrations, and [³H]-pirenzepine

to measure M1 receptors; M2 receptor concentrations were inferred by the [^3H]-QNB/[^3H]-pirenzepine ratio. In contrast to the previous report, Tonnaer and colleagues observed that M1 receptors were dense in the subiculum and in the stratum oriens/pyramidale of CA1. Less binding was evident in the stratum radiatum. While these discrepancies may be due partly to the more histologically specific approach of the authors, the more likely reason for the marked difference in reported M1 receptor levels in the subiculum may be differences in the ligand-binding protocols. It is possible that the low subicular density of M1 receptors noted by Mash and Potter (1986) represents an action of the M2 displacer carbachol on M1 receptors. It has been suggested that some binding conditions uncouple receptor sub-types such that "high and low" affinity sites for carbachol binding correspond to M2 and M1 receptors respectively, (see Mash & Potter, 1986 for discussion), so that carbachol under certain conditions may not be selective for M2 receptors. Further, Regenold et al. (1989) have shown that [^3H]-AF-DX 116, the highly selective M2 antagonist, binds in large quantities in the subiculum: it is possible that these discrepancies are due to the existence of a sub-type of muscarinic receptors, for which [^3H]-AF-DX 116 has high affinity, in the subiculum.

4.2. ACETYLCHOLINE AND THE SEPTOHIPPOCAMPAL PATHWAY

The involvement of cholinergic neurones in septohippocampal transmission is well-documented (see Nicoll, 1985 for review), and stems from the observation that whereas much of the cerebral cortex is innervated diffusely by cholinergic afferents, the hippocampus receives a dense cholinergic projection from the medial septum. The hippocampus is well-defined in terms of its other major, glutamate afferent (Swanson et al., 1987), and therefore provides a rare opportunity to study in detail

the modulatory actions of acetylcholine on glutamatergic transmission.

Pharmacological studies have demonstrated that application of acetylcholine or muscarinic agonists to the hippocampus results in increased firing of hippocampal pyramidal cells (Cole & Nicoll, 1984a). Further, electrical stimulation of the medial septum results in facilitation of glutamatergic-mediated pyramidal cell firing within the hippocampal CA1-2 regions; the facilitation is comparable to that produced by iontophoretic application of acetylcholine (Krnjevic & Ropert, 1982), providing evidence for the involvement of the medial septum in the cholinergic modulation of hippocampal transmission. Conversely, removal of the medial septum in rats resulted in impaired function in cognitive tasks thought to involve hippocampal activity (Hagan & Morris, 1988).

Electrophysiological analysis of cholinergic septohippocampal transmission has revealed that acetylcholine acts primarily to abolish two K^+ currents, an afterhyperpolarisation current (I_{AHP}) and the M-current. The M-current is a voltage- and time-dependent K^+ current which has some activity when the cell is at rest, and which acts to repolarise the cell: Cole and Nicoll, (1984a) postulated that the value of the membrane potential in hippocampal neurones may reflect a balance between the actions of the M-current and the continuous leakage of K^+ ions across the membrane according to their concentration gradient. Thus the M-current under resting circumstances helps to maintain the polarity of the neurone. When the cell membrane is depolarised by firing of its glutamatergic afferents, the M-current becomes fully activated, thus acting to repolarise the cell membrane.

The afterhyperpolarising current, the I_{AHP} is a Ca^{2+} -activated K^+ current which becomes active during cell firing, and results in hyperpolarisation of the membrane following the action potential discharge, thus inhibiting further cell membrane depolarisation. Both currents are inhibited by muscarinic agonists and acetylcholine, resulting

in an increased cell excitability: abolition of the M-current facilitates depolarisation of the cell membrane, while removal of the afterhyperpolarisation current reduces the delay between action potential discharge.

Despite the apparently well-understood mechanisms by which acetylcholine exerts its actions on hippocampal neurones, the degree of involvement of individual muscarinic receptor sub-types in the cellular response to cholinergic stimulation is less clear. In a recent report, Dutar and Nicoll (1988) examined the electrophysiological responses to pharmacological manipulations of muscarinic receptors in the hippocampus. The authors were able to demonstrate that the M2 receptor antagonist gallamine prevented the muscarinic blockade of the M-current, suggesting a role for M2 receptors; in contrast, the I_{AHP} was unaffected by gallamine, and was therefore presumed to be linked to an M1 receptor-mediated mechanism. However, the M1-selective antagonist pirenzepine did not display a discriminatory effect, and blocked both the M-current and the I_{AHP} in a dose-dependent fashion, suggesting that M1 receptors may be involved in both components.

The M-current has been demonstrated to be insensitive to the actions of phorbol esters (Baraban et al., 1985) and muscarinic drugs which act as partial agonists such as arecoline and oxotremorine (Dutar & Nicoll, 1988). However, full agonists such as carbachol and oxotremorine-M are able to inhibit the M-current; further, increasing intracellular concentrations of inositol tris-phosphate markedly reduced the size of the M-current, suggesting that inositol tris-phosphate, but not protein kinase C activation, is involved in the muscarinic receptor-mediated abolition of the M-current. However, inositol tris-phosphate may exert some of its actions non-specifically, through release of calcium from intracellular stores, resulting in widespread cellular modifications such as phosphorylation of ion channels. In contrast, phorbol esters have potent ability to abolish the I_{AHP} (Baraban et al., 1985), promoting a role for

protein kinase C. This observation at least is in accordance with the view that M1 receptors mediate blockade of the I_{AHP} in the hippocampus, through stimulation of the phosphoinositide system.

Finally, it has been demonstrated that both the I_{AHP} and the M-current are insensitive to treatment with pertussis toxin (Dutar & Nicoll, 1988) suggesting that pertussis toxin-sensitive G-proteins, such as G_i or G_o , and hence muscarinic-mediated inhibition of adenylate cyclase, are not involved in these mechanisms.

5. NEUROPATHOLOGY OF THE HIPPOCAMPUS

The hippocampus is vulnerable to a number of neurodegenerative diseases, which appear to result in particular patterns of pathology within specific neurotransmitter systems. Alzheimer's Disease is associated with profound neurodegeneration in the hippocampus, neocortex, and destruction of large numbers of neurones in the cholinergic basal forebrain nuclei; the cognitive impairments of the disease have been attributed to the loss of cholinergic innervation of the cortex and hippocampus (Perry et al., 1978); however, recent evidence implies a role for glutamate in the observed neurodegenerative alterations (Greenamyre et al., 1987).

Cerebral ischaemia has also been shown to be associated with specific neurodegeneration in the hippocampus and neocortex (Kirino, 1982; Volpe & Hirst, 1983); there is a correlation between the areas vulnerable to ischaemic damage and the densities of glutamate receptors within the brain, and the extremely high levels of glutamate found in the brain during ischaemia have been implicated in the ischaemic damage.

The evidence for cholinergic and glutamatergic mechanisms in the pathophysiology of Alzheimer's Disease, and the role of glutamate in the neurodegeneration which accompanies cerebral ischaemia is reviewed below.

5.1. ALZHEIMER'S DISEASE

By far the most common dementia in the developed world is Alzheimer's Disease, a progressive disorder characterised by severe memory loss and general cognitive decline (Huppert & Tym, 1986). In Britain, it has been estimated that 5% of the population over the age of 65, and almost 25% of those over 80 have Alzheimer's Disease (Deary &

Whalley, 1988); however, despite concentrated research efforts, the aetiology of Alzheimer's Disease remains obscure.

Alzheimer's Disease may be separated from other types of dementia by neuropathological diagnosis post-mortem. There is atrophy of the brain, particularly of the temporal and frontal lobes, manifested by shrinkage of the gyri and widening of the sulci. Microscopical examination reveals a diffuse loss of neurones in the cortex and hippocampus, and a profound loss of cells in the cholinergic basal forebrain nuclei. The most striking feature, however, and that upon which positive diagnosis of Alzheimer's Disease is based (Khachaturian, 1985) is the presence of large numbers of senile plaques and neurofibrillary tangles.

The general histological features of plaques are usually described in terms of a central spherical amyloid "core" surrounded by degenerating neurites (presynaptic nerve terminals) and glial cells (Brun 1983). Wisniewski and Terry (1973) have, however, sub-divided plaques into three categories depending on their stage of development: first, a primitive plaque, consisting of a small number of neurites and a small amount of amyloid, found typically in young Alzheimer patients; second, a mature plaque consisting of a dense core of amyloid and numerous neurites, found in greater quantities in older patients; and third, a "burnt-out" plaque which consists almost entirely of amyloid. Plaque amyloid is composed predominantly of β -amyloid, a low molecular weight protein which is also found in cerebrovascular amyloid (Selkoe, 1987). Analysis of the plaque core has suggested the presence of a form of aluminosilicate, lending support to the hypothesis that mineral deposition may be a stimulus for plaque formation (Bertholf, 1987). Plaque neurites appear to derive from a variety of neurone types, including cholinergic, noradrenergic, somatostatinergic (Walker et al., 1988), and possibly glutamatergic (Perry, 1986) neurones.

Plaques are found in high quantities in the hippocampus, frontal and temporal cortex, and amygdala, but are sparse in other cortical areas

(Mann 1988), suggesting that some selective process for plaque formation exists.

Neurofibrillary tangles are also present in large numbers in the hippocampus and cortex, but are also found in subcortical structures such as the cholinergic forebrain nuclei, the raphé nuclei and the locus coeruleus (Mann et al., 1985; Perry, 1986; Wilcock & Esiri, 1982). Tangles appear to be an accumulation of filamentous material within the neuronal perikarya (Brun, 1983), and electrosopy has revealed their structure to be a pair of tightly adhered, helically wound filaments, referred to as paired helical filaments (Kidd, 1963). It is unclear whether these represent a modification of normal cytoskeletal elements, or the synthesis of an abnormal protein. However, considerable cross-reactivity has been demonstrated immunologically between tangles and the microtubule-associated proteins, MAP2 and tau.

The formation of tangles within the neuronal perikarya has been postulated to underlie the cell loss in Alzheimer's Disease (Saper et al., 1985), and it is possible that accumulation of tangles results in progressive disruption of essential intracellular functions such as protein synthesis, and oxidative metabolism (Sumpter et al., 1986), leading ultimately to neuronal death.

Although diagnosis of Alzheimer's Disease is based on the presence of neuronal plaques and tangles, their functional significance remains obscure. Numbers of plaques have been correlated positively by some researchers with the degree of cognitive decline in Alzheimer patients (Blessed et al., 1968; Wilcock & Esiri, 1982), while other researchers found no relationship between dementia and tangle or plaque counts (Neary et al., 1986)

5.1.1. Cholinergic Dysfunction in Alzheimer's Disease and the Cholinergic Hypothesis of Learning and Memory

Of the many neurotransmitter systems which have been observed to suffer a degree of disruption in the course of Alzheimer's Disease, the most consistent neurochemical alterations are related to the cholinergic system. With few exceptions, reductions in choline acetyltransferase (ChAT) activity have been demonstrated in the cerebral cortex and hippocampus of Alzheimer patients (Davies & Terry, 1981; Mountjoy et al., 1984; Perry et al., 1977; White et al., 1977). Reduction in ChAT activity is most likely to stem from the vast degeneration of cholinergic neurones in the basal forebrain nuclei (McGeer et al., 1984; Saper et al., 1985; Whitehouse et al., 1982), which provide the cortex and hippocampus with their major cholinergic innervation. The degree of reduction in ChAT activity has been correlated with plaque counts and the degree of cognitive impairment in Alzheimer patients (Perry et al., 1978), and this has led to the formation of the "cholinergic hypothesis" of memory, which postulates that the cognitive impairments of Alzheimer's Disease are linked directly to the degree of disturbance in cholinergic transmission. The cholinergic hypothesis has been reviewed critically by Bartus and colleagues (1982), who put forward three criteria which should be satisfied if such a hypothesis were to receive credence. The first criterion, which requires that Alzheimer's Disease is associated with specific alterations in cholinergic markers, is satisfied by the consistent observation of depleted ChAT in Alzheimer brains. In addition, deficits in high affinity choline uptake (Rylett et al., 1983) have been observed in Alzheimer hippocampus and cortex, while reduced concentrations of acetylcholine have been measured in the cortex of Alzheimer patients (Richter et al., 1980).

The second criterion requires that if cognitive deficits are due to dysfunction of cholinergic neurones, then these deficits should be able to be reproduced in animals, through pharmacological blockade of

cholinergic mechanisms or through destruction of cortical or hippocampal cholinergic afferent pathways. This criterion is satisfied to a large extent: administration of the muscarinic antagonist scopolamine to rodents and primates results in generally impaired performance of cognitive tasks such as discriminatory and acquisition learning (see Collerton et al., 1986 for review). Secondly, lesions of cholinergic basal forebrain nuclei such as the medial septum or nucleus basalis, or the transection of forebrain cholinergic projections to the cortex and hippocampus, have yielded some success in producing cognitive impairments in a number of behavioural tasks (Collerton, 1986).

The third criterion to be satisfied in the cholinergic hypothesis is that enhancement of cholinergic function should reverse the cognitive deficit in Alzheimer patients and the behavioural deficits produced by cholinergic denervation in animals. However, pharmacological attempts to improve cognitive ability in Alzheimer patients have produced at best equivocal results (Bartus et al., 1982), while little or no improvement has been demonstrated in lesion-induced behavioural deficits following administration of cholinomimetic agents (Collerton, 1986). The failure to satisfy this final criterion, therefore, suggests that the dementia associated with Alzheimer's Disease cannot be explained solely by cholinergic mechanisms.

While deficits in presynaptic cholinergic markers are detected consistently in Alzheimer brain, ligand binding studies of muscarinic receptor density have demonstrated less consensus. Muscarinic receptors labelled with non-specific muscarinic antagonists have been found to be unaltered (Davies & Verth, 1978; Greenamyre et al., 1987) or moderately reduced (Rinne et al., 1984) in Alzheimer brains. Binding to M1 receptors has been detected to be normal, while M2 receptors are found to be decreased (Mash et al., 1985; Perry et al., 1986) in Alzheimer's Disease post-mortem. In a similar manner, nicotinic receptors have been demonstrated to be both decreased (Whitehouse et al., 1986) or unaltered

(Shimohama et al., 1986b). Consistent loss of presynaptic CAT activity, therefore, is not associated with any consistent cholinergic receptor alteration.

An increasing number of neurotransmitter systems have been demonstrated to be disrupted in the neuropathological degeneration of Alzheimer's Disease. For example, biochemical markers for dopaminergic, noradrenergic, serotonergic, peptidergic, GABAergic and glutamatergic transmission have been shown to be altered in the hippocampus and cortex of Alzheimer brains (Hardy et al., 1987; Lowe et al., 1988; Quirion et al., 1986; Rossor & Iversen, 1986). Further, cortical deficits in adrenergic receptors (Shimohama et al., 1986a, 1987), 5HT₁ and 5HT₂ receptors (Cross et al., 1984, 1988), somatostatin and corticotrophin-releasing factor receptors (Beal et al., 1985; DeSouza et al., 1986), GABA_A and GABA_B receptors, benzodiazepine receptors (Shimohama et al., 1988) and glutamate receptors (Greenamyre & Young, 1989) have been reported in Alzheimer brains. Statistical correlations have been made between many neurotransmitter receptor abnormalities and neuropathological changes of Alzheimer's Disease (Mountjoy et al., 1984; Mountjoy 1986). The contributions of these alterations to the clinical manifestations and neuropathological progression of the disease, however, are unknown.

5.1.2. Glutamate and Alzheimer's Disease

The role of glutamate in long-term potentiation and the ability of glutamate antagonists to disrupt memory in behaving animals (Morris et al., 1986; Morris, 1989) has no doubt enhanced the interest in glutamate as a contributory factor in Alzheimer's Disease. While the significance of the widespread pattern of neuronal degeneration is unclear, studies of the neuroanatomical distribution of Alzheimer pathology indicate that these alterations affect specific hippocampal and cortical regions which are interconnected by well-defined groups of neuronal projections, and

that the disease may progress along connecting fibres to sub-cortical regions (Pearson et al., 1985). Thus, the glutamatergic pyramidal cells of the hippocampus and interconnected olfactory and "association" areas of cortex exhibit severe neuropathology, while somatosensory areas are affected minimally. The role for glutamate as the major excitatory neurotransmitter in the hippocampus and cortex, and the neurotoxic properties of glutamate, have been the basis for the hypothesis that the glutamatergic system is involved in the pathophysiology of Alzheimer's Disease; further, these observations fuel the postulation that the primary lesion in Alzheimer's Disease occurs in the cortex, with the subsequent occurrence of sub-cortical lesions. It has been demonstrated that a close correspondence exists between the ability of glutamate and its analogues to depolarise neurones and their neurotoxic potency (Olney et al., 1971): thus, Olney suggested the term "excitotoxin" to emphasise that the neurotoxic effect of these compounds was mediated through a prolonged depolarising action at post-synaptic receptor sites. Therefore if glutamate were to mediate in neuronal death in Alzheimer's Disease, it would be expected that the neuropathological alterations would occur in a pattern similar to the disruption of the terminal fields of glutamatergic pathways. Consistent with this hypothesis, neurofibrillary tangles have been found to be most dense in the terminal zones for presumably glutamatergic "association" fibres (Pearson et al., 1985).

The suggestion that the primary lesion of Alzheimer's Disease is glutamatergic, and that the neuropathological degeneration is propagated along associational pathways is strengthened further by the observation that application of glutamate to human neurones in culture induces the formation of paired helical filaments similar to those which constitute neurofibrillary tangles in Alzheimer's Disease (De Boni & Crapper-McLachlan, 1985). Retrograde cellular degeneration has been found in the nucleus basalis of Meynert in the human brain following hemidecortication, and in the monkey following large lesions of the

neocortex (Pearson et al., 1983); in addition, Sofroniew and Pearson (1985) have demonstrated that application of NMDA or kainate to the cortical surface in rats results in retrograde degeneration of cholinergic neurones in the nucleus basalis; the degeneration was similar to that produced by mechanical destruction of the cholinergic terminals, and indicates that excitotoxic damage in the cortex, presumably mediated through post-synaptic excitation, can produce pathological changes in subcortical regions similar to those which occur in Alzheimer's Disease.

However, Sanfeliu and colleagues (1990) have demonstrated that exposure of NMDA to septal cells in culture did not result in typically prolonged cell activity, and suggested that glutamate-mediated toxicity is not likely to be the cause of cell death in septal cholinergic neurones at least in Alzheimer's Disease.

An inevitable consequence of excitotoxic cell death is the loss of glutamate receptors and terminals as cells are lost. However, evidence for glutamatergic receptor alterations indicated by ligand binding studies of Alzheimer's Disease post-mortem is less clear cut. NMDA receptors have been reported by some groups to be reduced in the cortex and hippocampus in Alzheimer brains (Greenamyre, 1986; Greenamyre et al., 1987; Represa et al., 1988); however, others have reported that NMDA receptors are unaltered in the cortex or hippocampus (Cowburn et al., 1988a,b; Geddes et al., 1986). Similar controversy reigns over studies of [³H]-TCP binding to the NMDA ion channel: a loss of [³H]-TCP binding in the hippocampus has been reported (Maragos et al., 1987; Monaghan et al., 1987), although [³H]-TCP binding in homogenate preparations has been demonstrated to be unaltered in the hippocampus, but decreased in the frontal cortex, of Alzheimer brains (Simpson et al., 1988).

The status of other glutamatergic receptor sub-types in Alzheimer's Disease has been equally difficult to establish. Greenamyre and colleagues (1987) have reported a reduction in [³H]-glutamate binding to quisqualate receptors in the CA1 and dentate gyrus, while Dewar et al.

(1991) reported deficits in [³H]-AMPA binding to quisqualate receptors in the CA1 and subiculum of Alzheimer brains. Finally, an expansion of the kainate receptor field has been reported to occur in the dentate gyrus (Geddes et al., 1985); however, this result has not been reproduced by other researchers, and Represa et al. (1988) reported a loss of [³H]-kainate receptors from Alzheimer hippocampus, with no alteration in the kainate receptor distribution field.

5.1.3. Second Messenger Systems and Alzheimer's Disease

It has become evident that neuronal transmission is dependent not only on the integrity of the neurotransmitter receptor, but also on the integrity of the second messenger signalling systems within the cell. Consequently, a number of diseases have been identified in which second messenger dysfunction may contribute to their aetiology. However, despite the massive disruption of neuronal transmitter systems known to occur, little attempt has been made to characterise the functional state of second messengers in Alzheimer's Disease.

There is evidence to suggest that dysfunction of second messenger systems may underlie the clinical manifestations of affective disorders. Decreased activity in the adenylate cyclase system, and the relative dominance of the phosphoinositide system has been proposed to occur during depression, while during mania the converse has been suggested (Wachtel, 1988, 1989). Thus the therapeutic efficacy of lithium in the treatment of depression may be explained by its ability to inhibit the hydrolysis of inositol phosphate, therefore preventing the re-synthesis of phosphatidyl inositol 4,5 bisphosphate (see Methods section 3) and further activity of the phosphoinositide system. Alternatively, lithium at therapeutic concentrations has been shown to inhibit adenylate cyclase (Newman et al., 1983); therefore in the treatment of mania, lithium may act to inhibit the overactive adenylate cyclase system.

Second messenger abnormalities have been proposed to occur in epilepsy, a condition characterised by spontaneous, recurrent epileptic seizures in the absence of a known precipitatory cause or illness. Electroconvulsive shock therapy and administration of a number of convulsants have been observed to increase markedly the concentrations of cAMP in the brain; in contrast, cAMP levels may be reduced by anticonvulsants (Wasterlain & Dwyer, 1983). During seizures, activity of the phosphoinositide system is enhanced, possibly through activation of protein kinase C (Wasterlain, 1989), and an increase in protein kinase C activity has been proposed to be associated with neuronal death and apparent around epileptic foci in human brains.

Recently, post-mortem studies of Alzheimer's Disease have demonstrated that despite widespread neuronal cell loss, [³H]-phorbol ester binding to protein kinase C is preserved in the hippocampus and cortex of Alzheimer patients (Horsburgh et al., 1991a). In contrast, using immunohistological staining, alterations in distinct isozymes of protein kinase C have been found in Alzheimer brain: in particular, intensely increased staining occurred in the hippocampal CA3-4 region compared with controls (Masliah et al., 1990).

In an effort to investigate the plasticity of second messenger systems, with reference to alterations in second messenger function in Alzheimer's Disease, some attempt has been made to measure the response of second messenger systems to experimental denervation in animals. Increases in cholinergic-mediated phosphoinositide hydrolysis have been demonstrated following disruption of the septohippocampal fibres (Connor & Harrell., 1989; Court et al., 1990; Smith et al., 1989). While some researchers report alterations in cholinergic-mediated phosphoinositide in the cortex following lesions of the nucleus basalis, (Reed & de Belleruche, 1988), these results have not been replicated by others (Raulli et al., 1989; Scarth et al., 1989). More subtle alterations in second messenger distribution have been measured using ligand binding

techniques. In contrast to the lack of alterations observed in Alzheimer hippocampus, following medial septal lesions in rats, [³H]-forskolin binding to adenylate cyclase was demonstrated to increase in the dentate gyrus-CA3 region of the hippocampus, whereas [³H]-phorbol ester binding to protein kinase C increased in the entorhinal cortex (Horsburgh et al., 1991b). These results would suggest that following denervation at least, second messenger systems are capable of plastic alterations. The success of pharmacological approaches to the treatment of cognitive deficits in Alzheimer's Disease is dependent on the integrity of intracellular transduction systems, and thus expanded research into the functional state of second messenger systems in Alzheimer's Disease and animal models of denervation is merited.

5.1.4. Animal Models of Alzheimer's Disease: Cholinergic Denervation

The diversity of neuropathological and neurochemical abnormalities in Alzheimer's Disease has posed a complex problem in the aim to provide animal models which mimic adequately the disease state. No animal model has been developed which replicates all the elements of Alzheimer's Disease; however, a number of experimental models have been useful in challenging hypotheses based on individual components of the disease.

The most consistent neurochemical alterations in Alzheimer's Disease are the depletions in presynaptic cholinergic markers in the cortex and hippocampus, and loss of cholinergic cell bodies from the basal forebrain. This has led to the development of a number of animal models in which the cortical or hippocampal cholinergic afferents are denervated, either through transection of afferent fibre pathways, or through specific lesions of cholinergic cells within the nucleus basalis or medial septal area. These lesions result in depletion of choline acetyltransferase activity in the cortex or hippocampus, and the impaired

performance in specific tasks; the degree of cognitive impairment has been correlated positively with the depletion of choline acetyltransferase in the denervated area (Everitt et al., 1987).

A number of approaches have been used to denervate the cortex and hippocampus. Knife-cut lesions of cholinergic afferent fibres, and electrolytic and excitotoxin-induced lesions of the nucleus basalis or septal area have been commonly used (Fisher & Hanin, 1986; Smith, 1988). Such models have been used with variable success in order to demonstrate the plastic response of the cholinergic system to denervation, in the hope that alterations in receptor density may help to clarify the somewhat obscure status of cholinergic receptors in Alzheimer's Disease. However, studies of cholinergic receptor binding following experimental denervation have to date demonstrated equally diverse alterations in hippocampal muscarinic receptor density. Cholinergic denervation has been shown by some groups to result in an increase in muscarinic receptor density (Dawson & Wamsley, 1990; Joyce et al., 1989; McKinney & Coyle, 1982; Westlind et al., 1981); however, other studies have not provided evidence for muscarinic receptor regulation (Court et al., 1990; Kamiya et al., 1981; Overstreet et al., 1980; Smith et al., 1989; Yamamura & Snyder, 1974), and some have demonstrated decreased muscarinic receptor density (Mash et al., 1985; Watson et al., 1985) following cholinergic denervation.

The demonstrated role for muscarinic mechanisms in modulating glutamatergic firing in the hippocampus lead Monaghan and colleagues (1982) to examine the effects of entorhinal cortex ablation on muscarinic receptor density in the hippocampus: the authors reported decreased muscarinic receptor binding in the hippocampus, and suggested that hippocampal muscarinic receptors were regulated by the entorhinal cortex, rather than the septum. Further, it has been demonstrated that removal of the septum in neonatal rats does not affect the development of muscarinic receptor populations in the hippocampus (Ben-Barak &

Dudai, 1980), despite the lack of development of the presynaptic cholinergic marker, acetylcholinesterase. The entorhinal cortex is known to suffer severe neuronal degeneration in Alzheimer's Disease, and therefore if the maintenance of hippocampal cholinergic receptors depends on the integrity of the entorhinal cortex, then the role of the septohippocampal pathway in the neurodegenerative alterations in Alzheimer's Disease must be re-examined. Despite the importance of these findings, there has been little emphasis on the possible effects of cholinergic denervation on glutamatergic systems in the hippocampus. The use of animal models of cholinergic denervation may clarify whether glutamatergic mechanisms are implicated in the cholinergic deficits of Alzheimer's Disease; furthermore, their use provides a rare opportunity to manipulate neurotransmitter systems in the attempt to elucidate the relationship between cholinergic and glutamatergic systems in the normal functions of the brain.

5.2. CEREBRAL ISCHAEMIA

In order to fuel cerebral metabolism, the brain receives a continuous supply of oxygen and glucose from its arterial blood supply. If the blood flow to the brain is interrupted for more than a few minutes, then cerebral tissue is irreversibly damaged. Ischaemic attacks commonly occur either localised to individual vascular territories in the form of stroke, or globally as a cardiac arrest, and are a major cause of death in the western hemisphere (Grotta et al., 1987).

Despite the prevalence, and consequently socioeconomic impact, of ischaemia-induced neuronal damage, and in the wake of intense research, little is known about the cellular pathogenesis of ischaemic cell death, and there exists to date no effective therapy for ischaemic damage.

It has been observed that while the brain in comparison with other organs is particularly susceptible to ischaemic damage, a distinct pattern of vulnerability exists within the brain itself: the hippocampus, particularly the neurones in CA1, and areas of the neocortex are inordinately vulnerable to ischaemic damage (Cummings et al., 1984; Kirino, 1982; Pulsinelli et al., 1982a; Volpe & Hirst, 1983) and are characteristically destroyed after even brief periods of ischaemia which spare most other brain regions. The observation that these areas contain large quantities of glutamate receptors (Monaghan et al., 1983) has led to the "excitotoxic hypothesis" of ischaemic damage: that during ischaemic attack, glutamate is released and accumulates within the brain in toxic amounts.

5.2.1. Glutamate Neurotoxicity and Ischaemia

A link between glutamate and cerebral ischaemia was anticipated by Van Harreveld (1959), who demonstrated that spreading depression in the rabbit could be produced by application of glutamate to the cortical

surface, and suggested that the phenomenon of spreading depression was in some way connected to neuronal hypoxia. Since then, a wealth of evidence has accumulated to support this speculation. Early research in the field of glutamate transmission in the CNS revealed that exposure of the retina to glutamate resulted in the destruction of the inner neuronal cell layer of the retina (Lucas & Newhouse, 1957). Further, Olney demonstrated that rats fed with large quantities of monosodium glutamate sustained neuronal lesions in brain regions which lacked a blood-brain barrier (Olney, 1969).

Two other factors have been pivotal in the establishment of the excitotoxic hypothesis of cerebral ischaemia. Firstly, the use of *in vivo* dialysis techniques has demonstrated raised extracellular concentrations of glutamate following both focal (Bullock et al., 1991a; Graham et al., 1990) and global (Benveniste et al., 1984) ischaemia. Secondly, there is extensive evidence that glutamate antagonists, particularly those which act at the NMDA receptor or its associated ion channel, afford neuroprotection in the ischaemic brain (Bullock et al., 1990; Frandsen et al., 1989; Gill et al., 1987; Ozyurt et al., 1988; Park et al., 1988a,b; Simon et al., 1984), and NMDA-treated neuronal tissue (Foster et al., 1987; Goldberg et al., 1988; Olney et al., 1987). The enormous therapeutic potential of glutamate antagonists in the clinical prevention of ischaemic damage has led to intensive research into the mechanisms underlying neurotoxicity in cerebral ischaemia.

5.2.2. Mechanisms of Excitotoxicity

Excitotoxicity exhibits a characteristic, acute cytopathology, which is post-synaptic, sparing axons and presynaptic terminals. Dendrites are found to have focal swelling, while in the initial stages of excitotoxic damage, the mitochondria of the perikarya become swollen, and the endoplasmic reticulum becomes dilated in appearance. Secondary

alterations include condensation of nuclear chromatin, and cytoplasmic condensation with multiple vacuolations; these alterations are identical to those observed in the hippocampus and cortex following transient forebrain ischaemia (Arsenio-Nunez et al., 1973; Brown & Brierley, 1972; Simon et al., 1984).

The primary effects of activating glutamate receptors are to open ion channels (MacDermott & Dale, 1987), resulting in a cascade of cellular events, including elevated intracellular calcium and second messenger activation. Stimulation of kainate and AMPA receptors results in entry of sodium and potassium ions through ion channels in the cell membrane, while stimulation of NMDA receptors results in the additional entry of calcium. Depolarisation of the cell membrane will result in activation of voltage-dependent calcium channels on the cell membrane, resulting in further elevation in the intracellular calcium concentration; an increase in calcium will activate chloride and potassium conductances, with the resultant flow of water from the cell according to an osmotic gradient. As a response to the ionic redistribution across the cell membrane, activation of ATPases in the cell membrane occurs in order to restore the ionic gradients, with the result of increased demand for ATP and therefore enhanced mitochondrial oxidative metabolism.

While these cellular events are normally short-lived – neuronal and glial re-uptake mechanisms result in the rapid removal of glutamate from the synapse – under excitotoxic conditions in which glutamate receptors are stimulated for prolonged periods, the ionic changes within the cell are greatly augmented, resulting in widespread disruption of cellular events. Prolonged stimulation of glutamate receptors while the blood supply to the brain remains compromised, leads to rapid depletion of existing cellular ATP supplies, thus preventing restoration of the cellular ionic balance. Raised calcium is unable to be removed either by ATP-dependent plasma membrane transport or mitochondrial buffering,

with the result of massive disruption of intracellular mechanisms, and the eventual death of the cell.

5.2.3. Cytotoxicity and Calcium

Raised intracellular calcium appears to play an important role in the excitotoxic and ischaemic cell death (Choi et al., 1987). Calcium has been shown to result in the activation of protein kinases, proteases and phospholipases. The production of second messengers such as inositol phosphates may act to release calcium from intracellular stores, thus cytosolic calcium concentrations are increased further. The activation of protein kinases may influence the activity of many enzymes and proteins including ion channels and receptors: for example phosphorylation of GABA_A receptors decreases the cellular response to GABA, while phosphorylation of NMDA receptors enhances the post-synaptic response (Mody et al., 1988). There is evidence that protein kinase C is involved in excitotoxic cell death: increased [³H]-phorbol ester binding to protein kinase C has been reported in the hippocampus of rats following ischaemia (Onodera et al., 1989), and gangliosides which inhibit glutamate- and kainate-induced translocation of protein kinase C to the cell membrane are neuroprotective (Vaccharino et al., 1987). Further, ischaemic damage in the CA1 region of the gerbil hippocampus can be prevented by pre-treatment with a protein kinase C antagonist (Hara et al., 1990).

Increasing the cytosolic calcium concentration results in the stimulation of calcium-dependent proteases, or calpains, which are able to effect changes in cytoskeletal elements and integral membrane proteins. Calpain I has been shown to be activated in hippocampal neurones by excitotoxic doses of kainate or NMDA (Siman et al., 1989). Calpain I-mediated spectrin breakdown is evident in the CA3 region following intraventricular injections of kainate, while in CA1, the rapid

proteolysis of spectrin in response to ischaemia appears to be dependent on NMDA receptor activation (Seubert et al., 1989); these observations are in accordance with the high densities of NMDA receptors in CA1, and the high levels of kainate receptors in CA3 (Cotman et al., 1987). Disruption of the cytoskeleton and consequently impaired transport of proteins to nerve terminals (Persson et al., 1989) may underlie in part the "delayed neuronal death" which has been observed to accompany ischaemia (Kirino, 1982).

Increased intracellular calcium will also result in a marked elevation in the concentration of the second messenger arachidonic acid, and initiation of the arachidonic acid cascade, through stimulation of phospholipase A₂. Further metabolism of arachidonic acid by cyclooxygenases and lipoxygenases may lead to the production of free radical groups, and results in lipid peroxidation (Werns et al., 1990). The role of free radicals in ischaemic damage is strengthened by the observation that free radical scavenging agents exhibit neuroprotection from excitotoxicity in cell culture (Dykens et al., 1987), and in global and focal ischaemia (Panetta et al., 1989). Free radicals are also possibly formed as a consequence of calcium-induced activation of a protease which converts xanthine dehydrogenase to xanthine oxidase. Xanthine is produced by the breakdown of AMP in the cell, to yield ultimately uric acid. Xanthine oxidase utilises molecular oxygen to generate superoxide radicals, which are directly cytotoxic, but may also be converted into hydroxyl radicals in the presence of transition metals. This mechanism is thought to occur when kainate is applied to cultured cerebellar neurones (Dykens et al., 1987) and poses another problem in the treatment of ischaemia: during reperfusion following an ischaemic insult, xanthine and oxygen levels are high, and therefore may contribute to reperfusion injury within previously ischaemic tissue.

Finally, increased calcium concentrations are able to influence the activity of genome-linked enzymes such as endonucleases. In the

normal cell, a number of morphological changes | presage the natural death of the cell, such as plasma and nuclear membrane blebbing, compacting of organelles, and chromatin condensation (See Orrenius et al., 1989). The most characteristic marker for cell death is calcium-dependent activation of endonucleases, which results in the cleavage of chromatin into fragments (Orrenius et al., 1989). Thus, marked elevation of calcium may induce prematurely those processes which result in cell death.

In the light of such findings, it appears, therefore, that to prevent ischaemic damage would require prompt pharmacological intervention, either at the level of the receptor or ion channel, in order to prevent toxic influx of calcium, or at an intracellular level, to prevent the actions of augmented cytosolic calcium on a range of cellular systems. With these aims, a number of pharmacological approaches have been advocated. It is clear, however, that to prevent the initial increase in calcium influx, and thus avoid the subsequent, marked cellular disruption, the most successful method of preventing ischaemic damage would be expected to be through antagonism of glutamate receptors.

5.2.4. Neurochemical Alterations in Response to Cerebral Ischaemia

A limited number of reports deal with the possibility that alterations in receptor density occur following cerebral ischaemia. Westerberg and colleagues (1987, 1989) examined the time-course of alterations in excitatory amino acid binding sites following transient global cerebral ischaemia, and reported a transient decrease in [³H]-AMPA binding in the dentate gyrus and CA1 of the hippocampus immediately after the ischaemic insult, and a more prolonged, severe decrease which became apparent two days after ischaemia and developed over two to four weeks. [³H]-Glutamate binding to NMDA receptors was not found to be altered acutely after the ischaemic insult, but decreased moderately in the CA1

stratum radiatum between four days and four weeks after the ischaemic insult. Additionally, [³H]-kainate binding was decreased in the CA4 region one and four weeks after the ischaemic insult. The authors suggested that AMPA receptors become desensitised acutely following ischaemia, while subsequent long-term reduction in [³H]-AMPA binding may reflect cell loss in regions of the hippocampus damaged by ischaemia. The relative preservation of the NMDA receptor binding sites has been replicated in a model of focal ischaemia in the rat (Dewar et al., 1989), and transient global ischaemia in the gerbil (Bowery et al., 1988), with the suggestion that although damaged neurones fail to take up histological stains, binding sites for the NMDA receptor are preserved.

5.2.5. Animal Models of Cerebral Ischaemia

The number of animal models of ischaemia is perhaps reflective of the diversity of manifestations, causes, and anatomical sites of human ischaemic stroke. The situation is further complicated by the lack of opportunity to study in detail the pathophysiological sequelae of the condition in humans: events occurring during the first minutes of an ischaemic insult may only be studied in laboratory animals. This necessitates careful modelling of the condition to provide a variety of circumstances which mimic as closely as possible one or more of the features of stroke (for review see Ginsberg and Busto, 1989).

Laboratory rodents, particularly rats and gerbils, are readily available at low cost, and are highly suitable for investigations into cerebral ischaemia: there is a close resemblance between the cerebrovascular anatomy and physiology of rodents and that of higher species, and the small brain size of rodents and studies of tracer analysis, which in larger species would be limited by cost. Nevertheless, several studies have employed higher, gyrencephalic species such as cats or primates, in order to produce ischaemia in animal models which resemble closely the

human brain.

Global Cerebral Ischaemia

While these may be criticised due to their lack of specificity, models of global cerebral ischaemia have provided an opportunity to study the effects of transient ischaemia and subsequent reperfusion. The advantages of global models such as two- or four-vessel occlusion are their manipulation and theoretically their reproducibility. Blood flow to the brain is interrupted by ligating the common carotid arteries, with or without cauterization of the vertebral arteries, to produce reversible forebrain ischaemia. While these techniques have been used to assess behavioural and neurochemical alterations at time-points other than acutely after the ischaemic insult, the mortality rate and the vast differences in the reproducibility of ischaemia between strains of rats has limited the use of four-vessel occlusion (Blomqvist et al., 1984), while the anaesthesia required to perform two-vessel occlusion raises questions on its suitability in drug studies aimed at neuroprotection.

Focal Cerebral Ischaemia

Models of focal cerebral ischaemia are now generally preferred to those of global ischaemia: focal lesions are discrete and reproducible, and allow observations of pathophysiological events in sites remote from the ischaemic insult. Moreover, focal ischaemic models appear to reflect more closely the sequence of events which occur in human stroke.

Possibly the most commonly employed model of focal cerebral ischaemia is occlusion of the middle cerebral artery (MCA) in the rat; this has gained increasing respect in recent years due to its similarity with human stroke. In simple terms the MCA is occluded unilaterally (see Tamura et al., 1981, for example), resulting in the interruption of the major blood supply to the ipsilateral caudate nucleus, olfactory and frontal cortices. The relative reproducibility of this model has propelled

its use in studies which assess the neuroprotective effect of drugs (for example, see Park et al., 1988). However, study of its events following ischaemia is limited to the dynamic alterations which surround the area of infarction. In order to estimate the direct effects of ischaemia on other brain regions, other models of focal cerebral ischaemia are required.

The most common mass CNS lesion to occur in the clinic is acute subdural haematoma, and it provides a major clinical challenge: although 80% of patients with acute subdural haematoma are conscious at some time after the injury, 60% die or remain severely disabled (Jamieson and Yelland, 1972, Stone et al., 1983). Thus it appears that some mechanism secondary to the initial insult is involved in the onset of much of the ischaemic damage. Again, a major problem in elucidating these putative mechanisms has been the inability to study the events which occur in the patient's brain during the initial insult. Despite the enormous cost of management of patients, however, and the potential benefits which an animal model may provide in order to test therapeutic regimes, there has to date been no altogether suitable model of acute subdural haematoma.

To this end, there has been developed in this laboratory a new rat model of acute subdural haematoma, designed to imitate as closely as possible those events which occur following subdural haematoma in humans (Miller et al, 1990). Briefly, the model involves injection of 0.4ml autologous venous blood into the subdural space. This results in an immediate rise in intracranial pressure, which is maintained above normal values for at least three hours. Histological examination of cerebral tissue at four and 24 hours reveals an extensive infarcted area directly below the haematoma, easily distinguishable from the underlying normal tissue. At a survival time of 72 hours, there is evidence of hippocampal damage, especially in the CA1 sector (Bullock, personal communication). These findings are consistent with the neuropathological alterations following ischaemic infarct in humans,

and hence this method provides a model of ischaemia in which other secondary mechanisms leading to ischaemic damage in vulnerable regions such as the hippocampus may be investigated.

5.2.6. Neuroprotection and Ischaemia: NMDA Antagonists

While it is clear that there exist a number of possible sites of action at which pharmacological prevention of ischaemic neuronal death may be successful, the most effective neuroprotection has been observed following treatment with glutamate antagonists specific for sub-types of glutamate receptor. The development of highly specific NMDA antagonists with high potency has propelled research into the ability of this class of drug to prevent ischaemic neuronal damage. Table 1 presents selected studies in which NMDA antagonists have been shown to be neuroprotective in focal cerebral ischaemia. Competitive and non-competitive NMDA antagonists differ in their site of action: competitive NMDA antagonists bind to the recognition site for glutamate and therefore exert their action by direct competition with the endogenous agonist; non-competitive NMDA antagonists on the other hand bind to a site within the associated ion channel, and therefore depend on the presence of the endogenous agonist to open the channel. In treatment of ischaemic damage, this represents an important difference in drug action, for while the action of non-competitive antagonists will be potentiated by the raised extracellular concentration of glutamate, competitive antagonists will be displaced by the increased concentration of glutamate, and thus may not be effective in antagonising glutamatergic responses.

The hydrophilic nature of competitive antagonists may limit their efficacy as anti-ischaemic drugs further. Non-competitive antagonists such as MK-801 are highly lipophilic, and therefore cross the blood brain barrier freely; thus they are able rapidly to achieve therapeutic concentrations within the cerebral tissue. Competitive antagonists,

NMDA ANTAGONISTS WITH DEMONSTRATED NEUROPROTECTIVE EFFECTS IN ISCHAEMIA

Competitive NMDA Antagonists:				
<u>DRUG</u>	<u>ADMINISTRATION</u>	<u>SPECIES</u>	<u>MODEL</u>	<u>REFERENCE</u>
CGS 19755	i.p. post-	Gerbil	2-VO (Global)	Boast et al. 1988
CPP	i.p. pre-	Gerbil	2-VO (Global)	Boast et al. 1988
AP7	i.h. pre-	Rat	2-VO + ↓ BP	Simon et al. 1984
D-CPP-ene	i.v. pre-	Cat	MCAO	Bullock et al. 1990
Non-Competitive NMDA Antagonists:				
<u>DRUG</u>	<u>ADMINISTRATION</u>	<u>SPECIES</u>	<u>MODEL</u>	<u>REFERENCE</u>
TCP	i.p. pre-	Rat	MCAO	Duverger et al. 1987
PCP	i.v. pre-	Rat	2-VO + ↓ BP	Sauer et al. 1988
MK-801	i.v. pre-	Rat	MCAO	Park et al. 1988a
	i.v. post-	Rat	MCAO	Park et al. 1988a
	i.v. pre-	Cat	MCAO	Ozyurt et al. 1988
	i.v. post-	Cat	MCAO	Park et al. 1988b

however, have relatively low lipophilicity, and therefore enter the brain slowly, where they attain only a fraction of the total plasma concentration (McCulloch & Iversen, 1991). The slow brain entry of competitive antagonists, and the likelihood that the raised extracellular glutamate concentration will overcome the competitive antagonist blockade, may explain the failure of these drugs to provide neuroprotection in ischaemia; for example, although MK-810 administration after induction of the ischaemic insult has been shown to reduce ischaemic damage (Park et al., 1988), D-CPP-ene administration following occlusion of the MCA in cats did not produce significant reduction in infarct size (Chen et al., 1991).

A limiting factor in the use of non-competitive NMDA antagonists such as MK-801 and phencyclidine, however, is that they induce pathomorphological alterations in certain cortical regions (Olney et al., 1989): single peripheral injections of these drugs at neuroprotective doses were found to cause cytoplasmic vacuolation and pyramidal cell swelling. Further, the [¹⁴C]-deoxyglucose autoradiographic technique has been used to demonstrate marked functional disturbances in these areas (Kurumaji et al., 1989). It is thought that these side effects might be controlled by the use of anaesthetics such as halothane, which abolish the marked increases in cortical glucose use produced by MK-801 (Kurumaji & McCulloch, 1989). However, the possible potentiation of these side effects as a consequence of the raised extracellular levels of glutamate in the ischaemic tissue, combined with the use-dependency of the drug, is an important consideration in the choice of glutamate antagonist for treatment of ischaemic damage in humans (see McCulloch & Iversen, 1991 for discussion). In this respect, competitive antagonists, due to their apparent lack of side effects, may be more beneficial in ischaemic injury, and have therefore received increasing attention as potential therapeutic agents.

6. AUTORADIOGRAPHIC IMAGING OF THE CENTRAL NERVOUS SYSTEM

The manufacture of the radio-labelled analogues specific for receptors or uptake by other cellular components, and the development of quantitative densitometric techniques has in recent years permitted high-resolution mapping of receptors and cellular pathways within the CNS. This study employs two autoradiographic techniques: the [^{14}C]-deoxyglucose autoradiographic technique for estimation of local cerebral glucose utilisation, and radio-ligand receptor autoradiography for estimation of specific receptor densities within the CNS. These are considered separately below.

6.1. DEOXYGLUCOSE AUTORADIOGRAPHY

The energy which fuels cerebral metabolism is provided, under normal physiological conditions, almost exclusively by the oxidative catabolism of glucose. Consequently, the functional activity within a region of cerebral tissue is directly proportional to the energy consumption within that region.

Estimation of glucose utilisation and hence functional activity within distinct brain regions has been made possible with the [^{14}C]-deoxyglucose autoradiographic technique (Sokoloff et al., 1977). Deoxyglucose, a structural analogue of glucose is transported across the blood-brain barrier, and enters the glycolytic pathway. It competes with glucose for hexokinase, and is phosphorylated to deoxyglucose-6-phosphate, at a defined rate relative to that of phosphorylation of glucose. While however glucose-6-phosphate undergoes metabolism by hexokinase, deoxyglucose-6-phosphate is not a substrate for further phosphorylation, and remains essentially trapped within the cerebral tissues. When the

radio-labelled analogue, [^{14}C]-deoxyglucose, is administered intravenously to animals, it is taken up and phosphorylated rapidly within the tissues; thence it is possible to produce autoradiograms of deoxyglucose uptake by exposure of brain sections to radiation-sensitive film. In order to measure precisely local cerebral glucose utilisation within discrete CNS regions, Sokoloff and colleagues (1977) developed a mathematical model which incorporates the biochemical properties of deoxyglucose and glucose, the plasma history of the tracer uptake within the animal, and the concentration of ^{14}C in the CNS as measured by densitometric analysis of the autoradiograms (see Methods Section 1 for details of mathematical model and autoradiographic routines). Thus the advent of this technique has provided an opportunity to investigate, within defined physiological parameters (Sokoloff et al., 1977; Sokoloff, 1981), the functional consequences of pharmacological, physiological and pathological manipulations within the CNS.

Pharmacological Investigations

Analysis of cerebral glucose utilisation in response to a variety of pharmacological agents has revealed in many cases striking patterns of functional activation or depression (for review, see McCulloch, 1982). For example, dopaminergic influences upon cerebral glucose utilisation have been studied extensively, and alterations in glucose use appear to be restricted in their distribution to a few neuronal circuits. However, altered glucose use is not confined to those regions which receive dopaminergic innervation (Moore & Bloom, 1978). Further, in regions known to contain dopaminergic receptors, there is no direct relationship between the magnitude of alterations in glucose use and the density of dopaminergic receptors within those regions.

Similar patterns have been observed in response to other pharmacological agents. Kurumaji and colleagues (1989) demonstrated that administration of the non-competitive NMDA antagonist MK-801

effected large alterations in glucose use in areas of cortex associated with limbic function known to contain high densities of NMDA receptors. However, regions of sensory cortex were unaffected. Additionally, alterations in glucose use in the hippocampus were not localised within those regions which display high densities of NMDA receptors. Therefore cerebral glucose use appears to reflect the functional consequences of pharmacological agents not only directly at the site of drug action, but also within remote sites which are neuroanatomically connected with the site of drug-receptor interaction.

Physiological Investigations

Whereas administration of pharmacological agents has been demonstrated to produce marked alterations in cerebral glucose use, responses to physiological challenges are mostly subtle alterations in glucose use. [¹⁴C]-Deoxyglucose autoradiography has been used to measure subtle circadian variations in glucose use in unrestrained rats (Room & Tielemans, 1989). The authors reported that glucose use was altered in cortical and extrapyramidal regions, and in the suprachiasmatic nucleus, which has been suggested to play a role in maintenance of circadian rhythms. Friedman & Goldman-Rakic (1988) used deoxyglucose autoradiography to investigate responses to cognitive memory tasks in primates, and measured subtle increases in glucose use in specific layers of the dentate gyrus and CA1 regions of the hippocampus; in contrast, glucose use was unaltered in the amygdalar nuclei, which are known to be involved in learning and memory (Mishkin, 1978). Finally, Porrino et al. (1990) have demonstrated alterations in glucose use in a number of brain regions following self-stimulation of electrodes previously implanted in the medial forebrain bundle: this regime is believed to be an artificial activation of brain systems that normally mediate the reinforcing effects of natural rewards. The authors reported alterations in a number of limbic brain regions

such as the diagonal band nucleus, nucleus accumbens, lateral septum and cingulate cortex. Thus deoxyglucose autoradiography is a potentially powerful technique in estimating the extent of cerebral activation in response to a range of physiological challenges.

Pathological Manipulations

The deoxyglucose technique has also been used extensively to illustrate alterations in cerebral glucose utilisation during types of pathological insult. For example, a large body of work has examined the alterations in glucose use which occur following cerebral ischaemia, and has provided evidence for dynamic functional disturbances within the brain (for review see Ginsberg et al., 1990). Although the effects of pathological insult on the stability of the kinetic data incorporated into the deoxyglucose operational equation must be considered, use of the deoxyglucose technique has demonstrated that increased deoxyglucose uptake may be observed in the region surrounding the infarct, or the penumbral region (Nedergaard et al., 1986; Shiraishi et al., 1989). Thus the suggestion has been made that infarction is a dynamic, progressive event, in which the cells in the penumbral region are compromised, and finally infarcted.

Several attempts have been made to demonstrate subtle alterations in glucose use in the CNS following lesions specific neuronal pathways. Local cerebral glucose utilisation has been measured at several time-points following unilateral ocular enucleation in the rat (Chalmers & McCulloch, 1989). The authors reported that while glucose use fell dramatically in structures associated with visual processing directly after enucleation, functional recovery occurred, inferring that plastic mechanisms exist within the CNS. It was also possible to correlate alterations in glucose use with alterations in receptor densities in those areas (Chalmers, D. T., Ph. D. Thesis, University of Glasgow, 1989), demonstrating that deoxyglucose may be used to illustrate functionally

the plastic processes which occur in response to denervation.

More subtle alterations have been measured in response to discrete lesions of specific nuclei or fibre tracts. Harrell and Davis (1984) report alterations in hippocampal glucose use following electrolytic lesions of the medial septal area, and found evidence for long-term functional recovery within the hippocampus. In contrast, Kelly et al. (1985b) demonstrated that decrements in glucose use in the hippocampus did not recover with time following fimbria fornix transection, but that the decrements could be ameliorated by grafting septal tissue; the authors suggested therefore that sprouting of grafted cholinergic cells are able to make synaptic contacts with hippocampal cells, and thus restore functional activity within the hippocampus. using fluoro-deoxyglucose in a positron emission tomography (PET) study of primates, Kiyosawa and colleagues (1989) found that amelioration of nucleus basalis-induced decreases in cortical glucose use are not accompanied by recovery of choline acetyltransferase activity in the cortex; the authors suggested therefore that functional plasticity within the cortex was due to non-cholinergic mechanism, rather than recovery of cholinergic neuronal connections from the nucleus basalis.

Deoxyglucose autoradiography therefore has proved to be pivotal in demonstration of functional relationships between specific populations of neurones in the CNS, and has provided novel insights into the effects in vivo of pharmacological, physiological and pathological manipulation of neurotransmitter systems in the brain.

6.2. QUANTITATIVE LIGAND-BINDING AUTORADIOGRAPHY

While deoxyglucose autoradiography has provided novel insights into the state of functional state of discrete CNS regions, ligand-binding autoradiography has been readily employed in the estimation of receptor

densities in the CNS. The development of radio-labelled ligands specific for receptors within the CNS has enabled high-resolution anatomical mapping of receptor distributions in the brain. The technique relies on knowledge of receptor ligand kinetics (see Methods Section 2 for theory and methodology); brain sections are incubated for a fixed period in the presence of radio-labelled ligand, rinsed and dried, and opposed to radiation-sensitive film in order to produce an autoradiographic image of receptor densities in anatomically discrete areas.

Ligand-binding kinetics have been determined for a large range of receptors and receptor sub-types. The use of these techniques has permitted quantitative anatomical mapping of receptors in the CNS. A large body of work has been dedicated to elucidating alterations in receptor densities in a number of CNS diseases such as Alzheimer's Disease (Geddes et al., 1985; see Greenamyre et al., 1987; Mash et al., 1985; Perry et al., 1986). Additionally, ligand-binding autoradiography in animal models of disease states has been crucial in the estimation of the degree of plasticity of specific neurotransmitter systems (for example see Joyce et al, 1989; Mash et al., 1985; Ulas et al., 1990a,b), confirming or reforming hypotheses which may explain alterations in receptor density following the onset of neurodegenerative disease.

7. AIMS OF THESIS

The aims of this thesis are firstly to investigate functional activity in the hippocampal formation in response to pharmacological and pathological manipulation of cholinergic and glutamatergic transmission, and secondly to investigate the plastic modification of hippocampal cholinergic and glutamatergic receptors after removal of the cholinergic input.

Quantitative *in vivo* [¹⁴C]-deoxyglucose autoradiography and quantitative *in vitro* ligand-binding autoradiography have been used extensively in order to examine critically the role of glutamatergic and cholinergic neurotransmitter systems in the hippocampus, and associated limbic regions. These aims are discussed specifically below.

7.1. EFFECTS OF GLUTAMATERGIC AND CHOLINERGIC AGENTS ON CEREBRAL GLUCOSE UTILISATION

Deoxyglucose autoradiography has been employed to estimate the effects of three pharmacological agents on local cerebral glucose utilisation in the conscious, lightly restrained rat. Detailed measurements of glucose use in the hippocampus have provided a focus for discussion. In addition, glucose use in limbic structures associated closely with hippocampal have been examined. Finally, measurements have been compared to alterations in glucose use in other, non-limbic regions in order to provide a full profile of drug action.

7.1.1. D-CPP-ene, a Novel Competitive NMDA Antagonist

The novel competitive NMDA antagonist, (E)-4-(3-phosphonoprop-2-enyl)- piperazine-2-carboxylic acid (D-CPP-ene) is a drug with high

potency, and is potentially therapeutic in the prevention of neuronal damage following ischaemia (Aebischer et al., 1989). Recently, administration of the non-competitive NMDA antagonists MK-801 and phencyclidine have been shown to result in pathomorphological alterations in areas of cortex and hippocampus (Olney et al., 1989); further, deoxyglucose autoradiography has demonstrated marked functional disturbances in these areas following administration of MK-801 (Kurumaji et al., 1989).

In the present study, cerebral glucose utilisation have been measured in conscious, lightly restrained rats following administration of saline or D-CPP-ene (0.3, 3 or 30mgkg⁻¹), in order to assess fully the functional effects of D-CPP-ene. The pattern of alterations in glucose utilisation are discussed with reference to the neuroanatomical organisation of glutamatergic pathways in the CNS; further, the patterns of altered glucose use are discussed with reference to the functional alterations elicited by other NMDA antagonists.

7.1.2. L-679-512, a Novel Muscarinic Agonist

L-679-512 is a novel muscarinic agonist with high efficacy which is able to pass the blood-brain barrier freely, and stimulate maximally phosphoinositide turnover in the brain (Saunders & Freedman, 1989; Freedman et al., 1990). There is considerable interest in cholinomimetic compounds as therapeutic agents in the treatment of the dementia of Alzheimer's Disease. Previously, only quaternary compounds, such as carbachol and muscarine have been able to stimulate maximal phosphoinositide turnover; however, these compounds have only a limited ability to cross the blood-brain barrier, thus limiting their central effects.

The aim of this series of experiments was to estimate the functional consequences, as measured by [¹⁴C]-deoxyglucose autoradiography, of

administration of L-679-512. Local cerebral glucose utilisation was measured in fully conscious, lightly restrained rats, following administration of L-679-512 (3, 10 or 30 μgkg^{-1}) or saline. The patterns of cerebral glucose use have been compared to those patterns produced by other cholinomimetic agents, and evidence for neuroanatomical organisation of alterations in function is reviewed.

7.1.3. 9-Amino-1,2,3,4-Tetrahydroacridine (THA), a Cholinesterase Inhibitor with Potential Glutamatergic Activity.

THA is a cholinesterase inhibitor, which has been suggested to be efficacious in the amelioration of cognitive deficits in Alzheimer's Disease (Summers et al., 1986). The drug has recently been introduced into clinical trials; however, to date, there has been no study of its effects on functional activity *in vivo*.

The therapeutic effects of THA have been attributed not only to its effects at cholinergic synapses, but also to an action at glutamatergic synapses (Albin et al., 1988). Using deoxyglucose autoradiography, the patterns of cerebral glucose utilisation in response to THA (2.5 mgkg^{-1}) or saline administration were measured in the conscious rat. Patterns of glucose utilisation are discussed in comparison to those produced by other cholinergic or glutamatergic drugs.

7.2. FUNCTIONAL PLASTICITY OF THE HIPPOCAMPUS IN RESPONSE TO LESIONS OF THE MEDIAL SEPTUM

Quantitative [^{14}C]-deoxyglucose autoradiography and quantitative receptor autoradiography has been employed three weeks after ibotenate lesions of the medial septum in order to estimate the effects of cholinergic denervation on transmission in the hippocampus. In addition, the integrity of muscarinic receptor coupling to phosphoinositide turnover was investigated using biochemical assay three weeks after medial septal lesions.

7.2.1. Functional Activity in the Hippocampus After Ibotenic Acid Lesions of the Medial Septum

In contrast to previous investigations which involved the use of non-specific lesion techniques (Harrell & Davis, 1984; Kelly et al., 1985b), this study examines the functional consequences of discrete ibotenate-induced lesions of the medial septal area in rats. Measurements of glucose utilisation have been made three weeks after medial septal lesions in discrete hippocampal regions and limbic areas associated with hippocampal function.

7.2.2. Alterations in Ligand-Binding to Hippocampal Cholinergic and Glutamatergic Receptors After Ibotenic Acid Lesions of the Medial Septum

The effects of cholinergic denervation on the hippocampal cholinergic and glutamatergic receptor binding have been assessed three weeks after lesions of the medial septum. Sub-types of glutamate receptor densities were measured using [^3H]-AMPA, [^3H]-kainate, and NMDA-sensitive [^3H]-glutamate binding, to image AMPA-sensitive quisqualate, kainate

and NMDA receptors respectively. Muscarinic receptor densities were measured using [³H]-QNB. The aim of this approach was to determine firstly, whether discrete, axon-sparing lesions of the medial septum would result in alterations in hippocampal muscarinic receptor densities; and secondly, whether hippocampal glutamatergic receptor integrity is altered by removal of the modulatory cholinergic input. The results of this study are discussed in relation to the role of cholinergic and glutamatergic receptors in hippocampal function; the significance of plastic mechanisms is discussed with respect to current theories regarding the neurochemical deficits in Alzheimer's Disease.

7.2.3. Muscarinic-Mediated Phosphoinositide Hydrolysis in the Hippocampus Following Ibotenic Acid Lesions of the Medial Septum

The final aim addressed in this series of experiments was to assess whether muscarinic-coupled second messenger turnover was preserved in the hippocampus. Carbachol-stimulated phosphoinositide hydrolysis was assayed biochemically in hippocampal slices from rat brains three weeks after lesions of the medial septum. The results are discussed with respect to measurements of muscarinic receptor density within the lesioned hippocampus.

7.3. THE CEREBRAL METABOLIC EFFECTS OF ACUTE SUBDURAL HAEMATOMA IN THE RAT.

The aims of this series of experiments were firstly to measure the effects on local cerebral glucose utilisation of a novel cortical ischaemic insult, acute subdural haematoma in the rat, and secondly to assess the ability of the competitive NMDA antagonist D-CPP-ene to ameliorate these effects.

Local cerebral glucose use was measured in the conscious rat, two hours after acute subdural haematoma had been induced by injection of autologous venous blood. Cerebral glucose use was estimated in areas directly vulnerable to ischaemic damage, such as the underlying cortex, and discrete hippocampal regions remote from the site of infarct. Additionally, rates for cerebral glucose use were estimated in limbic areas associated with hippocampal function and sensory regions. These were compared with rates for local cerebral glucose utilisation in sham-operated control rats, and rats which had received D-CPP-ene prior to acute subdural haematoma.

Alterations in local cerebral glucose use, and the ability for D-CPP-ene to ameliorate these alterations are discussed with reference to the excitotoxic hypothesis of ischaemia; the role of glutamatergic circuitry in the vulnerability of hippocampal ischaemic damage is discussed. Finally, the results of this study are compared with those of similar studies of the functional consequences of ischaemia, and the impact of the results on the attempts to elucidate the mechanisms which underlie ischaemic damage are discussed.

CHAPTER II

METHODS

1. QUANTITATIVE AUTORADIOGRAPHY

1.1. *IN VIVO* [¹⁴C]-2-DEOXYGLUCOSE AUTORADIOGRAPHY

1.1.1. Theory: Mathematical Model and the Operational Equation

Sokoloff and colleagues made use of an operational equation to calculate rates of cerebral glucose utilisation in the conscious albino rat. This equation is derived mathematically from a theoretical model which incorporates the rate constants of uptake and phosphorylation of glucose and deoxyglucose (Figures 4 & 5). The operational equation describes the rates of cerebral glucose use (R_i), following injection of a bolus of intravenous [¹⁴C]-2-deoxyglucose, in terms of the concentrations of [¹⁴C]-2-deoxyglucose and glucose in arterial plasma (C_p^* and C_p) and the total concentration of ¹⁴C within the CNS (C_i^*). The equation also incorporates a "lumped" constant, which represents the relative distribution volume of deoxyglucose and glucose, the Michaelis-Menten constants and maximal velocities of hexokinase for phosphorylation of deoxyglucose and glucose, and a factor which predicts the fraction of glucose which, once phosphorylated, will continue to be metabolised via the glycolytic pathway.

In the application of the operational equation, a number of assumptions are necessary:-

1. Measurements may only be made within a localised area in which rates of blood flow and rates of uptake and phosphorylation of deoxyglucose and glucose are constant.
2. The concentrations of deoxyglucose and glucose within each element of tissue are constant, and deoxyglucose and glucose are present in a single compartment, and may exchange freely between plasma and tissue.
3. The arterial plasma concentrations of deoxyglucose and glucose

represent accurately their cerebral capillary concentrations.

4. Carbohydrate metabolism is in a steady state.

Additionally, [^{14}C]-2-deoxyglucose and [^{14}C]-2-deoxyglucose-6-phosphate must be present in tracer amounts, and must be pharmacologically inactive.

A criticism of the deoxyglucose technique is that it does not account for the breakdown of deoxyglucose-6-phosphate to deoxyglucose by glucose-6-phosphatase (Hawkins & Miller, 1978). However, glucose-6-phosphatase is believed to be contained within the endoplasmic reticulum, and is not free within the cytosol; Sokoloff and colleagues have demonstrated that its activity in the brain is so low that in the 45 minute experimental period the effect of the enzyme on the total amount of phosphorylated deoxyglucose is negligible (Sokoloff, 1979).

Using a 45 minute period also diminishes the errors involved in using the fixed rate constants k_1^* , k_2^* , and k_3^* , which define the distribution of tracer within the various compartments of the model (Figure 4). A possible source of error in calculating local cerebral glucose utilisation with the operational equation exists in the assumption that the constants for transfer of [^{14}C]-2-deoxyglucose between plasma and tissue (k_1^* , k_2^*), and its subsequent phosphorylation in cerebral tissue (k_3^*), do not change over a given range of physiological conditions. Since, however, C_p^* diminishes with time, the elements of the operational equation which contain the term C_p^* will likewise diminish with respect to time, and hence if the experimental period is lengthened, the error inherent in these elements will also be reduced. This has been demonstrated by Sokoloff and colleagues experimentally (Sokoloff et al., 1977; Sokoloff, 1979).

$$R_i = \frac{C_i^*(T) - k_1^* e^{-(k_2^* + k_3^*)T} \int_0^T C_p^* e^{-(k_2^* + k_3^*)t} dt}{\left[\frac{\lambda V_m^* K_m}{\phi V_m K_m^*} \right] \left[\int_0^T (C_p^*/C_p) dt - e^{-(k_2^* + k_3^*)T} \cdot \int_0^T (C_p^*/C_p) e^{-(k_2^* + k_3^*)t} dt \right]}$$

FIGURE 5: THE OPERATIONAL EQUATION

Glucose utilisation, R_i is calculated in terms of the total ^{14}C concentration in tissue at the end of the experiment ($C_i^*(T)$) and the concentrations of [^{14}C]-2-deoxyglucose and glucose in plasma (C_p^* and C_p respectively); k_1^* , k_2^* , and k_3^* are the rate constants for uptake of deoxyglucose and its subsequent phosphorylation in tissue by hexokinase. The lumped constant incorporates the following elements:- λ is the ratio of tissue distribution volumes for [^{14}C]-2-deoxyglucose and glucose; ϕ is the fraction of glucose during steady state metabolism which, once phosphorylated, will continue down the glycolytic pathway; and K_m^* and V_m^* and K_m and V_m are the Michaelis-Menten constants and the maximal velocities of hexokinase for deoxyglucose and glucose respectively (Sokoloff et al. 1977).

1.1.2. Methodological Considerations

Although the constants incorporated in the operational equation appear to be stable for a range of physiological values, in theory the value of the rate constants and lumped constants might be expected to be altered by factors producing an imbalance between glucose supply and utilisation.

Outwith normoglycaemia, the ratio of distribution between glucose and deoxyglucose is altered: in hyperglycaemia decreases in the brain distribution spaces of deoxyglucose and glucose occur; thus λ , the ratio of distribution volumes for glucose and [^{14}C]-2-deoxyglucose, will decrease. The consequential decrease in the absolute value of the lumped constant renders the operational equation inaccurate, and leads to an underestimation of cerebral metabolic rate.

Conversely, in hypoglycaemia, the distribution volume of glucose is decreased, while that of deoxyglucose is increased, leading to a marked elevation in the value of the lumped constant. This in turn leads to an overestimation of cerebral metabolic rate.

The former case is particularly important in situations where stress-induced hyperglycaemia is evident; the latter is likely to occur if food has been withheld for a number of days, or if experimental procedures disable the animal sufficiently to prevent it feeding normally over an extended period.

While it is often possible to maintain normoglycaemia by simple adjustment of experimental procedures (for example see Methods Section 1.1.8., THA), more caution must be applied in situations where regional supply and utilisation of glucose may be altered. In focal cerebral ischaemia, marked reductions of blood flow, and hence glucose supply, may interfere with the quantitative estimation of cerebral metabolism. In the present study, deoxyglucose autoradiography was used to measure cerebral glucose use in response to acute subdural haematoma in the rat. The effects of ischaemia on the rate and lumped

constants are discussed within the relevant section (Results and Discussion Section 3).

1.1.3. Animals

All deoxyglucose investigations were performed on adult male Sprague Dawley rats (Harlan Olac, Oxfordshire, UK). Prior to investigations, the rats were housed in a naturally lit, temperature-controlled environment, and unless stated otherwise (see Methods Section 1.1.8, THA) all had free access to food and water.

1.1.4. Surgical Preparation

Rats were placed in a perspex chamber into which flowed an anaesthetic gas composed of 5% halothane in a nitrous oxide: oxygen mixture (70%: 30%). Once anaesthesia was induced, halothane was reduced to 1-1.5%, and rats were maintained, spontaneously breathing, in an unconscious state for the implantation of femoral arterial and venous cannulae. The femoral vessels were exposed bilaterally through a small incision in the skin overlying the pelvic muscles, proximal to the femur. A polyethylene cannula (Portex, external diameter 0.96mm, internal diameter 0.58mm), 15cm in length and filled with heparinised saline (10 IUml⁻¹), was inserted approximately 2cm into the vessel. The cannulae were tied in place with fine suture material, and the wound was infiltrated with local anaesthetic gel (lignocaine hydrochloride, 2%) and sutured.

Externally, the wound was smeared with local anaesthetic gel, and covered in gauze pads. The lower torso was enveloped in a surgical stocking, and a plaster cast was applied loosely around the hindlimbs and abdomen. The plaster cast and the hindlimbs of the animal were taped to a lead brick for purposes of restraint, anaesthesia was terminated, and

the rats allowed to regain consciousness. A recovery period of at least two hours was given, prior to autoradiographic measurements to allow dissipation of anaesthetic; during this period, arterial blood pressure was monitored continuously, and normothermia maintained with a heating lamp.

1.1.5. Autoradiographic Sampling and Preparation of Autoradiograms

The autoradiographic procedure was initiated by the intravenous infusion over 30 seconds of [^{14}C]-2-deoxyglucose (125 μCi in 0.7ml saline). Concurrent with the start of isotope injection, a 45 minute experimental period commenced, in which 14 timed arterial samples were collected and immediately centrifuged. The plasma from each sample was assayed for ^{14}C activity by liquid scintillation and for glucose concentration (Glucose Analyzer 2, Beckman, High Wycombe, UK), in order to calculate the history of the isotope. At 45 minutes, the animal was killed by decapitation, and the brain wholly dissected out and frozen in isopentane cooled to -45°C in dry ice. The brain was mounted on a swivel-headed microtome chuck using embedding matrix (Tissue-Tek, Miles Inc., Elkhart, USA), and coronal sections 20 μm thick were cut serially in a cryostat. Three adjacent sections were thaw-mounted onto glass coverslips, and rapidly dried on a hot-plate. The following ten sections were discarded. This cycle was repeated throughout the brain (medulla to frontal lobes).

The coverslips were glued to card, and placed in X-ray cassettes, adjacent to ^{14}C -sensitive film, along with a set of pre-calibrated epoxy-resin standards (concentration range 44-1475 nCi g^{-1}), for approximately two weeks. Films were processed using a standard Kodak automatic processor, in order to generate deoxyglucose autoradiograms.

1.1.6. Liquid Scintillation Analysis

The concentration of ^{14}C in plasma was estimated for each animal during the [^{14}C]-2-deoxyglucose autoradiographic routine. A 20 μl aliquot was pipetted into a scintillation vial containing 1ml of water. To each vial was added 10ml of scintillation fluid (Ecoscint, National Diagnostics, New Jersey, USA), and the vials shaken thoroughly. The radioactivity in each vial was counted in a refrigerated scintillation counter using an external standard channels-ratio method (Peng, 1977) together with a standard calibration curve for quench correction. Vials were counted on three separate occasions, and the mean values for disintegrations per minute used in the calculation of the plasma integral.

1.1.7. Calculation of Local Cerebral Glucose Utilisation

Local tissue concentrations of ^{14}C were measured in each region of interest, using computerized densitometry (Methods section 1.3.). Local cerebral glucose utilisation for each region was calculated from these values and the plasma values for tracer and glucose concentration, by application of the deoxyglucose operational equation derived by Sokoloff et al. (1977).

1.1.8. Drug Administration

In three series of animals, deoxyglucose autoradiography was performed after administration of one of the following pharmacologically active agents, in order to assess its effects on cerebral metabolism.

1. D-(E)-4-(3-phosphonoprop-2-enyl)-piperazine-2-carboxylic acid (D-CPP-ene), a competitive glutamate antagonist

Competitive antagonists such as D-CPP-ene are highly hydrophilic, and therefore the rate at which they penetrate the blood brain barrier is slow, and the CNS concentration they achieve is low relative to their plasma concentration. The blood-brain barrier permeability-surface area product (PS) of D-CPP-ene has been estimated to be less than 0.0001ml/min/g (Pardridge et al., 1990), a figure in agreement with its octanol/water partition coefficient (Rapoport et al., 1979). The entry into the brain of drugs with low blood-brain barrier permeability may be estimated by the equation:-

$$C_B(T) = PS \int_0^T C_A(t) dt$$

where C_B is the concentration of drug in the brain at time T, and $C_A(t)$ is the arterial plasma concentration of the drug at variable time t after its administration into the bloodstream. This equation has been used to suggest that the CNS concentration of D-CPP-ene reaches a plateau at 120 minutes after administration into the bloodstream (McCulloch & Iversen, 1991). Therefore, in order that the effects of D-CPP-ene on cerebral metabolism could be assessed at steady-state conditions in terms of drug concentration, D-CPP-ene was administered intravenously two hours prior to administration of isotope, at a dose of 0.3, 3 or 30 mgkg⁻¹.

2. L679-512, a novel muscarinic agonist

L679-512, a novel muscarinic agonist of high efficacy, was administered intravenously 15 minutes prior to administration of [¹⁴C]-2-deoxyglucose, at a dose of 3, 10, or 30mgkg⁻¹.

3. 9-Amino-1,2,3,4-tetrahydroacridine (THA), a Cholinesterase Inhibitor with Potential Glutamatergic Activity

9-Amino-1,2,3,4-tetrahydroacridine (THA) was administered intravenously 15 minute prior to isotope injection at a dose of 2.5mgkg⁻¹. In this series, it was found that THA induced a degree of hyperglycaemia; in order that plasma glucose levels did not exceed those values for which the operational equation is accurate, food was withdrawn from these animals 12 hours prior to autoradiographic measurement.

1.1.9. Chemicals

[¹⁴C]-2-deoxyglucose (50Ci mmol⁻¹) was supplied by Amersham International, Buckinghamshire, England.

D-(E)-4-(3-phosphonoprop-2-enyl)-piperazine-2-carboxylic acid (D-CPP-ene) was obtained from Sandoz Research Institute Berne Ltd., Berne, Switzerland.

9-Amino-1,2,3,4-tetrahydroacridine hydrochloride (THA) was purchased from Sigma Chemical Company Ltd., Poole, Dorset, UK.

L679-512 was obtained from Merck Sharpe Dohme, Harlow, Essex, UK.

1.2. *IN VITRO* LIGAND-BINDING AUTORADIOGRAPHY

1.2.1. Theory

Ligand-binding autoradiography involves the interaction of a radio-labelled drug with a receptor, according to classical ligand-receptor kinetics. A simple model is described by the bimolecular action:-



RL, the product is more commonly known as B, the amount bound. At equilibrium:-

$$K_d = \frac{[R][L]}{[B]} \quad (2)$$

where K_d is the dissociation constant. The total number of receptors, B_{max} , will be equal to the amount of free receptors plus the amount bound, i.e.:-

$$B_{max} = [R] + [B] \quad (3)$$

Substitution for [R] in equation (2) yields:-

$$K_d = \frac{(B_{max} - [B])[L]}{[B]} \quad (4)$$

Rearrangement of equation (4) gives:-

$$[B] = \frac{B_{max}[L]}{[L] + K_d} \quad (5)$$

This equation is used in saturation analysis to provide estimates of K_d and B_{max} . [B] is measured as a function of the radio-ligand, and will increase as [L], the concentration of the ligand, is increased. K_d , the dissociation constant, which describes the equilibrium condition of

binding, will be equal to $1/2 B_{\max}$.

Non-specific binding, that is, binding to components of the tissue other than the receptor, is non-saturable, and proportional to the concentration of the radio-ligand. The portion of non-specific binding may be estimated by displacement of the radio-ligand with a non-labelled ligand specific for the receptor.

Analysis of binding data is more commonly performed using a Scatchard plot. Further rearrangement of equation (4) yields:-

$$\frac{[B]}{[L]} = \frac{B_{\max}}{K_d} + \frac{[B]}{K_d} \quad (6)$$

When the ratio of the concentrations of bound (B) and free (L) ligand is plotted against the concentration of bound ligand, a straight line is produced, with a gradient equal to $-1/K_d$. The intercept of the line on the x-axis is B_{\max} (Scatchard, 1949). This analysis allows estimation of B_{\max} by extrapolation, and hence negates the need to use saturating concentrations of ligand.

This method has been used extensively in the calculation of receptor-binding kinetics, in order to establish protocols for binding with each radio-ligand. The present study employs kinetic analysis of ligand-binding which has been calculated elsewhere (Monaghan & Cotman, 1985; Walmsley et al., 1984; Westerberg et al., 1987); details of methods used, and the source reference are found in Table 2.

1.2.2. Preparation of Sections for Ligand-Binding Autoradiography

Adult male Sprague Dawley rats were killed by decapitation, and the brains rapidly dissected out and frozen in isopentane cooled to -42°C . Coronal sections, $20\mu\text{m}$ thick were cut in a cryostat, and collected on

TABLE 2: SUMMARY OF LIGANDS AND BINDING PROTOCOLS

RECEPTOR	LIGAND	DISPLACER	PRE-INCUB.	INCUBATION	WASH	BUFFER	REFERENCE
NMDA	[³ H]-Glutamate 100nM	NMDA	1 Hour 0° C 15 Min. 30° C	10min. 4° C +5µM Quisqualate +100µM SITS	4 x 5 Sec. Buffer 1 x 5 Sec. H ₂ O 4° C	50mM Tris/ Acetate pH7.2	Monaghan & Cotman 1985
Quisqualate	[³ H]-AMPA 50nM	Quisqualate	1 Hour 0° C 15 Min. 30° C	30 Min. 4° C +100mM KSCN	4 x 5 Sec. Buffer 1 x 5 Sec. H ₂ O 4° C	50mM Tris/ Acetate pH7.2	Westerberg et al. 1987
Kainate	[³ H]-Kainate 50nM	Kainate	1 Hour 0° C 15 Min. 30° C	30 Min. 4° C	4 x 5 Sec. Buffer 1 x 5 Sec. H ₂ O 4° C	50mM Tris/ Citrate pH7.0	Westerberg et al. 1987
Muscarinic M1/M2	[³ H]-QNB 2nM	Atropine	20 Min Room Temp.	120 Min. Room Temp.	2 x 5 Min. Buffer 1 x 30 Sec. H ₂ O 4° C	50mM Sodium Phosphate pH7.4	Wamsley et al. 1984

SITS: 4-acetomido-4'-isothiocyanatostilbene-2, '2-disulphonic acid
KSCN: potassium thiocyanate

gelatin-coated microscope slides: three adjacent sections in 27 were serially collected throughout the brain (cerebellum to frontal lobes) for each ligand-binding experiment.

The sections were dried at room temperature, and stored at -20°C , in enclosed containers for up to 12 months prior to autoradiography.

1.2.3. Procedure

A general outline of the method employed in receptor autoradiography is given in Figure 6, and the protocol employed for binding experiments with each ligand is found in Table 2, together with details of the publication which describes the particular method used.

Briefly, tissue sections were incubated in the appropriate buffer for a period of time (the pre-incubation period) in order to remove endogenous ligands which might inhibit or displace the binding of the radio-ligand. Tissue sections were then incubated with the radio-ligand for a given period; non-specific binding was estimated in adjacent sections by inclusion of a non-radio-labelled displacer in the incubation medium. At the end of the incubation period, the sections were washed in buffer and rinsed in water to remove unbound radio-ligand, and dried in a stream of cool air. Because of the short dissociation time of glutamate receptor ligands, sections incubated with these ligands were dried rapidly by application of 2.5% glutaraldehyde in acetone (approximately .1ml per section). Finally, sections were apposed to radiation-sensitive film in sealed X-ray cassettes for an appropriate length of time, to produce autoradiograms. Films were developed manually in Kodak D-19 developer for five minutes at 17°C , with intermittent agitation. Development was terminated by placing the films in de-ionised water at 20°C for 30 seconds, and the films were fixed in Kodak Kodafix at 20°C for ten minutes. Finally, films were washed with running water and rinsed in de-ionised water, and suspended in a

RECEPTOR AUTORADIOGRAPHY

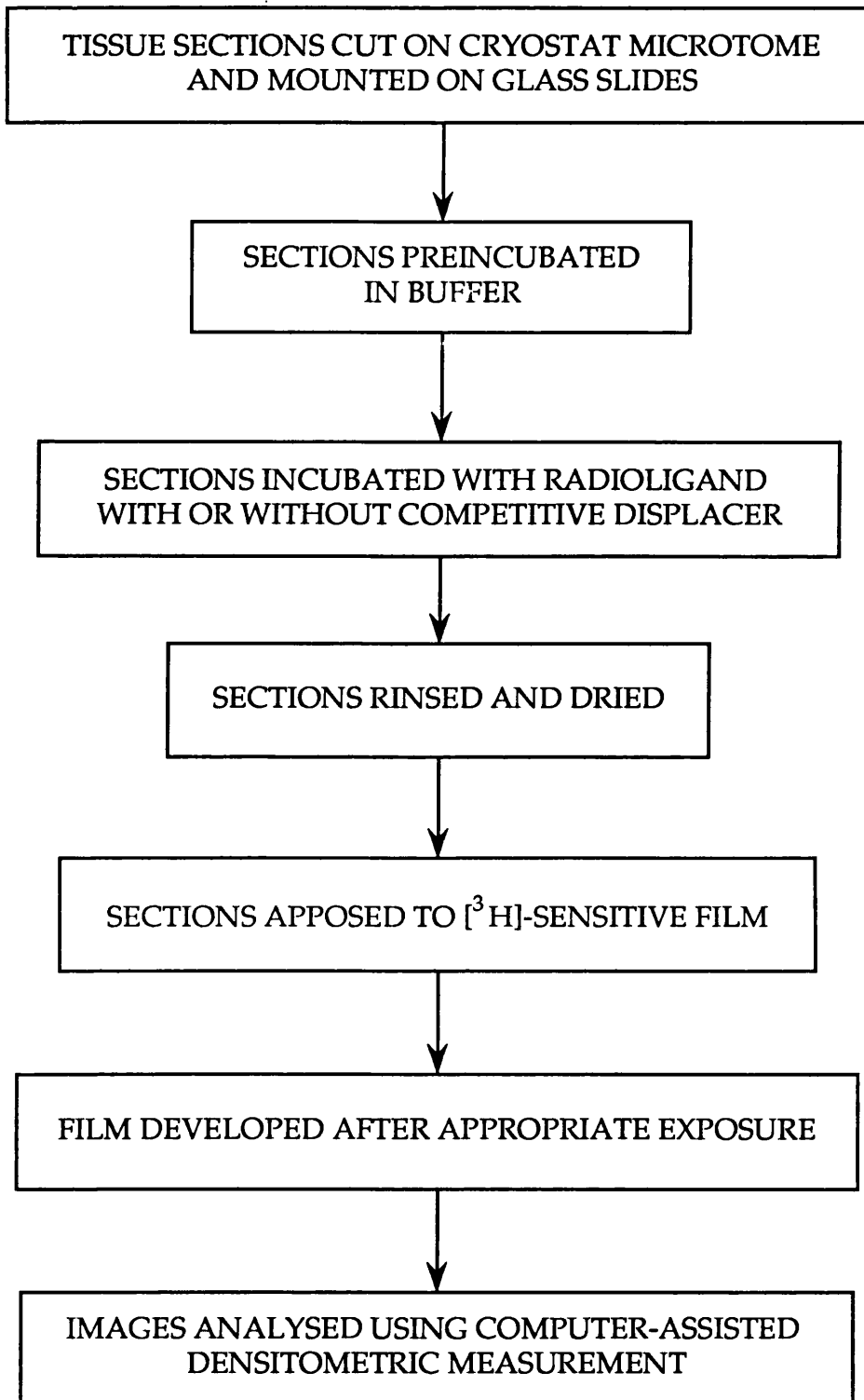


FIGURE 6: GENERAL PROCEDURE FOR QUANTITATIVE RECEPTOR AUTORADIOGRAPHY *IN VITRO*

drying cabinet.

Ligand concentrations (pmoles of ligand bound/g tissue) were estimated from the autoradiograms using computerised densitometry (Methods Section 1.4.), with reference to pre-calibrated tritium standards of known radioactivity (range 1060-17720 nCi/g tissue equivalent).

1.2.4. Chemicals

[³H]-Quinuclidinyl benzilate ([³H]-QNB, 44 Ci mmol⁻¹) and [³H]-glutamate (46 Ci mmol⁻¹) were purchased from Amersham International, Buckinghamshire, UK. [³H]-Kainate (59 Ci mmol⁻¹) and [³H]- α -3-hydroxy-5-methylisoxazole-4-propionic acid ([³H]-AMPA, 29.2 Ci mmol⁻¹) were obtained from New England Nuclear, Herts., UK.

Atropine sulphate, N-methyl-D-aspartate, kainate, quisqualate and potassium thiocyanate were purchased from Sigma Chemicals, UK. 4-Acetamido-4'-isothiocyano-stilbene-2,2'-disulfonic acid (SITS) was obtained from Fluka, Buchs, Switzerland.

1.3. ANALYSIS OF AUTORADIOGRAMS

Two computer-based densitometry systems were employed in the analysis of the autoradiograms. For most optical density measurements, a Quantimet 970 image analyser (Cambridge Instruments, England) was used. The autoradiograms were suspended on a fixed glass plate above a white stage, illuminated by four 24W lamps, whose intensity was controlled by the computer. Light from the lamps was reflected by the white stage, through the glass plate and autoradiogram, and was detected by a video camera. The image was digitised into pixels with a grey level in the range of 0-255 (grey-level of 255 corresponds with an optical density of 0; grey level of 1 corresponds to an optical density of 2.41). The

image was projected onto a live video screen for the user's reference.

The system was calibrated against each film, so that a calibration curve between 100% transmission (obtained when a blank part of film was in view) and zero transmission (measured when the lens cap was in place) was achieved.

Once the system had been calibrated, optical densities of the images produced by the pre-calibrated standards were measured, to provide a calibration curve of optical density versus radioactivity (nCi/g tissue equivalent). The optical densities of the images produced by the radio-labelled sections were subsequently quantified in terms of isotope concentration by reference to the standard curve. For each anatomical region of interest, the image analyser calculated three integrated optical density measurements, within a given frame of reference superimposed upon the region. The size of the reference frame could be altered between 9 and 900 pixels/frame (900 pixels represented 9mm²), but was kept constant between animals for each particular structure. Structures were defined anatomically with reference to a stereotaxic atlas (Paxinos and Watson 1986), and for each animal 3-6 sections were measured to give a mean optical density value for a given structure.

A modified densitometric approach was used in the analysis of several series of films in order to measure discrete regions of the hippocampus (Room & Tieleman, 1989). Following the production of autoradiograms, the radio-labelled sections were histologically stained, and superimposed on the autoradiographic image: this allowed detection of discrete "cortical" layers, which would not have been possible from the autoradiograms alone. For this procedure the IBAS 2000 analyser (Kontron, Munich, Germany) was used. This system differs substantially from the Quantimet 970 in its method of analysis. A light-box provided a diffuse light source upon which the autoradiogram or histological section was placed. The host computer was connected to a video camera suspended above the light-box: using the light-box as a reference the

system was calibrated, by detecting the grey level (range 0-255) of each pixel in view (field of view: 1.75 x 1.25cm, equal to 512 x 768 pixels). Thus a maximal transmission level was set for each pixel, and an allowance made for the possibility of uneven illumination from the light-box. Once the system had been calibrated, the autoradiogram was placed on the light-box. The whole image was digitised by averaging over 10 successive measurements, and the grey level for each pixel was stored. The autoradiogram was replaced by the corresponding histologically-stained section, the image of which in turn was stored. A Helmert transformation technique was used to measure the positions of at least four markers (such as bubbles in the section, etc.) and then rotate and magnify the histological image, with respect to the autoradiographic image, so that the two were aligned.

Densitometric measurements were made by drawing the outlines of distinct histologically-defined layers and regions on a digitiser tablet; the path of the pen was observed as a red line on the histological image stored and displayed on the video screen. Concurrently, the grey level of the outlined area was calculated from the stored autoradiographic image. Following measurement of each section, transmission from the light-box was re-measured, as a control against changing levels of light.

Optical density measurements were quantified in terms of radioactivity, as previously, with reference to pre-calibrated standards which were measured prior to analysis of each section. A total of 3-6 sections were measured for each given region of interest, and the mean values of radioactivity calculated.

1.4. STATISTICAL ANALYSIS

In studies with two groups, statistical analysis of results was performed using a two-tailed, unpaired Student's t-test. In studies with three or more groups, Bonferroni correction was used for multiple group comparisons (Wallenstein et al., 1980). Statistical significance was deemed to be achieved when $p < 0.05$.

2. LESIONS OF THE CNS

2.1. STEREOTAXIC LESIONS OF THE MEDIAL SEPTAL NUCLEUS

2.1.1. Theory: The Use of Ibotenic Acid as a Neurotoxin

Ibotenic acid is an analogue of glutamate with neurotoxic actions, and which has been employed widely to lesion specific cellular populations within the CNS (Fisher & Hanin, 1986; Smith, 1988). Injection of ibotenate has been shown to produce marked destruction of neurones, while axons of passage are spared (Schwarcz et al., 1979).

Ibotenic acid-induced lesions of the hippocampal afferents are now well established models of amnesia (Fisher & Hanin, 1986; Hagan & Morris, 1988; Smith, 1988); the advantage of ibotenic acid in this particular field of study is the lack of epileptogenic effects known to occur in glutamatergic systems following injection of kainic acid.

2.1.2. Animals

Surgery was performed on either adult male Sprague Dawley rats (Harlan Olac, Oxfordshire, UK), and Wistar rats (Cpb: Wu, TNO Zeist, Netherlands). Prior to surgery, rats were kept in a temperature-controlled environment, and fed ad libitum.

2.1.3. Chemicals

Ibotenic Acid (Cambridge Research Biochemicals Ltd, or Sigma Chemical Company Ltd, England) was dissolved in phosphate-buffered saline (0.1M, pH7.2) at a concentration of 10mg ml⁻¹. Once prepared, the solution was stored frozen until use, for a maximum period of two months.

2.1.4. Surgical Procedure

Injection into the medial septum of the buffered ibotenic acid solution was achieved using stereotaxic procedures. The rat was anaesthetised with chloral hydrate (400mgkg^{-1}) and diazepam (Valium, Roche England) (2mgkg^{-1}) injected intraperitoneally. The scalp was shaved and cleaned with an antiseptic surgical swab, and the rat was placed in a stereotaxic frame and restrained by use of ear bars and an incisor bar. The incisor bar was lowered 3.3mm, according to Paxinos and Watson (1986). The scalp was incised, and the underlying tissue retracted from the skull. Using a dental drill, a burrhole was made anterior to Bregma. The buffered ibotenic acid solution was delivered into the medial septum through a $1\mu\text{l}$ syringe (SGE, Ringwood, Australia), the needle of which had been placed 0.8mm anterior to Bregma, at the midline, and lowered 5.8mm below the surface of the dura. These coordinates have been previously defined (Wenk et al., 1984).

A total volume of $0.6\mu\text{l}$ ($6\mu\text{g}$ ibotenic acid) was injected into the medial septum at a rate of $0.1\mu\text{l min}^{-1}$. Following completion of the injection, the syringe was left in place for five minutes, to allow diffusion of the toxin away from the injection site; the syringe was then slowly withdrawn. Antibiotic powder (neomycin sulphate) was applied to the exposed skull and scalp, and the wound was sutured. The animal was removed from the frame, and maintained on a thermal blanket until recovery from anaesthesia was complete.

In order to control for surgical damage to the medial septum and surrounding tissues, sham-operated rats underwent a surgical procedure identical to that outlined above, but phosphate buffered saline medium only was injected into the medial septum.

2.1.5. Quantification of Extent of Lesion

The size and position of the lesion were assessed using the following histological methods.

Initially, a series of rats were placed in the stereotaxic frame as described, with the exception that no vehicle was injected; the rats were sacrificed immediately following the surgical procedure. The brains were rapidly dissected out and frozen, and the frontal portion was cut into 20 μ m sections in a cryostat. Sections were thaw-mounted on glass microscope slides, and the tissue was fixed and stained using thionine, cresyl violet/luxol fast blue, or haematoxylin and eosin. Under light microscopy, the position of the syringe was identified by a straight line of disrupted cells and fibres. Thus the accuracy of the chosen coordinates, was confirmed. A second series of experiments was performed to estimate the reproducibility of the lesion. Animals were allowed to survive post-operatively for three weeks. After this time, the animal was placed under deep halothane anaesthesia, and the brain was fixed by perfusion of approximately 200ml of 40% formaldehyde: acetic acid: methanol mixture (1:1:8 v/v/v). The brain dissected out and cryostat-sectioned, and alternate tissue sections were stained with either haematoxylin and eosin, or cresyl violet-luxol fast blue. The lesion site was quantified by light microscopy in order to determine both the size and position of the lesion. In two brains: one sham and one ibotenate-lesioned, staining for glial fibrillary acidic protein (GFAP) was performed by an independent neuropathologist (Professor D. I. Graham, Institute of Neurological Sciences, Southern General Hospital, Glasgow) to confirm the presence of glial cells within the lesioned tissue.

In subsequent series, rats were prepared surgically as described, and killed by decapitation, and the brains dissected out and frozen rapidly. The method of collection of material for histology was dependent on the protocols subsequently applied to the lesioned animals. In those brains which were used in autoradiographic investigations, cryostat cut sections

were collected adjacent to those sections used for autoradiography (Methods Section 1.2.2.). For all other brains, the portion rostral to the optic chiasma was separated and frozen. This portion was cryostat-cut into 20µm sections, and stained using one of the methods previously used. The extent of the lesion was assessed using light microscopy.

2.2. ACUTE SUBDURAL HAEMATOMA: A RAT MODEL OF FOCAL CEREBRAL ISCHAEMIA

2.2.1. Surgical Preparation

Under halothane anaesthesia, femoral arterial and venous cannulae were implanted in adult, male Sprague Dawley rats, in preparation for autoradiographic measurements (Methods Section 1.1.4). The rats were then turned prone, and a midline incision was made in the scalp. Using a dental drill, a 3mm burrhole was drilled approximately 2mm left of the sagittal suture and 3mm anterior to Bregma, over the parietal cortex. The dura was incised, and a J-shaped 23 gauge needle inserted into the subdural space. The burrhole was sealed around the needle with rapidly-setting glue. A haematoma was produced by injection of 0.4ml of non-heparinised autologous venous blood into the subdural space: the total injection time was seven minutes. The needle was then cut and the open end sealed to prevent back-flow of injected blood. Local anaesthetic gel was applied to the scalp and the wound was sutured. Animals were restrained and allowed to regain consciousness in preparation for autoradiography. Sham-operated control rats underwent the same surgical procedure, including placement of the needle, with the exception that no blood was injected into the subdural space.

2.2.3. Experimental Routines and Drug Administration

Two hours following production of ASDH, [^{14}C]-2-deoxyglucose (125 μCi in 0.7ml saline) was administered, and the deoxyglucose autoradiographic procedure was initiated. Prior to commencement of autoradiography, arterial blood pressure and rectal temperature were monitored continually. Arterial blood gases were sampled regularly, and normothermia was maintained with the use of a heating lamp.

In a series of animals, administration of the competitive glutamate antagonist, D-CPP-ene (Sandoz Research Institute Bern Ltd, Switzerland) was administered intravenously, at a concentration of 15mgkg $^{-1}$ in saline, 15 minutes before the ASDH was produced. Despite its apparently limited penetration of the CNS at short times after administration (McCulloch & Iversen, 1991) D-CPP-ene administration according to this regime has been shown to be neuroprotective in focal cerebral ischaemia in the cat (Bullock et al., 1990). Deoxyglucose autoradiography was performed two hours after production of the haematoma; at this time D-CPP-ene is predicted to reach its maximal CNS concentration, and the effects of D-CPP-ene could be compared with those produced in control animals (Methods Section 1.1.8.)

Twenty five minutes after the administration of deoxyglucose, 6.1 mCi of the blood flow tracer, $^{99\text{m}}$ -technecium-labelled Hexamethethylpropyleneamine oxime ([$^{99\text{m}}\text{Tc}$]-HMPAO; half life 6 hours) was injected intravenously, in order to measure blood flow and cerebral glucose use concurrently (Kuroda et al., 1992). Following deoxyglucose autoradiographic measurements, the animals were killed by decapitation, and the brains rapidly dissected and frozen in isopentane at -45°C and cut into 20 μm sections in a cryostat. Blood flow autoradiograms of [$^{99\text{m}}\text{Tc}$]-HMPAO were prepared by exposing the sections to radiation-sensitive film (LKB-Ultrafilm) for six hours. The sections were set aside for 72 hours to allow for decay of $^{99\text{m}}\text{Tc}$, then re-exposed to ^{14}C -sensitive film for two weeks. Deoxyglucose

autoradiograms were analysed as described previously; the results of blood flow measurements have been described elsewhere (Kuroda et al., 1992), and are not included as part of this study.

2.2.4. Quantification of Ischaemic Lesion

Quantitative neuropathological studies have been described in detail (Miller et al., 1990). At four hours after production of the haematoma, the region of infarct is clearly visible in sections stained with haematoxylin and eosin. The infarcted area can be defined as a sharply delineated region of pallor, bordering normal, densely stained tissue (Figure 7). Within the infarcted area, there is vacuolation of the neuropil and swelling of astrocytes. Hippocampal damage was not observed up to 24 hours following production of the haematoma; however, after four days, gross ultrastructural abnormalities were apparent in the nucleus, cytoplasm and endoplasmic reticulum (Bullock et al., 1991b).

Following production of autoradiograms in the present study, coronal sections were stained with haematoxylin and eosin, and the damage assessed by an independent neuropathologist (Professor D. I. Graham, Institute of Neurological Sciences, Southern General Hospital, Glasgow).

LEGEND TO FIGURE 7: HISTOLOGICAL ANALYSIS OF ACUTE
SUBDURAL HAEMATOMA IN THE RAT

- A. Diagram of the distribution of ischaemic damage at various stereotaxic planes through the rat brain.
- B. & C. Coronal sections stained with hematoxylin and eosin after acute subdural haematoma in the rat. Sections at the level of the frontal cortex (B) and the hippocampus (C) in a rat four hours after acute subdural haematoma. Note the region of **pallor** with a clearly defined margin beneath the haematoma.

Reproduced with kind permission from Mr Ross Bullock and colleagues (Miller et al., 1990).

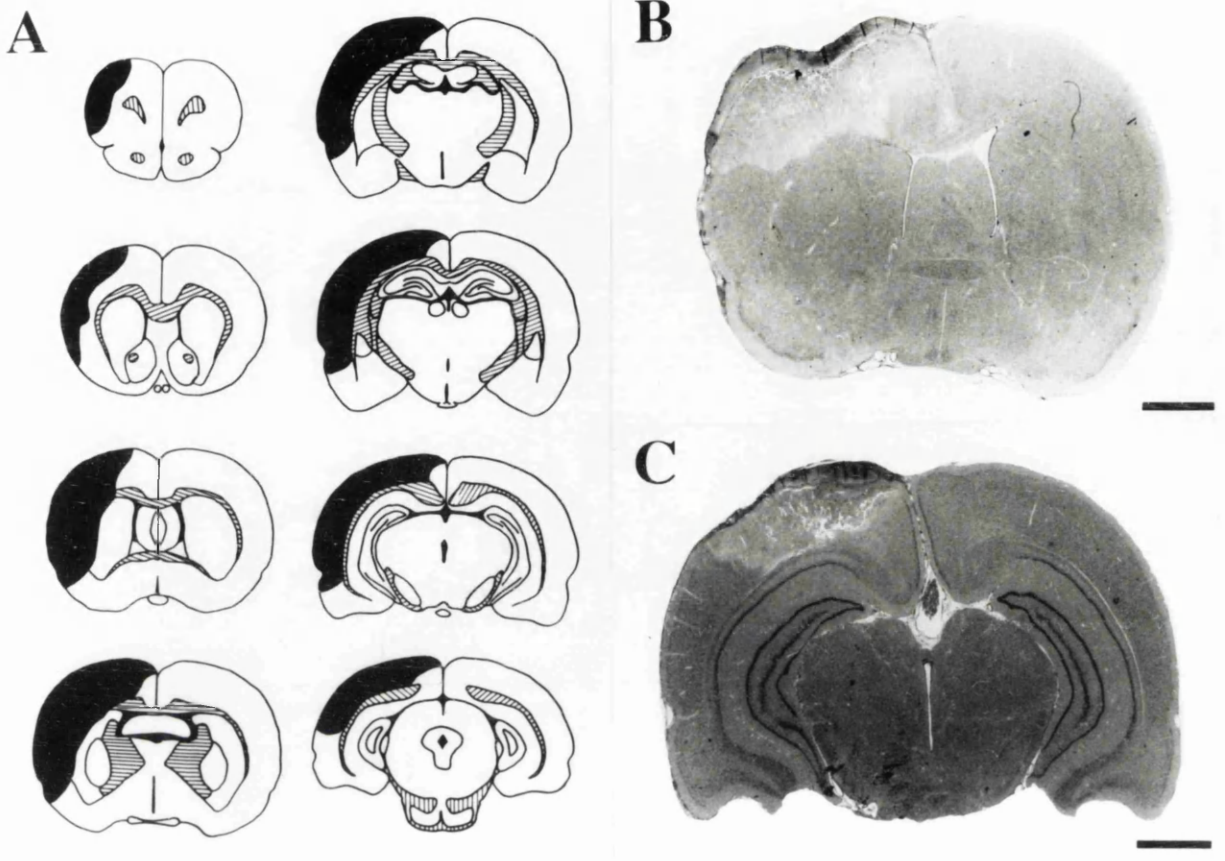


FIGURE 7: HISTOLOGICAL ANALYSIS OF ACUTE SUBDURAL HAEMATOMA IN THE RAT

3. BIOCHEMICAL ANALYSIS OF SECOND MESSENGER SYSTEMS IN THE HIPPOCAMPUS: ESTIMATION OF PHOSPHOINOSITIDE TURNOVER

3.1. Theory and Background to Assay

There are now known to exist several second messenger systems, which are activated by the association of a specific receptor and its neurotransmitter, resulting in the modification of cellular responses. One of these is the phosphoinositide cycle, (Figure 8) and activation of a number of receptor types and sub-types is thought to be linked to phosphoinositide metabolism.

When an agonist binds to a receptor linked to the phosphoinositide signalling system, the resultant agonist-receptor complex leads to the stimulation of a phosphoinositide-specific phospholipase C. Activation of this enzyme results in the hydrolysis of phosphatidyl-inositol 4,5-bisphosphate (PIP_2) to form diacylglycerol (DAG) and inositol 1,4,5-trisphosphate (IP_3). Both products have second messenger actions: IP_3 has been demonstrated to mobilise calcium ions from endoplasmic reticulum, the putative stimulus for many enzymes and cellular reactions, while DAG activates protein kinase C thus resulting in protein phosphorylation, and further modification of cell function.

DAG is inactivated by its conversion to phosphatidic acid by DAG kinase; phosphatidic acid reacts with cytidine triphosphate, resulting in the formation of cytidine diphosphodiacylglycerol (CDP-DAG), which is ultimately used in the re-synthesis of PIP_2 . IP_3 is broken down and thus inactivated by a phosphatase, yielding inositol 1,4-bisphosphate (IP_2). Further metabolism of IP_2 leads to formation of inositol phosphate and subsequently myo-inositol, which combines with CDP-DAG in the re-synthesis of PIP_2 . Re-synthesis involves a number of intermediary stages: CDP-DAG and myo-inositol combine to form phosphatidylinositol, which is phosphorylated to form

LEGEND TO FIGURE 8: THE PHOSPHOINOSITIDE CYCLE

Schematic diagram of agonist-dependent phosphoinositide hydrolysis. Activation of phospholipase leads to hydrolysis of phosphatidylinositol 4,5 bisphosphate (PIP₂), resulting in the formation of diacylglycerol (DAG) and inositol 1,4,5 trisphosphate (IP₃). DAG and IP₃ have second messenger activities: DAG activates protein kinase C (PKC), while IP₃ mobilises intracellular Ca²⁺ stores, resulting in phosphorylation of phosphoproteins (PP) such as membrane channels. DAG is converted to phosphatidic acid (PA) via DAG kinase; PA reacts with cytidine diphosphate (CDP) to form cytidine diphosphodiacylglycerol (CDP-DAG). IP₃ is metabolised to myo-inositol via inositol bisphosphate (IP₂), and inositol phosphate (IP); lithium chloride prevents the breakdown of PI to myo-inositol. IP₃ may also be metabolised to other inositol phosphates with second messenger activity, such as IP₄.

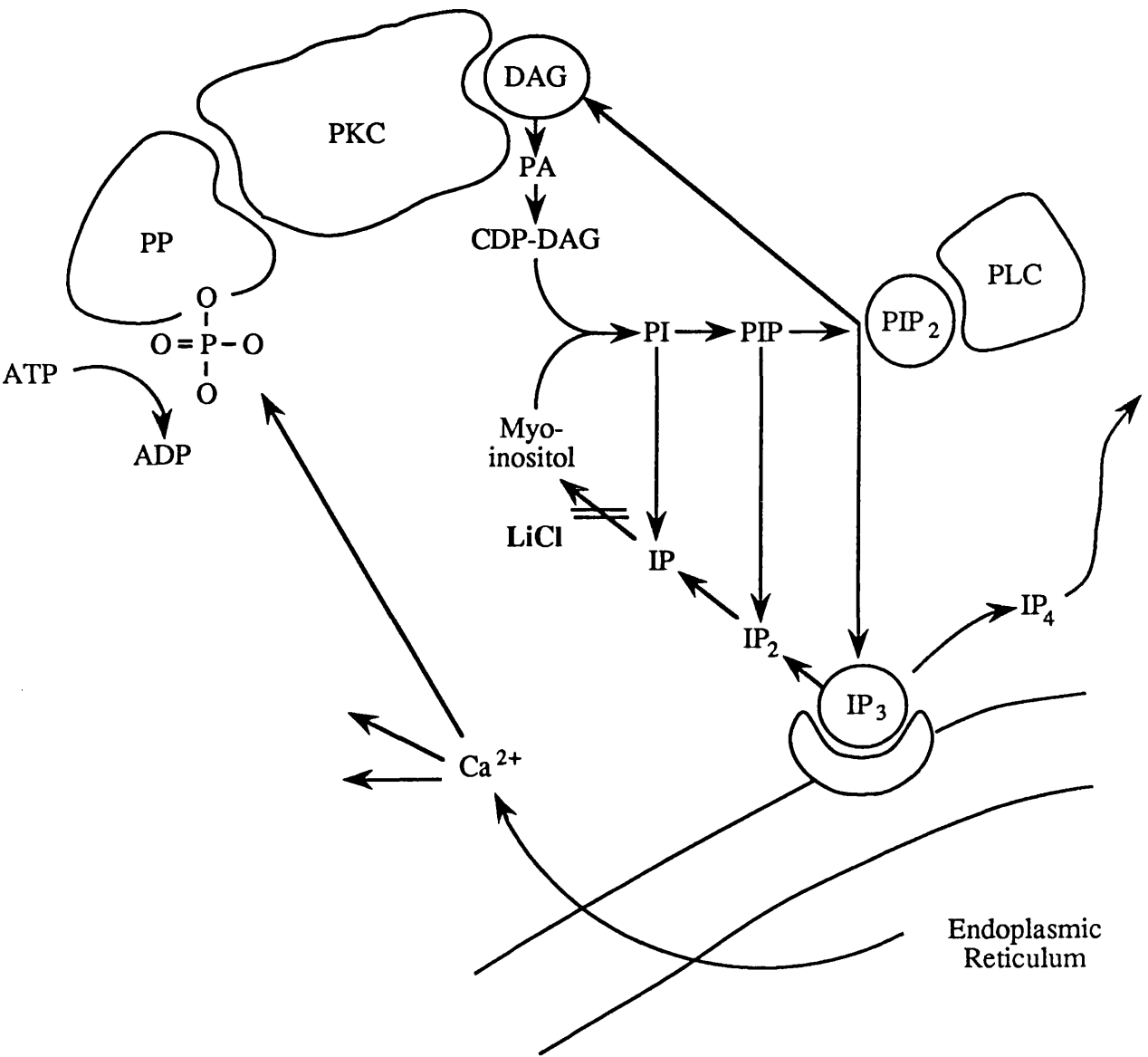


FIGURE 8: THE PHOSPHOINOSITIDE CYCLE

phosphatidylinositol 4-phosphate (PIP), and then further phosphorylated to PIP₂ by two distinct kinases. Thus, the cyclic breakdown and re-synthesis of PIP₂ in response to receptor-agonist interaction represents a complex second messenger signalling system which results in the modulation of cell function.

The discovery that lithium inhibits the phosphatase enzyme which mediates the breakdown of inositol phosphate to myo-inositol provided an indirect method for the estimation of the total amount of phosphatidyl hydrolysis in a given period (Gonzales & Crews, 1984; Janowsky et al., 1984). Briefly, tissue slices are incubated with [³H]-labelled myo-inositol, which is incorporated into phosphatidylinositol, and further metabolised to PIP₂. To the medium is added lithium chloride, and an agonist known to exert its effects through activation of the phosphoinositide cycle. Agonist-receptor interaction will thus result in the breakdown of PIP₂, and stimulation of phosphatidylinositol turnover, as described. The presence of lithium, however, prevents the hydrolysis of inositol phosphate and results in accumulation of [³H]-inositol phosphate, which may be separated from other inositol lipids by ion-exchange chromatography, and quantified using liquid scintillation analysis. The total accumulation of [³H]-inositol phosphate may thus be used as an indication of agonist-induced activity of the phosphoinositide cycle.

3.2. Method

Experiments were performed on adult male Wistar rats (Cpb: Wu, TNO, Zeist, Netherlands), which had previously undergone surgery to lesion the medial septal nucleus of the brain (Methods Section 2.1.4.). Rats were killed by decapitation, and the brains rapidly removed and placed on ice. The frontal portion of the brain was removed and processed histologically for quantification of the lesion. The

hippocampus was dissected out and chopped into 0.35mm² slices using a McIlwain tissue chopper, and suspended in 50ml Kreb's Ringer bicarbonate buffer (KRBB) at room temperature. Sections were washed once with KRBB at 37°C and re-suspended in 50ml fresh KRBB. To remove endogenous agonists, slices were incubated for 30 minutes at 37°C in a shaking waterbath, under a constant stream of 95% oxygen: 5% carbon dioxide. Following the incubation, the buffer was aspirated, and 50ml aliquots of the remaining slurry (containing approximately 15mg tissue) were transferred to glass micromedia tubes (Otan, Rijsbergen, Netherlands). For each brain, a total of four samples were collected. To each sample was added 200µl [³H]-myo-inositol (final concentration 250 nM), and the samples were incubated as previously for 45 minutes. Following the incubation, 25µl of lithium chloride solution (final concentration 10mM) was added, and the sections further incubated for 10 minutes. Agonist-induced phosphoinositide turnover was estimated in two of the four samples for each brain, by the addition of the muscarinic agonist carbachol (25µl, final concentration 500µM). Basal phosphoinositide turnover was estimated in the remaining two samples, following the addition of 25µl KRBB. The final incubation solutions were incubated under the conditions described for 60 minutes.

Accumulation of inositol phosphate was terminated by the addition of 2.5ml ice-cold KRBB to the medium. The buffer and incubation solutions were aspirated, and the slices were washed twice with 2.5ml ice-cold KRBB. Following the second wash the KRBB was aspirated and 0.9ml of a chloroform and methanol mixture was added to elute the inositol compounds from the tissue slices. After 10 minutes, 0.3ml chloroform and 0.3ml ultrapure water (Milli-Q 200µm filter) were added, and the mixture was centrifuged at 500g_{avc} for 15 minutes. This resulted in a separation of the solution into aqueous and organic layers: 0.8ml of the aqueous supernatant, containing the inositol compounds, was transferred to a polypropylene column filled with 1ml anion exchange

resin (AG1-X8 formate form, 100-200 mesh, and Econo-Column, Bio-Rad, California, USA). The column was washed with 10ml ultrapure water to remove uncharged moieties, and 0.6ml ammonium formate to elute non-metabolised [^3H]-myo-inositol. Finally, [^3H]-inositol phosphate was eluted with 1.6ml ammonium formate, and the filtrate was collected in scintillation vials. To each vial was added 8ml liquid scintillant (Picofluor 30), and the concentration of isotope was determined by liquid scintillation analysis. Finally, choline acetyltransferase (ChAT) activity was measured in hippocampal slices according to the micro-assay developed by Fonnum (1975).

3.3. Analysis of Results

[^3H]-inositol phosphate accumulation for each animal was calculated from the data obtained by liquid scintillation analysis and expressed in DPM. Basal and carbachol-stimulated [^3H]-inositol phosphate accumulation in sham and lesioned rats, and the percentage of carbachol stimulation of [^3H]-inositol phosphate accumulation for sham and lesioned rats, were compared statistically using unpaired, 2-tailed Student's t-test. ChAT activity in lesioned and sham-operated animals was compared statistically using Student's t-test, and the relationship between ChAT activity and basal and stimulated [^3H]-inositol phosphate accumulation were determined using linear regression analysis.

3.4. Materials

Kreb's Ringer bicarbonate buffer (KRBB; NaCl, 118mM; KCl, 5mM; $\text{CaCl}_2 \cdot 2\text{H}_2\text{O}$, 2.5mM; KH_2PO_4 , 2mM; $\text{MgSO}_4 \cdot 7\text{H}_2\text{O}$, 2mM; Na_2 EDTA, 0.2mM; NaHCO_3 , 24mM; glucose, 10mM) was prepared using ultrapure water (MilliQ). All reagents were of analytical grade, and were obtained from Baker Chemicals, Netherlands.

Myo-inositol (Sigma Chemical Co., St. Louis, USA), Carbachol (Brocacef, Maarsden, Netherlands), and Lithium chloride (Baker Chemicals, Deventer, Netherlands) were dissolved in KRBB.

[2-³H(N)]-myo-inositol (specific activity 16Ci/mmol) was obtained from New England Nuclear, Boston, USA.

The liquid scintillation fluid used was Picofluor 30 and was obtained from Packard Instruments, Downer's Grove, Illinois, USA).

CHAPTER III

RESULTS

1. EFFECTS OF GLUTAMATERGIC AND CHOLINERGIC AGENTS ON CEREBRAL GLUCOSE USE

1.1. GENERAL OBSERVATIONS

Administration of the competitive glutamate antagonist D-CPP-ene resulted in a marked dose-dependent sedation in conscious, restrained rats: exploratory behaviour, present in saline-treated control animals was abolished following administration of 30mgkg^{-1} D-CPP-ene. In these animals a slight tail tremor was present. Mean arterial blood pressure was seen to increase slowly over a two hour period; however, neither the mean arterial pressure nor the average increase in blood pressure was significantly different in the D-CPP-ene treated rats compared to control animals (Appendix I, Table 1). Finally, two hours and 35 minutes after administration of 30mgkg^{-1} D-CPP-ene, rats had significantly lower arterial pH than saline-treated controls. Other physiological parameters remained unchanged after administration of D-CPP-ene.

Animals treated with the muscarinic agonist L-679-512 showed a marked accentuation of exploratory behaviour, coupled with signs of stress: sniffing and chewing became more frequent, and lacrimation was apparent. Muscle fasciculation and a tail tremor were also observed. These responses were dose-dependent, and most evident following the highest dose of $30\mu\text{gkg}^{-1}$. In rats which received $30\mu\text{gkg}^{-1}$ L-679-512, a profound bradycardia occurred within a minute of intravenous administration of the drug; this was accompanied by a transient decrease in blood pressure. At the time of deoxyglucose administration, however, the mean arterial pressure and the average change in blood pressure were not significantly different to that measured prior to drug injection (Appendix II, Table 1). A decrease in

arterial CO_2 (PaCO_2) was apparent following administration of L-679-512 (3 and $30\mu\text{gkg}^{-1}$). Additionally, L-679-512 (10 and $30\mu\text{gkg}^{-1}$) induced an increase in plasma glucose, which persisted until the end of the experiment. Other physiological parameters were unaltered after drug administration.

The cholinesterase inhibitor amino-tetrahydroacridine (THA) also induced a marked accentuation of exploratory behaviour, sniffing, chewing and lacrimation. In addition, muscle fasciculation and a tail tremor were also present. Mean arterial pressure increased in response to THA administration, and was significantly elevated at the time of deoxyglucose administration; furthermore, the average change in arterial pressure was found to be significantly increased in the THA-treated group (Appendix III, Table 1). A decrease in arterial CO_2 (PaCO_2) and an increase in arterial plasma glucose was observed in response to THA administration. Other physiological parameters were unaltered following drug administration.

1.2. LOCAL CEREBRAL GLUCOSE UTILISATION

Local Cerebral Glucose Utilisation was estimated in 76 anatomically defined areas following intravenous administration of D-CPP-ene (0.3, 3 or 30mgkg^{-1}), L-679-512 (0.3, 10 or $30\mu\text{gkg}^{-1}$), amino-tetrahydroacridine (THA, 2.5mgkg^{-1}). Patterns of glucose utilisation produced by each drug were compared with glucose use in groups of contemporaneous saline-treated control rats. Details of mean rates of glucose utilisation in each structure are given in Appendices I-III.

1.2.1. D-CPP-ene, a Competitive NMDA Antagonist

D-CPP-ene, a competitive glutamate antagonist, induced heterogeneous alterations in glucose use (Appendix I). In 52 of the 76 regions analysed, D-CPP-ene administration did not at any dose produce significant alterations in glucose utilisation compared to saline-treated controls. Of the remaining 24 regions, significant functional alterations were measured only in those animals which received 3 or 30mgkg⁻¹ D-CPP-ene. Significant decreases in glucose use occurred in twelve regions of brain: these were mostly cortical areas, or subcortical structures involved in processing sensory information. In contrast, significant increases in glucose use were measured in four regions involved in olfaction. In another eight regions involved mostly in limbic function, a biphasic response to D-CPP-ene was observed: glucose use was significantly depressed after the intermediate dose of 3mgkg⁻¹ D-CPP-ene, but was not significantly different from control value in those animals which received 30 mgkg⁻¹ D-CPP-ene.

Hippocampal Region

Following the intermediate dose of 3 mgkg⁻¹ D-CPP-ene, glucose use was decreased significantly in two hippocampal areas (Appendix I, Table 2 and Figures 9 & 10): rates of glucose utilisation were decreased in the subiculum and the pyramidal layer of the CA4 region by 22% and 31% respectively. Glucose utilisation in these structures remained unchanged with respect to control values following administration of 0.3 or 30mgkg⁻¹. Although there were no other significant alterations in the hippocampus in response to D-CPP-ene administration, it was noted that the mean value for glucose use in response to 3mgkg⁻¹ in each hippocampal area measured was lower than the control value, while rates of glucose use following 3 or 30mgkg⁻¹ D-CPP-ene were comparable to control values.

LEGENDS TO FIGURES 9 AND 10

FIGURE 9: Local cerebral glucose utilisation in the hippocampus following D-CPP-ene administration: Ammon's Horn.

FIGURE 10: Local cerebral glucose utilisation in the hippocampus following D-CPP-ene administration: Dentate gyrus, presubiculum and subiculum.

Data are presented as mean glucose utilisation ($\mu\text{mol } 100\text{g}^{-1} \text{ min}^{-1}$) \pm S.E.M. * $p < 0.05$ relative to control (Student's unpaired t-test, two-tailed, with Bonferroni correction for multiple group comparison).

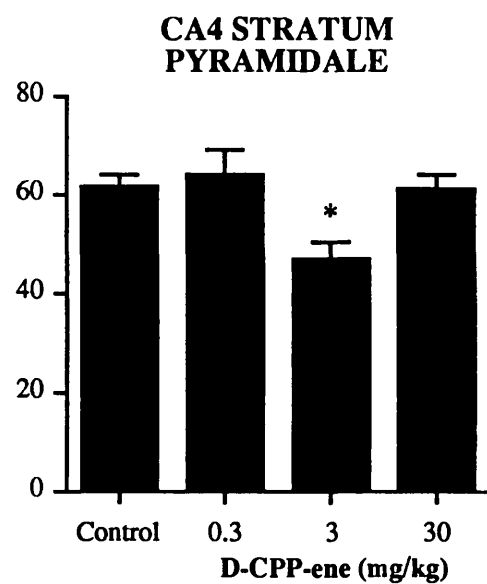
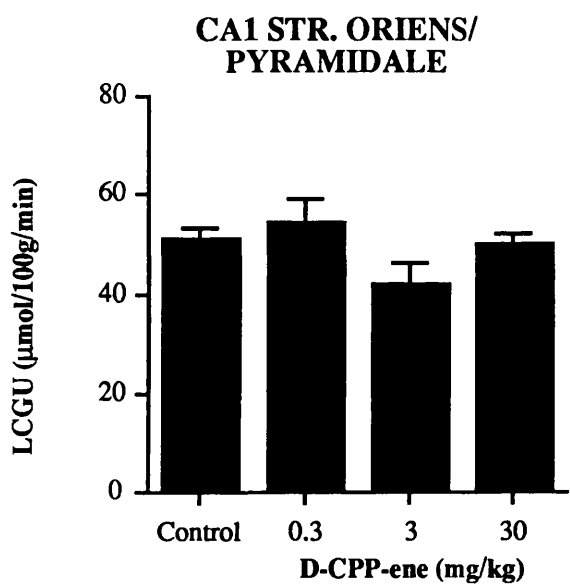
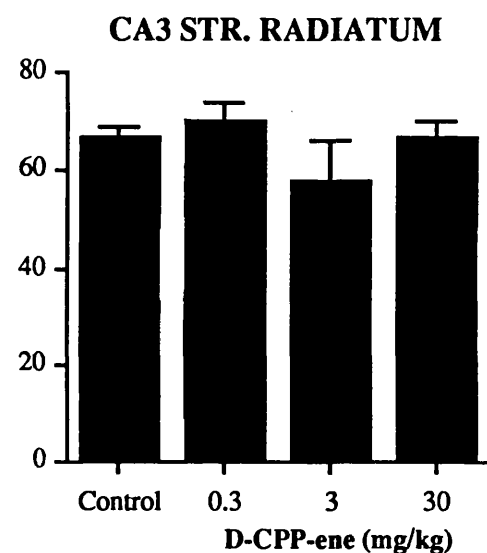
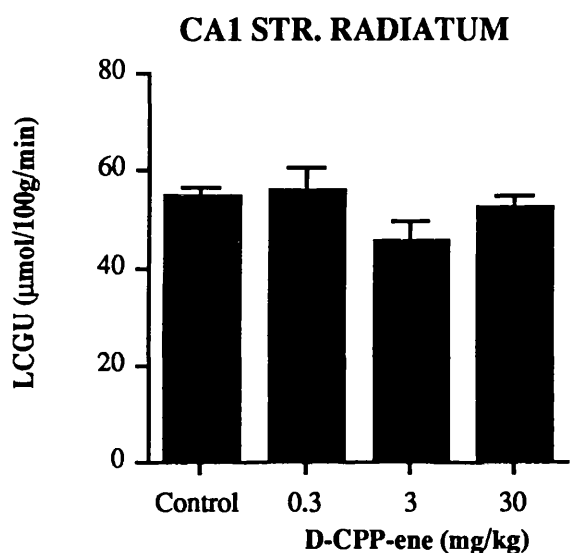
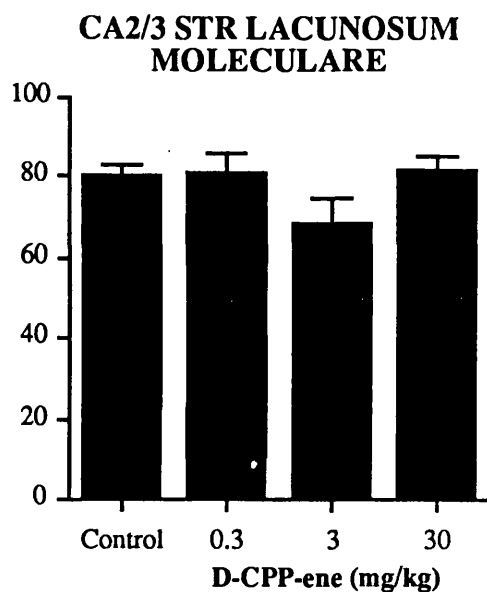
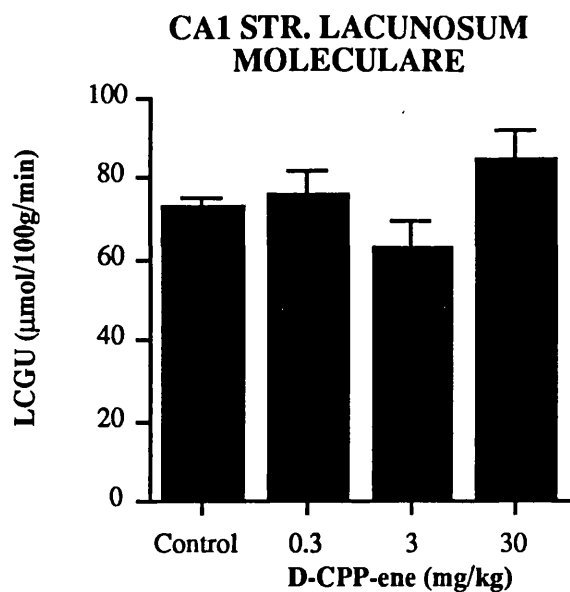


FIGURE 9 : LOCAL CEREBRAL GLUCOSE UTILISATION IN THE HIPPOCAMPUS FOLLOWING D-CPP-ENE ADMINISTRATION: AMMON'S HORN

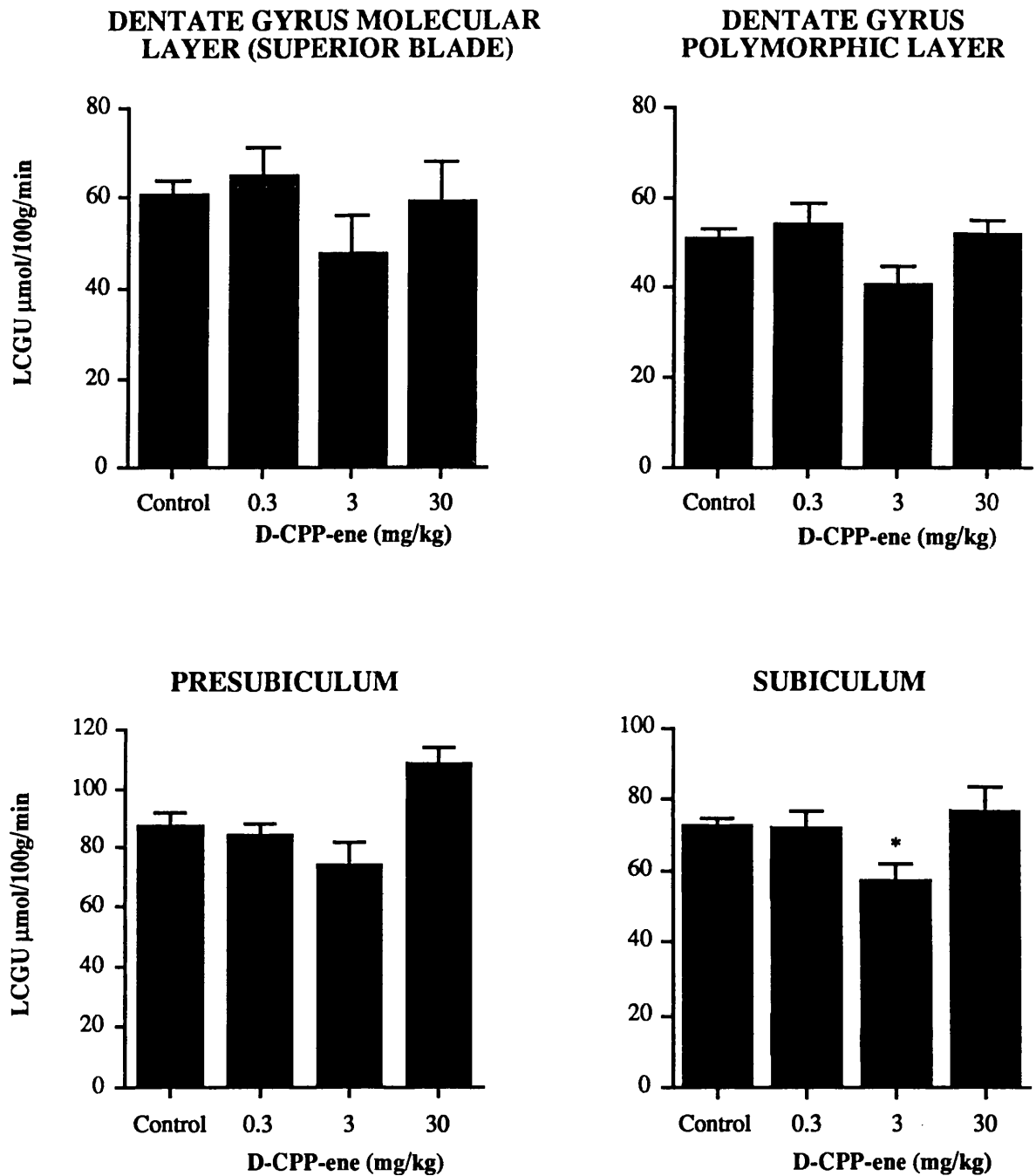


FIGURE 10 : LOCAL CEREBRAL GLUCOSE UTILISATION IN THE HIPPOCAMPUS FOLLOWING D-CPP-ENE ADMINISTRATION: DENTATE GYRUS, PRESUBICULUM AND SUBICULUM

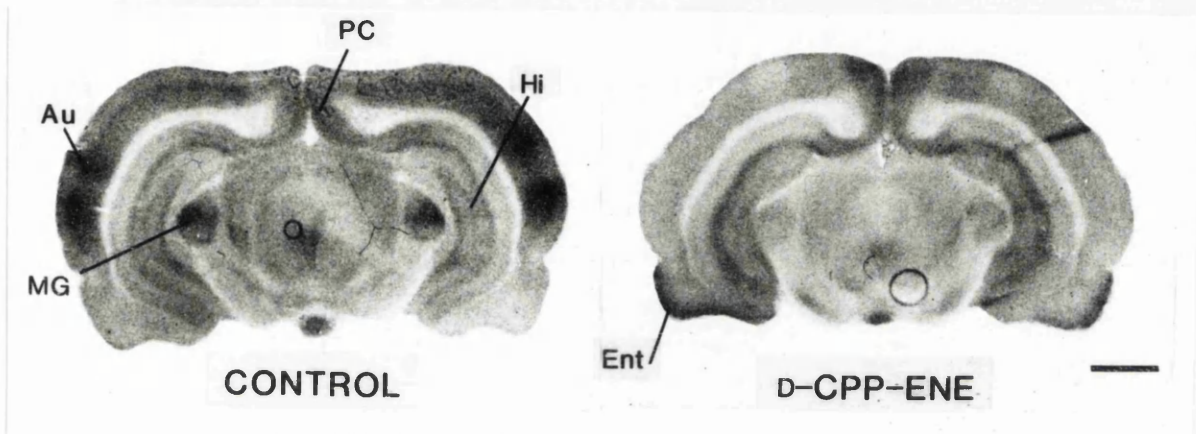


FIGURE 11: AUTORADIOGRAMS OF GLUCOSE UTILISATION IN THE RAT BRAIN FOLLOWING D-CPP-ENE: HIPPOCAMPUS, AUDITORY AND VISUAL REGIONS

Representative autoradiograms of glucose use in the rat brain at the level of the ventral hippocampus, auditory and visual regions following D-CPP-ene administration. Left: control animal. Hippocampus (Hi), posterior cingulate cortex (PC), auditory cortex (Au), and medial geniculate nucleus (MG) are indicated by solid lines. Right: D-CPP-ene-treated (30 mgkg^{-1}) animal. Note the increased deoxyglucose uptake in the entorhinal cortex (Ent) and decreased deoxyglucose uptake in auditory and visual structures in the D-CPP-ene-treated animal compared to control. Scale bar equals 2mm.

Areas Associated with Limbic Function

Rates of glucose use following D-CPP-ene administration in limbic structures other than the hippocampus are given in Appendix I, Table 3. Heterogeneous functional alterations were recorded in response to 3 and 30mgkg⁻¹ D-CPP-ene. In three cortical areas, the anterior cingulate, frontal and parietal cortices, a marked dose-dependent decrease in glucose utilisation was observed: a dose of 30mgkg⁻¹ D-CPP-ene effected a reduction in glucose use of 44% in the parietal cortex relative to the control value. In contrast, glucose utilisation in the posterior cingulate cortex was not significantly altered with respect to the control value (Figure 12).

In four limbic subcortical structures, the dorsal tegmental nucleus, the medial and lateral portions of the mamillary body, and the nucleus accumbens, glucose use was significantly suppressed following 3mgkg⁻¹ D-CPP-ene, but not different from control values following 0.3 or 30mgkg⁻¹ D-CPP-ene. Finally, glucose utilisation in the lateral amygdalar nucleus decreased in a dose-dependent manner, and was significantly lower than the control value after administration of 30mgkg⁻¹ D-CPP-ene (Figure 13).

Olfactory Areas

D-CPP-ene effected the largest increase in glucose utilisation in areas involved in the processing of olfactory information (Appendix I, Table 4). Of six olfactory regions measured, significantly increased glucose utilisation was observed in four regions following administration of 30mgkg⁻¹ (Figures 15 & 16). In two, the lateral olfactory tract and the posterior piriform cortex, there was evidence of a dose-dependent mechanism of drug action. In the lateral olfactory tract the largest elevation in glucose use was recorded: 30mgkg⁻¹ D-CPP-ene induced a 62% increase with respect to control values. In the entorhinal cortex and anterior olfactory nucleus significant increases in glucose use (43%)

LEGENDS TO FIGURES 12 AND 13

FIGURE 12: Local cerebral glucose utilisation in cortical areas associated with limbic function following D-CPP-ene administration.

FIGURE 13: Local cerebral glucose utilisation in subcortical limbic areas following D-CPP-ene administration.

Data are presented as mean glucose utilisation ($\mu\text{mol } 100\text{g}^{-1} \text{ min}^{-1}$) \pm S.E.M. * $p < 0.05$, ** $p < 0.01$ relative to control (Student's unpaired t-test, two-tailed, with Bonferroni correction for multiple group comparison).

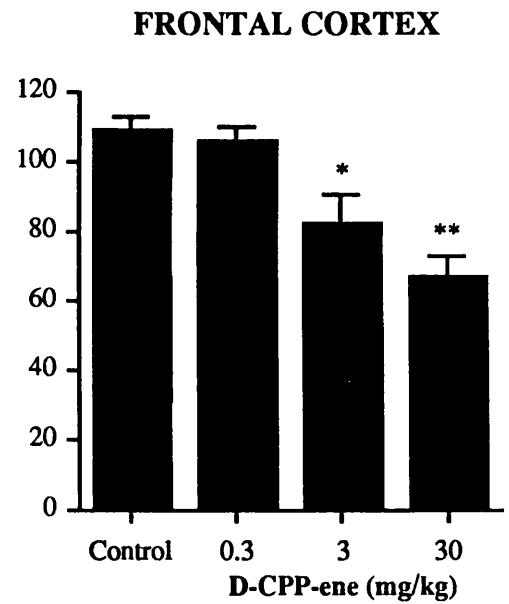
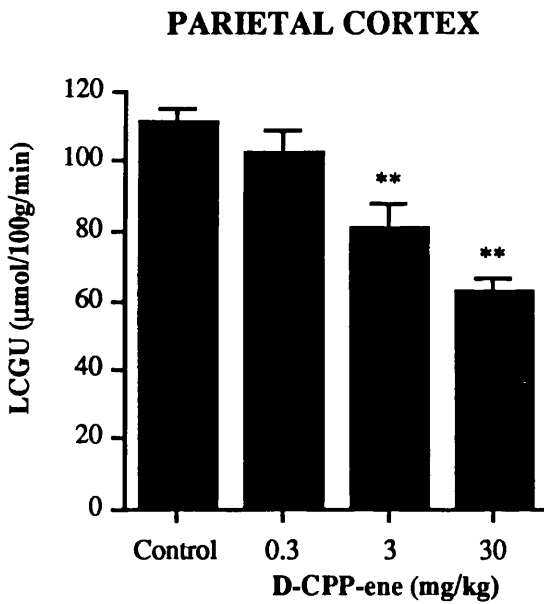
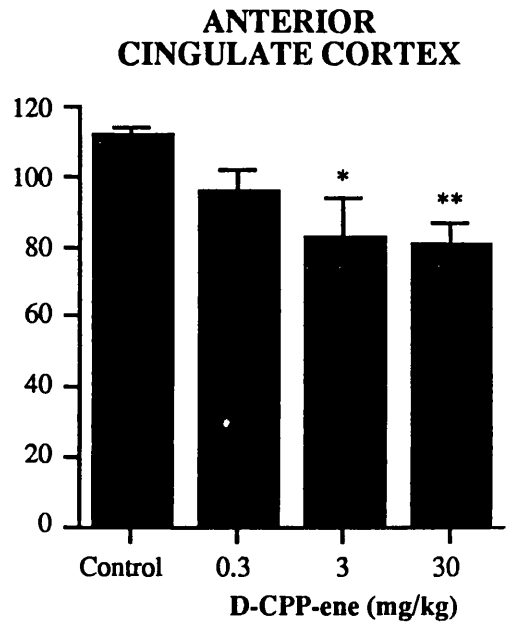
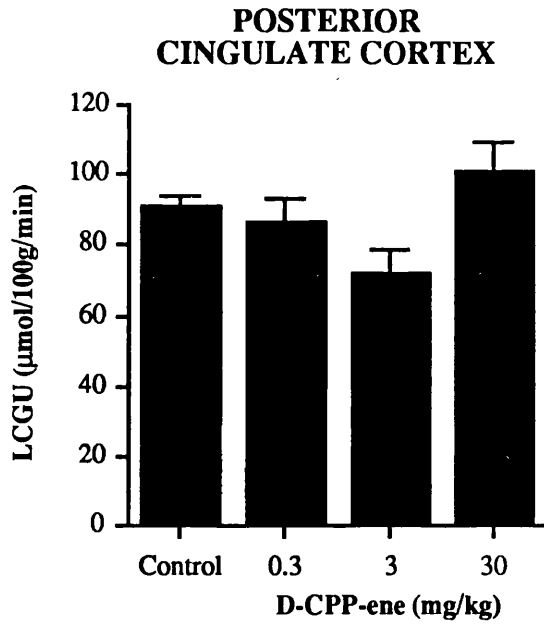


FIGURE 12 : LOCAL CEREBRAL GLUCOSE UTILISATION IN CORTICAL AREAS ASSOCIATED WITH LIMBIC FUNCTION FOLLOWING D-CPP-ENE ADMINISTRATION

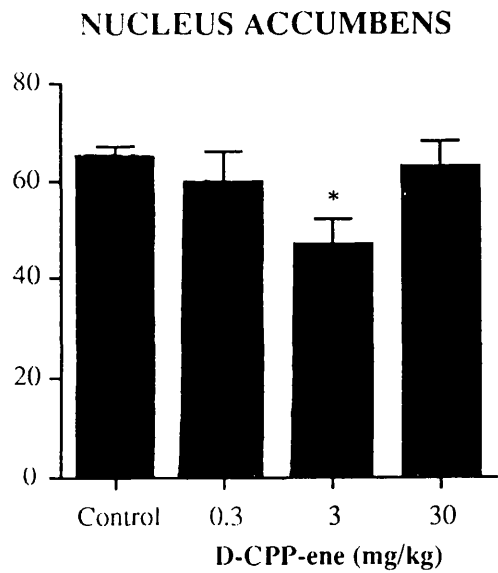
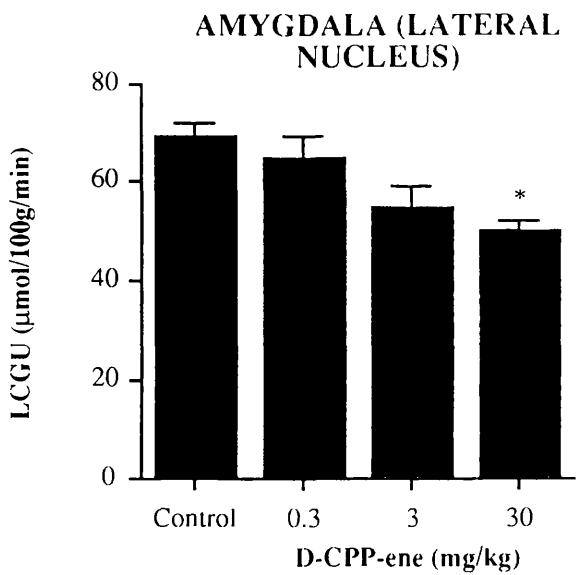
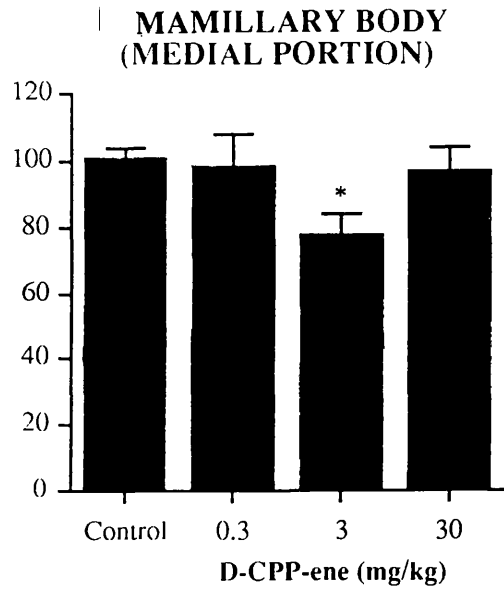
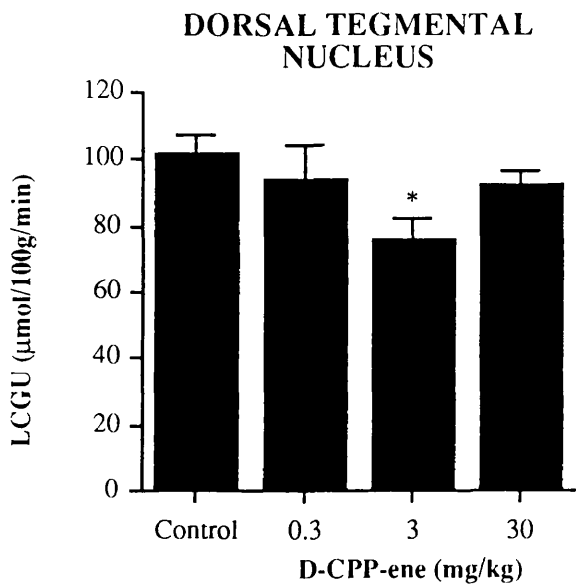


FIGURE 13 : LOCAL CEREBRAL GLUCOSE UTILISATION IN LIMBIC STRUCTURES FOLLOWING D-CPP-ENE ADMINISTRATION: SUBCORTICAL AREAS

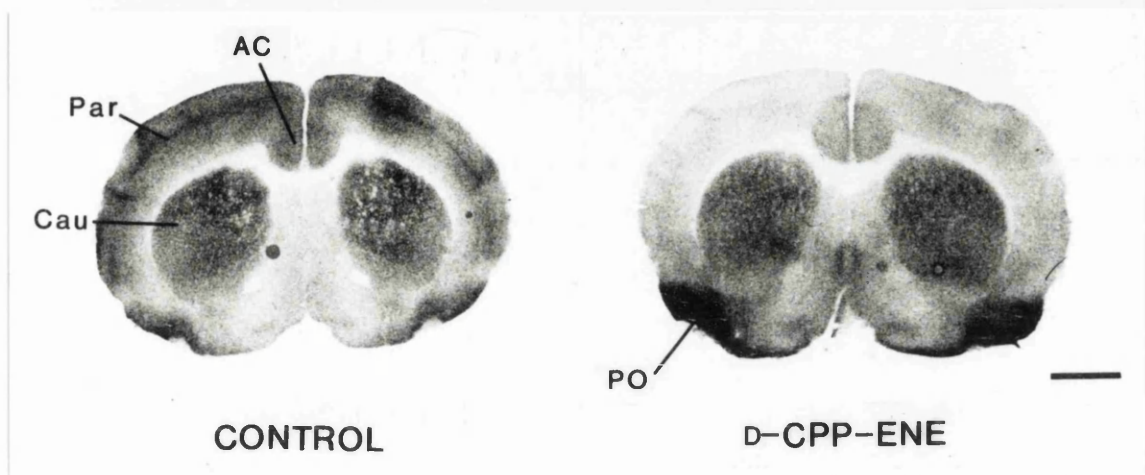


FIGURE 14: AUTORADIOGRAMS OF GLUCOSE UTILISATION IN THE RAT BRAIN FOLLOWING D-CPP-ENE: PARIETAL CORTEX

Representative autoradiograms of glucose use in the rat brain at the level of the parietal cortex in response to D-CPP-ene administration. Left: control animal. Anterior cingulate cortex (AC), parietal cortex (Par) and caudate (Cau) are indicated by solid lines. Right: D-CPP-ene-treated (30 mgkg^{-1}) animal. Note the reduction in optical density in parietal and anterior cingulate cortices in the D-CPP-ene-treated animal compared to control. In contrast, the optical density of the primary olfactory cortex (PO) is increased in the D-CPP-ene-treated animal compared to control. Scale bar equals 2mm.

were evident after administration of 30mgkg^{-1} D-CPP-ene (Figure 15).

Auditory and Visual Structures

Administration of D-CPP-ene produced profound dose-dependent alterations in glucose utilisation within structures involved in processing auditory and visual information (Appendix I, Table 5 and Figures 11 & 17). Significantly decreased glucose utilisation was observed after administration of 30mgkg^{-1} D-CPP-ene in eight out of fourteen regions in this group; in six of these, glucose utilisation was also suppressed significantly following 3mgkg^{-1} D-CPP-ene. The largest reductions in glucose utilisation were measured in cortical areas: in layer IV of the auditory and visual cortices, in which 30mgkg^{-1} D-CPP-ene induced 49% and 41% reductions respectively, and in layer II of the auditory cortex a decrease of 40% was measured. The medial geniculate body and the inferior colliculus were also greatly affected, with respective reductions of 39% and 35% in response to 30mgkg^{-1} D-CPP-ene. Other alterations in glucose use occurred in the dorsolateral geniculate body, the anterior pretectal nucleus, and the superficial layer of the superior colliculus following 3 and 30mgkg^{-1} D-CPP-ene.

Extrapyramidal and Sensorimotor Areas

Few alterations in glucose utilisation could be evoked in extrapyramidal and sensorimotor regions by D-CPP-ene (Appendix I, Table 6). Administration of D-CPP-ene at a dose of 3mgkg^{-1} evoked a decrease in glucose use in two structures, the cerebellar hemisphere, and the inferior olive. Administration of 3 or 30mgkg^{-1} D-CPP-ene, however did not produce a significant deviation from the control value for either structure. Glucose use was unchanged by D-CPP-ene administration at any dose in ten other structures within this group.

LEGEND TO FIGURE 15

FIGURE 15: Local cerebral glucose utilisation in olfactory areas in response to D-CPP-ene administration.

Data are presented as mean glucose utilisation ($\mu\text{mol } 100\text{g}^{-1} \text{ min}^{-1}$) \pm S.E.M. ** $p < 0.01$ relative to control (Student's unpaired t-test, two-tailed, with Bonferroni correction for multiple group comparison).

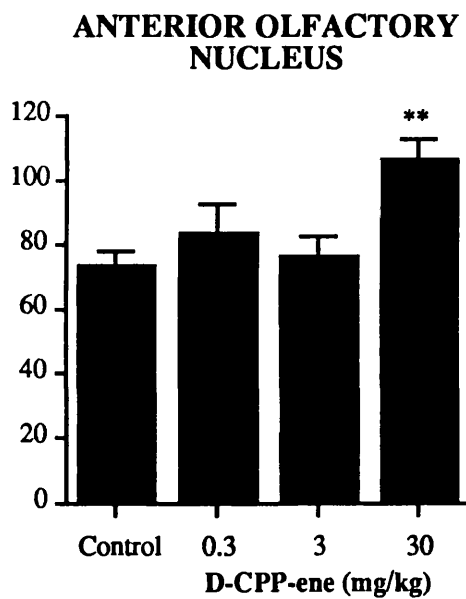
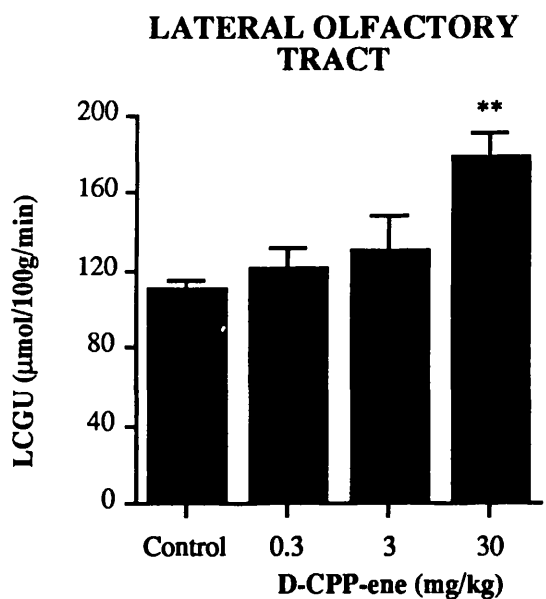
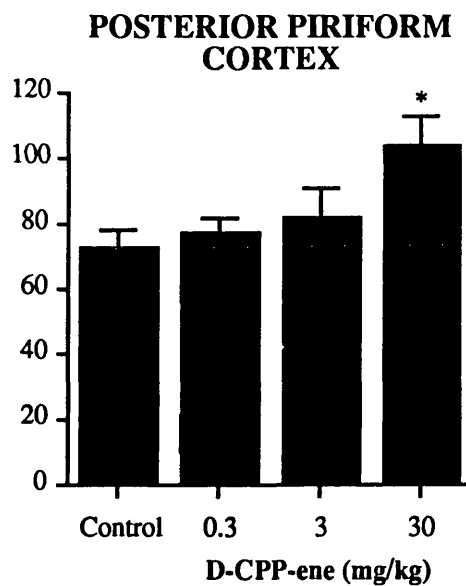
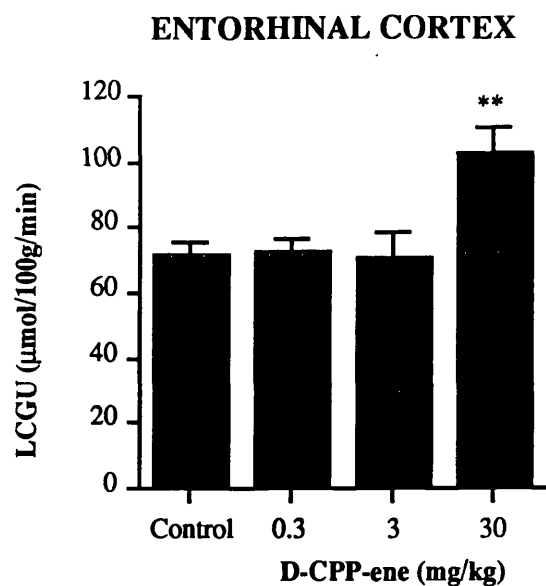


FIGURE 15 : LOCAL CEREBRAL GLUCOSE UTILISATION IN OLFACTORY AREAS FOLLOWING D-CPP-ENE ADMINISTRATION

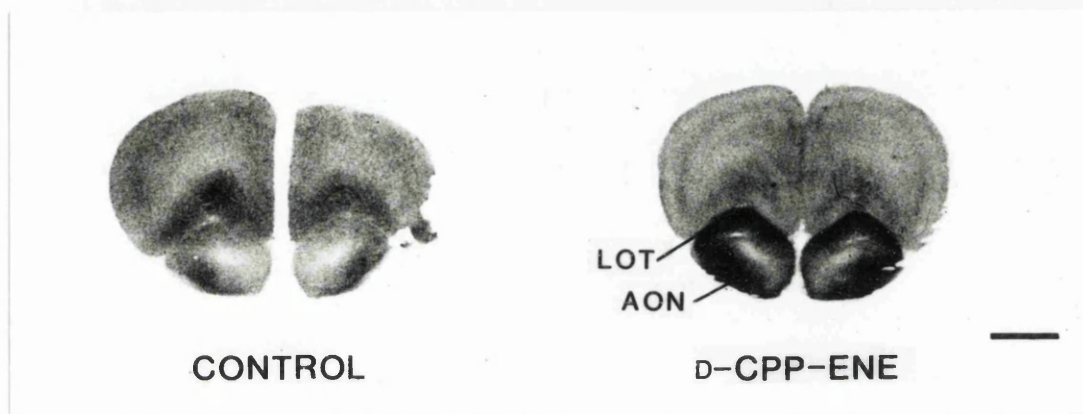


FIGURE 16: AUTORADIOGRAMS OF GLUCOSE UTILISATION IN THE RAT BRAIN FOLLOWING D-CPP-ENE: OLFACTORY CORTEX

Representative autoradiograms of glucose use in the rat brain at the level of olfactory areas in response to D-CPP-ene administration. Left: control animal. Right: D-CPP-ene-treated (30 mgkg^{-1}) animal. Optical densities of the lateral olfactory tract (LOT) and the anterior olfactory nucleus (AON), indicated by solid lines, are increased in the D-CPP-ene-treated animal compared to control. Scale equals 2mm.

LEGEND TO FIGURE 17

FIGURE 17: Local cerebral glucose utilisation in auditory and visual structures in response to D-CPP-ene administration.

Data are presented as mean glucose utilisation ($\mu\text{mol } 100\text{g}^{-1} \text{ min}^{-1}$) \pm S.E.M. * $p < 0.05$, ** $p < 0.01$ relative to control (Student's unpaired t-test, two-tailed, with Bonferroni correction for multiple group comparison).

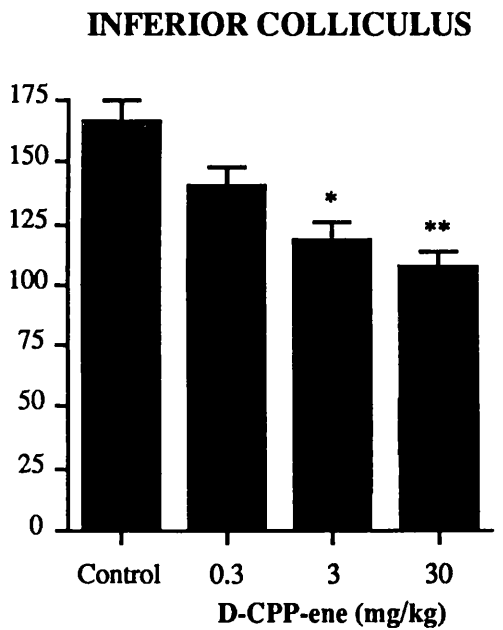
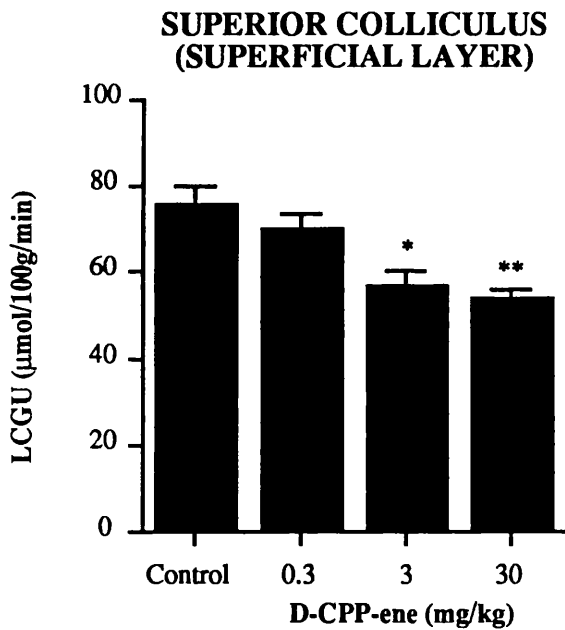
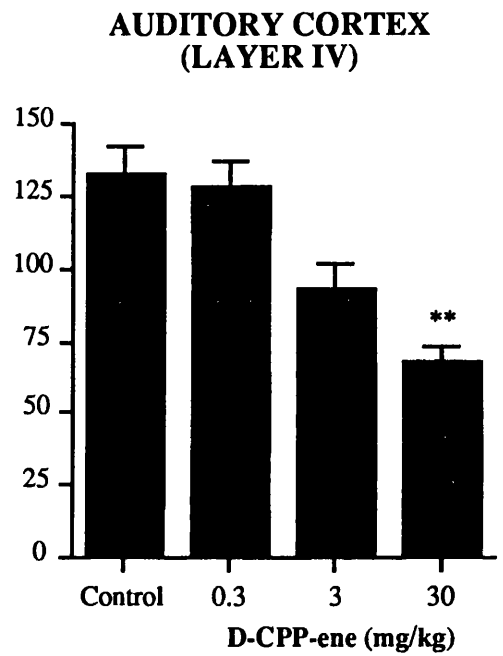
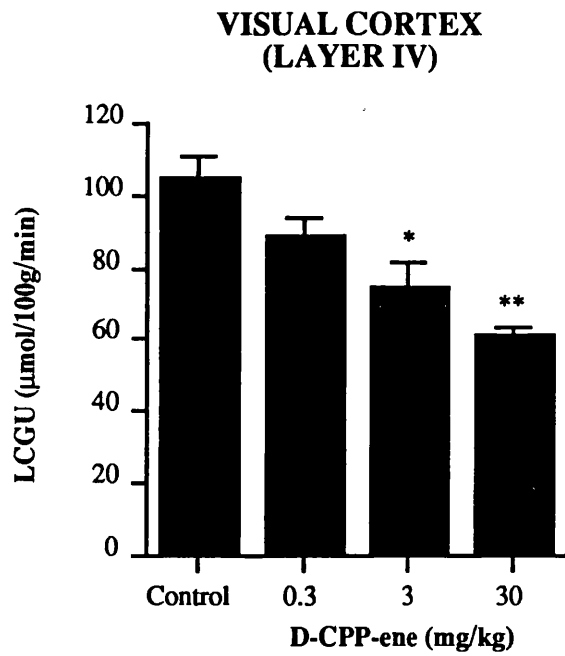


FIGURE 17 : LOCAL CEREBRAL GLUCOSE UTILISATION IN VISUAL AND AUDITORY STRUCTURES FOLLOWING D-CPP-ENE ADMINISTRATION

Myelinated Fibre Tracts

Glucose use was measured in five regions of white matter to examine the metabolic effects D-CPP-ene on fibre tracts of the brain (Appendix I, Table 7). D-CPP-ene had no effects at any dose on glucose utilisation in five regions of white matter.

1.2.2. L-679-512, a Novel Muscarinic Agonist

The effects of L-679-512 on cerebral glucose utilisation are given in Appendix II. Alterations in glucose utilisation were observed in only twelve of the 76 regions of brain analysed, and in every case glucose utilisation decreased following L-679-512 administration. These effects were concentrated particularly in hippocampal and limbic structures, and regions of the brain involved in olfactory transmission.

Hippocampal Region

Administration of L-679-512 resulted in essentially the same biphasic depression of glucose use in the hippocampus: in most cases a dose of $10\mu\text{gkg}^{-1}$ L-679-512 resulted in a suppression of glucose utilisation, while administration of 3 or $30\mu\text{gkg}^{-1}$ did not result in deviation from control values (Figures 18 & 19). Glucose use was significantly lowered by L-679-512 in three hippocampal areas, in the stratum lacunosum moleculare of the CA1 and CA2/3 sectors (11% and 14%, respectively) and in the stratum oriens/pyramidale of CA2 (15%). No other significant decreases in glucose utilisation were observed.

Areas Associated with Limbic Function

L-679-512 induced alterations in five of 25 limbic structures measured (Appendix II, Table 3). In one cortical area, the parietal cortex, a dose-dependent decrease in glucose utilisation was observed; glucose use was decreased significantly in response to a dose of $30\mu\text{gkg}^{-1}$ L-679-

LEGENDS TO FIGURES 18 AND 19

FIGURE 18: Local cerebral glucose utilisation in the hippocampus following L-679-512 administration: Ammon's Horn.

FIGURE 19: Local cerebral glucose utilisation in the hippocampus following L-679-512 administration: Dentate gyrus, presubiculum and subiculum.

Data are presented as mean glucose utilisation ($\mu\text{mol } 100\text{g}^{-1} \text{ min}^{-1}$) \pm S.E.M. * $p < 0.05$ relative to control (Student's unpaired t-test, two-tailed, with Bonferroni correction for multiple group comparison).

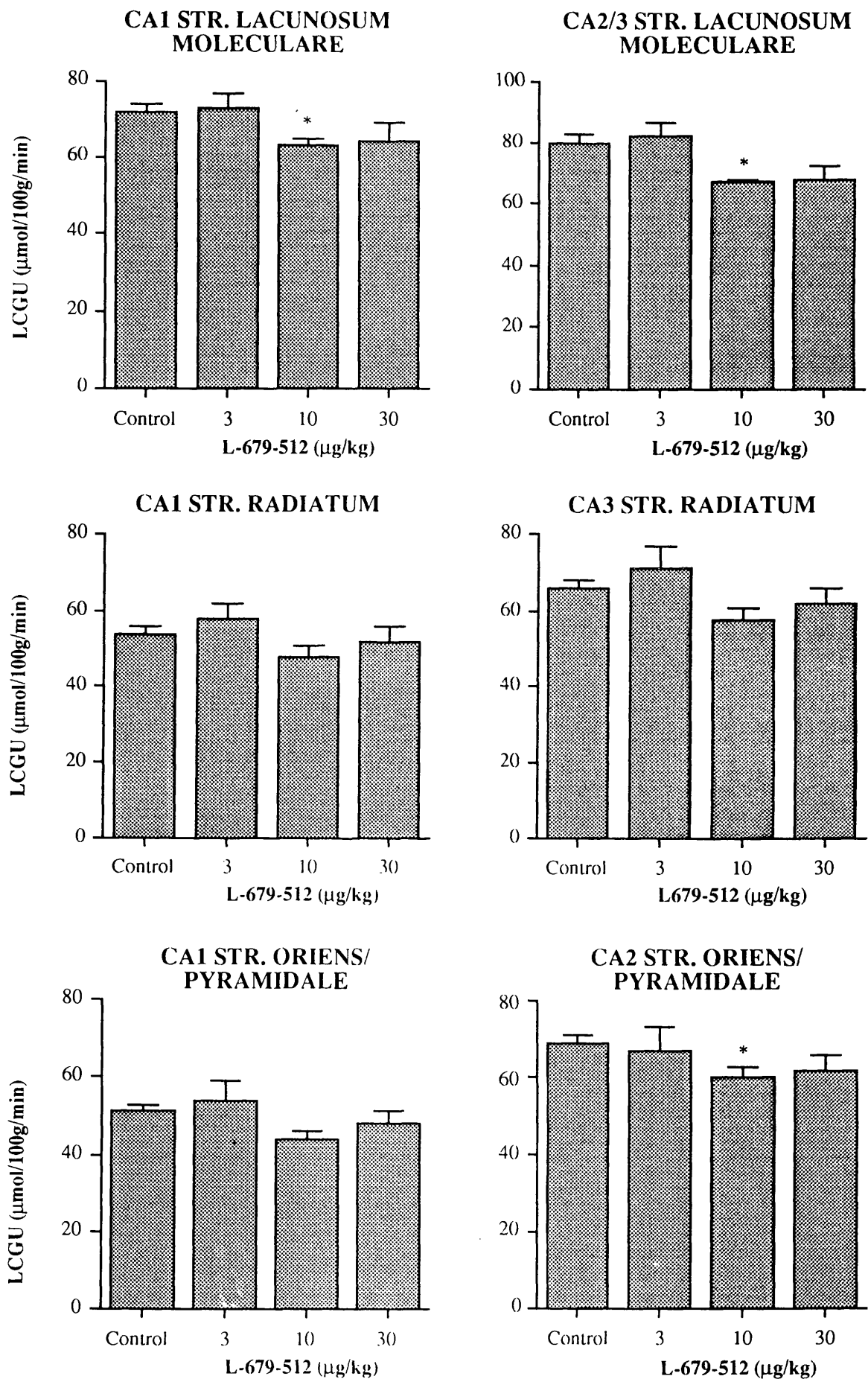
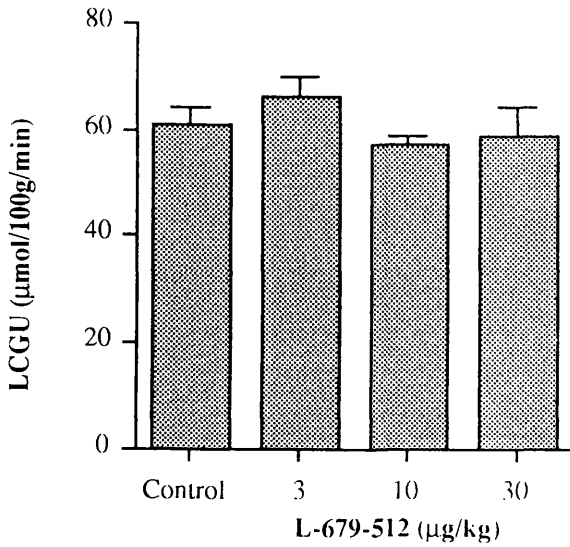
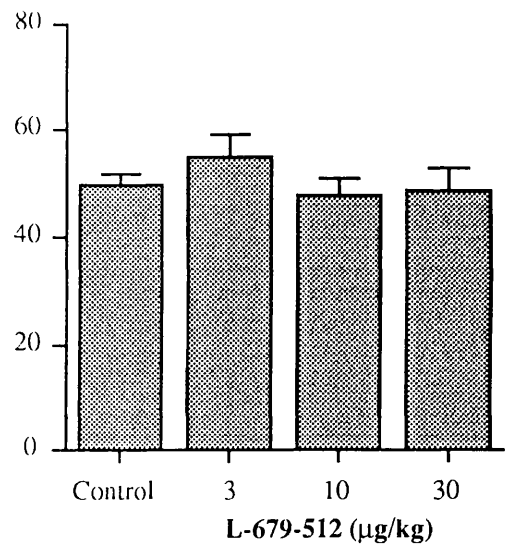


FIGURE 18 : LOCAL CEREBRAL GLUCOSE UTILISATION IN THE HIPPOCAMPUS FOLLOWING L-679-512 ADMINISTRATION: AMMON'S HORN

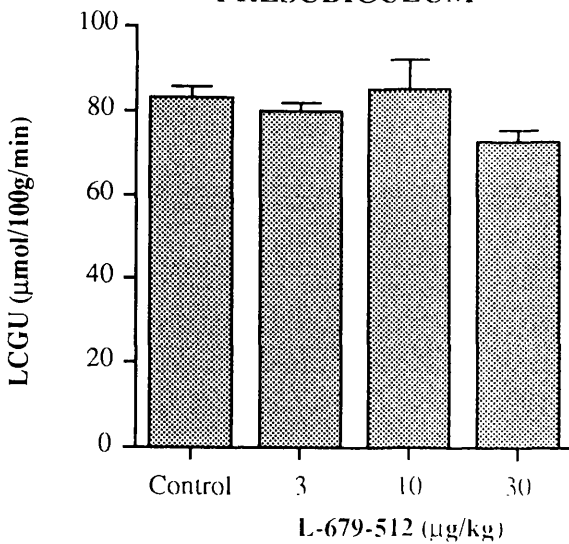
DENTATE GYRUS MOLECULAR LAYER (SUPERIOR BLADE)



DENTATE GYRUS POLYMORPHIC LAYER



PRESUBICULUM



SUBICULUM

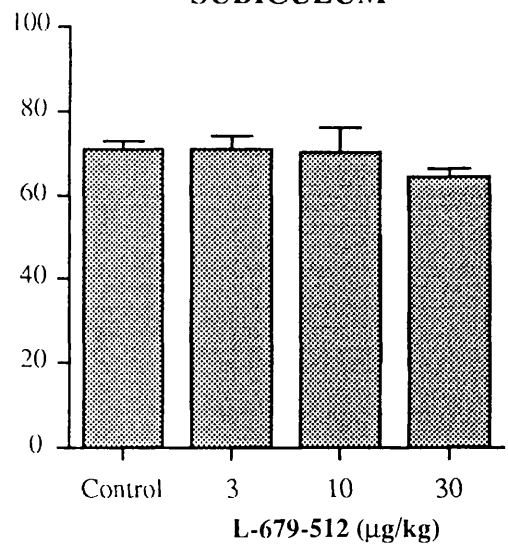


FIGURE 19 : LOCAL CEREBRAL GLUCOSE UTILISATION IN THE HIPPOCAMPUS FOLLOWING L-679-512 ADMINISTRATION: DENTATE GYRUS, PRESUBICULUM AND SUBICULUM

512. In the medial and lateral portions of the | mamillary body, glucose use decreased significantly following 3 and 30 μgkg^{-1} L-679-512 and in the lateral portion glucose use remained significantly lower than the control value after 10 μgkg^{-1} L-679-512 (Figure 20). In the medial forebrain bundle and the horizontal limb of the diagonal band glucose utilisation decreased in a dose-dependent manner, and was significantly lower than the control value after 30 μgkg^{-1} L-679-512.

Olfactory Areas

L-679-512 produced functional changes in glucose utilisation in olfactory areas: in three of the six structures, decreases in glucose utilisation were observed in response to 30 μgkg^{-1} L-679-512 (Appendix II, Table 4). In the lateral olfactory tract, the primary olfactory cortex, and the entorhinal cortex, decreases were measured of 23%, 25% and 20% respectively (Figure 21). In every other structure, glucose use was suppressed, though not significantly, following 30 μgkg^{-1} L-679-512. Doses of 3 or 10 μgkg^{-1} did not result in functional alterations in any olfactory region.

Auditory and Visual Structures

L-679-512 evoked significant alterations in glucose utilisation in only two structures (Appendix II, Table 5). A dose of 30 μgkg^{-1} L-679-512 caused a reduction in glucose use of 23% in the medial geniculate body and 27% in layer IV of the visual cortex; lower doses of drug failed to produce significant functional alterations in auditory or visual structures. In auditory structures, although no further significant alterations were observed, there was evidence of a dose-dependent mechanism of suppression of glucose use (Figure 22). This pattern of alteration was not evident in visual structures.

LEGENDS TO FIGURES 20 & 21

FIGURE 20: Local cerebral glucose utilisation in regions associated with limbic function following L-679-512 administration.

FIGURE 21: Local cerebral glucose utilisation in olfactory structures following L-679-512 administration.

Data are presented as mean glucose utilisation ($\mu\text{mol } 100\text{g}^{-1} \text{ min}^{-1}$) \pm S.E.M. * $p < 0.05$ relative to control (Student's unpaired t-test, two-tailed, with Bonferroni correction for multiple group comparison).

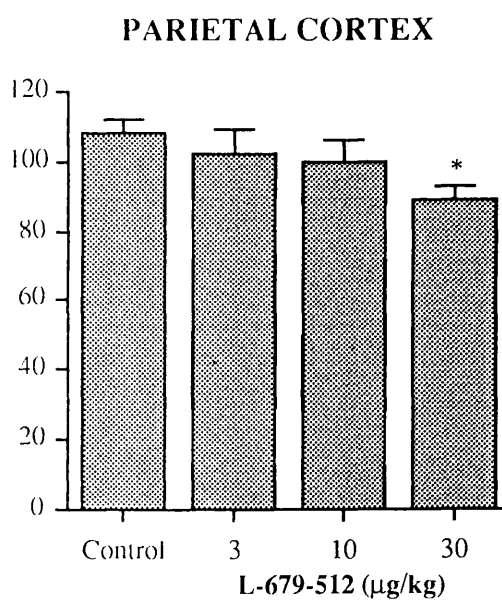
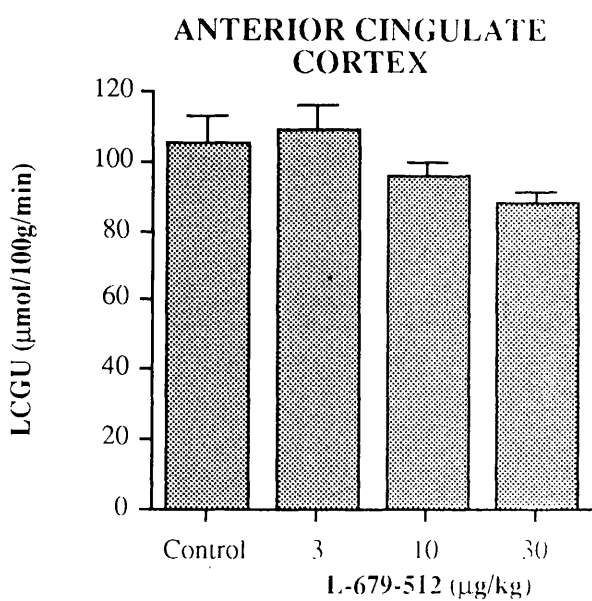
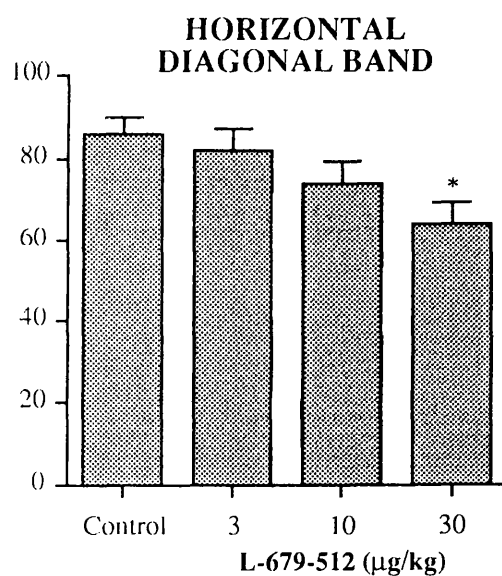
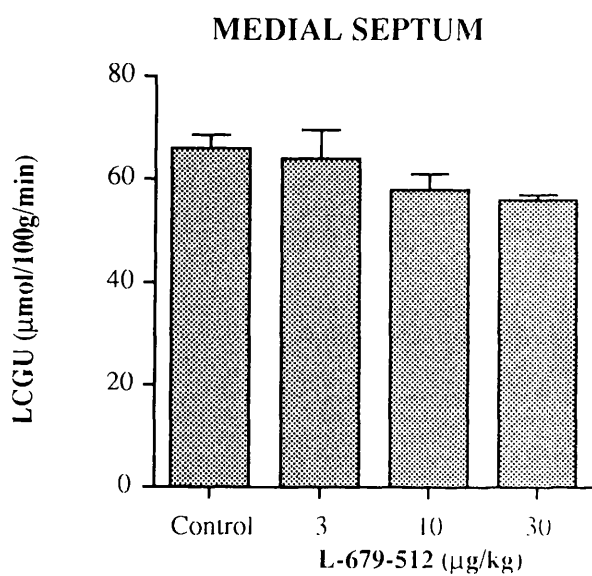
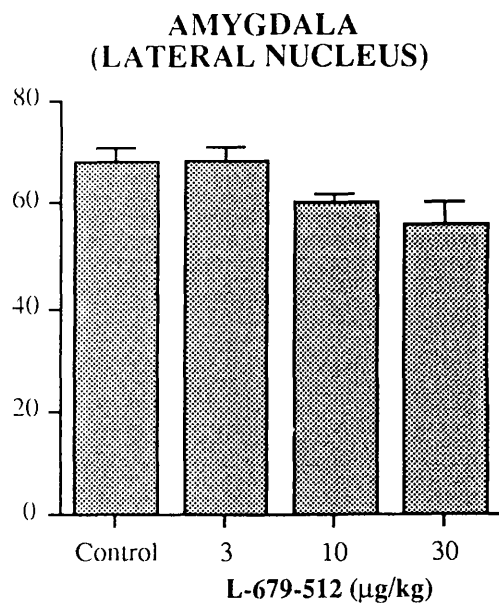
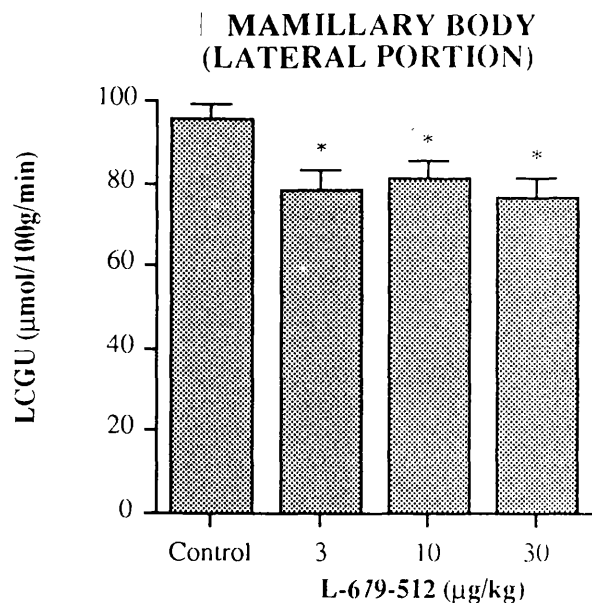


FIGURE 20 : LOCAL CEREBRAL GLUCOSE UTILISATION IN LIMBIC STRUCTURES FOLLOWING L-679-512 ADMINISTRATION

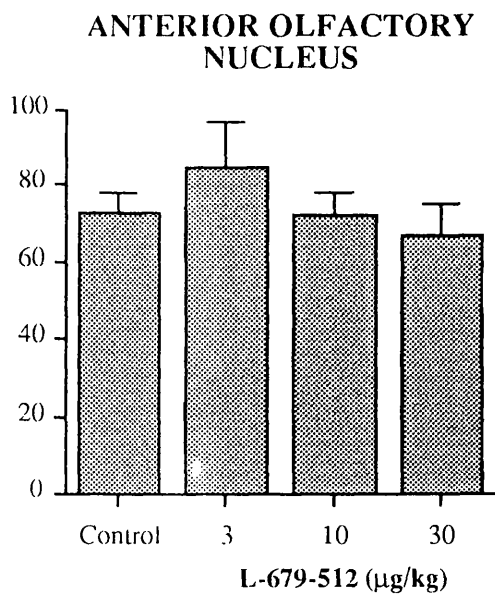
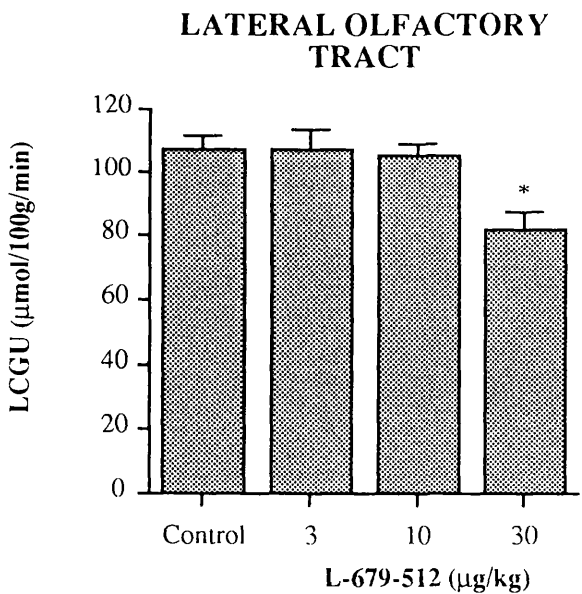
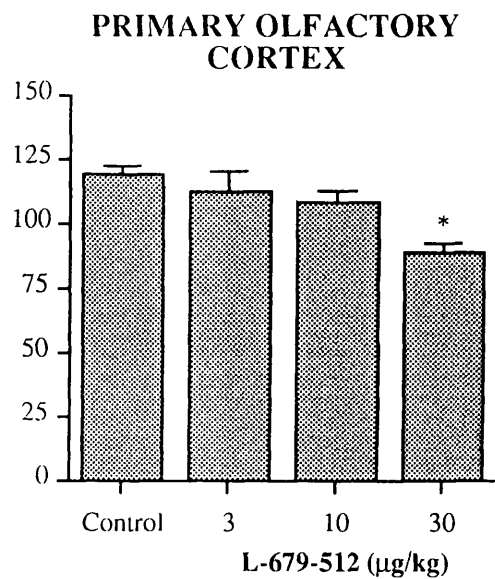
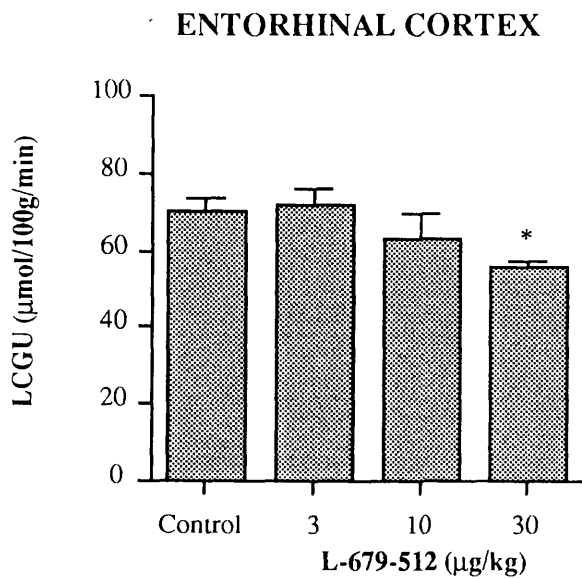


FIGURE 21 : LOCAL CEREBRAL GLUCOSE UTILISATION IN OLFACTORY STRUCTURES FOLLOWING L-679-512 ADMINISTRATION

LEGEND TO FIGURE 22

FIGURE 22: Local cerebral glucose utilisation in auditory and visual regions following L-679-512 administration.

Data are presented as mean glucose utilisation ($\mu\text{mol } 100\text{g}^{-1} \text{ min}^{-1}$) \pm S.E.M. * $p < 0.05$ relative to control (Student's unpaired t-test, two-tailed, with Bonferroni correction for multiple group comparison).

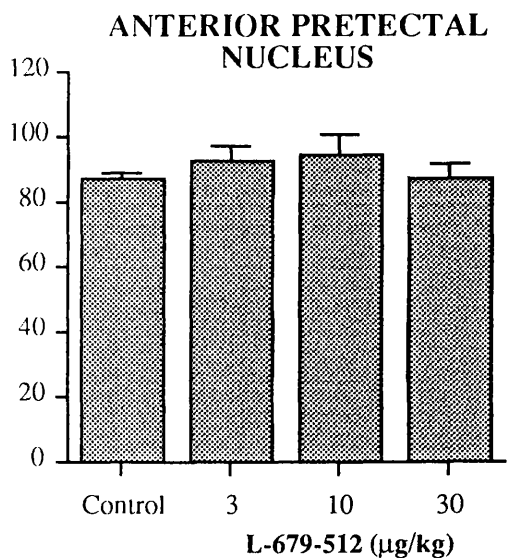
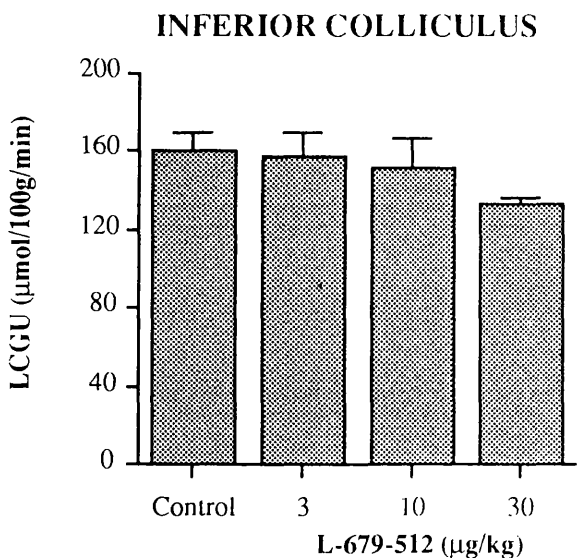
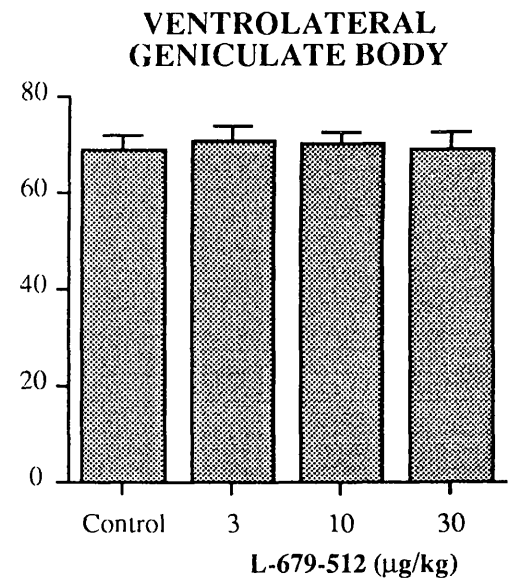
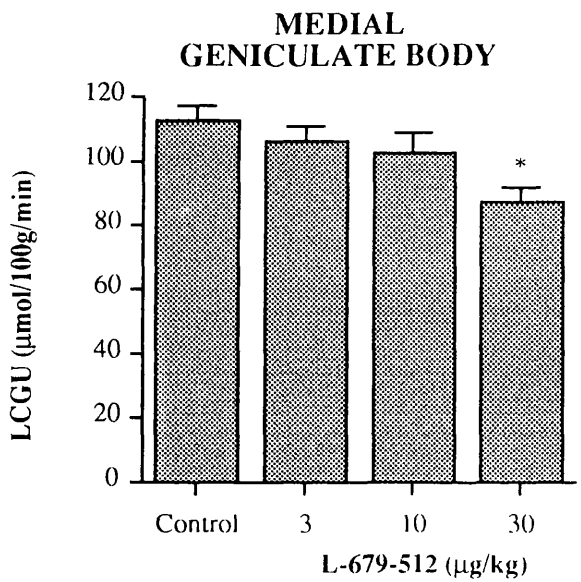
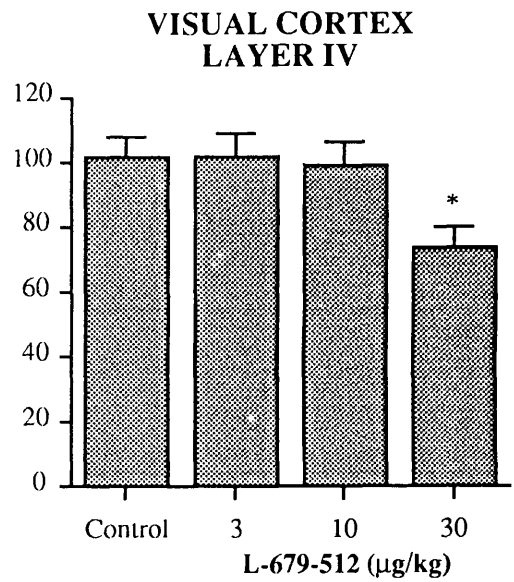
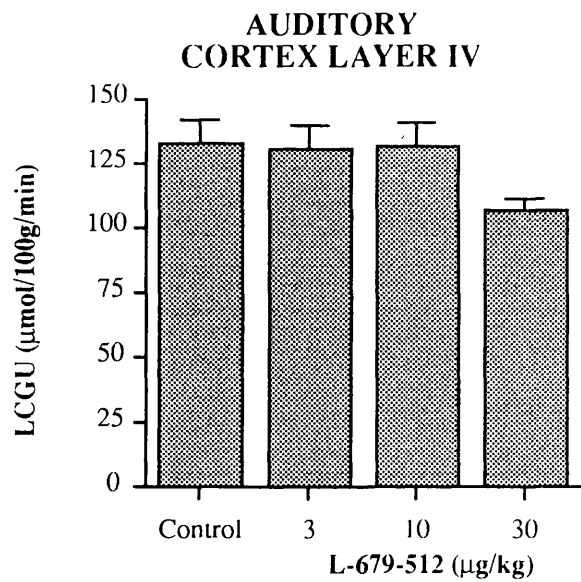


FIGURE 22 : LOCAL CEREBRAL GLUCOSE UTILISATION FOLLOWING L-679-512 ADMINISTRATION: AUDITORY AND VISUAL STRUCTURES

Extrapyramidal and Sensorimotor Areas

L-679-512 administration produced only one significant functional alteration in this group of structures: in the caudate nucleus, glucose use was reduced by 22% in response to $30\mu\text{gkg}^{-1}$ L-679-512. Glucose use remained unchanged in all other structures in the group in response to L-679-512 administration.

Myelinated Fibre Tracts

L-679-512, had no effects at any dose on glucose utilisation in five regions of white matter.

1.2.3. **9-Amino-1,2,3,4-tetrahydroacridine (THA), a Cholinesterase Inhibitor with Potential Glutamatergic Activity**

Despite the overt changes in behaviour and physiological parameters which accompanied THA administration, functional alterations in response to the drug were observed in only eight of the 76 regions analysed. In seven of these regions, glucose utilisation increased following THA administration, while in one other structure there was a significant decrease in glucose use. The most marked alterations in function occurred in regions involved in visual processing.

Hippocampal Region

Glucose utilisation was increased significantly in the subiculum following THA administration; there were no significant alterations in glucose use in other hippocampal regions (Appendix III, Table 2, and Figure 23).

LEGENDS TO FIGURES 23 AND 24

FIGURE 23: Local cerebral glucose utilisation in hippocampal and limbic structures following THA administration.

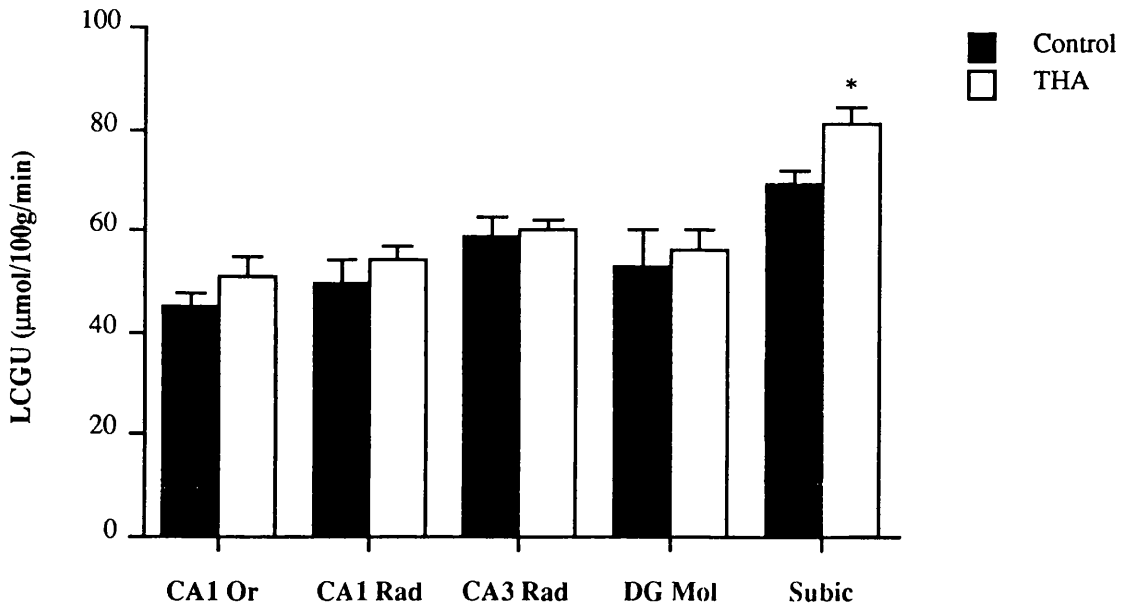
Abbreviations: Or: stratum oriens; Rad: stratum radiatum; Mol: molecular layer; Subic: subiculum; PCC: posterior cingulate cortex; Mam B (Med): mamillary body, medial portion; Thal AVN: thalamus, anteroventral nucleus; N Acb: nucleus accumbens.

FIGURE 24: Local cerebral glucose utilisation in auditory and visual structures following THA administration.

Abbreviations: Aud (IV): auditory cortex, layer IV; IC: inferior colliculus; MGB: medial geniculate body; Co N: cochlear nucleus; SON: superior olivary nucleus; Vis (IV): visual cortex, layer IV; SC (Sup): superior colliculus, superficial layers; SC (Deep): superior colliculus, deep layers; DLG: dorsolateral geniculate body; APN: anterior pretectal nucleus.

Data are presented as mean glucose utilisation ($\mu\text{mol } 100\text{g}^{-1} \text{ min}^{-1}$) \pm S.E.M. * $p < 0.05$, ** $p < 0.01$ relative to control (Student's unpaired t-test, two-tailed).

HIPPOCAMPUS



LIMBIC STRUCTURES

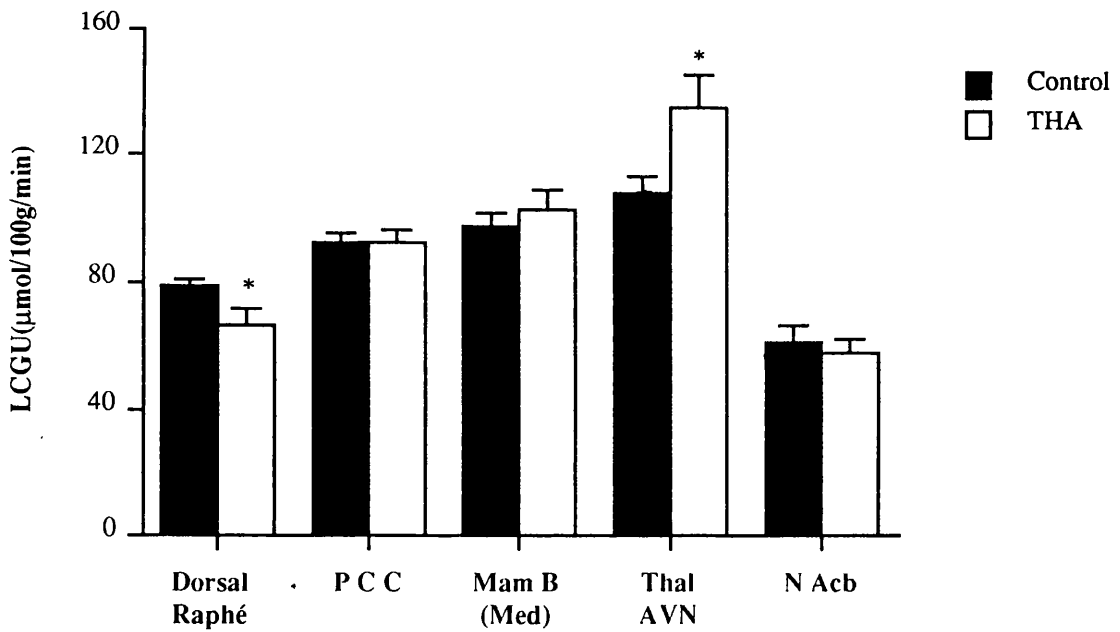
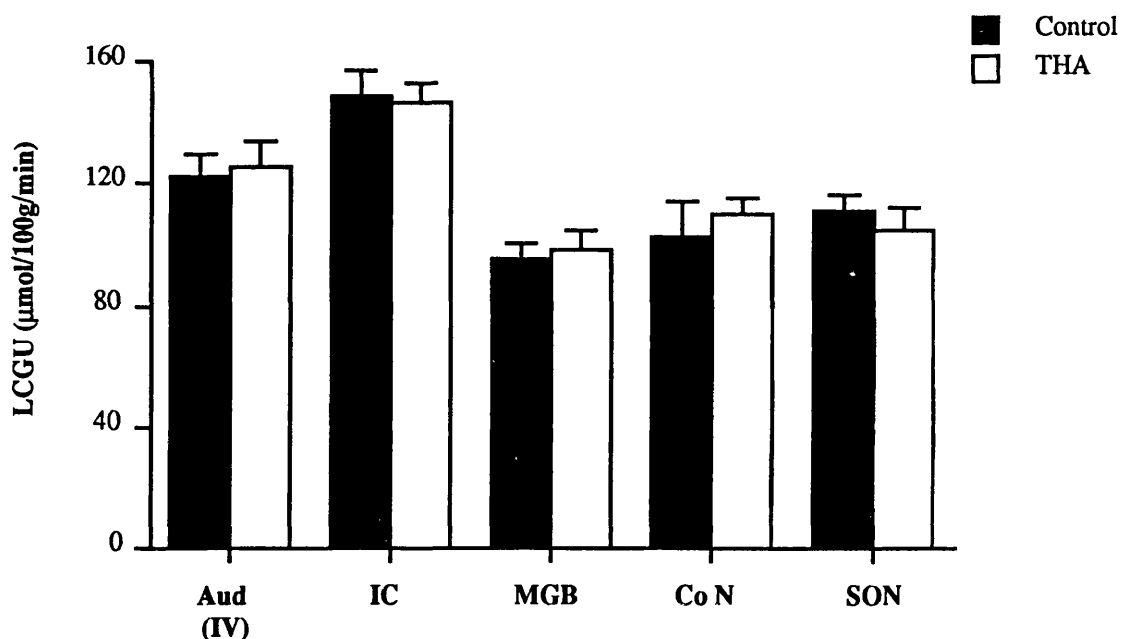


FIGURE 23 : LOCAL CEREBRAL GLUCOSE UTILISATION IN HIPPOCAMPAL AND LIMBIC STRUCTURES FOLLOWING THA ADMINISTRATION

AUDITORY STRUCTURES



VISUAL STRUCTURES

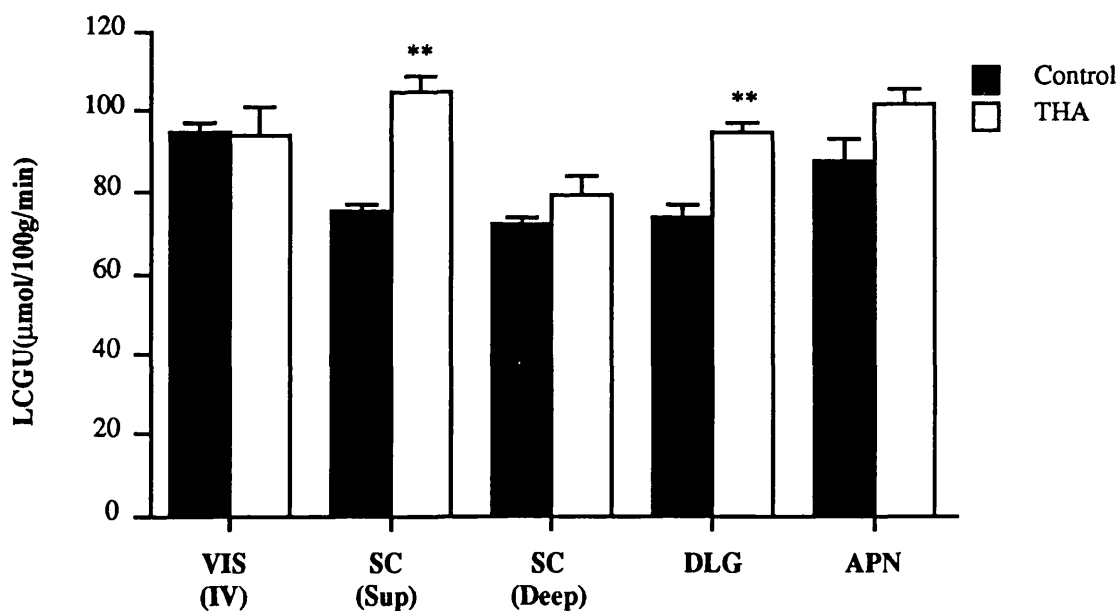


FIGURE 24 : LOCAL CEREBRAL GLUCOSE UTILISATION IN AUDITORY AND VISUAL STRUCTURES FOLLOWING THA ADMINISTRATION

Areas Associated with Limbic Function

THA administration resulted in significantly altered glucose utilisation in two regions of brain involved in limbic function. Glucose utilisation was decreased in the dorsal raphe nucleus by 15% following THA; this represented the only region to exhibit reduced glucose utilisation in response to THA. THA elicited a significant functional increase in the anteroventral thalamus: glucose use was increased by 25%.

Olfactory Areas

In contrast to the extensive effects of D-CPP-ene and L-679-512 on local glucose utilisation within olfactory areas, THA administration did not produce significant alterations in glucose utilisation within these regions, in comparison to saline-treated controls.

Auditory and Visual Structures

The effects of THA on cerebral glucose utilisation in auditory and visual structures were qualitatively different from those which accompanied D-CPP-ene or L-679-512 administration (Appendix III, Table 5). No alterations in glucose use occurred in response to THA in any of seven auditory structures measured. However, in three regions involved in visual function increases in glucose utilisation were observed. THA effected a 40% increase in glucose use in the superficial layer superior colliculus (Figures 24 & 25). Glucose use was also elevated in the dorsolateral and ventrolateral portions of the geniculate body by 28% and 25% respectively, relative to control values. In four other structures involved in visual processing, glucose use remained unchanged.

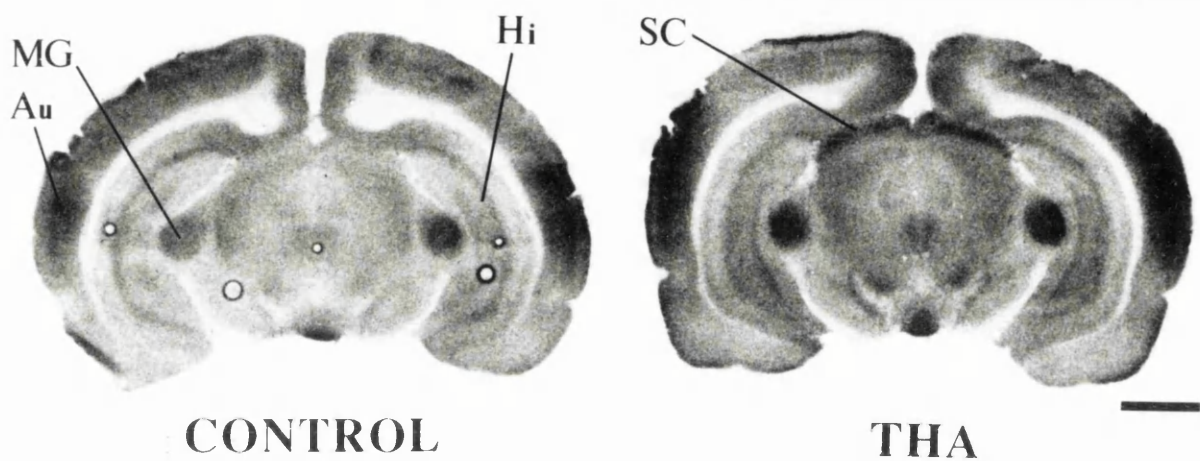


FIGURE 25: AUTORADIOGRAMS OF GLUCOSE UTILISATION IN THE RAT BRAIN FOLLOWING THA: HIPPOCAMPUS, AUDITORY AND VISUAL REGIONS

Representative autoradiograms of glucose use in the rat brain at the level of the ventral hippocampus, auditory and visual regions in response to THA administration. Left: control animal. Hippocampus (Hi), auditory cortex (Au), and medial geniculate nucleus (MG) are indicated by solid lines. Right: THA-treated (2.5 mgkg^{-1}) animal. Note the increased deoxyglucose uptake in the superficial layers of the superior colliculus (SC) compared to control. Scale equals 2mm.

Extrapyramidal and Sensorimotor Areas

THA effected only one alteration in glucose utilisation within this group of structures: in the cerebral hemisphere, a significant increase in glucose use was measured in response to 2.5mgkg^{-1} THA.

Myelinated Fibre Tracts

THA however evoked a significant increase in glucose use in the genu of the corpus callosum. Although glucose use was slightly increased in the four other regions, these increases were not significantly different from control values.

2. FUNCTIONAL PLASTICITY OF THE HIPPOCAMPUS IN RESPONSE TO LESIONS OF THE MEDIAL SEPTUM

2.1. CHARACTERISATION OF IBOTENIC ACID-INDUCED LESIONS OF THE MEDIAL SEPTUM

Ibotenate infusion into the medial septum resulted in a loss of neuronal cell bodies in the medial septal area revealed with light microscopy. Lesions involved typically the entire medial septal nucleus, rostral to the anterior commissure through to its termination caudal to the septo-hippocampal nuclei (Paxinos and Watson, 1986), with minimal damage to the surrounding lateral septum or vertical diagonal band nucleus (Figure 26).

Quantitatively, the lesion extended to the extreme dorsal regions of the lateral septum bordering the medial septum, while the diagonal band was largely intact. The corpus callosum suffered consistent but discrete damage, probably due to the passage of the syringe needle. A needle tract lesion was frequently visible in the cingulate cortex overlying the septal region, possibly due to diffusion of ibotenate up the syringe barrel tract upon removal of the syringe. In some cases, damage was recorded in more ventral portions of the lateral septum and in the dorsal extremity of the vertical diagonal band. These nuclei, however, were largely conserved. Only in a very small number of animals did the lesion lie outwith these limits. Animals with more extensive lesions, or incomplete lesions of the medial septum, were discarded. Brains in which the lesion appeared to be unilateral fell naturally into either of these categories, and were also excluded. In no animal was there histological evidence at the light microscopy level to indicate direct ibotenate-induced damage of the hippocampus or other structures distant from the septal area.

The lesion could be identified easily from the surrounding non-

LEGEND TO FIGURE 26

QUANTIFICATION OF IBOTENATE LESIONS OF THE MEDIAL SEPTUM

Diagrammatic illustration of coronal sections at the level of the medial septal region, illustrating the extent of a representational ibotenic acid-induced lesion.

(A) 0.2 mm, (B) 0.7 mm, and (C) 1.00 mm anterior to bregma. The lesioned area, which encompassed the entire medial septal nucleus, is represented by the blackened area.

Abbreviations: LS: Lateral septum; VDB: vertical diagonal band; HDB: horizontal diagonal band; CP: Caudate Putamen.

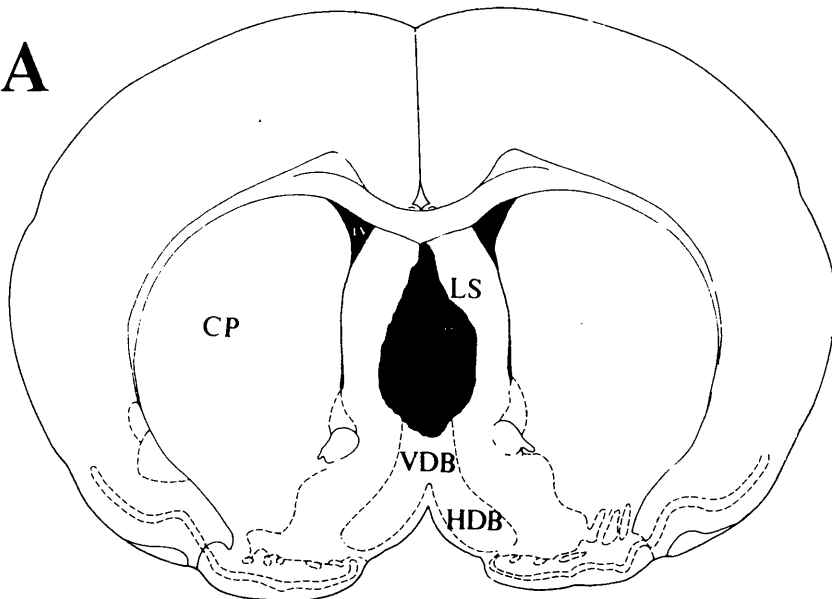
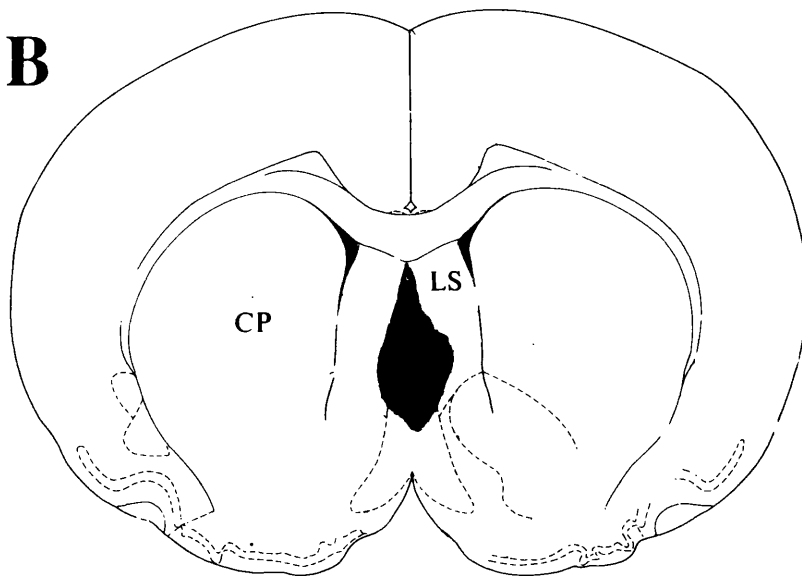
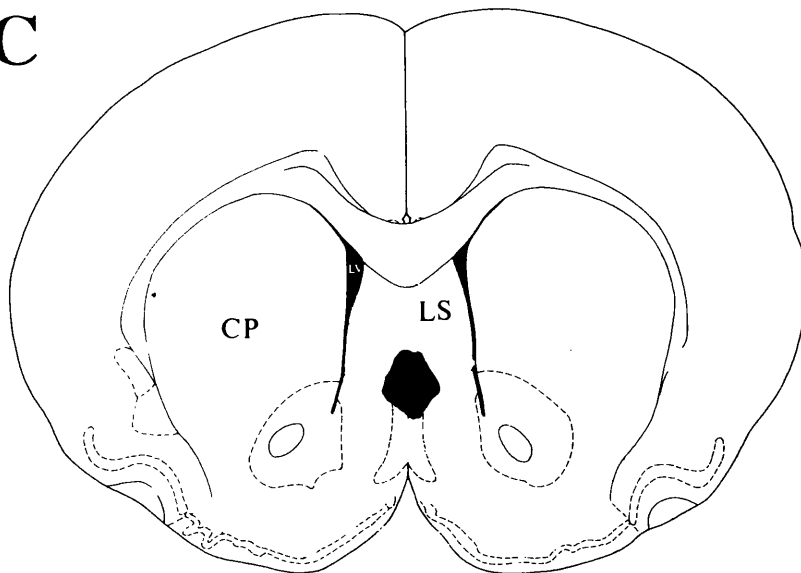
A**B****C**

FIGURE 26: QUANTIFICATION OF IBOTENATE LESIONS OF THE MEDIAL SEPTUM

LEGEND TO FIGURE 27: HISTOLOGICAL PROFILE OF IBOTENATE
LESIONS OF THE MEDIAL SEPTUM

A.-D. Cresyl violet-stained coronal sections taken at the level of the medial septum three weeks after injection of phosphate buffered saline (A & C) or ibotenic acid (B & D).

A and B: gross histological evaluation of lesioned area (Magnification approximately $\times 30$). CC, corpus callosum; MS, medial septum; LS, lateral septum; lv, lateral ventricle. Note the presence of magnocellular, putatively cholinergic cells in the medial septal area of the sham-operated control rat (A). In contrast, the ibotenate-lesioned septum (B) is devoid of magnocellular cells; instead, intense gliosis is present. The small arrowheads indicate the border between lesioned and normal tissue.

C and D: photographs of medial septal tissue (magnification approximately $\times 185$). Magnocellular cells in the normal (sham-operated) septum (C) are indicated by large arrowheads. Note the absence of magnocellular cells, and the large numbers of glial cells (tailed arrows) in the lesioned tissue (D).

E.-F. Sections from the medial septum stained for glial fibrillary acidic protein (GFAP). E: sham-operated control rat. F: the lesioned septum is densely stained, indicating the presence of reactive astrocytosis, and inherent cell loss (Hume-Adams & Graham, 1988).

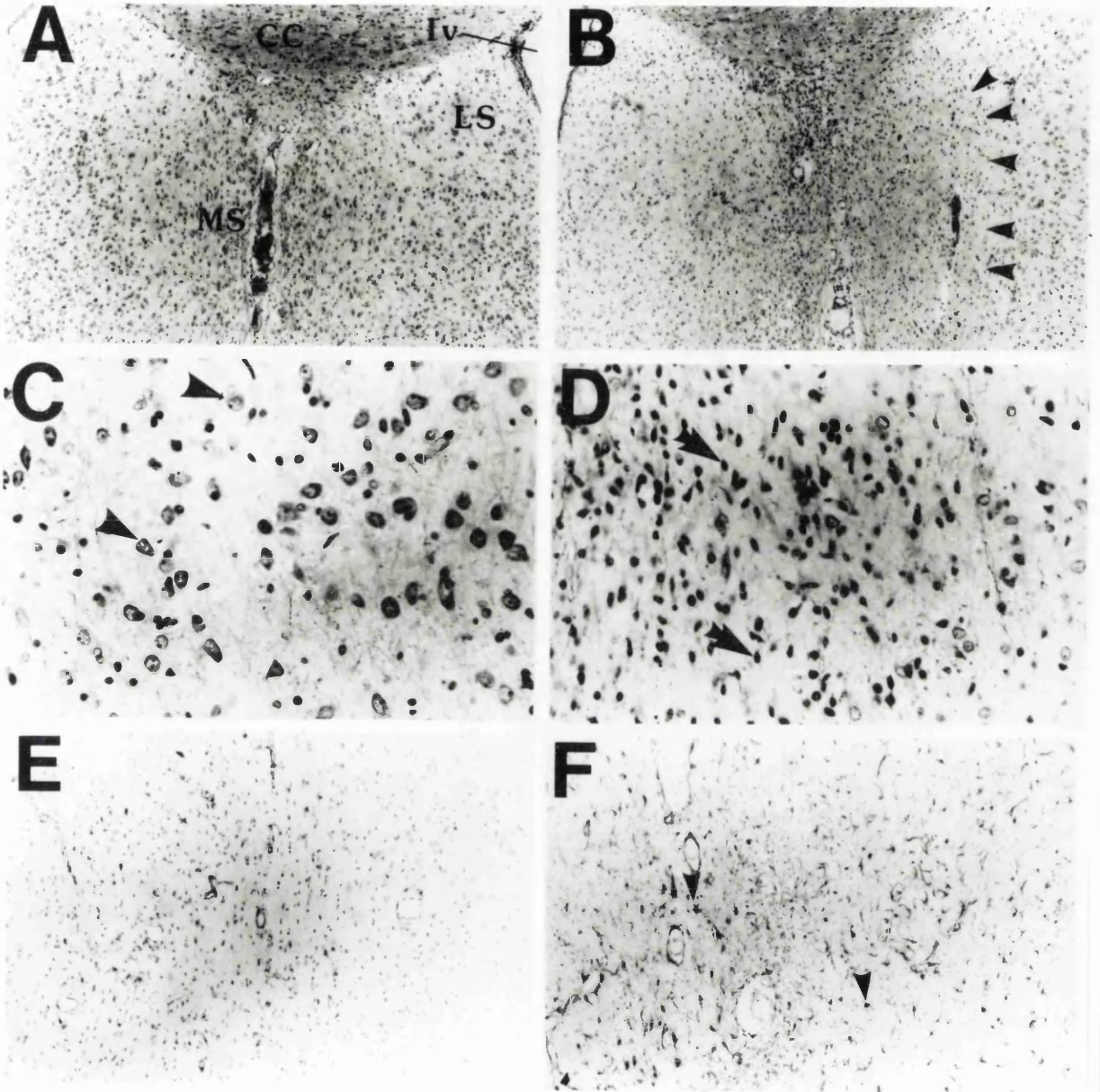


FIGURE 27: HISTOLOGICAL PROFILE OF IBOTENATE LESIONS
OF THE MEDIAL SEPTUM

lesioned tissue. The lesion site was bordered by a wall of typically small glial cells, and the lesioned tissue was characteristically devoid of large, putatively cholinergic cell bodies; instead, the area was infiltrated with glial cells and irregular shaped macrophages (Figure 27). In two brains, staining for glial fibrillary acidic protein (GFAP) confirmed the presence of glial cells within the lesioned tissue (Figure 27).

2.2. LOCAL CEREBRAL GLUCOSE UTILISATION FOLLOWING LESIONS OF THE MEDIAL SEPTUM

2.2.1. Local Cerebral Glucose Utilisation Within the Hippocampus

The heterogeneous pattern of glucose utilisation within the normal rat hippocampus is illustrated in Figure 28. Glucose utilisation is generally higher within the CA region, particularly CA2, than in the dentate gyrus, although glucose use within the CA region is highly stratified: high levels of glucose utilisation are measured within the stratum lacunosum moleculare, and the pyramidal layer exhibits greater levels of glucose utilisation than in the bordering strata oriens and radiatum. Within the dentate gyrus, glucose utilisation is higher in the granular and molecular layers than in the infragranular region.

In comparison to the diversity of functional activation in the CA and dentate regions, glucose use within the subiculum and presubiculum is more heterogeneous. Additionally, in the entorhinal cortex, glucose utilisation varies little within specific layers, although higher levels of functional activity are observed superficially compared to deep levels.

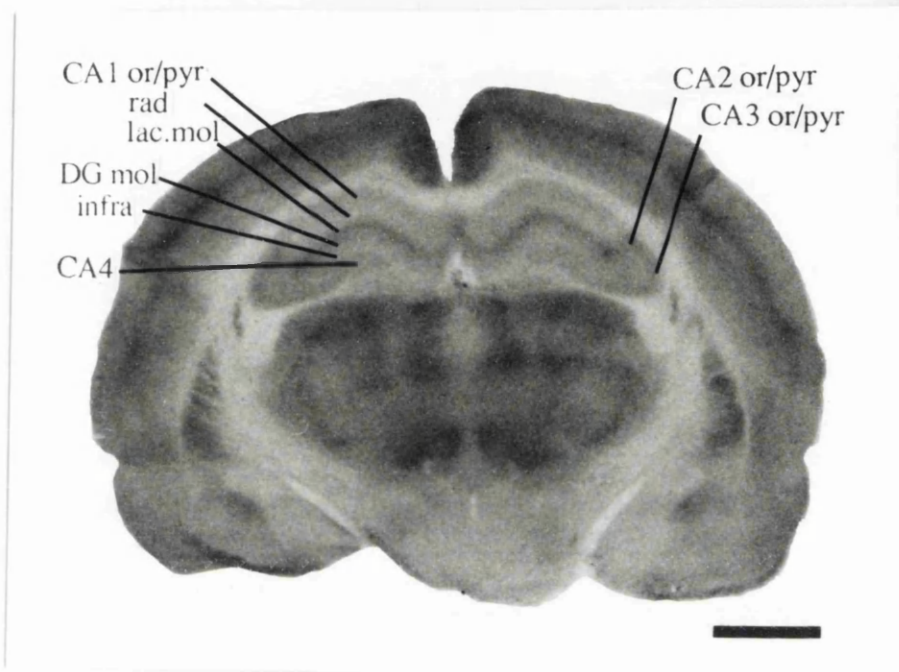


FIGURE 28: AUTORADIOGRAM OF GLUCOSE UTILISATION IN THE RAT HIPPOCAMPUS

Representative autoradiogram of glucose use in the rat brain at the level of the dorsal hippocampus. Abbreviations: or/pyr: strata oriens/pyramidale; rad: stratum radiatum; lac. mol: stratum lacunosum moleculare; DG mol: dentate molecular layer; DG infra: dentate infragranular layer. Scale equals 2mm.

LEGEND TO FIGURE 29

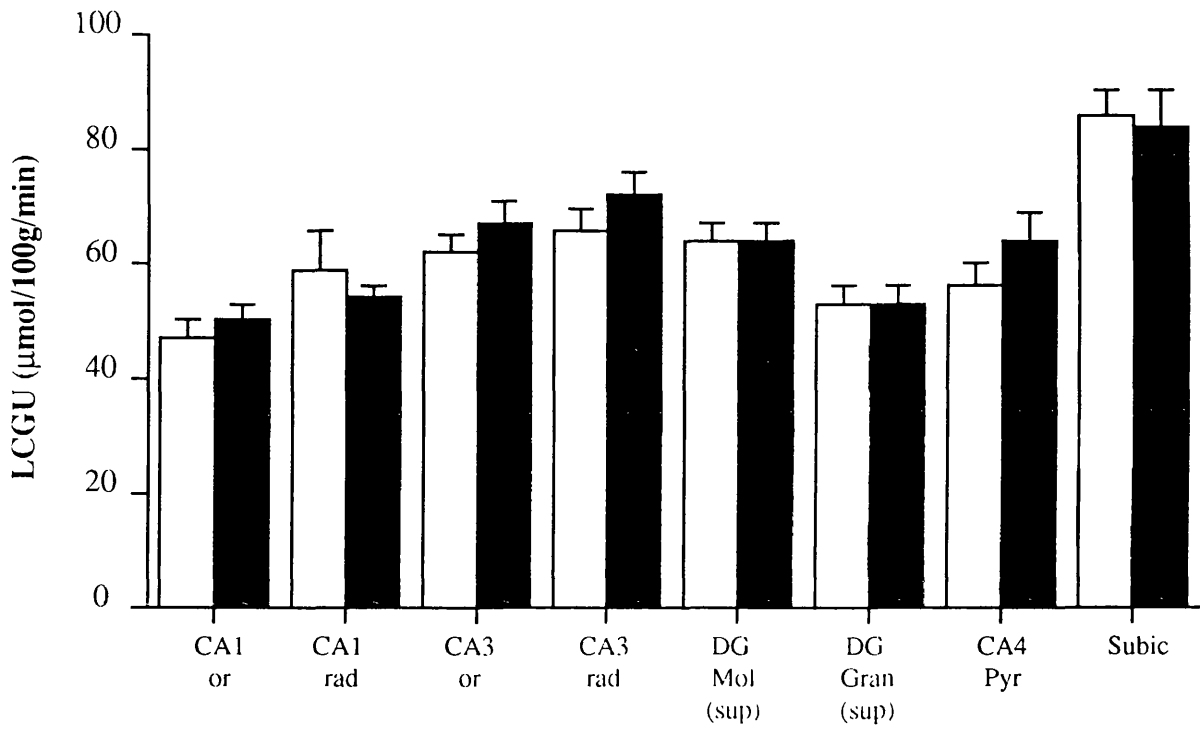
FIGURE 29: Local cerebral glucose utilisation in hippocampal and limbic regions following lesions of the medial septum.

Abbreviations: or: stratum oriens; rad: stratum radiatum; DG Mol (sup): dentate gyrus, molecular layer, superior blade; DG Gran (sup): dentate gyrus, granular layer, superior blade; Ent L I-II: entorhinal cortex, lateral portion layers I-II; Ent L III-VI: entorhinal cortex, lateral portion, layers III-VI; MS: medial septum; LS: lateral septum; Amyg BL: amygdala, basolateral nucleus; Thal AVN: thalamus, anteroventral nucleus; PCC: posterior cingulate cortex; Par C: parietal cortex.

Data are presented as mean glucose utilisation ($\mu\text{mol } 100\text{g}^{-1} \text{ min}^{-1}$) \pm S.E.M. There were no significant differences between sham-operated control and lesioned animals (Student's unpaired t-test, two-tailed).

HIPPOCAMPAL REGIONS

□ SHAM
 ■ LESION



LIMBIC REGIONS

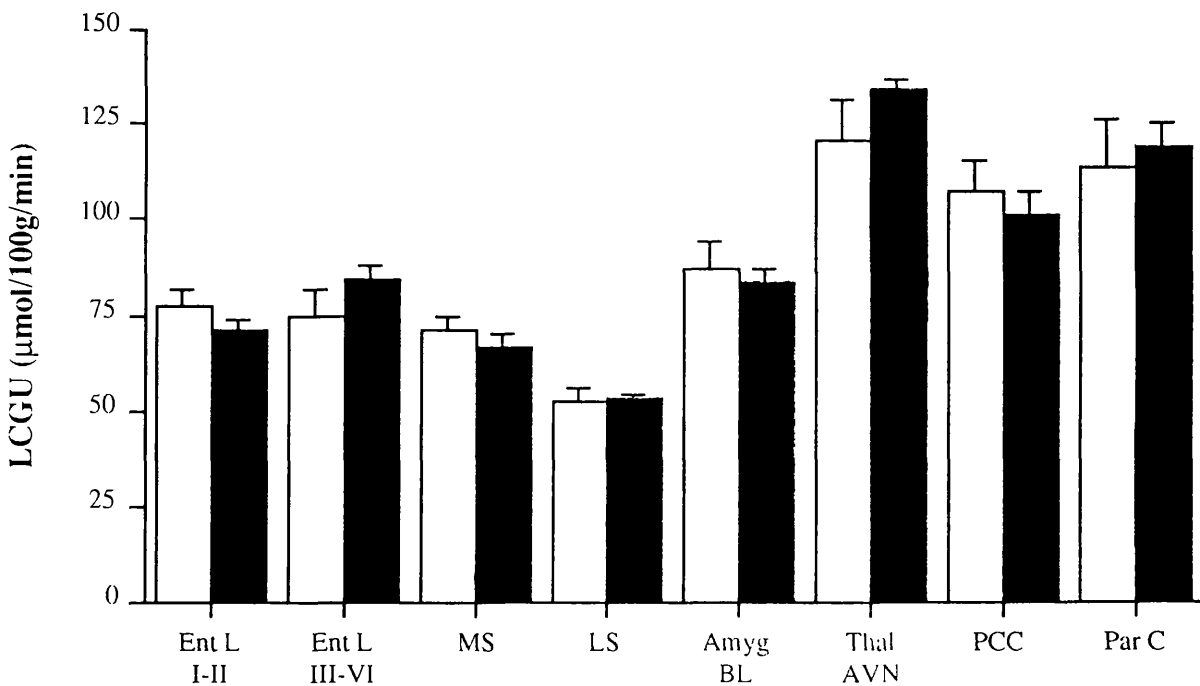


FIGURE 29 : LOCAL CEREBRAL GLUCOSE UTILISATION FOLLOWING LESIONS OF THE MEDIAL SEPTUM: HIPPOCAMPAL AND LIMBIC AREAS

2.2.2. Cerebral Glucose Utilisation in Hippocampal and Limbic Regions Following Lesions of the Medial Septum

Local cerebral glucose utilisation was measured in rats three weeks after medial septal lesions or sham operation in 57 anatomically defined regions of brain: these comprised of 22 hippocampal regions, 23 structures associated with limbic function, and twelve other brain regions. In each case, glucose utilisation was unaltered in response to lesions of the medial septum in comparison to sham-operated control animals (Figure 29).

2.3. MUSCARINIC AND GLUTAMATERGIC RECEPTOR BINDING IN HIPPOCAMPAL REGIONS FOLLOWING LESIONS OF THE MEDIAL SEPTUM

2.3.1. Anatomical Distribution of Muscarinic and Glutamatergic Binding Sites Within the Hippocampus and Associated Regions.

The regional distributions of glutamatergic and muscarinic binding sites within the hippocampus are illustrated in Figure 30.

[³H]-QNB Binding Sites

The observed distribution of muscarinic receptors, as measured by [³H]-QNB binding, was generally in agreement with previous reports (Mash & Potter, 1986; Tonnaer et al., 1988). [³H]-QNB binding to muscarinic receptors was highest within the CA1 strata radiatum and pyramidale, and dense labelling was also present in CA1 strata oriens and lacunosum moleculare and throughout the dentate gyrus. In the CA2 and CA3 regions, [³H]-QNB binding was slightly lower.

The entorhinal cortex contained high levels of binding sites, which were distributed more densely in superficial layers: this contrasts with the pattern of binding in other cortical regions in which dense bands of

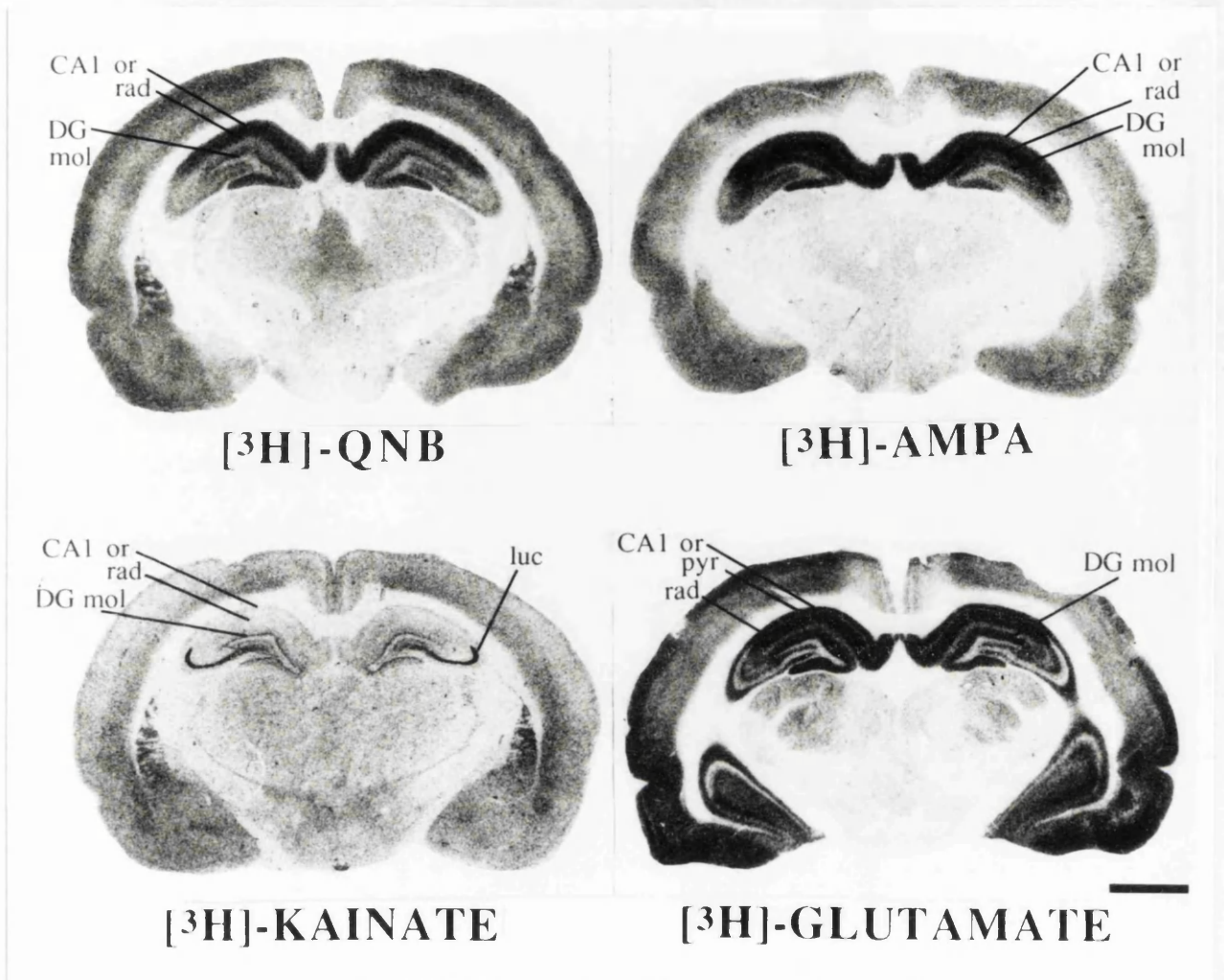


FIGURE 30: AUTORADIOGRAMS OF LIGAND BINDING TO GLUTAMATERGIC AND MUSCARINIC RECEPTORS IN THE RAT HIPPOCAMPUS

Representative autoradiograms of [³H]-QNB (A), [³H]-AMPA (B), [³H]-kainate (C) and [³H]-glutamate (D) binding in the rat brain at the level of the dorsal hippocampus. Abbreviations: or: stratum oriens; pyr: stratum pyramidale; rad: stratum radiatum; luc: stratum lucidum; DG mol: dentate molecular layer. Scale equals 2mm.

labelling in superficial and deep layers border an intermediate band of more diffuse binding.

In agreement with Tonnaer et al. (1988), [^3H]-QNB binding was dense in the subiculum, and less dense in the presubiculum. In the septal area, moderate levels of binding occurred, and these were concentrated in the lateral septum.

[^3H]-AMPA Binding Sites

[^3H]-AMPA binding sites are dense within the hippocampal formation. In contrast with a previous report that [^3H]-AMPA-binding is highest in the stratum pyramidale (Cotman et al., 1987), the use of histological overlay in the present series demonstrated that binding was most dense in the stratum radiatum, with moderately less binding in the stratum pyramidale. Other CA1 regions were also densely labelled. Within CA2/3 [^3H]-AMPA binding was also highest in the stratum radiatum, although binding is generally lower than in CA1. In the dentate gyrus, [^3H]-AMPA binding was concentrated within the molecular layer. In the cortex, [^3H]-AMPA binding was distributed evenly throughout superficial and deep cortical layers. Dense [^3H]-AMPA binding was also measured in the subiculum; in the septal area, binding was dense in the lateral septum, and moderate within the medial septum.

[^3H]-Kainate Binding Sites

The distribution of [^3H]-kainate binding was observed to be markedly different to that of [^3H]-AMPA binding. In the stratum lucidum, situated lateral to the CA2/3 pyramidal cell layer, [^3H]-kainate binding sites were extremely dense, and the CA4 pyramidal layer also exhibited relatively high amounts of binding. Little binding occurred elsewhere within the hippocampus, although the dentate gyrus, particularly the infragranular layer and the inner portion of the

molecular layer, was generally more densely labelled than the CA sector. Low levels of kainate binding were measured in the subicular complex.

Within cortical regions, [^3H]-kainate binding was generally associated with deep cortical layers; however, this trend is absent in the entorhinal cortex, which contained higher densities of binding within superficial layers. In the septal area, low amounts of [^3H]-kainate binding occurred throughout the septal nuclei and diagonal band.

NMDA-Displaceable [^3H]-L-Glutamate Binding Sites

NMDA-displaceable [^3H]-glutamate binding sites were found in extremely high quantities in the hippocampus, and were concentrated in CA1 strata oriens and radiatum. The inner portion of the dentate molecular layer was also densely labelled, while binding was lower in the outer portion and in CA2 and CA3.

NMDA-sensitive [^3H]-glutamate binding was dense within cortical areas, and was particularly dense within the entorhinal cortex; binding sites were concentrated in the outer cortical layers. The subiculum and presubiculum were observed to contain moderate levels of NMDA-sensitive binding sites, while in the septal area NMDA-sensitive binding was low.

2.3.2. Alterations in Muscarinic and Glutamatergic Receptor Binding Within Hippocampal and Associated Regions Following Lesions of the Medial Septum

Exact values for [^3H]-QNB, [^3H]-AMPA, [^3H]-kainate and NMDA-displaceable [^3H]-glutamate binding to muscarinic, AMPA, kainate and NMDA receptors respectively are found in Appendix V, Tables 1-4.

LEGENDS TO FIGURES 31 & 32

FIGURE 31: [³H]-Quinuclidinyl Benzylate ([³H]-QNB) binding in the hippocampal formation and associated regions following lesions of the medial septum: Ammons horn and the dentate gyrus.

Abbreviations: or: stratum oriens; pyr: stratum pyramidale; rad: stratum radiatum; lac mol: stratum lacunosum moleculare; mol (outer): molecular layer, outer portion; mol (inner): molecular layer, inner portion; gran: granular layer; infragran: infragranular layer.

FIGURE 32: [³H]-Quinuclidinyl Benzylate ([³H]-QNB) binding in the hippocampal formation and associated areas following lesions of the medial septum: subicular area, entorhinal cortex and septal area.

Abbreviations: Sub: subiculum; Pres: presubiculum; Medial: Entorhinal cortex, medial portion; Lateral: entorhinal cortex, lateral portion; I-II: cortical layers I-II; III-VI: cortical layers III-VI; LS: lateral septum; MS: medial septum; VDB: vertical diagonal band nucleus.

Data are presented as mean ligand bound (pmol/g tissue) ± S.E.M. *p<0.05, **p<0.01 relative to control (Student's unpaired t-test, two-tailed).

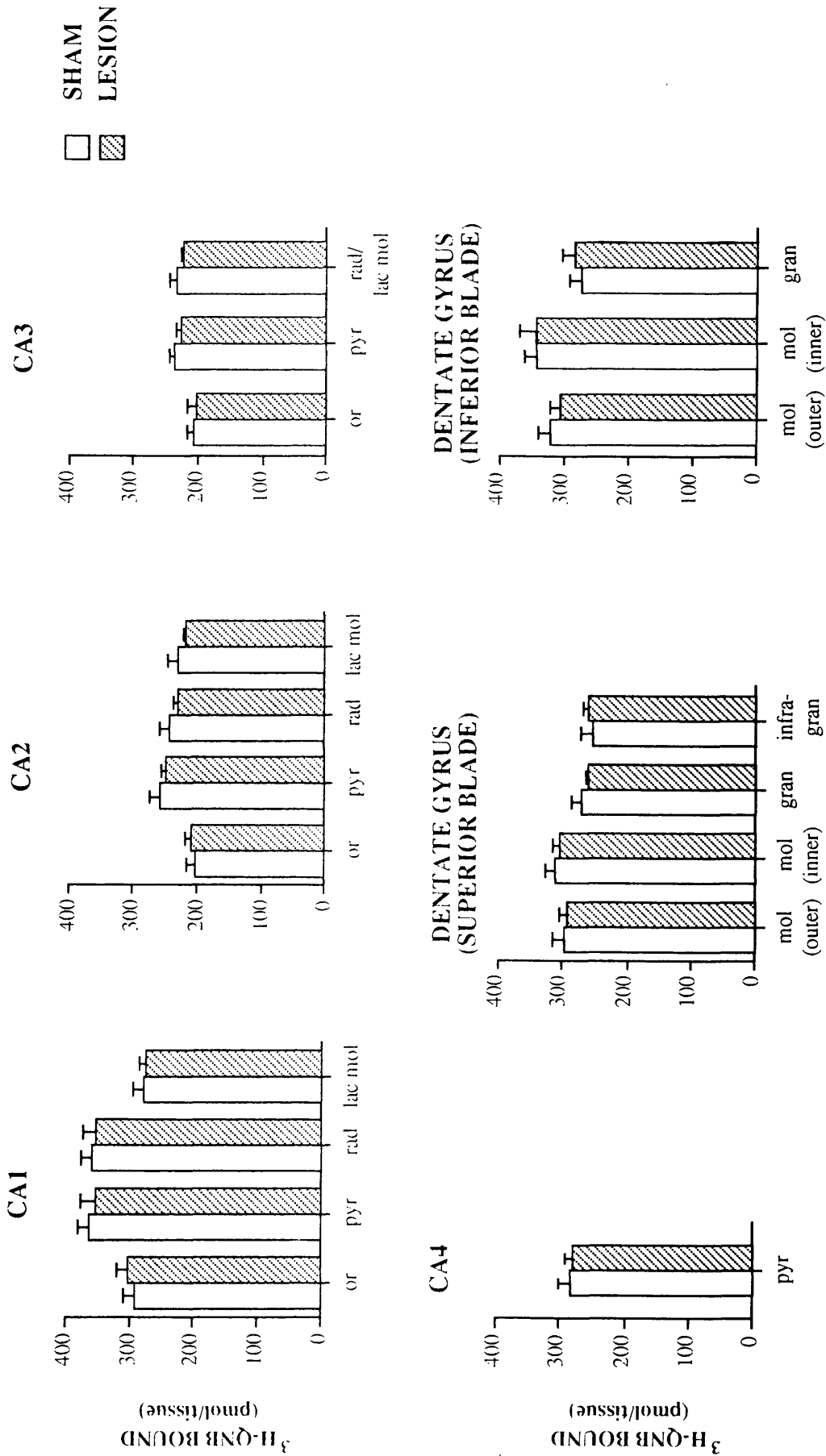


FIGURE 31: [³H]-QNB BINDING IN THE HIPPOCAMPAL AREA: CA AND DENTATE GYRUS

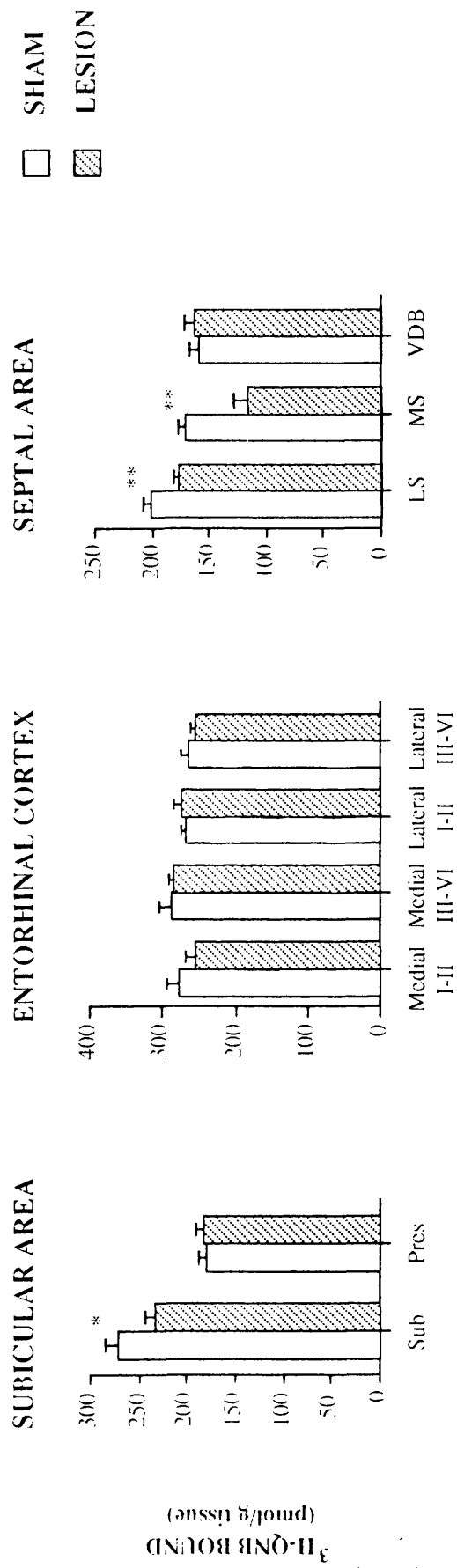


FIGURE 32 : [³H]-QNB BINDING IN THE HIPPOCAMPAL REGION: SUBICULAR AREA, ENTORHINAL CORTEX AND SEPTAL AREA

LEGENDS TO FIGURES 33 & 34

FIGURE 33: [³H]-AMPA binding in the hippocampal formation and associated regions following lesions of the medial septum: Ammons horn and the dentate gyrus.

Abbreviations: or: stratum oriens; pyr: stratum pyramidale; rad: stratum radiatum; lac mol: stratum lacunosum moleculare; mol (outer): molecular layer, outer portion; mol (inner): molecular layer, inner portion; gran: granular layer; infragran: infragranular layer.

FIGURE 34: [³H]-AMPA binding in the hippocampal formation and associated areas following lesions of the medial septum: subicular area, entorhinal cortex and septal area.

Abbreviations: Sub: subiculum; Pres: presubiculum; Medial: Entorhinal cortex, medial portion; Lateral: entorhinal cortex, lateral portion; I-II: cortical layers I-II; III-VI: cortical layers III-VI; LS: lateral septum; MS: medial septum; VDB: vertical diagonal band nucleus.

Data are presented as mean ligand bound (pmol/g tissue) \pm S.E.M. * $p < 0.05$, ** $p < 0.01$ relative to control (Student's unpaired t-test, two-tailed).

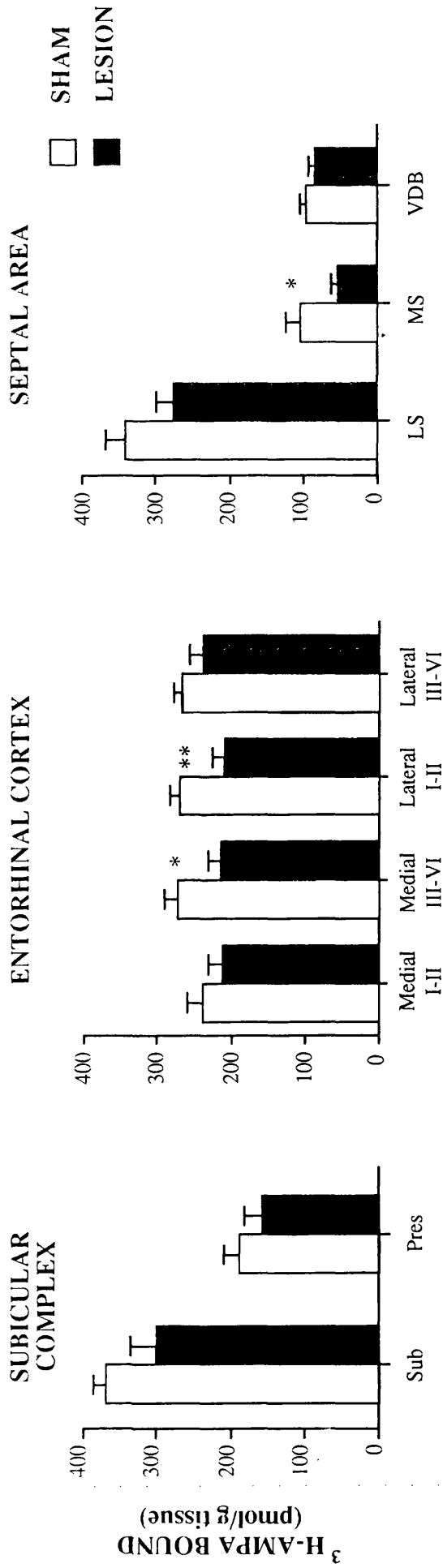


FIGURE 34 : [³ H] - AMPA BINDING IN THE HIPPOCAMPAL REGION: SUBICULUM, ENTORHINAL CORTEX AND SEPTAL AREA

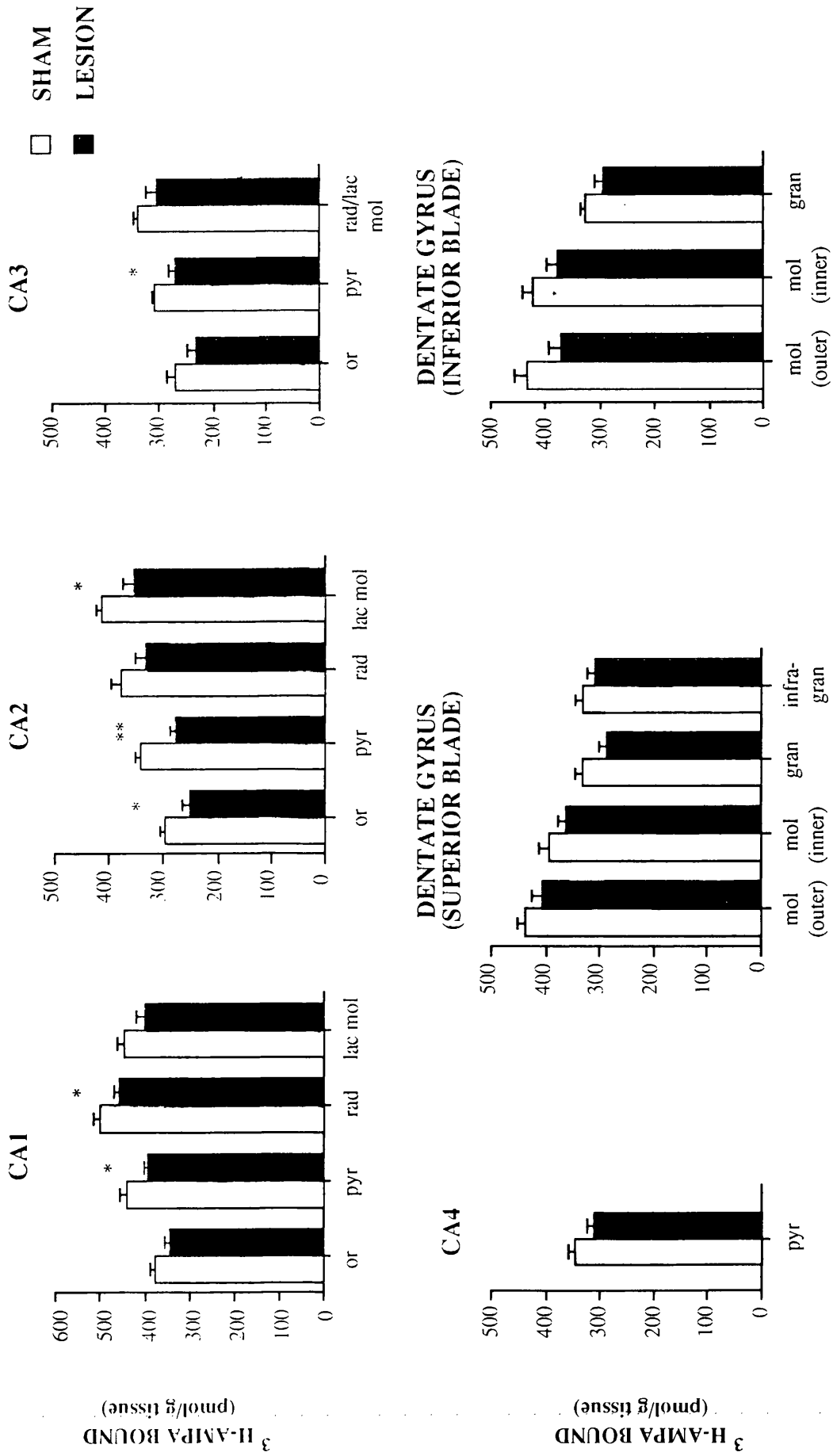


FIGURE 33 : [³H]-AMPA BINDING IN THE HIPPOCAMPAL REGION: CA AND DENTATE GYRUS

[³H]-QNB Binding

In Ammon's Horn and the dentate gyrus, muscarinic binding sites, measured by [³H]-QNB binding were unaltered following lesions of the medial septum (Appendix V Table 1; Figures 31 & 32). In the subiculum, however, a significant decrease (14%) was observed in the lesioned group. In the septal area, further reductions in [³H]-QNB binding were apparent: binding was reduced in the medial septum by 32% and in the lateral septum by 13% relative to control values.

[³H]-AMPA Binding to Quisqualate Receptors

Significantly decreased [³H]-AMPA binding was measured in a number of hippocampal and associated regions in response to lesions of the medial septum (Appendix V, Table 2). Within the CA region, significantly decreased levels of binding occurred in the stratum pyramidale of CA1-3. The largest decrease, which represented 18% of the control value, occurred in CA2 (Figure 33). Significant decreases in [³H]-AMPA binding were also measured in the stratum radiatum of CA1 and the strata oriens and lacunosum moleculare of CA2. No significant alterations in binding were measured in the dentate gyrus or subicular area.

In the entorhinal cortex, [³H]-AMPA binding was significantly decreased in layers III-VI of the medial portion, and in layers I-II of the lateral portion following medial septal lesions. In the septal area, binding was decreased by 49% in the medial septal nucleus, but was unaltered in the lateral septal nucleus and diagonal band (Figure 34).

[³H]-Kainate Binding

In contrast to the localised alterations in [³H]-AMPA binding in response to lesions of the medial septum, there were no significant alterations in [³H]-kainate binding in the 29 hippocampal and associated areas following septal lesions (Appendix V, Table 3, and Figures 35 &

LEGENDS TO FIGURES 35 & 36

FIGURE 35: [³H]-Kainate binding in the hippocampal formation and associated regions following lesions of the medial septum: Ammons horn and the dentate gyrus.

Abbreviations: or: stratum oriens; pyr: stratum pyramidale; rad: stratum radiatum; lac mol: stratum lacunosum moleculare; mol (outer): molecular layer, outer portion; mol (inner): molecular layer, inner portion; gran: granular layer; infragran: infragranular layer.

FIGURE 36: [³H]-Kainate binding in the hippocampal formation and associated areas following lesions of the medial septum: subicular area, entorhinal cortex and septal area.

Abbreviations: Sub: subiculum; Pres: presubiculum; Medial: Entorhinal cortex, medial portion; Lateral: entorhinal cortex, lateral portion; I-II: cortical layers I-II; III-VI: cortical layers III-VI; LS: lateral septum; MS: medial septum; VDB: vertical diagonal band nucleus.

Data are presented as mean ligand bound (pmol/g tissue) ± S.E.M. There were no significant differences between control and lesioned animals (Student's unpaired t-test, two-tailed).

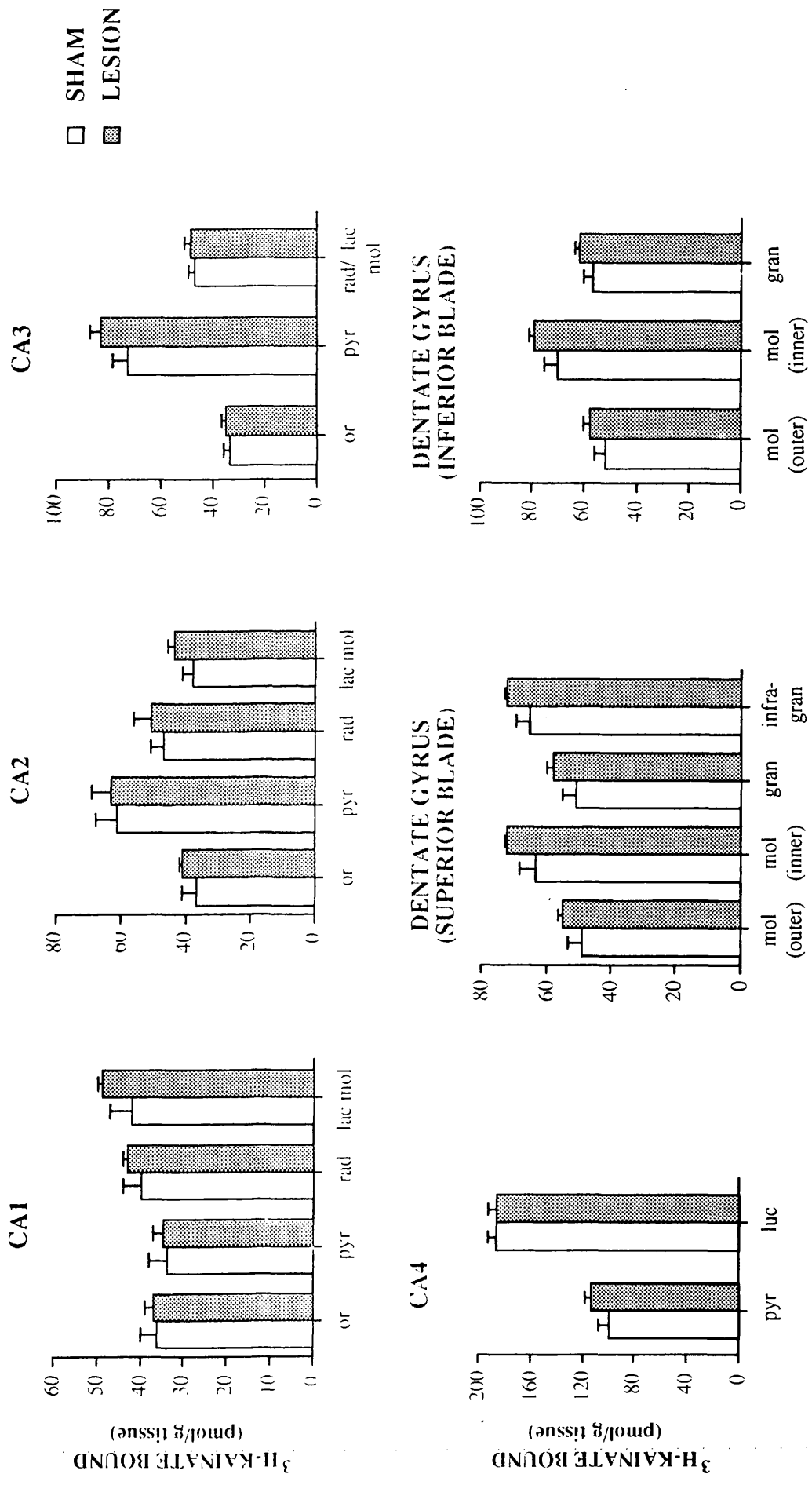


FIGURE 35 : [³H]-KAINATE BINDING IN HIPPOCAMPAL REGIONS FOLLOWING LESIONS OF THE MEDIAL SEPTUM: CA REGION AND DENTATE GYRUS

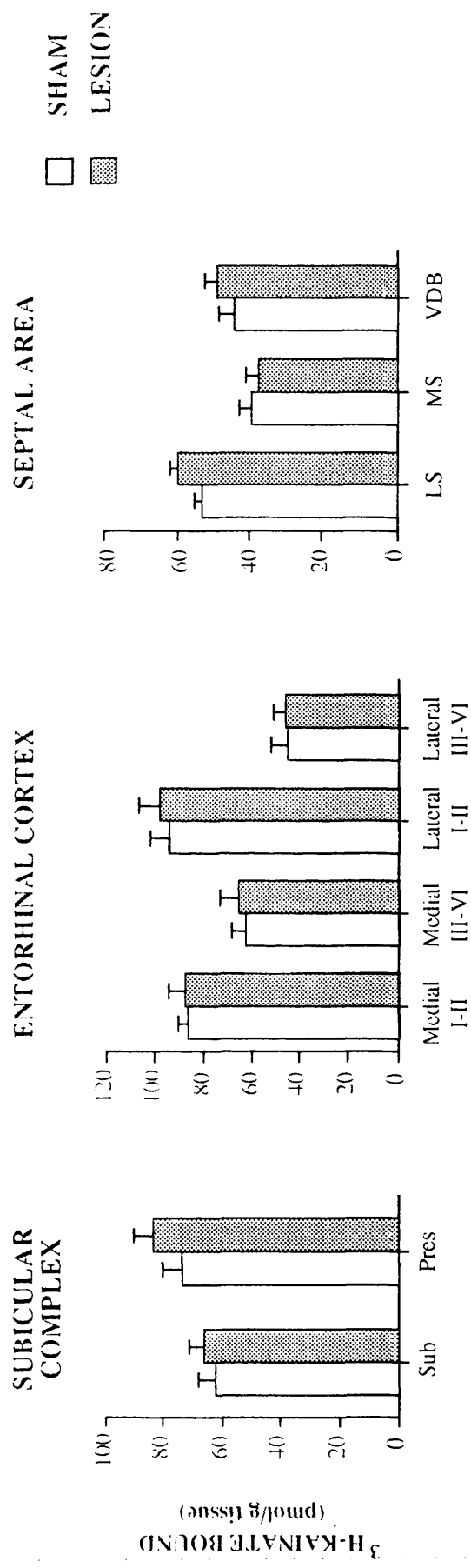


FIGURE 36 : [^3H]-KAINATE BINDING IN THE HIPPOCAMPAL REGION: SUBICULAR COMPLEX, ENTORRHINAL CORTEX AND SEPTAL AREA

LEGENDS TO FIGURES 37 & 38

FIGURE 37: NMDA-displaceable [³H]-glutamate binding in the hippocampal formation and associated regions following lesions of the medial septum: Ammons horn and the dentate gyrus.

Abbreviations: or: stratum oriens; pyr: stratum pyramidale; rad: stratum radiatum; lac mol: stratum lacunosum moleculare; mol (outer): molecular layer, outer portion; mol (inner): molecular layer, inner portion; gran: granular layer; infragran: infragranular layer.

FIGURE 38: NMDA-displaceable [³H]-glutamate binding in the hippocampal formation and associated areas following lesions of the medial septum: subicular area, entorhinal cortex and septal area.

Abbreviations: Sub: subiculum; Pres: presubiculum; Medial: Entorhinal cortex, medial portion; Lateral: entorhinal cortex, lateral portion; I-II: cortical layers I-II; III-VI: cortical layers III-VI; LS: lateral septum; MS: medial septum; VDB: vertical diagonal band nucleus.

Data are presented as mean ligand bound (pmol/g tissue) ± S.E.M. There were no differences between control and lesioned animals (Student's unpaired t-test, two-tailed).

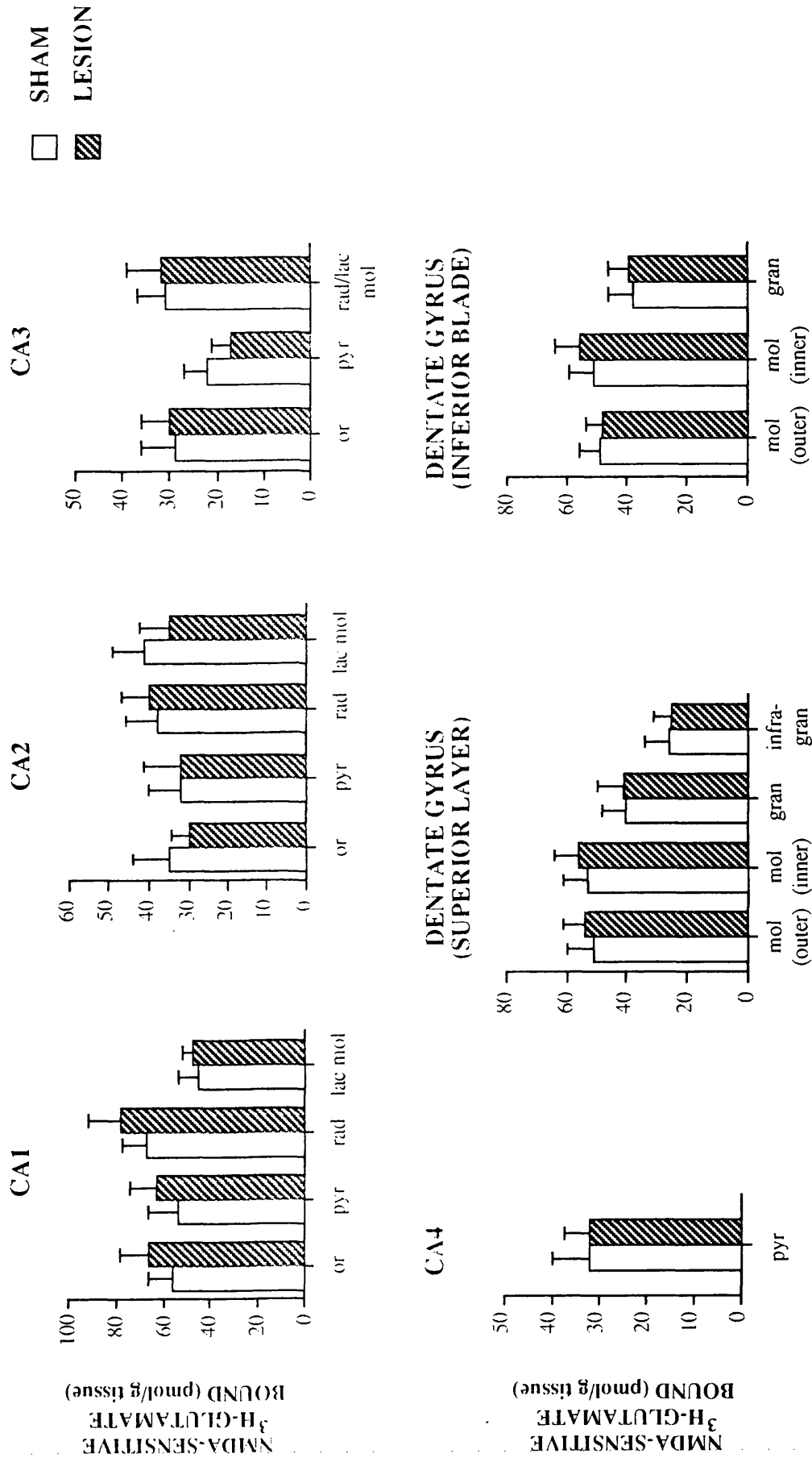


FIGURE 37: NMDA-SENSITIVE [³H]-GLUTAMATE BINDING IN THE HIPPOCAMPAL AREA: CA AND DENTATE GYRUS

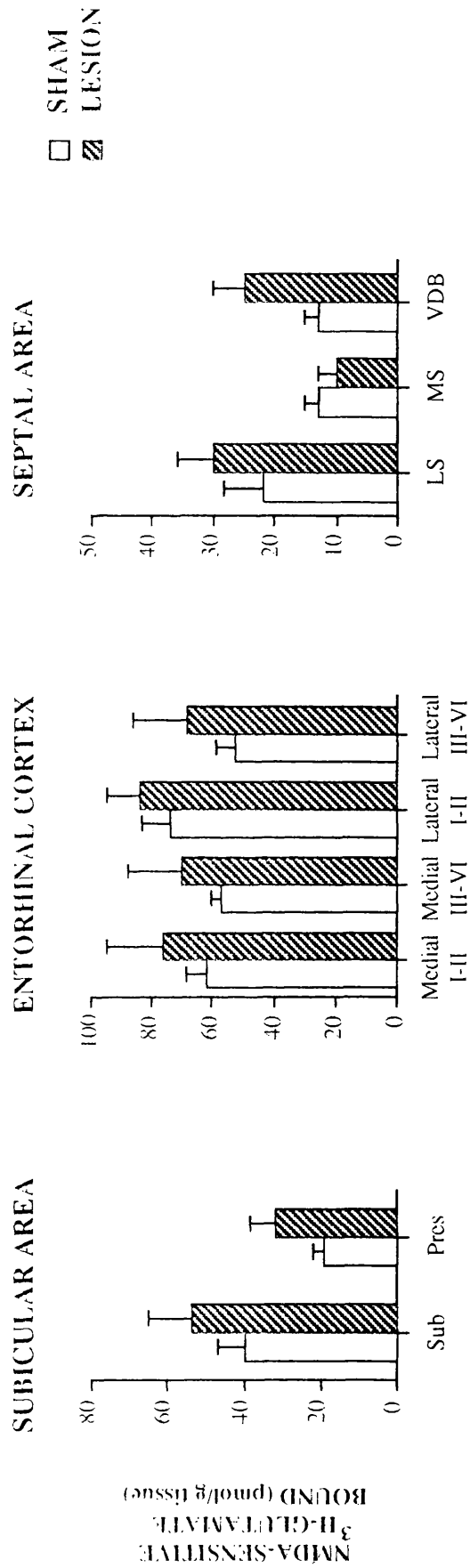


FIGURE 38 : NMDA-SENSITIVE [³H]-GLUTAMATE BINDING IN THE HIPPOCAMPAL AREA: SUBICULAR, ENTORHINAL AND SEPTAL AREAS

36). The largest deviations from sham operated control values occurred in the stratum lacunosum moleculare, where increases of 17% and 16% were measured in the CA1 and CA2 regions respectively in response to septal lesions. Binding was unaltered in the lesioned medial septal area.

NMDA-Displaceable [³H]-Glutamate Binding

There were no significant alterations in NMDA-sensitive [³H]-glutamate binding sites in any of 29 structures measured (Appendix V, Table 4 and Figures 37 & 38). In the presubiculum, binding was increased by 68%, and in the vertical limb of the diagonal band nucleus, binding was increased by 92% in lesioned animals compared to values for sham operation; however, the variability of binding in these animals was high, reflected by the relatively large standard errors, and these results were not significant.

2.4. MEASUREMENT OF PHOSPHOINOSITIDE TURNOVER FOLLOWING LESIONS OF THE MEDIAL SEPTUM

Accumulation of [³H]-inositol phosphate was measured in the presence of lithium in rat hippocampal slices 21 days after lesions of the medial septum or sham operation. Choline acetyltransferase activity was assayed in homogenate preparations from the hippocampus of each rat.

Mean values for phosphoinositide hydrolysis, as indicated by inositol phosphate accumulation, and choline acetyltransferase activity are given in Table 3. Following lesions of the medial septum, a decrease in choline acetyltransferase activity of 25% was measured in the hippocampus; this reduction was statistically significant. However, no significant difference in either basal or carbachol-stimulated inositol

TABLE 3: BASAL AND CARBACHOL-STIMULATED [³H]-INOSITOL PHOSPHATE ACCUMULATION AND ChAT ACTIVITY IN THE RAT HIPPOCAMPUS FOLLOWING LESIONS OF THE MEDIAL SEPTUM

	SHAM (n=10)	LESION (n=10)
[³ 1,1]-Inositol-phosphate incorporated (DPM):-		
BASAL	735 ± 98	707 ± 66
CARBACHOL (500µM)	2425 ± 248	2134 ± 138
% [³ H]-Myo-inositol incorporated:-		
BASAL	0.69 ± 0.09	0.65 ± 0.07
CARBACHOL (500µM)	2.35 ± 0.33	1.95 ± 0.23
% STIMULATION:	264 ± 53	227 ± 41
ChAT Activity (nmol/h/mg protein):-	27.0 ± 1.4	20.5 ± 2.1*

ChAT: Choline acetyltransferase; *p<0.02, Student's unpaired t-test, two-tailed.

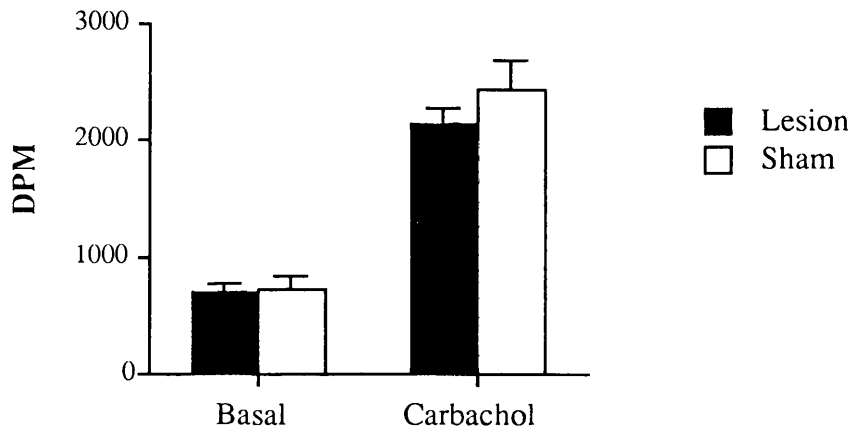
LEGEND TO FIGURE 39

FIGURE 39: Phosphoinositide hydrolysis in the rat hippocampus following lesions of the medial septum

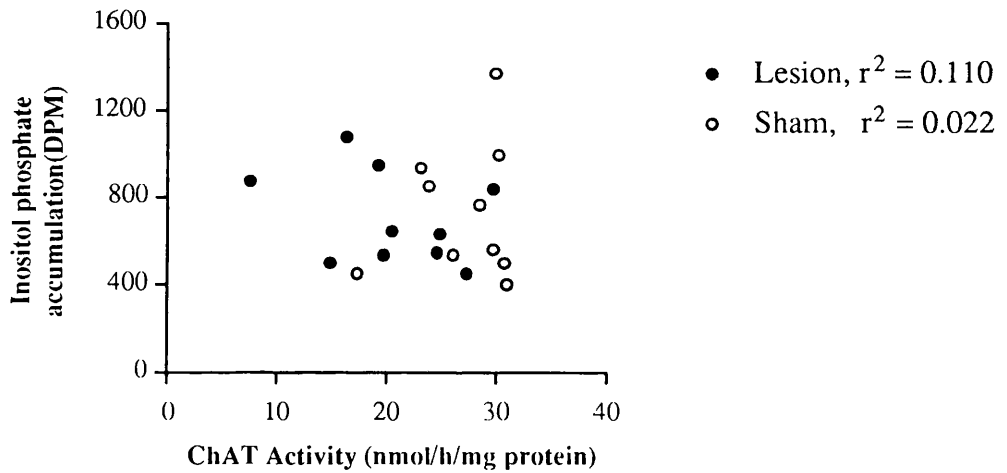
- A. [³H]-Inositol phosphate accumulation: Basal and carbachol-stimulated [³H]-inositol phosphate accumulation is expressed as DPM for lesioned (n=10) and control (n=10) rats. There were no significant differences between control and lesioned rats (Student's unpaired t-test, two-tailed).
- B. & C. Basal (B.) and carbachol-stimulated (C.) [³H]-inositol phosphate accumulation (DPM) vs. ChAT activity. [³H]-inositol phosphate accumulation (DPM) is plotted against ChAT activity (nmol/h/mg protein) within the hippocampus. Correlation coefficients for [³H]-inositol phosphate accumulation vs. ChAT activity in sham-operated control and lesioned animals are given as r² values. There was no correlation between ChAT activity and [³H]-inositol phosphate accumulation. Note the relative loss of ChAT activity in lesioned animals.

ChAT: Choline acetyltransferase

A. [³H]-INOSITOL PHOSPHATE ACCUMULATION



B. BASAL [³H]-INOSITOL PHOSPHATE ACCUMULATION VS ChAT ACTIVITY



C. CARBACHOL-STIMULATED [³H]-INOSITOL PHOSPHATE ACCUMULATION VS ChAT ACTIVITY

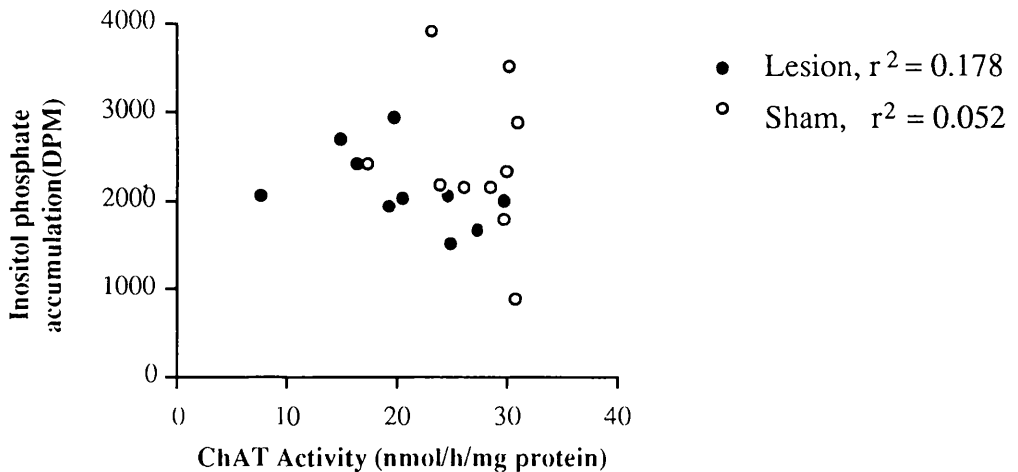


FIGURE 39: PHOSPHOINOSITIDE HYDROLYSIS IN THE RAT HIPPOCAMPUS FOLLOWING LESIONS OF THE MEDIAL SEPTUM

phosphate accumulation occurred in the hippocampus following septal lesions (Figure 39). Finally, there was no correlation between phosphoinositide hydrolysis and ChAT activity in control or lesioned animals.

3. THE CEREBRAL METABOLIC EFFECTS OF ACUTE SUBDURAL HAEMATOMA IN THE RAT.

3.1. EFFECTS OF ACUTE SUBDURAL HAEMATOMA ON LOCAL CEREBRAL GLUCOSE UTILISATION

Local cerebral glucose utilisation two hours after acute subdural haematoma alone, haematoma with prior administration of D-CPP-ene, or sham surgery are given in Appendix V. Rates of cerebral glucose use were calculated using the rate and lumped constants described by Sokoloff et al. (1977). Glucose use was measured in twelve hippocampal regions, nineteen other regions associated with limbic function, and nine additional regions of interest.

Visual inspection of the autoradiograms (Figure 40) from animals with subdural haematoma alone revealed an area of hypometabolism, presumably caused by loss of perfusion, and thence impeded tracer delivery, in the region of infarct, which extended from the posterior parietal cortex to the occipital cortex; in some animals, a lack of deoxyglucose uptake was observed in visual cortical areas. The lack of deoxyglucose uptake was limited to the cortex; there was no evidence of impeded uptake in the underlying hippocampal formation in any animal. Surrounding the area of diminished deoxyglucose uptake was a rim of apparent hypermetabolism, presumed to be the ischaemic penumbral region. In those animals which had received acute subdural haematoma with prior administration of D-CPP-ene, the area of decreased deoxyglucose uptake was on inspection smaller than in the non-pretreated group. Additionally, D-CPP-ene abolished the appearance of the rim of increased deoxyglucose phosphorylation bordering the infarcted area. In the sham-treated rats, a slight depression of glucose utilisation was observed in the area directly below the inserted needle, and was probably due to heat-damage in the course

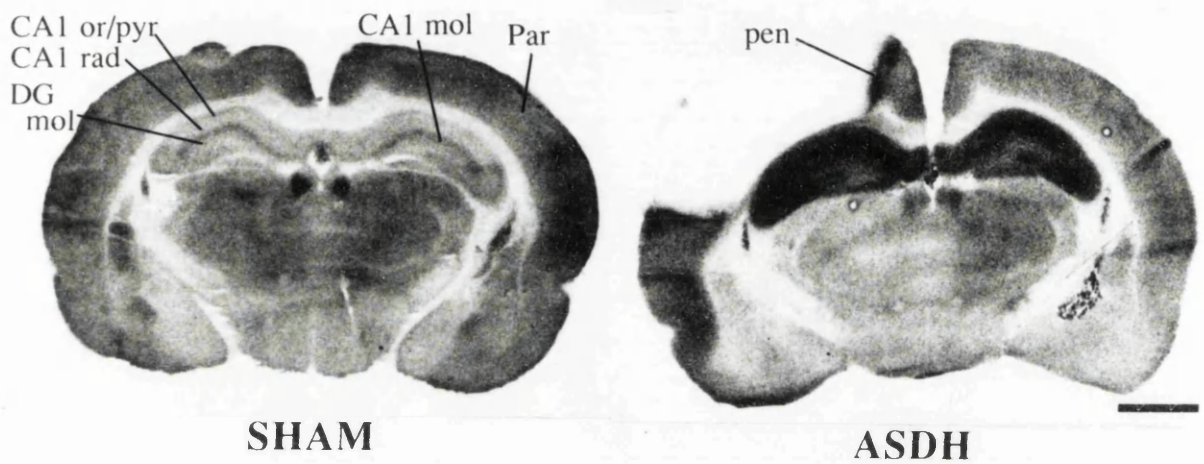


FIGURE 40: AUTORADIOGRAMS OF GLUCOSE UTILISATION IN THE RAT BRAIN HIPPOCAMPUS FOLLOWING ACUTE SUBDURAL HAEMATOMA

Representative autoradiograms of glucose use in the rat brain at the level of the dorsal hippocampus. Left: sham-operated control. Right: acute subdural haematoma. Note the large parietal cortical region of markedly reduced deoxyglucose uptake and the degree of increased deoxyglucose uptake throughout the hippocampal formation in response to haematoma.

Abbreviations: CA1 or/pyr: CA1 strata oriens/pyramidale; CA1 rad: CA1 stratum radiatum; CA1 mol: CA1 stratum leucosum moleculare; DG mol: dentate molecular layer. Par: parietal cortex; Pen: penumbral region. Scale bar equals 2mm.

of drilling through the skull. No hypermetabolism was evident in the surrounding cerebral tissues.

Following acute subdural haematoma, glucose utilisation was markedly increased in the hippocampus bilaterally. When compared statistically to rates of glucose utilisation in sham-operated rats, all values for glucose utilisation in the hippocampal CA and dentate gyrus ipsilateral to the haematoma were significantly increased: in the CA1 stratum radiatum the largest increase of 142% was measured (Figure 41). Contralaterally, glucose utilisation was increased less than ipsilaterally; the largest increase occurred in the CA1 radiatum. Variability was greater contralaterally, and consequently, increases were significant in only three hippocampal regions: the CA3 stratum oriens, the CA1 stratum lacunosum moleculare, and the dentate molecular layer. In animals which had received D-CPP-ene prior to the haematoma, glucose utilisation was lower than in the group with haematoma alone (Figure 41). Significant difference in comparison to the haematoma group was achieved in three hippocampal regions, the CA3 stratum oriens, and the stratum radiatum of CA1 and CA3. D-CPP-ene also induced an increase in glucose utilisation in the presubiculum contralaterally to the haematoma.

In other regions associated with limbic function, a number of alterations were observed, which can be related to either the haematoma or the action of D-CPP-ene. In the group of animals with the haematoma alone, glucose utilisation was increased in the laterodorsal thalamic nucleus in comparison with sham-treated rats. In contrast, glucose utilisation was significantly increased in the anteroventral thalamic nucleus in the D-CPP-ene pretreated group compared with values for acute subdural haematoma alone. A number of cortical regions were likewise affected: glucose utilisation was raised significantly in the entorhinal cortex and lateral olfactory tract contralaterally, and in the posterior cingulate cortex bilaterally,

LEGEND TO FIGURE 41

FIGURE 41: Local cerebral glucose utilisation in hippocampal regions following acute subdural haematoma.

Abbreviations: ASDH: acute subdural haematoma; or: stratum oriens; rad: stratum radiatum; pres: presubiculum; subic: subiculum; DG Mol (sup): dentate gyrus, molecular layer, superior blade; DG Infra (sup): dentate gyrus, infragranular granular layer, superior blade; Ent L I-II: entorhinal cortex, lateral portion layers I-II.

Data are presented as mean glucose utilisation ($\mu\text{mol } 100\text{g}^{-1} \text{ min}^{-1}$) \pm S.E.M. All measurements were made ipsilateral to the haematoma. * $p < 0.05$, ** $p < 0.01$ for comparisons of ASDH with controls; † $p < 0.05$ for comparisons of ASDH alone with D-CPP-ene pre-treated ASDH (15 mgkg^{-1}) (Student's unpaired t-test, two-tailed, with Bonferroni correction).

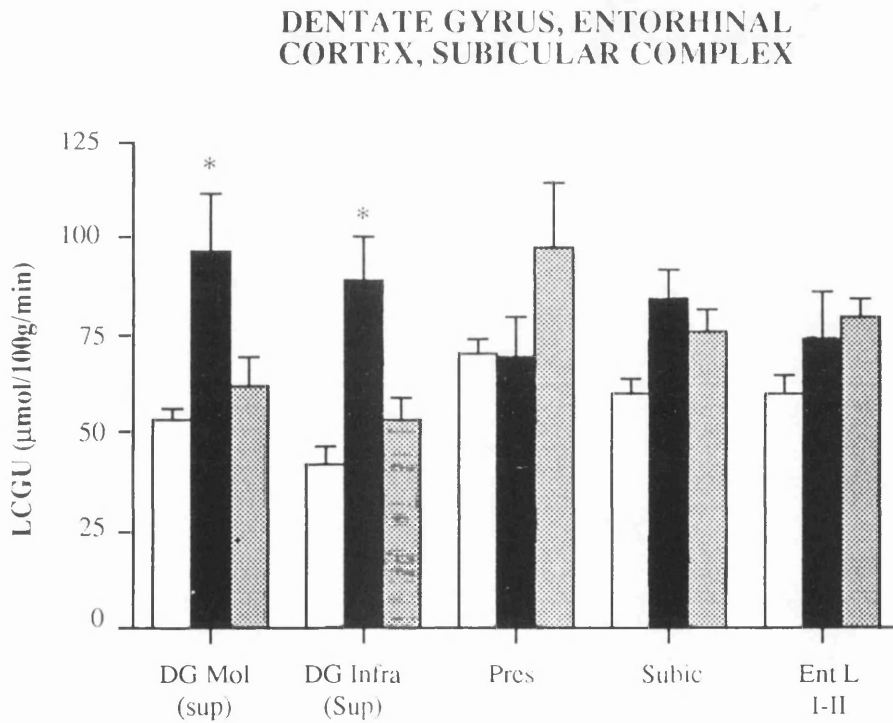
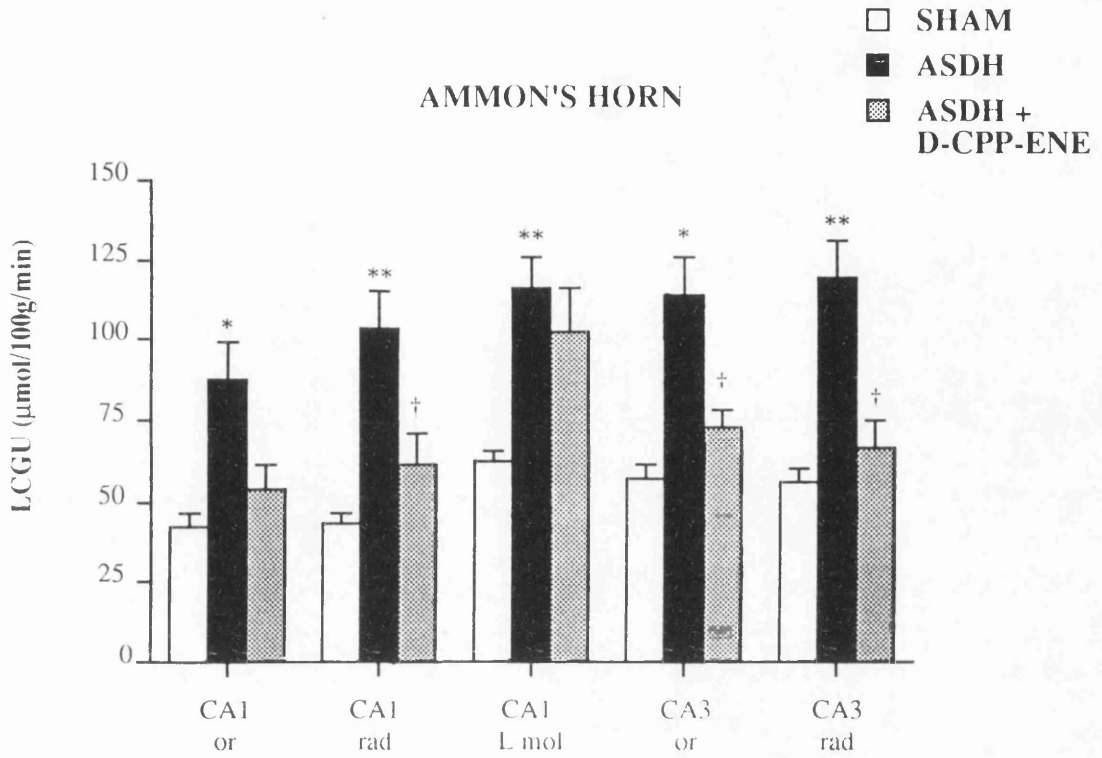


FIGURE 41 : LOCAL CEREBRAL GLUCOSE UTILISATION FOLLOWING ACUTE SUBDURAL HAEMATOMA : HIPPOCAMPAL FORMATION

following D-CPP-ene pretreatment. In one cortical area, layer IV of the frontal cortex, glucose utilisation was reduced significantly following D-CPP-ene treatment.

Finally, acute subdural haematoma was seen to alter glucose utilisation in several other regions (Figure 42). In auditory and visual regions, values for glucose utilisation were significantly lower following acute subdural haematoma in the ipsilateral medial and dorsolateral geniculate bodies, and a depression of glucose use, though not significant, was observed in the auditory cortex. In the caudate nucleus ipsilateral to the haematoma, glucose utilisation was lower than in sham-treated rats, but this result was not significant. D-CPP-ene pretreatment failed to alter significantly rates of glucose utilisation in any of these structures, although values for the medial and dorsolateral geniculate bodies were higher than in the group which had received the haematoma alone.

LEGEND TO FIGURE 42

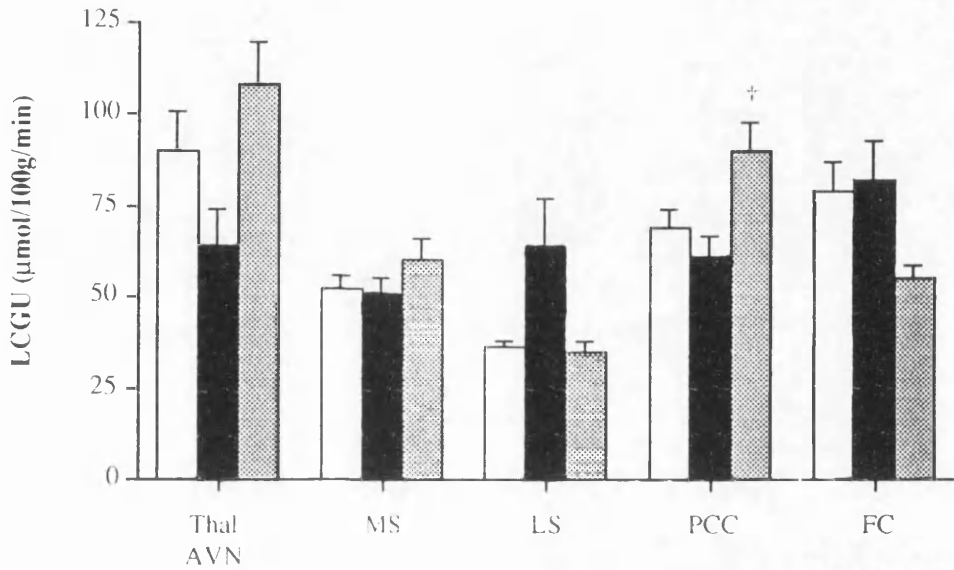
FIGURE 42: Local cerebral glucose utilisation in limbic, auditory and visual regions following acute subdural haematoma.

Abbreviations: ASDH: acute subdural haematoma; Thal AVN: thalamus, anteroventral nucleus; MS: medial septum; LS: lateral septum; PCC: posterior cingulate cortex; FC: frontal cortex; Aud C IV: auditory cortex layer IV; MGB: medial geniculate body; DLG: dorsolateral geniculate body; SC (sup): superior colliculus, superficial layer.

Data are presented as mean glucose utilisation ($\mu\text{mol } 100\text{g}^{-1} \text{ min}^{-1}$) \pm S.E.M. All measurements were made ipsilateral to the haematoma. * $p < 0.05$, ** $p < 0.01$ for comparisons of ASDH with controls; † $p < 0.05$ for comparisons of ASDH alone with D-CPP-ene pre-treated ASDH (15 mgkg^{-1}) (Student's unpaired t-test, two-tailed, with Bonferroni correction).

- SHAM
- ASDH
- ▨ ASDH + D-CPP-ENE

AREAS ASSOCIATED WITH LIMBIC FUNCTION



AUDITORY AND VISUAL STRUCTURES

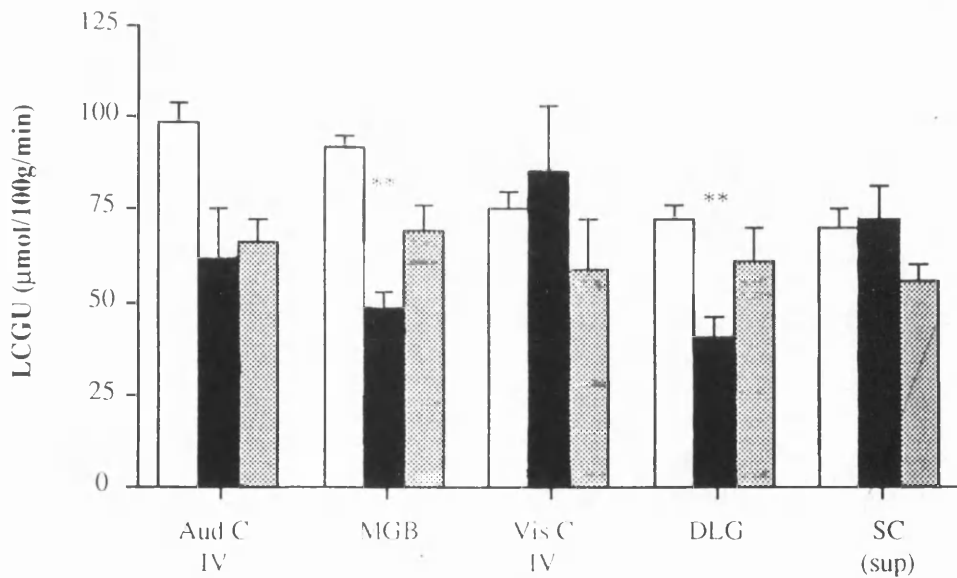


FIGURE 42 : LOCAL CEREBRAL GLUCOSE UTILISATION FOLLOWING ACUTE SUBDURAL HAEMATOMA: LIMBIC, AUDITORY AND VISUAL REGIONS

CHAPTER IV

DISCUSSION

1. EFFECTS OF GLUTAMATERGIC AND CHOLINERGIC AGENTS ON CEREBRAL GLUCOSE USE

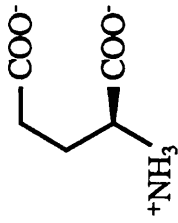
1.1. THE COMPETITIVE NMDA ANTAGONIST D-CPP-ENE

The development of antagonists specific for the NMDA receptor and its associated ion channel (Figure 3), and the use of the deoxyglucose technique has provided considerable insight into the function of glutamatergic systems in the brain (McCulloch & Iversen, 1991). Further, the deoxyglucose autoradiographic technique has proved informative in the study of differences between competitive and non-competitive antagonists: while the general distribution of alterations is similar, the functional effects of non-competitive antagonists differ greatly in their magnitude. While non-competitive antagonists such as MK-801 (Kurumaji et al., 1989) and phencyclidine (Weissman et al., 1987) produce marked increases in glucose use in limbic and olfactory regions, the competitive NMDA antagonists 3-(2-carboxypiperazin-4-yl)-propyl-1-phosphonic acid (CPP, Kurumaji et al., 1989) and 2-amino-7-phosphonoheptanoate (AP7; Chapman et al., 1989) produce few significant alterations in cerebral glucose use.

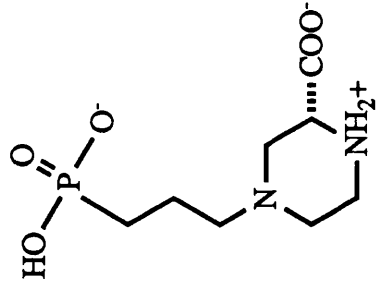
Kurumaji and colleagues (1989) suggested that the difference in patterns of altered glucose use produced by MK-801 and CPP was due to the different modes of action of the drugs: the action of non-competitive antagonists, because of their use-dependency, is potentiated in areas of high glutamatergic activity, while in these regions, competitive antagonists which bind to the recognition site for glutamate are readily displaced by the endogenous agonist during intense glutamatergic activity. Thus, the increased functional activity in limbic and olfactory regions in response to MK-801 was interpreted as a futile attempt to overcome the non-competitive glutamatergic blockade within these regions.

In contrast to previous studies, D-CPP-ene administration resulted in much less overt alterations in glucose utilisation in limbic regions including the Papez circuit (hippocampal formation, mamillary bodies, anterior thalamic nucleus and cingulate cortex), but produced marked dose-dependent reductions in glucose use in areas involved in sensory processing, such as auditory and visual structures. Therefore, the results presented here are notably different to those of glucose use following administration of classical competitive antagonists. Indeed, while non-competitive antagonists produce largely similar patterns of altered glucose use (Crosby et al., 1982; Hammer et al., 1982; Kurumaji et al., 1989; Weissman et al., 1987), competitive antagonists display heterogeneity in their ability to produce functional alterations in discrete CNS regions. It might be presumed that the present results differ from previous reports of competitive NMDA antagonists on the basis of the high potency of D-CPP-ene (Chapman et al., 1990; Lowe et al., 1990). However, a recent study of the effects of CGP39551 (2-amino-4-methyl-5-phosphono-3-pentenoic acid 1-ethyl ester), an orally active, unsaturated analogue of AP7 with high potency (Schmutz et al., 1989), demonstrated large increases in glucose utilisation in the Papez circuit, extrapyramidal system and olfactory regions (Chapman et al., 1991), while sensory regions were largely unaltered.

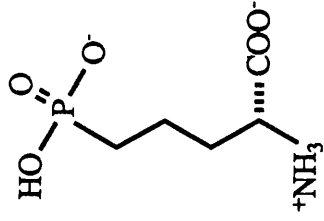
Different patterns of functional activity may represent the affinities which some drugs have for other classes of receptor such as the β -adrenergic, dopaminergic, and sigma-opiate receptor (Snell et al., 1988, Kozlowski, 1986). The non-competitive antagonist phencyclidine has been shown to interact with the sigma-opiate binding site in the brain, for which MK-801 has little affinity (Wong & Nielsen, 1989), and phencyclidine also displays some dopamine agonist properties (Snell et al., 1988). In addition to the functional activation of the Papez and olfactory structures, phencyclidine has been shown to increase glucose use in regions such as the anterior cingulate cortex, amygdala, caudate



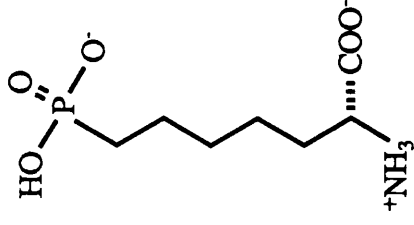
L-glutamate
(endogenous agonist)



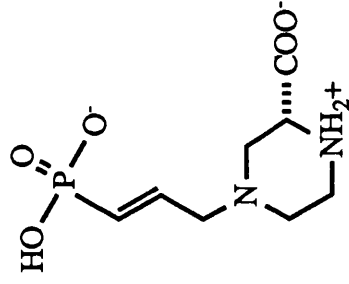
CPP



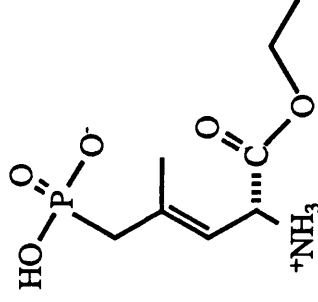
APV (AP5)



APH (AP7)



CPP-ene



CGP 39551

FIGURE 43: COMPETITIVE NMDA ANTAGONISTS

nucleus and globus pallidus, while MK-801 has no effect: and it has been suggested that these differences represent the action of phencyclidine at opiate or dopamine receptors. While there is little evidence from deoxyglucose studies that selective sigma-opiate ligands induce altered glucose use in these areas (della Puppa & London, 1989; Kozłowski 1986), the dopaminergic agonist apomorphine increases glucose utilisation in striatal regions (Kelly & McCulloch, 1987). It is possible, therefore, that the ability of CGP39551 to activate dopaminergic areas such as the caudate nucleus, substantia nigra, and globus pallidus may be due to the actions of the drug at dopaminergic sites. In contrast, Lehmann et al. (1987) have shown that CPP has little affinity for dopaminergic receptors, and none at all for β -adrenergic receptors, at a concentration which maximally displaces [3 H]-AP5 binding (Davies et al., 1986).

Additionally, variant patterns of glucose use produced by different competitive NMDA antagonists may be explained by the existence of sub-populations of NMDA receptors within the brain. Comparisons between the distribution of [3 H]-CPP, [3 H]-AP5, and NMDA-displaceable [3 H]-glutamate binding have led to the speculation that at least two sub-types of NMDA receptor exist (Cotman et al., 1987): both [3 H]-CPP and [3 H]-AP5 bind in relatively higher amounts in the thalamus, and lower amounts in the striatum, septal area and cerebellum compared to NMDA-displaceable [3 H]-glutamate. Recently it has been shown that [3 H]-MK-801 binds differentially in a number of brain regions, including regions of the hippocampus and entorhinal cortex, and this suggests the existence of at least two active subpopulations of NMDA receptors (Monaghan, 1991). Therefore, the discrepancies in patterns of *in vivo* action of D-CPP-ene compared with other NMDA antagonists may be explained by different affinities for subpopulations of NMDA receptors within different regions of the brain.

Comparisons of the functional responses to D-CPP-ene and other

NMDA antagonists thus provides an insight into the diversity of NMDA-mediated cerebral events, and illustrates a complex relationship between glucose use and NMDA receptor occupancy. The regional changes in glucose utilisation in response to D-CPP-ene, and their implications for the local function of NMDA receptors are discussed in further detail below.

The Hippocampal Formation and Limbic Areas

The highest density of NMDA-displaceable glutamate binding in the entire brain occurs in the hippocampus, in the strata oriens and radiatum (Monaghan & Cotman, 1985; Monaghan et al., 1983). On this basis alone it would be expected that NMDA antagonists such as D-CPP-ene would produce substantial alterations in hippocampal function. On the contrary, D-CPP-ene had little effect on glucose utilisation within the hippocampus, and indeed resulted in decreased glucose use in two areas of the hippocampal formation – the CA4 pyramidal layer and the subiculum – which show little affinity for NMDA-sensitive glutamate binding. There is much evidence, however, to suggest that while NMDA receptors are involved in the high-frequency synaptic transmission which results in the establishment of long-term potentiation (LTP; Collingridge, 1985), under normal low frequency cell-firing, the NMDA-associated channel is blocked by magnesium and hence contributes little to synaptic activity (Collingridge & Bliss, 1987; Collingridge et al., 1988).

In contrast to the present results are reports by a number of authors that both competitive and non-competitive NMDA antagonists increase glucose utilisation in the hippocampal CA region (Chapman et al., 1991; Hammer et al., 1982; Hammer & Herkenham, 1983; Lund et al., 1981; Oguchi et al., 1982) and dentate gyrus (Chapman et al., 1991; Kurumaji et al., 1989; Weissman et al., 1987). It has been noted also that alterations in glucose use were not related simply to the density of

NMDA receptors within a particular region: for example, both CPP and MK-801 administration increased glucose use in the relatively NMDA receptor-sparse hippocampal CA stratum lacunosum moleculare, while glucose use in the stratum radiatum, which contains high densities of NMDA receptors, was unaltered (Kurumaji et al., 1989). In view of the pattern of functional alterations in the limbic system, Kurumaji and colleagues suggested that contrary to electrophysiological evidence, antagonism of hippocampal NMDA receptors is probably responsible for the marked alterations in glucose utilisation throughout the Papez circuit following MK-801 administration: the Papez circuit represents a network of fibres between the hippocampal formation, diencephalon and the cingulate cortices and thus forms an anatomical basis for a relay circuit between the anterior and posterior limbic areas and the hippocampus. However, the authors observed in a subsequent series of experiments that intrahippocampal injection of MK-801 resulted in altered glucose use throughout the stratum lacunosum moleculare and the dentate gyrus ipsilateral to the site of the injection, but functional activity in major hippocampal efferents was unaltered (Kurumaji & McCulloch, 1990a). This would imply that blockade of NMDA receptors in the hippocampus was not responsible for the altered function measured in the Papez circuit and rhinencephalon in response to systemic administration of MK-801 and other NMDA antagonists.

The pattern of intrahippocampal association fibres is complex and highly organised (Swanson et al., 1987): the afferents and efferents of the hippocampal formation are highly interconnected ipsilaterally and contralaterally. The medial and lateral portions of the entorhinal cortex, which give rise to the medial and lateral perforant pathway respectively, innervate distinct areas of the dentate gyrus to form the first synapse in the trisynaptic path. Fibres from the lateral entorhinal cortex synapse within the CA stratum lacunosum moleculare (Gottlieb & Cowan, 1972) and the outer two thirds of the dentate molecular layer

(Storm-Mathisen, 1977); these inputs account for 85% of the synapses within the dentate molecular layer area and are putatively glutamatergic (Matthews et al., 1976). In contrast, synaptic contacts from the medial perforant path are restricted to the inner third of the dentate molecular layer. The medial and lateral entorhinal cortex are innervated by separate structures: the lateral entorhinal cortex receives a major afferent from the olfactory cortex, which terminates in layers I and II of the entorhinal area, and is thus in a position to influence events in the deeper layers of the cortex through an extensive system of interneurons (Köhler et al., 1986). The medial entorhinal cortex, on the other hand, receives dense inputs particularly in layers I and III from the pre- and parasubiculum (Köhler et al., 1978; Swanson & Cowan, 1977), which in turn are innervated to a greater extent by visual areas. In functional terms, therefore, the two portions of the perforant path provide the hippocampus with information from two distinct sensory systems.

Glucose utilisation in the entorhinal cortex has been demonstrated to increase in response to a variety of NMDA antagonists: for example, a three-fold increase in glucose use occurred in the posterior entorhinal cortex in animals treated with MK-801 (Kurumaji et al., 1989), and D-CPP-ene (30mgkg⁻¹) induced a 43% increase in the same area. Since the functional activation in response to each drug occurred in the outer layers of the entorhinal cortex, it may be surmised that they were associated with olfactory transmission; and further evidence for this is provided by the increased glucose utilisation throughout the rhinencephalon and lateral olfactory tract. In the hippocampus, the terminal regions for projections of the lateral perforant pathway, that is the CA lacunosum moleculare and the dentate molecular layer, were functionally activated following MK-801 administration, but were unchanged in response to D-CPP-ene.

In a further series of experiments, Kurumaji and McCulloch (1990b)

attempted to determine whether the functional integrity of the entorhinal cortex was required for activation of the hippocampus by MK-801. Systemic administration of MK-801 in animals with lesions of the entorhinal cortex resulted in a pattern of glucose utilisation different to that seen in sham-operated rats. While increased glucose use was measured in the CA lacunosum moleculare and dentate gyrus contralateral to the lesion, these regions were functionally unaltered by MK-801 ipsilaterally. This suggests that cell firing in the entorhinal cortex in response to NMDA antagonists leads to the functional changes observed in the hippocampus.

In contrast, the lack of alterations in the hippocampus in response to D-CPP-ene are surprising. However, D-CPP-ene induced a much smaller increase in glucose utilisation in the entorhinal cortex, and this putative increase in cell firing may have a much lesser impact on hippocampal function. Additionally, competitive blockade of NMDA receptors may be overcome by an increase in the release of the endogenous agonist glutamate, presumably without significant increase in functional activity. If the functional alterations observed in the entorhinal cortex represent an attempt to surmount the NMDA receptor blockade by increased activity, it follows that the difference in magnitude of the increase in glucose use effected by the two drugs will be due to the distinction between their competitive and non-competitive action. However, the competitive NMDA antagonist CGP39551 did not alter significantly glucose use in the entorhinal cortex, but resulted in significantly increased glucose use in the piriform cortex and the hippocampus: thus the reason for the activation of the hippocampus in response to some, but not all, NMDA antagonists is obscure.

There is growing support for existence of glutamatergic autoreceptors within the CNS; thus, blockade of these may contribute to the sustained neuronal firing in limbic areas following administration

of NMDA antagonists. Using electrophysiological recording techniques, Coan & Collingridge (1987) measured the response of CA1 neurons in hippocampal slices to high-frequency stimulation of the Schaffer collateral fibres, and observed that in the absence of magnesium, application of AP5 or magnesium to the hippocampal slice resulted in an increase in the size of the population spike. The authors suggested that NMDA receptors therefore may be involved in presynaptic autoregulation, and removal of this component resulted in an increase in cell firing. Further, it has been demonstrated that MK-801 administration increases extracellular glutamate levels, measured with high performance liquid chromatography (HPLC) within distinct brain regions including the olfactory bulb and piriform cortex (Löscher et al., 1991), while CGP39551 did not have significant effects on glutamate release in these areas. These observations would support the view that increased neuronal activity represents an attempt to overcome the glutamatergic blockade, and that in the case of the competitive antagonist, the blockade is readily overcome by moderate increases in glutamate release. The authors also demonstrated that in these and other areas such as the hippocampus, release of the inhibitory transmitter γ -amino-butyric acid (GABA) is significantly increased by MK-801 but not by CGP39551; this may be due to either the activation of recurrent GABAergic inhibitory neurones (Andersen et al., 1964a, b; Wouterlood et al., 1985), or enhanced turnover of glutamate in these areas.

There is, however, little other evidence to support such a feedback mechanism. The concentration of glutamate within the synaptic cleft is controlled rapidly by presynaptic regulatory mechanisms and uptake sites (Nicholls & Attwell, 1990), and other authors have reported that pharmacological blockade of the NMDA receptor in the hippocampus inhibits glutamate release (Chapman & Bowker, 1987; Connick & Stone, 1988; Crowder et al., 1987; Nadler et al., 1990).

D-CPP-ene significantly reduced glucose utilisation in the CA4 region and subiculum following the intermediate dose of 3mgkg^{-1} , and in the mamillary body following 3 and 30mgkg^{-1} ; the subiculum appears to perform an important role in the relay of information from the hippocampus to many cortical and sub-cortical regions such as areas involved in visual processing (Swanson et al., 1987). Subicular fibres project to the mamillary body and nucleus accumbens, and a glutamatergic mechanism has been implicated (Walaas & Fonnum, 1980). Further, in the nucleus accumbens, glucose utilisation was affected in a similar manner to that in Papez areas; functional suppression occurred following 3mgkg^{-1} but not 30mgkg^{-1} D-CPP-ene. The failure of D-CPP-ene to produce increased glucose utilisation in Papez structures, such as the posterior cingulate cortex and mamillary bodies, is in contrast with the report that MK-801 produced marked increases in glucose use in these structures (Kurumaji et al., 1989), but accords with the lack of alterations reported in these areas in response to other competitive antagonists (Chapman et al., 1989, 1991; Kurumaji et al., 1989). Kurumaji and McCulloch (1990a) noted that Papez structures were functionally activated by MK-801 despite removal of the entorhinal cortex, supporting an additional mechanism for functional activation of the Papez circuit. Bearing in mind the anatomical complexity of subicular (and hippocampal) connections, it is not unlikely that this response is due to two distinct mechanisms of functional alteration. It is possible that the initial decrease in glucose utilisation reflects a local inhibition of cell firing due to the action of D-CPP-ene on NMDA receptors within that region. It is notable that all areas of the hippocampus measured are found to have a slightly decreased rate of glucose utilisation following 3mgkg^{-1} compared with 0.3mgkg^{-1} or 30mgkg^{-1} D-CPP-ene. Equally, reversal of this trend with a higher dose of drug might not represent a local effect, but is the result of increased firing within distant afferents, such as the entorhinal cortex,

with larger doses of drug.

Olfactory Areas

Increases in glucose utilisation in olfactory regions represent the most consistent alterations in glucose utilisation in response to NMDA antagonists, and occur following administration of both competitive and non-competitive antagonists (Chapman et al., 1989, Chapman et al., 1991; Kurumaji et al., 1989, Weissman et al., 1987). The olfactory cortex, as discussed, projects extensively to the lateral entorhinal cortex and hence constitutes a major input of the lateral perforant path. Stimulation of the olfactory bulb leads to kindling in rats, a process which is sensitive to blockade by NMDA antagonists (Millan et al., 1988; Piredda & Gale, 1986). However, a large projection from the olfactory bulb terminates in the cortical amygdalar nuclei, which thence project directly to the hippocampus (Carlsen et al., 1982). The entorhinal cortex also projects to the basolateral and lateral amygdalar nuclei (Ottersen, 1982). Amygdala-induced kindling is evidence that activation of the perforant path by olfactory and entorhinal stimulation is not necessarily required for kindling; furthermore, studies suggest that glutamatergic transmission exists between the amygdalar nuclei and the hippocampus (Petersen et al., 1983). However, D-CPP-ene (30mgkg^{-1}) produced a moderate decrease in glucose utilisation in the lateral amygdalar nucleus (Figure 13), and did not alter glucose use in the medial amygdalar nucleus. Thus it appears that NMDA receptor blockade results in diverse functional alterations even within structures which are functionally related.

The piriform and associated cortices contain an extensive system of association and commissural fibres (Haberly & Price, 1978). The pharmacology of excitatory transmission within the olfactory cortical areas is complex: kainate and AMPA receptors are believed to mediate transmission in the commissural fibres of the lateral olfactory tract,

while NMDA receptors may be involved in polysynaptic excitation within the cortex (Collins & Howlett, 1988). The concentration of NMDA binding sites within the olfactory cortex is extremely high in comparison to other brain regions (Monaghan & Cotman, 1985). Additionally, the ability of the NMDA antagonist AP5 to antagonise transmission in the olfactory cortex when low frequency stimulation is applied points to evidence in this area at least of a role for NMDA receptors in the normal low frequency glutamate-mediated transmission. Although the polysynaptic nature of neuronal pathways merits caution in the interpretation of electrophysiological recording in the olfactory cortex, it may be significant that NMDA receptors in this region may show different characteristics from those in other limbic areas. A difference in the function of NMDA receptors in this area may underly the increases in glucose use which occur in olfactory areas in response to D-CPP-ene, in contrast to the marked depression produced in other cortical areas.

Finally, there is evidence to suggest that olfactory inputs to the entorhinal cortex form synapses not only directly with pyramidal cells, but also on GABAergic interneurons in layer I of the entorhinal area (Wouterlood et al., 1985). The olfactory cortex, therefore, has both an inhibitory and an excitatory control over entorhinal firing; blockade of GABAergic inhibition of entorhinal firing, may explain the metabolic activation to NMDA antagonists in the entorhinal area. The entorhinal cortex sends reciprocal projections to olfactory areas (Swanson et al., 1987), including the anterior olfactory nucleus, the only subcortical olfactory-associated region in which glucose utilisation was significantly increased after D-CPP-ene administration (Figures 15 & 16). Thus, within olfactory regions there appears to be evidence for a highly regulated glutamatergic transmission between adjacent cortical areas.

Auditory and Visual Areas

Within layers of the auditory and visual cortices, high numbers of NMDA-sensitive binding sites are known to exist (Monaghan & Cotman, 1985), and glutamate has been implicated in both retino-fugal (Crunelli et al., 1987), and cortico-fugal fibres (Fosse & Fonnum, 1987) to the superior colliculus and dorsolateral geniculate nucleus. Additionally, glutamate is a putative transmitter in intrahemispheric cortico-cortical connections throughout the cerebral cortex (Baughman & Gilbert, 1981; Peinado & Mora, 1986), and NMDA receptors appear to be important in plastic responses of the visual system (Artola & Singer, 1987; Chalmers & McCulloch, 1989; Kleinschmidt et al., 1987).

NMDA antagonists are known to possess anaesthetic, anxiolytic and anticonvulsant effects (Kleinschmidt et al., 1982; Domino et al., 1965; France et al., 1990). The widespread dose-dependent reductions in glucose use in subcortical auditory and visual structures represent the most robust alterations in response to D-CPP-ene; and probably reflect largely the degree of sedation produced by D-CPP-ene. However, the competitive NMDA antagonists CGP39551 and CPP had little effect on auditory and visual regions, even at high doses of drug, (Chapman et al., 1991; Kurumaji et al., 1989), while MK-801 administration produced limited reductions in glucose use in auditory areas; thus heterogeneity exists in the responses to NMDA antagonists in these regions.

The visual system projects densely to areas of subiculum, presubiculum, and distinct layers of the medial entorhinal cortex, and thus forms a major sensory afferent to the hippocampus. Therefore, it is feasible that the slight depression in glucose use within hippocampal areas at lower doses of D-CPP-ene may reflect the degree of reduced firing within visual afferents, while, as discussed, the reversal of this trend in hippocampal areas following 30mgkg^{-1} D-CPP-ene possibly reflects functional activation of other hippocampal afferents, such as regions of the Papez circuit, or olfactory areas.

In summary, these results provide further evidence for the functional heterogeneity of NMDA receptors in the brain, and illustrate an apparent functional divergence between NMDA receptors in olfactory areas and those in other sensory systems. The bi-phasic alterations in glucose use observed in the hippocampus and other limbic structures are perhaps indicative of the integrative role of the limbic system in cerebral transmission.

1.2. THE NOVEL MUSCARINIC AGONIST L-679-512

The use of the deoxyglucose autoradiographic technique has to date contributed minimally to the elucidation of the functional role of cholinergic systems within the CNS, and reflects the generally poor perception of the mechanisms involved in cholinergic transmission. While other transmitter systems have been characterised in detail in terms of electrophysiology, location, and anatomical circuitry, thus providing an interdisciplinary basis for hypotheses as to their precise function within the CNS, the same approach has not yet provided a clear understanding of cholinergic function. A number of factors contribute to this: high densities of cholinergic receptors are found in much of the brain, and the innervation of many such areas, especially cortical areas, is relatively diffuse (for a comprehensive study, see Lysakowski et. al., 1989), hence hindering studies which employ electrophysiological, deafferentation, and tract-tracing techniques. In addition, muscarinic and nicotinic cholinergic receptors may be subdivided into several sub-populations based on relative affinities of agonists and antagonists, structure, and transduction mechanism. A recent review described the existence of at least five structurally distinct sub-populations of muscarinic receptors (Bonner, 1989), although functional heterogeneity has not been demonstrated for all of these.

Therefore any systematic study of cholinergic transmission in the CNS is complicated by the apparent functional diversity of cholinergic receptors.

A number of studies have employed deoxyglucose autoradiography to examine the cerebral metabolic effects of muscarinic agents in the brain (Dam & London, 1984; Soncrant et al., 1985; Weinberger et al., 1979). The agonists oxotremorine and arecoline have been found to increase glucose utilisation in areas of the brain associated with cholinergic function, while scopolamine, a muscarinic antagonist was found to reduce glucose utilisation in almost every brain region analysed (Weinberger et al., 1979). In each study the magnitude of functional alteration correlated poorly with the receptor density of that area. These observations possibly reflect not only the functional diversity of muscarinic receptors, but also the vast degree to which acetylcholine regulates firing throughout the brain, directly, or indirectly in the non-cholinergic structures by modulation of their cholinergic afferents.

L-679-512 is one of a series of novel muscarinic antagonists derived from arecoline (Saunders & Freedman, 1989; Freedman et al. 1990), with similar affinity for M1 and M2 receptors (R. Hargreaves, Merck, Sharp and Dohme, Harlow, Essex; personal communication). It is able to cross the blood-brain barrier freely and to stimulate maximally muscarinic phosphoinositide hydrolysis in the brain. Previously, the only muscarinic agonists which were able to induce maximal phosphoinositide hydrolysis were quaternary ammonium-based agonists such as carbachol, oxotremorine-M, and muscarine (Saunders & Freedman, 1989). However, these are thought to have only a limited ability to cross the blood-brain barrier, and thus systemic administration limits their ability to produce centrally mediated effects. The present study, therefore, represents the first comprehensive examination of the *in vivo* functional consequences of maximally stimulating muscarinic

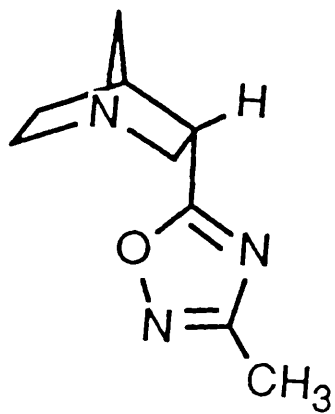


FIGURE 44: THE NOVEL MUSCARINIC AGONIST L-679-512:
CHEMICAL STRUCTURE

receptors in the CNS by administration of a muscarinic agonist.

In the present study, two observations are apparent immediately:- firstly, despite overt changes in behaviour and physiological parameters which are consistent with cholinomimetic effects (decreased heart rate and blood pressure, lacrimation, muscle fasciculation and tail tremor), few significant alterations in local cerebral glucose utilisation were observed. Secondly, while broadly speaking muscarinic agonists produce an elevated glucose utilisation whereas the muscarinic antagonist scopolamine causes widespread depression of glucose use, L-679-512 in contrast resulted in generally decreased rates of glucose use (Appendix II). While the different pattern of functional alterations observed in this study, compared to other studies may be explained partly in terms of the CNS penetration of L-679-512, the lack of any similarity between these responses and others, particularly in cholinergic regions, is surprising.

A number of factors may be important in these results. Firstly, L-679-512 induced a profound bradycardia, coupled with a decrease in blood pressure; these results were marked in animals which received $30\mu\text{gkg}^{-1}$ L-679-512. However, the effects were transient, and blood pressure had returned to the pre-injection level by the time deoxyglucose was administered. Therefore decreased rates of glucose use are unlikely to be due to decreased perfusion within the CNS. Secondly, it has been observed in other studies that cholinomimetics may induce hypothermia. Hypothermia has been reported to reduce cerebral glucose utilisation in most regions of brain (McCulloch, 1982). However, hypothermia did not occur in response to L-679-512 administration, and cannot account for the reductions in glucose use in this study. It must be concluded, therefore, that the different effects of L-679-512 on cerebral glucose use, in comparison to those produced by other cholinomimetics are due to the high potency of the compound, or its ability to penetrate freely the blood-brain barrier, or both.

The effects of L-679-512 are further discussed below, with reference to regional changes in glucose utilisation, and their implications for the local function of muscarinic cholinergic receptors in the CNS.

Hippocampal and Limbic Areas

Muscarinic agonists have produced a spectrum of effects on glucose utilisation in the hippocampus: arecoline, which displays some affinity for nicotinic receptors has been found to increase glucose use in a dose-dependent manner in most regions in the hippocampus (Soncrant et al., 1985), while the partial muscarinic agonist oxotremorine evoked increases in glucose utilisation in the presubicular area only (Dam & London, 1984). Conversely, L-679-512 induced significant decreases in glucose use in three hippocampal regions, the stratum lacunosum moleculare of the CA1 and CA2/3 regions and the stratum oriens/pyramidale region of CA2. As noted previously following the administration of glutamatergic agents, functional alterations do not necessarily occur in regions with high numbers of receptors: in the CA region, muscarinic receptors are particularly dense within the strata oriens and radiatum, with moderate amounts of binding in the stratum lacunosum moleculare. Nor do the regional functional reductions in the hippocampus correspond to the regional density of M1 or M2 receptor sub-types (Mash & Potter, 1986): M1 receptors account for the majority of muscarinic binding sites in the hippocampus; dense M2 receptor-binding is found in the pyramidal cell layer of the CA region, and the molecular layer of the dentate gyrus. In cortical areas, which contain dense amounts of M1 and M2 receptors, glucose utilisation was depressed following the highest dose of L-679-512; in contrast, in the M2 receptor-dense medial forebrain bundle and horizontal diagonal band nucleus, glucose use was significantly reduced following $30\mu\text{gkg}^{-1}$ L-679-512. Finally, the mamillary bodies exhibited the most robust alterations in glucose utilisation following L-679-512, despite relatively

low levels of both M1 and M2 receptors.

A possible reason for the discrepancies between the functional responses to L-679-512 and those to arecoline and oxotremorine is the ability of L-679-512, and the failure of arecoline and oxotremorine, to fully stimulate phosphoinositide activity, and presumably to abolish the M-current or the I_{AHP} in hippocampal cells. Since the maintenance of the membrane potential is an energy-demanding process, removal of this process would represent an energy saving, reflected in a decrease in deoxyglucose uptake. This may account for the decrease in glucose utilisation following low doses of L-679-512; as the concentration of agonist increases, it is likely that initial energy savings are offset by an increased energy demand to fuel the other consequences of muscarinic stimulation, such as phosphorylation of proteins by second messengers, activation of ion channels in response to an increasing frequency of depolarisation, or the activation of other sub-populations of muscarinic receptors, such as presynaptic inhibitory synapses. Indeed, recent evidence suggests that carbachol is able to inhibit firing of CA1 pyramidal neurons through presynaptic mechanisms (Sheridan & Sutor, 1990).

Dam and London (1984) proposed that the lack of alterations in glucose utilisation following oxotremorine administration was due to the ability of muscarinic receptor stimulation to modify membrane excitability without producing adequate depolarisation to alter glucose use measurably. In contrast, arecoline-induced increases in hippocampal glucose utilisation have been suggested to reflect the widespread metabolic activation observed throughout most of the brain (Soncrant et al., 1985). Although arecoline has affinity for nicotinic synapses, nicotine administration does not alter significantly hippocampal glucose utilisation (London et al., 1988) and therefore probably does not participate locally in the metabolic activation of the hippocampus produced by arecoline.

From these studies, there exists no overall evidence that alterations in hippocampal glucose utilisation represent altered activity in afferent neuron populations. Although oxotremorine did not alter hippocampal glucose utilisation, functional activation was apparent in several Papez structures, while arecoline administration resulted in functional activation of both the Papez circuit and the hippocampus. The Papez circuit, as discussed, is an anatomically-defined feedback loop, providing a connection between the forebrain, cingulate cortices and hippocampus. Contrary to these observations, glucose utilisation following L-679-512 administration was suppressed in the hippocampus and mamillary bodies, while other Papez structures remained functionally unaltered.

The *in vivo* consequences of muscarinic receptor stimulation in the hippocampus and structures remain unclear, and these studies highlight the reliance of the deoxyglucose technique upon parallel *in vitro* and *in vivo* studies of receptor and cell function. Undoubtedly, studies of the functional alteration in the hippocampus in response to muscarinic stimulation, coupled with a better understanding of (1) the role of second messenger systems in muscarinic action, (2) the function of distinct muscarinic receptor sub-types in the hippocampus, and (3) the role of presynaptic and post-synaptic muscarinic modulation of hippocampal firing would lead to a better comprehension of the precise consequences of muscarinic receptor activation in the brain.

Olfactory Areas

L-679-512 produced significant decreases in glucose utilisation in three out of six olfactory regions in the brain (Figure 21). The olfactory system, as discussed, represents a major afferent of the lateral perforant path; furthermore, cholinergic mechanisms in the olfactory cortices have been implicated in seizure activity: pilocarpine application to the

piriform cortex results in seizures in rats which can be prevented by glutamate antagonists (Millan et al., 1988), suggesting that acetylcholine modulates glutamate-mediated transmission in olfactory cortex. Pilocarpine-induced seizures, however, have been observed to increase markedly glucose utilisation in olfactory cortices in rats (Clifford et al., 1987), a result contrary to the present findings that L-679-512 induced decreased glucose utilisation in olfactory areas. The present results are also in contrast to those produced by arecoline and oxotremorine, which resulted in moderately increased glucose utilisation in the entorhinal cortex, and did not alter glucose utilisation in other olfactory areas (Soncrant et al., 1985; Dam et al., 1982). These observations therefore extend the evidence gained from the pattern of functional alterations in the hippocampus for a different mechanism of action of L-679-512 compared to other, partial muscarinic agonists.

Auditory and Visual Areas

Studies of function in the visual system have been facilitated by the ease of manipulating the system, for example by enucleation or light-deprivation, and these have led to the belief that acetylcholine has a modulatory role in neuronal firing within visual areas: for example, physostigmine and other cholinesterase inhibitors increase glucose utilisation in the superior colliculus (Nelson et al., 1978), a process dependent on retinal stimulation (Gomez-Ramos et al., 1982). However, the cholinergic component of visual transmission appears to be largely nicotinic, and this is reflected in the lack of functional alterations produced by L-679-512, and other muscarinic agonists (Dam & London, 1983). L-679-512 produced significantly reduced glucose utilisation in one visual and one auditory region of brain, the medial geniculate body and the auditory cortex; however, it was noted that there was a trend for glucose utilisation to decrease dose-dependently in auditory, but not visual, areas. There is no obvious

reason for the different patterns of glucose utilisation in the two sensory systems: both systems contain predominantly M2 receptors (Mash & Potter, 1986), and there was no apparent alteration in the conscious state of the animals, which might account for the loss of a particular sensory function. Nevertheless, the magnitude of altered glucose use in these areas does not suggest that functional alterations in the hippocampus and limbic areas result from altered activity in auditory or visual afferents.

These results illustrate overwhelmingly the complexity of cholinergic systems in the brain, and the difficulties involved in disseminating the precise functional role of cholinergic transmission. However, this study has provided evidence for an important difference between the *in vivo* functional alterations produced by partial and full agonists of phosphoinositide turnover, and thus the results have important implications in the use of such drugs to treat cholinergic disorders such as Alzheimer's disease. The unique effect of L-679-512 on glucose use in the rat brain in comparison to other muscarinic drugs may identify a possible method of cholinergic stimulation not achieved by administration of other muscarinic agonists.

1.3. 9-AMINO-1,2,3,4-TETRAHYDROACRIDINE (THA)

THA induced few alterations in local cerebral glucose utilisation, and therefore these results contribute little to existing evidence that THA interacts directly with glutamatergic receptors in the brain (Albin et al., 1988; Davenport et al., 1988). There appear to be few similarities between the pattern of functional alterations and the distribution of glutamatergic pathways in the brain: glucose use was unchanged in response to THA in all regions of sensory cortex, including olfactory

cortices, and the functional activity of the hippocampus was largely unaltered; in the subiculum, however, glucose use was significantly increased.

In the Papez circuit, glucose utilisation was increased in the anteroventral thalamic nucleus, but unaltered in the mamillary bodies and cingulate cortices; therefore on the basis of functional activity, THA does not appear to enhance transmission in key limbic areas.

The alterations in cerebral glucose use within visual structures evoked by THA administration are indicative of the cholinomimetic effect of THA. Markedly increased glucose use was measured in the superficial layer of the superior colliculus and in the lateral geniculate body (Figures 24 & 25). In the anterior pretectal nucleus glucose use was increased moderately but not significantly. Large increases in glucose utilisation have been reported to occur in response to cholinesterase inhibitors (Dam & London, 1983; Nelson et al., 1978), a response prevented by exposing the retina to the excitotoxin kainate (Gomez-Ramos et al., 1982), leading to the postulation that acetylcholine in these regions has a modulatory effect on glutamatergic transmission. The superior colliculus is also functionally activated by arecoline (Soncrant et al., 1985) and nicotine (London et al., 1988), but only slightly by the muscarinic agonist oxotremorine (Dam & London, 1983); thus it is probable that the cholinergic response in this area is largely nicotinic.

It has been suggested that THA and physostigmine exert some of their therapeutic effect in the treatment of the cholinergic dysfunction of Alzheimer's disease through nicotinic as well as muscarinic mechanisms (Nillson et al., 1987). Indeed, despite the lack of nicotinic involvement in septo-hippocampal transmission (Cole & Nicoll, 1984b), nicotine improves performance in learning and memory tasks (Flood et al., 1988; Gibson et al., 1983; Warburton & Wesnes, 1984), and nicotinic receptors are found to be reduced in regions which undergo

pathological degeneration typical of Alzheimer's disease, such as frontal (Nordberg & Winblad, 1986; Whitehouse et al., 1986), temporal and occipital cortices (Whitehouse et al., 1986), and cholinergic forebrain structures (Shimohama et al., 1986b). Nicotinic acid has been found to stimulate acetylcholine release in the cerebral cortex (Rowell & Winkler, 1984), and presynaptic nicotinic terminals have been found on catecholamine terminals in the brain (Schwartz et al., 1984), which are indicative of a modulatory role for nicotinic receptors. Moreover, the nucleus basalis of Meynert, a cholinergic forebrain nucleus, and a principal source of cholinergic fibres to the cortex, is reported to have the highest density of nicotinic receptors in the brain (Shimohama et al., 1985). In Alzheimer's disease, this region is subject to depletion of choline acetyltransferase activity and neuronal loss (Whitehouse et al., 1981), coupled with significant reduction in nicotinic binding sites (Shimohama et al., 1986b). An increase in nicotinic activity in this area, therefore may underlie in part the efficacy of THA in the treatment of Alzheimer's disease.

Nicotinic receptors predominate over muscarinic receptors in the habenulo-interpeduncular system (Clarke et al., 1984), and nicotine administration leads to markedly increased glucose utilisation in rats (London et al., 1988). The habenular nuclei are interconnected extensively with the midbrain raphé nuclei, and are believed to provide a link between forebrain and midbrain limbic systems. Nicotine administration produces antinociception in laboratory animals by an apparent central mechanism (Phan et al., 1973), and stimulation of the dorsal raphé attenuates nociceptive-evoked habenular neuronal firing (Dafny & Qiao, 1990). Although no alteration in glucose utilisation was measured in the habenula following THA administration, the decreased glucose utilisation in the dorsal raphé nucleus may indicate a nicotinic-mediated functional modification of its habenular afferent.

Finally, THA has been demonstrated to block potassium channels

(Osterreider, 1987), and thus facilitate presynaptic release of transmitter substance (Harvey & Rowan, 1990) and it has been postulated that this may contribute to the therapeutic effects of THA in Alzheimer's disease (Summers et al., 1986). Indeed, Stevens & Cotman (1987) observed that the excitation produced by THA on hippocampal pyramidal cells was not blocked by atropine, and therefore could not be explained by a cholinergic effect alone. It is possible, then, that several effects, including nicotinic, muscarinic and potassium channel-inhibiting actions are synergistic in the efficacy of THA in Alzheimer's disease. In the light of functional alterations in response to THA and other cholinergic and glutamatergic agents, the present results provide evidence for a cholinergic, possibly nicotinic, mode of action for THA, and demonstrate the novel perspective gained from deoxyglucose autoradiographic studies of *in vivo* drug action.

2. FUNCTIONAL PLASTICITY OF THE HIPPOCAMPUS IN RESPONSE TO LESIONS OF THE MEDIAL SEPTUM

2.1. GLUCOSE UTILISATION AND SYNAPTIC MODIFICATION

Previous attempts to examine functional activity in response to lesions of discrete neuronal populations have mostly demonstrated a bi-phasic response (Chalmers et al., 1989; Harrell & Davis, 1984; Kiyosawa et al., 1989; Yamaguchi et al., 1990): generally decreased glucose utilisation occurs acutely after the lesion, followed later by amelioration of the reduction in glucose utilisation over a variable period of time. The former phase of hypometabolism has been thought to reflect the decrease in activity of the target tissue due to the loss of its presynaptic input, while recovery of functional activity indicates synaptic reorganisation or restoration of the synaptic input within the target tissue.

A number of attempts have been made to examine the functional consequences of cholinergic denervation in the rat and primate brain. In baboons with unilateral lesions of the nucleus basalis of Meynert, decrements in glucose use have been observed in the cerebral cortex (Kiyosawa et al., 1989; Yamaguchi et al., 1990), linearly proportional to depletions in choline acetyltransferase (ChAT) activity. Although reduced ChAT activity persisted with time, however, glucose utilisation recovered gradually, to near normal levels after three months, inferring that functional recovery in the cortex was not dependent on the recovery of the deafferentated cholinergic input. Lamarca and Fibiger (1984) reported that nucleus basalis lesions were not associated with reduced cortical glucose utilisation ten days post-lesion, despite depletions in ChAT activity in the denervated cortex.

The functional response of the hippocampus in response to deafferentation has been less clearly defined. Harrell and Davis (1984)

observed increases in glucose utilisation in ipsilateral hippocampal regions one week after unilateral electrolytic ablation of the medial septal area, and decreases in the same regions three weeks after the lesion. The authors suggested that early increases in hippocampal glucose use represented gliosis in the deafferented hippocampus, and these initially masked reductions in glucose use due to the loss of the cholinergic input. The authors also reported that twelve weeks after denervation, hippocampal glucose utilisation was not significantly different from control values, suggesting that plastic responses had allowed restoration of hippocampal activity, as measured by deoxyglucose uptake. However, the lack of proper quantification within these experiments throws uncertainty on the validity of the results: these were comprised of measurements of [³H]-deoxyglucose uptake, estimated by counting silver grains, within very small experimental groups (one sham-operated and two lesioned animals); further, the control values reported were pooled data from the hippocampus bilaterally of the sham-operated rat and the contralateral hippocampus of the two lesioned rats, and there was a sizeable degree of variability within reported values for control rats. In contrast, Kelly et al. (1985b) reported that significant decreases in glucose utilisation measured using quantitative [¹⁴C]-deoxyglucose autoradiography persisted six months after severe cholinergic denervation of the hippocampus via fimbria fornix transection. When embryonic septal tissue was grafted into the lesioned area, functional activity recovered in the hippocampus, suggesting that the integrity of some cholinergic cells is required before functional recovery can occur. In comparison, the present results suggest that if functional alterations do occur in the hippocampus in response to ibotenate-induced medial septal lesion, these are ameliorated within three weeks after the lesion. Thus it would appear that the hippocampus is able to sustain the loss of part of its cholinergic input without significant long-term disruption of activity.

It has been suggested that partial cholinergic denervation results in sprouting of other cholinergic afferent fibres, and these result ultimately in the recovery of function in the denervated pathway. Indeed, the ability of the hippocampus to recover function can be correlated roughly with the severity of the lesion: confined ibotenate lesions, electrolytic medial septal lesions and fimbria fornix lesions result, in that order, in an increasing amount of disruption of both septal cholinergic hippocampal afferents and fibres of passage, while in the same order appear to decrease the ability of the hippocampus to recover functionally. However, the persistent decrease in choline acetyltransferase activity following apparent recovery of glucose utilisation (Harrell & Davis, 1984; Kiyosawa et al., 1989; Yamaguchi et al., 1990) suggests that functional recovery is dependent on non-cholinergic mechanisms. It is possible, therefore that the lack of recovery of glucose use in the hippocampus following fimbria fornix lesions (Kelly et al., 1985b) was due in part to the removal of non-cholinergic fibres which passed through the fornix.

The hippocampus receives a major noradrenergic projection from neurons which arise in the locus coeruleus and travel via the medial forebrain bundle to the hippocampus. At least part of these fibres pass via the fornix (Ungerstedt, 1971). Noradrenergic terminals are particularly dense within the infragranular region of the dentate gyrus and the stratum radiatum of CA3 (Crutcher & Davis, 1980). Noradrenaline is proposed to modulate long-term potentiation in the hippocampus: consequently, superfusion of noradrenaline during high frequency stimulation of the dentate mossy fibres in an *in vitro* hippocampal slice preparation results in an increased magnitude, duration and probability of induction of LTP in the CA3 sub-field (Hopkins & Johnston, 1984), while conversely, adrenergic antagonists block the production of LTP. This effect is thought to be mediated through β -adrenergic stimulation of adenylate cyclase (Stanton &

Sarvey, 1985).

There is evidence that noradrenergic fibres invade the hippocampus following removal of the septal cholinergic input, resulting in synaptic formation within the dentate-CA3 region (Crutcher et al., 1981), possibly due to the dendritic space vacated by the loss of septal cholinergic afferents. Further, in the dentate-CA3 region, an increase in [³H]-forskolin binding to adenylate cyclase has been measured following septal lesions (Horsburgh et al., 1991b), and has been attributed to axonal sprouting of noradrenergic fibres within this area.

In terms of functional recovery following cholinergic denervation, then, it is likely that an increased noradrenergic influence on the hippocampus would replace at least partly the modulatory role of the septal cholinergic afferent fibres destroyed by septal lesion. Following fimbria fornix lesion, however, both cholinergic fibres originating in the medial septum, and non-cholinergic fibres of passage, are destroyed. The latter include a proportion of noradrenergic fibres targeted for the hippocampus, and the removal of these during fimbria fornix lesion may explain the lack of functional recovery in the hippocampus at long time-points post-lesion (Kelly et al., 1985b).

Finally, a further explanation for the lack of alterations in glucose utilisation following ibotenate-induced lesions of the medial septum is that although denervation does result in synaptic reorganisation – and the existence of receptor alterations and significant choline acetyltransferase activity following medial septal lesion in the present series of experiments suggests that plastic alterations are in operation following septal lesion – these alterations do not represent in functional terms a significant portion of the total activity, reflected by glucose utilisation, to be detected using the present techniques. In either case, the lack of altered hippocampal glucose utilisation following medial septal lesion suggests that hippocampal function is preserved three weeks following the lesion, either by synaptic reorganisation in the

hippocampal formation, or by the maintenance of hippocampal activity by other cholinergic and non-cholinergic afferents.

2.2. MUSCARINIC RECEPTOR PLASTICITY AND MEDIAL SEPTAL LESIONS

The lack of consistent muscarinic receptor alterations in the cortex and hippocampus of Alzheimer's Disease has provided the impetus for expanded research into the role of muscarinic receptor plasticity in animals following cholinergic denervation; however, the results to date of these studies have not been less variable. While the small reductions in [³H]-QNB binding in the present study are in agreement with some studies which report the loss of muscarinic receptors following cholinergic denervation (Mash et al., 1985; Watson et al., 1985), the magnitude of these alterations does not provide convincing evidence for muscarinic receptor plasticity in the hippocampus following loss of the cholinergic input. It has been suggested that regulation of muscarinic receptor activity is achieved by a negative feed-back mechanism: administration of muscarinic agonists results in decreased receptor density (Gazit et al., 1979; Ehlert et al., 1980; McKinney & Coyle, 1982), while pharmacological blockade induces increased receptor concentrations (Ben-Barak & Dudai, 1980; McKinney & Coyle, 1982). Similarly, removal of cholinergic innervation by deafferentation should lead to an increase in post-synaptic densities of muscarinic receptors. However, with few exceptions (Joyce et al., 1989; McKinney & Coyle, 1982; Westlind et al., 1981), and including the present study, there has been little evidence for such a mechanism in the brain (Court et al., 1990; Kamiya et al., 1981; Mash et al., 1985; Norman et al., 1986; Overstreet et al., 1980; Smith et al., 1989; Yamamura & Snyder, 1974; Watson et al., 1985). A number of reasons may explain the apparent

lack of receptor plasticity in these studies. Firstly, small lesions of cholinergic inputs may lead to a partial denervation of the target organ, and consequently, only small alterations in synaptic receptor density, which were not detected by autoradiographic means. Secondly, discrete lesions resulting in an incomplete cholinergic denervation of the target tissue may allow presynaptic modifications, such as neuronal sprouting in the remaining cholinergic fibres, to replace the cholinergic function lost by the degeneration of lesioned cells. In the present case, there exist a number of other sources of hippocampal cholinergic innervation which arise in the diagonal band nucleus, immediately ventral to the medial septum. Cholinergic cells which project from the diagonal band through the fimbria fornix make synaptic contacts with all hippocampal fields (Nyakas et al., 1987). Additionally, two projections from the diagonal band reach the hippocampus: one projection courses over the genu of the corpus callosum and then runs caudally in or near the cingulum bundle (Milner et al., 1983; Swanson & Cowan, 1979). These fibres innervate the anterior cingulate and retrosplenial areas and finally end in temporal regions of the subiculum and presubiculum. The second projection from the diagonal band nucleus, which accounts for up to 10% of the cholinergic input into the hippocampal formation, runs ventrally through the amygdala and terminates within temporal hippocampal fields (Milner & Amaral, 1984; Gage et al., 1984). Thus restricted lesions of the medial septum afford the possibility of plastic modifications of the cholinergic innervation of the hippocampus.

In addition, ibotenic acid-induced lesions avoid to a large extent damage of fibres of passage in the lesioned area. The medial septal region supports fibres which arise predominantly in the hypothalamus and brainstem regions, and course through the medial septum and fornix, to terminate finally within the hippocampal formation (Swanson et al., 1987). The present lesion system, therefore, permits preservation of a large body of cholinergic hippocampal afferents, which

may be involved in plastic responses to partial cholinergic denervation.

A third reason for the lack of detectable alterations in muscarinic receptor binding following denervation may be due to the failure to differentiate between different muscarinic receptor types. Using autoradiographic analysis, two sub-types of muscarinic receptor are able to be distinguished in the mammalian brain (Mash & Potter, 1986; Tonnaer et al., 1988; Wamsley et al., 1980), based on the selective affinity of M1 receptors for pirenzepine and the apparent selectivity of M2 receptors for carbachol. However, discrepancies exist between the reported M1 and M2 receptor densities in the hippocampus, which may be due to less specific actions of these compounds (see Introduction Section 4.1.4.). It has been observed that M2 receptors are found co-localised with high densities of acetylcholinesterase and choline acetyltransferase, and a specific loss of M2 receptors has been observed in animals following cholinergic deafferentation (Mash et al., 1985, Watson et al., 1985) and in Alzheimer's Disease (Mash et al., 1985; Perry et al., 1986). On this basis it has been suggested that M2 receptors represent autoreceptors on the presynaptic cholinergic terminals (Mash & Potter, 1986), while M1 receptors have been suggested to be located post-synaptically. Accordingly, the M1 antagonist pirenzepine is ineffective at blocking acetylcholine-mediated autoinhibition (Meyer & Otero, 1985). Following deafferentation, therefore, M1 receptor density may be expected to increase, while M2 receptors would be reduced due to the loss of the presynaptic input. M2 receptors constitute 20% of total muscarinic receptors in the hippocampus, and thus failure to demonstrate alterations in muscarinic receptors in some studies may be due to the use of non-specific muscarinic ligands such as QNB, whereby small decreases in M2 receptors are either masked by increases in M1 receptors post-synaptically, or represent an immeasurably small fraction of the total ligand-binding to muscarinic receptors. However, observations of decreased M2 receptor density following cholinergic

denervation have not been replicated by others (Court et al., 1990; Norman et al., 1986; Smith et al., 1989), and Joyce and colleagues (1989) observed increases in both M1 and M2 receptors following almost complete cholinergic deafferentation of the hippocampus, suggesting that both M1 and M2 receptors were located postsynaptically.

The present study offers little evidence to support postsynaptic modification of muscarinic receptors. Instead, the moderate decrease in muscarinic binding in the subiculum is more likely to be due to the loss of presynaptic receptors situated on degenerating cholinergic afferents to the hippocampus. The use of [³H]-QNB prohibits distinction between M1 and M2 receptors; further, due to the lack of consensus as to whether M1 or M2 receptors predominate in the subiculum (Mash & Potter, 1986; Regenold et al., 1989; Tonnaer et al., 1988) it is unclear which receptor sub-type is likely to be affected.

Although the alterations in muscarinic receptor binding in the present study are small, it is of interest to examine more closely the pattern of hippocampal cholinergic innervation originating in the septum. The results of degeneration (Mellgren & Srebro, 1973), autoradiographic (Swanson & Cowan, 1979) and tract-tracing (Nyakas et al., 1987) studies indicate that neuronal fibres from the medial septum innervate all fields of the hippocampal formation (Figure 45). In turn, Ammon's Horn and the subicular region give rise to a massive projection via the fimbria fornix to the lateral septum, which itself sends a dense body of neuronal fibres to the medial septum. This circuit has been proposed as a feedback loop between the hippocampus and septal area (Swanson et al., 1987). In the present study, reductions in muscarinic binding observed in the medial and lateral septal nuclei and subicular region represent a consistent reduction throughout at least one complete hippocampal circuit.

Few investigators have examined plastic mechanisms within the septal region in response to selective lesion of the septohippocampal

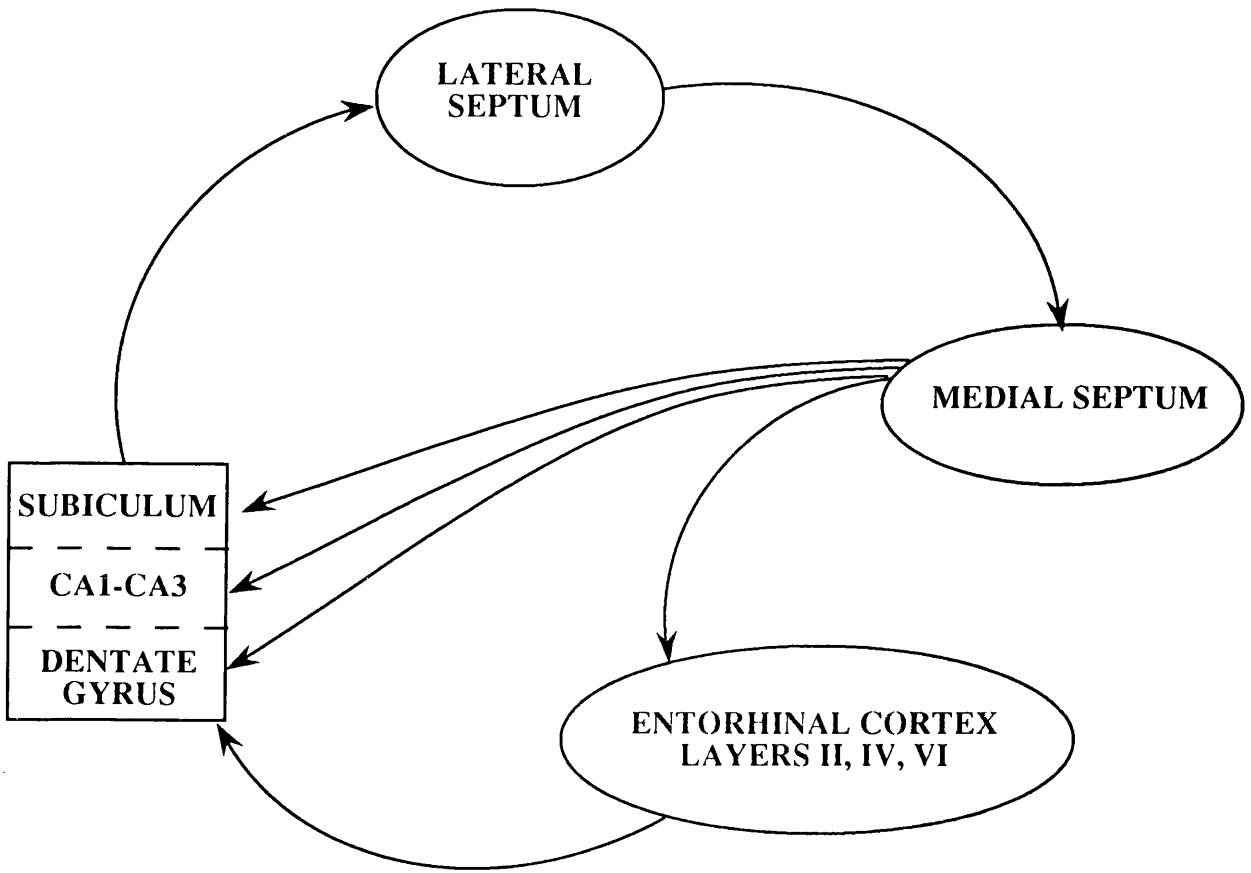


FIGURE 45: THE CHOLINERGIC SEPTOHIPPOCAMPAL PATH

Simple diagrammatic representation of the septal cholinergic input to the hippocampus. Arrows from the hippocampus to the septal area represent possible feedback systems (transmitter unknown).

path. Consequently, the role of putative septohippocampal feedback system has not been studied in detail. Furthermore, many lesion paradigms actively preclude these types of investigation: electrolytic lesions may result in anterograde and retrograde degeneration of neurones in tissue some distance from the site of the lesion, while transection of the fimbria fornix disrupts both septohippocampal and hippocampal-septal fibres, resulting in a complete loss of feedback mechanisms between the septum and hippocampus. The isolation of the hippocampus from the septal nuclei in this manner may itself provide a reason for conflicting results in terms of the muscarinic response to cholinergic denervation within the hippocampus, and advocates further investigation into the precise role of hippocampo-septal fibres in deafferentation-induced plasticity.

Finally, the lack of measurable alterations in muscarinic receptor binding in the hippocampus may be explained in part by an apparent modulatory role of the entorhinal area on hippocampal receptor plasticity. In an early study of receptor plasticity following entorhinal cortex lesions, Monaghan et al. (1982) demonstrated decreased [³H]-QNB binding to muscarinic receptors in the stratum lacunosum moleculare and the outer portion of the dentate molecular layer, and suggested that integrity of the entorhinal cortex was required for the control of muscarinic receptor densities in the hippocampus. Moreover, in rats which received lesions of the medial septum two to four days post-natally, i.e. prior to establishment of septohippocampal lesions (Ben-Barak & Dudai, 1980), the pattern of muscarinic binding sites was unaltered at maturity, compared to control rats. In the same groups of animals, however, a 70% deficit of acetylcholinesterase was observed post-lesion, in comparison to control values, and the authors concluded that the development of muscarinic binding sites in the hippocampal formation is not dependent upon normal establishment of presynaptic contacts. Therefore, the preservation of [³H]-QNB binding in the

present series of results may be a result of entorhinal control of muscarinic receptors, regardless of the cholinergic septohippocampal afferents.

2.3. GLUTAMATERGIC RECEPTOR PLASTICITY AND MEDIAL SEPTAL LESIONS

The role of glutamate in long-term potentiation (LTP) in the hippocampus and its involvement in learning and memory have been well established (Collingridge, 1985). The hippocampus, which contains extremely high densities of all sub-types of glutamate receptor, is profoundly affected by severe neurodegeneration in Alzheimer's Disease (Hyman et al., 1984), and it has been suggested therefore that disruption of glutamatergic neuronal firing within the hippocampal formation may underlie some of the cognitive impairments associated with the disease.

In associational cortical regions of brain, loss of pyramidal cells is a prominent feature of Alzheimer's Disease pathology (Mountjoy et al., 1983; Pearson et al., 1985; Terry et al., 1981), and has been demonstrated to be directly related to the level of cognitive impairment in Alzheimer patients (Neary et al., 1986). Thus a loss of glutamatergic function may contribute to the clinical manifestations of the disease.

Consequently, many groups have reported altered glutamate release and re-uptake, and altered ligand-binding to sub-types of glutamate receptors in Alzheimer brains (for review, see Greenamyre & Young, 1989). In the hippocampus, although there exist some discrepancies between individual results, possibly due to sub-populations of Alzheimer patients or different ligand-binding protocols, [³H]-glutamate binding to NMDA receptors or [³H]-TCP binding to the associated ion channels are reduced in Alzheimer hippocampus. The pyramidal cells

of CA1 and CA2 have been reported to be particularly affected (Greenamyre et al, 1987), perhaps reflective of the vast cell loss associated with the disease. Less emphasis has been placed on alterations in other glutamatergic receptor sub-types in Alzheimer's Disease. Geddes and colleagues (1985) reported expansion of the kainate receptor field in the hippocampus of Alzheimer brains, and suggested that this represented compensatory sprouting of dentate associational and commissural fibres into the space vacated by the loss of the entorhinal perforant path input in the course of the disease. The authors suggested that despite the massive pathomorphological disruption associated with Alzheimer's Disease the brain exhibits some capacity for plastic modification in response to denervation. However, the result was not reproduced by a similar study (Represa et al., 1988) in which markedly reduced densities of kainate receptors were measured in the hippocampus of severely demented Alzheimer patients, inferring that as the disease progresses, so does the inability of the diseased tissue to compensate for a reduction of excitatory input.

Additionally, AMPA-sensitive quisqualate receptors have been reported to be reduced in the hippocampus of Alzheimer patients (Dewar et al., 1991), and Greenamyre and colleagues (1987) have reported decreased hippocampal quisqualate-sensitive [³H]-glutamate binding in Alzheimer brains.

Severe pathological degeneration of the entorhinal cortex, in addition to that observed in the hippocampus, is also a prominent feature of Alzheimer's Disease, suggesting that atrophy of the perforant pathway to the dentate gyrus may account for some of the memory loss in Alzheimer patients. Thus, experimental lesions of the entorhinal cortex have been used as a model in which to investigate the plastic alterations in glutamatergic receptor densities in the hippocampus which may accompany entorhinal deafferentation in Alzheimer's Disease. These studies are of mixed success: Geddes and colleagues

(Geddes et al., 1985) were able to demonstrate that entorhinal cortex lesions lead to an expansion of the kainate receptor field in the rat hippocampus, a result which paralleled their observations in Alzheimer tissue. However, in contrast to the deficits demonstrated in Alzheimer brain, NMDA and quisqualate receptor densities have been reported to increase in the hippocampus following entorhinal cortex lesions; this suggests that the loss of the entorhinal perforant path input into the hippocampus cannot solely account for the decrements in quisqualate and NMDA receptors measured in Alzheimer brains.

Despite extensive evidence for the destruction of both the glutamatergic hippocampal perforant path and the cholinergic septohippocampal pathway in Alzheimer's Disease, and the apparently modulatory role which cholinergic systems exert upon glutamate-mediated neuronal firing in the hippocampus, few experimental approaches have examined the possibility of hippocampal glutamatergic receptor plasticity following removal of the cholinergic input. A previous report described decreases in muscarinic cholinergic receptor binding following lesions of the entorhinal cortex (Monaghan et al., 1982), and suggested that the integrity of the entorhinal cortex, rather than the medial septal area, was required for the maintenance of cholinergic receptors in the hippocampal formation. In comparison, the results presented here provide evidence for glutamatergic plasticity following cholinergic deafferentation via lesions of the medial septum. Further, the selective nature of alterations in receptor density suggest that sub-types of glutamatergic receptor are modulated differently. The basis for the pattern of alterations in glutamatergic receptor sub-type, in terms of their function and anatomical location within the hippocampus, is discussed in further detail below.

AMPA-sensitive Quisqualate Receptors

Electrophysiological evidence suggests that stimulation of either quisqualate or kainate receptors in conjunction with NMDA receptors is required for the production of LTP in the hippocampus, and blockade of the AMPA-sensitive quisqualate receptor with the selective antagonist CNQX prevented the formation of LTP in response to tetanic stimulation of the hippocampus (Kauer et al., 1988; Muller et al., 1988a).

The distribution of [³H]-AMPA binding to quisqualate receptors overlaps well with the distribution of NMDA-sensitive [³H]-glutamate binding sites in the brain (Monaghan et al., 1984; Rainbow et al., 1984): each ligand binds in high amounts in the hippocampal CA1 strata oriens and radiatum. [³H]-AMPA-binding to quisqualate receptors and quisqualate-sensitive [³H]-glutamate binding has been demonstrated to be reduced in the hippocampus of Alzheimer patients (Dewar et al., 1991; Greenamyre et al., 1987); however, little priority has been given to the mechanism underlying the loss of quisqualate binding sites in the process of the disease. It has been suggested that reductions in ligand-binding in Alzheimer brains may represent cell loss from pathologically affected regions of brain; evidence for this was provided by a recent study which demonstrated reduced [³H]-AMPA binding and a parallel cell loss in the subiculum (Dewar et al., 1991); however, the authors failed to correlate reduced cell loss in the CA1 with reduced [³H]-AMPA binding in that sector, and thus deficits in ligand-binding cannot simply be attributed to cell loss in the course of the disease. In this respect, the results presented here, in terms of the location of altered [³H]-AMPA binding in the hippocampus following medial septal lesions, and the direction of these alterations, namely decreases, are of some interest.

Removal of the cholinergic input to the hippocampus would be predicted to result in an upregulatory response within glutamatergic neurones in order to compensate for the lack of potentiation of glutamatergic neuronal firing by the septal cholinergic afferents: thus an

increase in glutamatergic receptor binding may be expected to occur following septal lesions. On the contrary, septal lesions were accompanied by a decrease in [³H]-AMPA binding in the entorhinal cortex and CA sector of the hippocampus. Thus it would appear that septal lesions mimic some of the glutamatergic receptor deficits which occur in Alzheimer's Disease. Whether these are truly representative of the altered glutamatergic receptor densities which accompany Alzheimer's Disease, however, is unclear.

In an attempt to elucidate the mechanisms underlying the maintenance of LTP in the hippocampus, Davies and colleagues (1989) observed that induction of LTP was associated with an increase in the sensitivity of CA1 neurones to quisqualate and AMPA; this developed slowly and was maximal one hour after the onset of LTP. The effect was blocked by the NMDA antagonist APV, suggesting that NMDA-mediated transmission, or the induction of LTP, was necessary for the increased neuronal sensitivity. It is possible, then, that the decreases in [³H]-AMPA binding described in the present study represent a decrease in the affinity of AMPA-sensitive quisqualate receptors due to the reduced induction of LTP following removal of modulatory cholinergic fibres in the hippocampus.

However, 21 to 60 days after lesions of the entorhinal cortex, increased [³H]-AMPA binding has been reported in the dentate gyrus (Ulas et al., 1990a), suggesting that in the absence of the major hippocampal excitatory input, AMPA receptors are up-regulated. At shorter times post-lesion, the authors reported a decrease in AMPA binding in the inner dentate molecular layer, a region which would not be denervated by entorhinal cortex lesion, and thus the transient reduction of [³H]-AMPA binding was unlikely to be due to loss of presynaptic AMPA receptors situated on the ablated entorhinal-hippocampal fibres. This observation would be consistent with the view that reduction in LTP, in this case due to the destruction of the

perforant path, leads to a decreased sensitivity of AMPA-sensitive quisqualate receptors in the hippocampus. Additionally, while activation of GABA receptors during neuronal discharge usually results in inhibition of firing (Andersen et al., 1964a, b; Wouterlood et al., 1985), it has been shown that during LTP in the hippocampus GABA_B autoreceptors act to depress the release of GABA, thus facilitating the induction of LTP (Davies et al., 1991). If GABAergic autoreceptors are situated on septohippocampal fibres, the removal of GABAergic cells following medial septal lesion may therefore prevent the increased sensitivity in AMPA receptors observed during LTP.

There exist a number of other possible explanations for the decreased [³H]-AMPA binding observed in the present study, based on the anatomical organisation of neuronal pathways within the hippocampus which employ excitatory amino acids as transmitter substances. In addition to the dense innervation of the hippocampus, septal fibres terminate in all layers of the entorhinal cortex, and particularly in layers II, IV and VI (Swanson et al., 1987). Thus reductions in [³H]-AMPA binding in the entorhinal cortex and the hippocampal CA sector following medial septal lesions may represent the loss of presynaptic glutamatergic receptors due to the removal of the septal-entorhinal input (Figure 46). However, although a significant proportion of cells in the medial septum have been identified as non-cholinergic, a large percentage of these are GABAergic (Köhler et al., 1984), and there is no evidence at present for the involvement of glutamate in the septal projection to the hippocampal and entorhinal areas.

Secondly, as has been discussed in previous sections, the hippocampal formation is interconnected by an extensive network of associational and commissural fibres (Swanson et al., 1987). While the entorhinal cortex provides the dentate gyrus with a major glutamatergic projection in the form of the perforant path, fibres from layer III of the entorhinal area synapse in the stratum lacunosum moleculare with what are assumed to be the distant dendrites of CA pyramidal neurones (Gottlieb & Cowan, 1973; Köhler, 1986). In turn, a projection from the pyramidal cell layer has been reported to innervate in particular layer IV of the entorhinal cortex (Swanson et al., 1978); the transmitter for this pathway has not been identified, but has been proposed to be an excitatory amino acid (Swanson et al., 1987). The significantly reduced [³H]-AMPA binding observed consistently throughout the pyramidal cell layer of

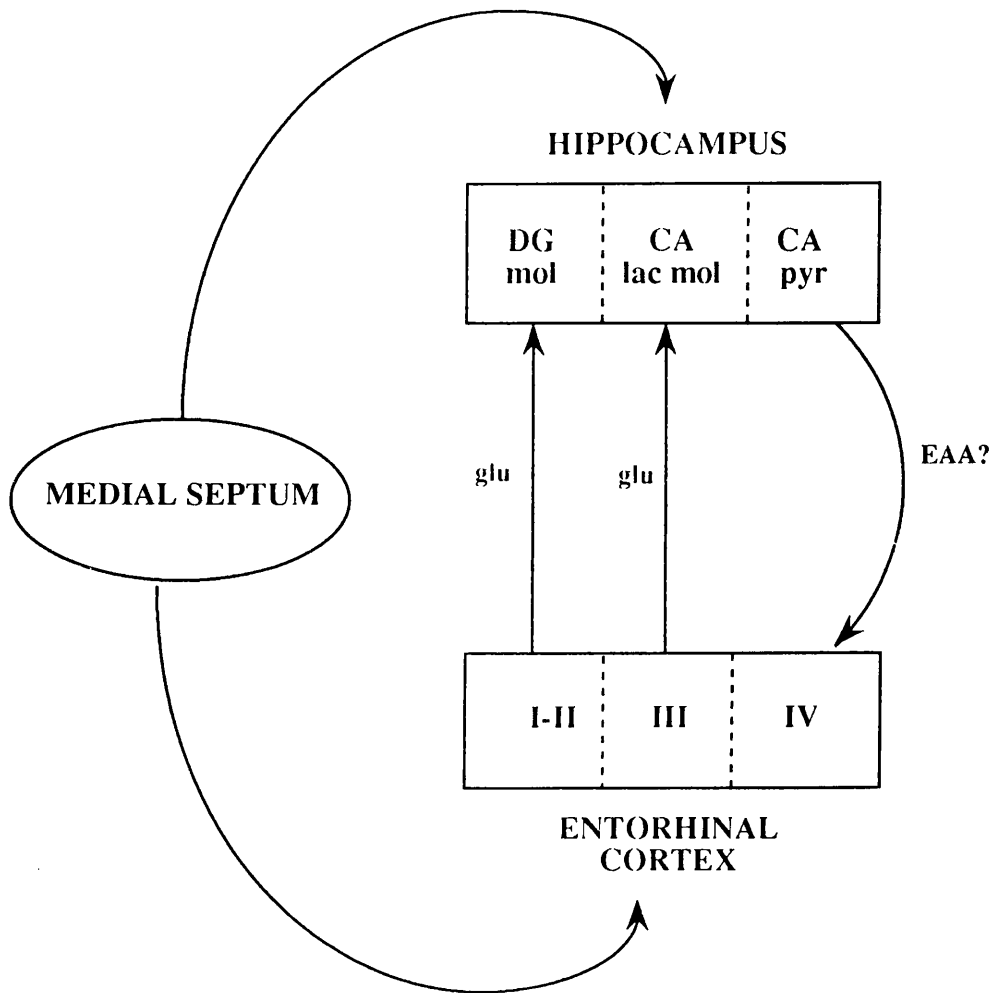


FIGURE 46: HIPPOCAMPAL ASSOCIATION SYSTEMS

Simple diagrammatic representation of the glutamatergic projections between the hippocampus and entorhinal cortex. The cholinergic septohippocampal path is also indicated.

glu: confirmed glutamatergic projection; EAA?: possible excitatory amino acid projection (Swanson et al., 1987).

the CA sector following septal lesions may represent therefore plastic modification of this particular association pathway following removal of the cholinergic input to the hippocampus.

It is of further interest to note that the reductions in [³H]-AMPA binding occur in those parts of the entorhinal cortex which support the two respective portions of the perforant path: consequently, decreased levels of [³H]-AMPA binding in the outer layers of the lateral entorhinal cortex may be associated with altered excitatory amino acid transmission within the lateral perforant path, whereas the reduction in [³H]-AMPA binding in the deep layers of the medial entorhinal cortex may represent modification of the medial perforant path input to the hippocampus.

Finally, studies of second messenger binding following medial septal lesions have also provided evidence for the involvement of the entorhinal cortex in hippocampal plasticity. [³H]-phorbol dibutyrate binding to protein kinase C was increased in the outer layers of the entorhinal cortex, but was unaltered in the hippocampus (Horsburgh et al., 1991b). The present report of altered [³H]-AMPA binding to quisqualate receptors, and the increase protein kinase C binding sites observed within the entorhinal cortex therefore indicate that the entorhinal cortex undergoes extensive synaptic reorganisation in response to septal lesions; the neuronal response of the entorhinal cortex to cholinergic deafferentation supports further the role for both cholinergic and glutamatergic mechanisms in hippocampal plasticity.

Kainate Receptors

Kainate receptors, like AMPA-sensitive quisqualate receptors, are involved in fast excitatory post-synaptic transmission in the hippocampus, (Jahr & Stevens, 1987). In contrast to [³H]-AMPA binding sites, however, which are concentrated in the CA1, co-localised with NMDA receptors, kainate receptors are sparse in CA1, but are found in

high quantities in the dentate gyrus-CA3 region (Monaghan & Cotman, 1985; Cotman et al., 1987). The stratum lucidum, which runs immediately medial to the CA3 stratum pyramidale (Figure 2), and represents the terminal region of the dentate mossy fibres (Swanson et al., 1987) contains the highest density of kainate receptors in the mammalian brain; this almost certainly underlies the susceptibility of CA3 pyramidal neurones to kainate toxicity in animals (Schwob et al., 1980) and man (Teitelbaum et al., 1990). The cholinergic septohippocampal input to the hippocampus is particularly dense within the dentate gyrus: thus it might be expected that medial septal lesions would result in upregulation of glutamatergic receptors in the CA3, manifested in an increase in glutamatergic receptor binding, to overcome the decreased facilitation of glutamatergic firing through the loss of the modulatory cholinergic input.

However, the little evidence which exists for plastic modifications of kainate receptors is controversial: in Alzheimer's Disease, an expansion in the dentate gyrus kainate receptor field has been reported by one group (Geddes et al., 1985), while other investigators found decreased kainate receptor binding in the hippocampus of severely demented patients (Represa et al., 1988). Chalmers and colleagues reported an increase in kainate receptors in the frontal cortex of Alzheimer brains (Chalmers et al., 1990), and suggested that this represented a "denervation supersensitivity" in the frontal cortex. While one group have replicated the apparent broadening of the kainate receptor field in the dentate molecular layer of rats with entorhinal cortex lesions (Ulas et al, 1990b), the present study provides no evidence for kainate receptor regulation in response to cholinergic denervation of the hippocampus. Although there exist differences in the precise method of analysis of autoradiograms employed in the present study, compared to that of Ulas and colleagues, the use of histological overlay in the present study (Methods Section 1.3.) in order to determine the precise hippocampal

layers precludes the possibility that the autoradiograms were misread and that an alteration in kainate receptor localisation had been overlooked. It is not impossible, however, that kainate receptor densities are modified with time following medial septal lesions: Ulas and colleagues report that kainate receptor densities are increased significantly at 30 to 60 days after entorhinal lesion, whereas no significant alterations in kainate binding were observed at shorter time-points post-lesion. Therefore, the present study of ligand-binding 21 days after medial septal lesion, may have been performed before significant modifications in kainate receptor densities occurred. However, in view of the significantly reduced densities of [³H]-AMPA binding to quisqualate receptors in the same brains, this study provides evidence for differential regulation of AMPA-sensitive quisqualate receptors and kainate receptors following cholinergic denervation of the hippocampus.

NMDA Receptors

The involvement of NMDA receptors in the induction of LTP is well established: NMDA antagonists prevent the formation of LTP in the hippocampus, and result in impaired learning and memory in behavioural paradigms. The apparent association between LTP and memory, therefore, has provided the impetus for expanded research into the role of NMDA receptors in neurodegenerative diseases such as Alzheimer's Disease, in which cognitive ability is profoundly reduced.

[³H]-NMDA binds with low affinity and specificity to the NMDA receptor (Foster & Fagg, 1987), and therefore has not been employed routinely as a ligand for quantitative autoradiography. However, the demonstration that chloride- and calcium-independent [³H]-glutamate binding to synaptic receptors is particularly sensitive to displacement by compounds specific for the NMDA receptor (Fagg et al., 1983) has led to the use of [³H]-glutamate as a ligand at this receptor. Consequently,

reductions in the NMDA binding site measured with NMDA-displaceable [^3H]-glutamate have been reported to occur in the hippocampus of Alzheimer patients (Greenamyre, 1986; Greenamyre et al., 1987; Represa et al., 1988). Greenamyre et al. (1987) reported a loss of up to 80% of [^3H]-glutamate binding in the CA1 and CA2 of Alzheimer hippocampus; however, this study did not account for chloride-dependent binding of [^3H]-glutamate to glial cells (Bridges et al., 1987). In contrast, others have found no consistent alteration in NMDA-sensitive [^3H]-glutamate binding in Alzheimer brains (Cowburn et al., 1988a,b; Geddes et al., 1986). Further, Geddes and colleagues (1986) reported that within their study, a single case which presented particularly severe neuronal cell loss was found to have markedly reduced NMDA receptor binding; this would infer that NMDA receptor density can be maintained at normal levels in the hippocampus of Alzheimer Patients, as long as a minimum level of cell survival is maintained. The existence of such a "threshold" phenomenon in the pathological alterations of Alzheimer's Disease would suggest that receptor plasticity is important in maintaining functional activity in the wake of cell loss which accompanies the disease.

The results of the present study do not provide evidence for NMDA receptor plasticity following medial septal lesions. However, the variability of NMDA-sensitive glutamate binding was higher than that for other ligands, as indicated by the larger degree of error associated with NMDA-sensitive [^3H]-glutamate binding (Figures 37 & 38, and Appendix V, Table 4), and this may mask subtle alterations which might occur in NMDA receptor binding. In the vertical limb of the diagonal band and the presubiculum [^3H]-glutamate binding to the NMDA receptor was increased by 92% and 68% respectively; however, these results were not significantly different from control values.

In contrast to the present study, increases in NMDA receptor binding (Ulas et al., 1990) have been demonstrated in the hippocampus

following entorhinal cortex lesions in the rat; the increased NMDA receptor density which accompanies entorhinal cortex lesions is in contradiction to the reports of either decreased, or unaltered receptor density in Alzheimer's Disease. However, in view of the cell loss which affects the hippocampus in Alzheimer's Disease, synaptic plasticity in response to deafferentation may underlie the maintenance of NMDA-sensitive [³H]-glutamate binding in the course of the disease.

As is the case with kainate receptors in the present study, an important consideration in evaluating the plastic response of NMDA receptors to medial septal lesion is the time post-lesion at which investigations were performed. In the studies by Ulas et al. (1990a,b), significantly increased kainate receptor densities were observed in the hippocampus 60 days after entorhinal cortex lesion, while NMDA receptor densities were increased 30 days post-lesion; however, the elevation in NMDA-sensitive [³H]-glutamate binding was much greater at 60 days post-lesion, suggesting that modulation of NMDA receptors following deafferentation is by no means complete at 21 days. It is possible, therefore, that medial septal lesion, combined with a longer survival time than the present 21 day period, may result in significant altered NMDA receptors.

In summary, these results provide further evidence for the differential regulation of glutamatergic receptor sub-types in the hippocampus following medial septal lesions. While the destruction of the medial septal input to the hippocampus has been demonstrated to result in modification of AMPA-sensitive quisqualate receptors, these results do not provide evidence for the involvement of NMDA and kainate receptors, at least at short survival times, in the plastic responses of the hippocampus to cholinergic denervation.

2.4. PHOSPHOINOSITIDE HYDROLYSIS: RESPONSE TO MEDIAL SEPTAL LESIONS

Increasing interest in the role of second messenger systems in cellular function can be accredited in part to the elucidation of altered levels of second messengers or second messenger activity in a number of diseases, including Alzheimer's Disease (Saitoh et al., 1991) and ischaemia (Onodera & Kogure, 1989; Onodera et al., 1989). Thus, although altered receptor numbers may not be apparent in diseased tissue, changes in activity of second messengers and their enzymes may indicate altered neuronal transduction and consequently loss of normal neuronal function. Altered muscarinic-stimulated phosphoinositide turnover in response to lesions of the cholinergic septohippocampal pathway may therefore provide evidence of altered signal transduction through occupancy of muscarinic receptors in the hippocampus, even in the absence of altered muscarinic receptor densities.

Although a number of attempts have been made to demonstrate altered phospholipase C activity in terms of inositol phospholipid turnover in response to discrete neuronal populations, no general pattern of alteration has emerged. The results described presently indicate that muscarinic stimulated phosphoinositide turnover is unaltered in the hippocampus following lesions of the medial septum and suggest that there is no upregulatory response of muscarinic-mediated signal transduction. However, this contrasts with a previous report that electrolytic lesions of the medial septal area result in chronically increased phosphoinositide turnover in response to cholinergic, but not noradrenergic stimulation (Connor & Harrell, 1989); in view of the sprouting of putatively noradrenergic fibres into the CA3-dentate region following medial septal lesions (Crutcher et al, 1981), this result is intriguing. Nonetheless, a similar study has shown that α_1 -adrenergic-mediated phosphoinositide hydrolysis in the

hippocampus is unaltered following removal of the noradrenergic hippocampal projection from the locus coeruleus and dorsal noradrenergic bundle (Fowler et al., 1986). Thus, noradrenergic innervation of the hippocampus would not seem to be associated with changes in phosphoinositide hydrolysis post-lesion.

The increased phosphoinositide hydrolysis in response to cholinergic denervation has been confirmed, albeit with shorter survival times post-lesion, by several other groups. Fimbria fornix transection has been demonstrated to result in increases in muscarinic-stimulated phosphoinositide turnover in young (Smith et al., 1989) and in aged rats (Court et al., 1990) fourteen days after surgery was performed, despite preservation of muscarinic receptor densities in the hippocampus. The authors noted that these results provide evidence for the post-synaptic location of the majority of muscarinic receptors in the hippocampus. In the cerebral cortex, Reed and de Belleruche (1988) observed an upregulation in muscarinic-mediated phosphoinositide turnover five days after removal of the cholinergic innervation via lesions of the nucleus basalis. However, the increase was largely diminished fourteen days post-lesion, and abolished completely fifty days post-lesion, in spite of evidence of long-term reductions of choline acetyltransferase activity and acetyl cholinesterase associated with the lesion (Reed & de Belleruche, 1985; Wenk & Olton, 1984). In comparison, phosphoinositide turnover has been shown to be unaltered one, six and twelve weeks after quinolinate lesions of the nucleus basalis (Scarth et al., 1989), and one and three weeks following ibotenate lesions of the nucleus basalis (Raulli et al., 1989) of rats. Furthermore, in the guinea pig, electrolytic destruction of the medial septum did not result in altered phospholipid turnover eight to ten days following surgery (Fisher et al., 1980). These results suggest that while the present time course of twenty one days survival following lesions of the medial septum may exclude the possibility of acute,

transiently altered phosphoinositide hydrolysis, enhancement of cholinergic-mediated phosphoinositide turnover in the acute period post-lesion is not a consistent finding.

It is likely that different lesion strategies are responsible for different interpretations of the consequences in terms of phosphoinositide hydrolysis following lesions of cholinergic forebrain nuclei. Most notable is the absence of altered phosphoinositide turnover after selective lesions produced with neurotoxins (Raulli et al., 1989; Scarth et al., 1989, and the present study). As has been stressed in earlier sections of this discussion, excitotoxic lesions afford recovery and sprouting of fibres of passage, and do not result in such widespread damage as do, for example electrolytic or knife-cut lesions.

Finally, it is important to realise that the method currently employed for estimation of phosphoinositide turnover, which involves measuring accumulation of inositol phosphate within whole hippocampal preparations, precludes the measurement of discrete, localised alterations within sub-fields of the hippocampus: thus, it cannot be concluded from this study that phosphoinositide turnover remains unaltered in local hippocampal regions. However, in a parallel investigation to the present study, Horsburgh and colleagues (1991) observed that three weeks following medial septal lesions, [^3H]-PDBu binding increased in the entorhinal cortex, but was unaltered in other hippocampal areas, suggesting that the distribution of protein Kinase C was preserved following septal lesions. Instead, the increased [^3H]-PDBu binding in the entorhinal cortex indicates that plastic alterations are present in response lesions of the medial septum, and provide further evidence for the involvement of the entorhinal cortex, rather than intrinsic hippocampal neuronal circuits, in the synaptic modification within the hippocampus following cholinergic deafferentation.

3. THE CEREBRAL METABOLIC EFFECTS OF ACUTE SUBDURAL HAEMATOMA IN THE RAT.

3.1. FUNCTIONAL ACTIVITY AND ACUTE SUBDURAL HAEMATOMA IN THE RAT

A large body of evidence has contributed to the currently well-established excitotoxic hypothesis of cerebral ischaemia: exposure to glutamate or its analogues results in neurodegeneration in cell culture (Choi et al., 1988; Frandsen et al., 1989) and in vivo (Foster et al., 1987). Elevated extracellular glutamate concentrations are demonstrated in response to both global (Benveniste et al., 1984) and focal cerebral ischaemia (Graham et al., 1990; Bullock et al., 1991), and there is widespread evidence that glutamate antagonists, particularly those which act at the NMDA receptor and its associated ion channel, afford protection in ischaemic (Bullock et al., 1990; Frandsen et al., 1989; Gill et al., 1987; Ozyurt et al., 1988; Park et al., 1988; Rod & Auer, 1989; Sauer et al., 1988; Simon et al., 1984), hypoxic (McDonald et al., 1987), and glutamate-treated neuronal tissue (Foster et al., 1987c; Goldberg et al., 1988; Olney et al., 1987). Additionally, the pattern of selective vulnerability of neurones to ischaemic damage corresponds well with the distribution of glutamate receptors in the brain: hippocampal CA1 pyramidal neurones, which contain the highest density of NMDA-sensitive binding sites within the brain (Monaghan & Cotman, 1985), are particularly susceptible to ischaemia-related damage in animal models (Kirino, 1982; Pulsinelli et al., 1982a) and man (Cummings et al., 1984; Volpe & Hirst, 1983).

The autoradiographic measurement of local metabolism in cerebral ischaemia has proved to be a powerful strategy in the investigation of both the anatomical location of ischaemic damage, and the mechanisms underlying ischaemic damage (for review, see Ginsberg, 1990). Such

studies have proved instrumental in a number of observations. Firstly, functional activity is affected in structures remote from, as well as structures directly within the infarcted region. Secondly, these functional changes are dynamic and progressive, and are suggestive of a time-course for the occurrence of ischaemic damage which determines the "therapeutic window" or absolute time in which compromised tissue may be saved from infarction. Thirdly, these techniques have been used recently as a basis for quantification of pharmacological efficacy: a number of groups have demonstrated the reduction by various pharmacological agents of functional disturbances produced by ischaemic insult.

This study has demonstrated that remote as well as local alterations in deoxyglucose phosphorylation occur following acute subdural haematoma in the rat. In addition, the vastly increased deoxyglucose phosphorylation around the site of infarct, and in the hippocampal area were prevented by the administration prior to production of haematoma of D-CPP-ene, a competitive NMDA antagonist with clinical potential. This suggests that a glutamatergic mechanism plays a role in the altered glucose utilisation, and subsequent ischaemic damage associated with this model. Evidence for this is reviewed below.

Local Mechanisms: The Ischaemic Penumbra

Several groups have reported the appearance of an "ischaemic penumbra" surrounding the infarcted region in models of focal cerebral ischaemia. The term was initially coined by Astrup and colleagues (1981) to describe the region immediately next to densely ischaemic tissue, with a higher perfusion rate than that of the densely ischaemic region. The concept of the ischaemic penumbra is derived initially from electrophysiological experiments in which baboons were subjected to occlusion of the middle cerebral artery (Astrup et al., 1977). Two ischaemic thresholds emerged: firstly, a reduction of flow sufficient to

abolish evoked cortical potentials did not result in a large elevation of potassium ions; by contrast, massive flux of potassium occurred only with greater reductions in flow. Thus there is a disparity between the level of ischaemia required for electrical failure and for disruption of membrane homeostasis, and the ischaemic penumbral region has been conceptualised as an area in which cerebral bloodflow falls between these two levels.

This observation is of great therapeutic relevance: while the cells within the penumbral region are compromised, they are potentially retrievable, if the process of ischaemic damage were to be halted by pharmacological intervention.

Using deoxyglucose autoradiography, various authors have reported the presence of a region of diminished glucose utilisation following focal ischaemia, surrounded by an area of apparently increased deoxyglucose phosphorylation (Ginsberg et al., 1977a,b; Shiraishi et al., 1989; Simon & Shiraishi, 1990). This increase is attributed to anaerobic glycolysis, since double-label experiments which employed [³H]-antipyrine to measure local cerebral bloodflow demonstrated a decrease in bloodflow concurrent with increased deoxyglucose uptake in the penumbral region (Ginsberg et al., 1977). Recently, Shiraishi and colleagues (1989) used the deoxyglucose technique to examine the time-course for metabolic alterations in response to occlusion of the middle cerebral artery in rats, observed that increased deoxyglucose uptake preceded decreased uptake in the same area; the rim of apparent hypermetabolism surrounding the infarct progressed outward, leaving infarcted tissue in its place. The same group (Graham et al., 1990) also reported increases in excitatory amino acids in the extracellular fluid in response to the ischaemic insult, and postulated that local release of glutamate and other excitatory amino acids was responsible for the apparent hypermetabolism in the ischaemic penumbra: in the absence of bloodflow to the ischaemic cells, these toxic substances may be

removed only by re-uptake and metabolism within neurons and glia; however, within the ischaemic zone, the energy stores which fuel the process of re-uptake are depleted rapidly. Diffusion of these amino acids from the centre of the ischaemic zone may jeopardise the cells within the ischaemic penumbra.

Support for this hypothesis comes from the observation in the present study that D-CPP-ene administration prior to production of acute subdural haematoma prevented hypermetabolism in the ischaemic penumbral region. Further, in a subsequent series of measurements, D-CPP-ene has been demonstrated to reduce the size of infarct produced by the subdural haematoma (Inglis et al., 1991), a result which confirms the findings of Simon and colleagues (Shiraishi et al., 1989; Simon & Shiraishi, 1990) who demonstrated reduction of ischaemic damage in the middle cerebral artery occlusion model with the use of the competitive NMDA antagonist CGS-19755; this suggests that blockade of NMDA receptors may prevent some spread of ischaemic damage in the area surrounding the infarct, and adds weight to the glutamatergic hypothesis of ischaemic damage.

However, a second mode of action may explain the efficacy of NMDA antagonists in the reduction of infarct size and preventing the hypermetabolism which occurs. Competitive NMDA antagonists cross the blood-brain barrier poorly, and therefore the CNS concentrations of these drugs rise slowly and remain only a fraction of the peripheral concentration (McCulloch & Iversen, 1991). However, in a double-label study Takizawa and colleagues (1991) demonstrated that treatment with CGS-19755 immediately after occlusion of the middle cerebral artery in rats corrected the ischaemia-induced decrease in local pH, and increased local cerebral bloodflow in several ischaemic areas. The authors suggested therefore that a potent increase in cerebral perfusion may aid the removal of compounds such as excitatory amino acids, lactic acid, and hydrogen ions which are present in toxic quantities as a result of

the ischaemic process; this may complement any NMDA receptor blockade induced by the small amounts of CGS-19755 able to penetrate the blood-brain barrier in the limited time in which the process of ischaemic damage can be impeded. Thus in the present study, the ability of D-CPP-ene to prevent hypermetabolism in the penumbral region may arise from both blockade of glutamate receptors and an increased perfusion of the compromised tissue in the penumbral zone.

Remote Mechanisms: The Hippocampus.

The most striking observations of this study were the massive increases in glucose utilisation produced by acute subdural haematoma in the hippocampus, and the ability of D-CPP-ene to prevent almost completely, or in some cases abolish, these increases. From the latter it may be inferred that functional activation of the hippocampus is produced by a glutamatergic mechanism; and indeed, *in vivo* dialysis of the extracellular fluid in the hippocampal area revealed elevated levels of glutamate and aspartate in the hippocampus following acute subdural haematoma, and these remained elevated for at least three hours (Bullock et al., 1991a).

To date, of the relatively few accounts of hippocampal glucose utilisation measured in response to ischaemia, both increased and decreased glucose utilisation have been reported in the hippocampal formation at some period after ischaemia (see Beck et al., 1990, for review). However, the majority of these describe the consequences of transient global ischaemia in the rat (Beck et al., 1989, 1990; Diemer & Siemkowicz, 1980; Kozuka et al., 1989; Pulsinelli et al., 1982b; Rischke & Kreiglstein, 1991) or gerbil (Izumiyama et al., 1987; Suzuki et al., 1983), and the discrepancies between the duration of ischaemic period, and the length of recovery time prior to deoxyglucose autoradiography (from four minutes to two days) have made comparison of these results difficult. While global reperfusion models of ischaemia are pivotal in

assessing the long-term consequences of ischaemia, these are complicated by issues such as reperfusion injury, and indicate little about the dynamic alterations which occur in the course of the initial ischaemic period. Furthermore, the susceptibility of gerbils to seizures introduces a confounding variable into the assessment of ischaemic damage in this species.

An advantage of this study is that not only does it represent a measure of functional alterations in the course of the ischaemic infarct, but these stem from an apparently confined focus; and there exists therefore the possibility to discuss these changes in terms of limited, anatomically defined circuitry. Disruption of the glutamatergic perforant pathway via lesions of the entorhinal cortex has been found to afford protection for the CA1 pyramidal cells against ischaemia (Weiloch et al., 1985), suggesting that over-stimulation of this particular hippocampal input is responsible for the ischaemia-induced neuronal damage within the hippocampus. In the rat, the entorhinal cortex receives inputs from cingulate, frontal and temporal cortices (See Swanson et al., 1987 for review), and also reciprocal connections from the hippocampal formation. The hippocampus receives a second major cortical connection, through the subicular complex from temporal, frontal and cingulate cortices, and additionally from parietal and visual cortical areas. Thus, the hippocampus receives extensive connections from many cortical areas. Glutamate is a major neurotransmitter in cortical synapses (Baughman & Gilbert, 1981; Crunelli et al., 1987; Fosse & Fonnum, 1987; Peinado & Mora, 1986), a factor which most probably underlies the vulnerability of the cortex and its glutamatergic efferents in ischaemia. The massive disruption of metabolism in cortical areas following acute subdural haematoma in this study, combined with the functional activation of the hippocampus may provide further evidence for a cortical role in hippocampal ischaemic damage.

Buchan & Pulsinelli (1990) have shown that in rats subjected to

transient four-vessel occlusion, fimbria fornix transection protects the hippocampus against ischaemic damage more effectively than lesions of the perforant path, suggesting that the cholinergic input into the hippocampus is more important in producing ischaemic damage than the integrity of the glutamatergic perforant path. However, due to the global nature of the ischaemic insult, increased neuronal activity in any number of areas, including the septohippocampal pathway itself, may underly the ischaemic damage observed in the hippocampus in the intact animal, and these results may not reflect events in a focal model of ischaemia such as acute subdural haematoma. There is little evidence however from the present study as to whether or not this input is important in the functional activation of the hippocampus in response to subdural haematoma.

Finally, given that acute subdural haematoma is associated with a concomitant increase in intracranial pressure, it is important to consider whether this global element could account for the functional activation observed in the hippocampus. Glucose utilisation was not significantly altered in any of the three hippocampal afferents discussed above, and this may on first inspection be considered as evidence that hippocampal activity was not mediated through stimulation of these afferents. However, in a separate group of animals, in which the subdural haematoma was replaced by an inert silicone mass injected underneath the dura in the same manner as blood, glucose utilisation was not increased in either the penumbral region or in the hippocampus (Kuroda et al., 1992). The presence of a Cushing's response in these animals indicated that intracranial pressure was increased in these rats. This would imply that raised intracranial pressure is not able alone to induce the increased hippocampal glucose utilisation, and that blood is required for the widespread cortical and hippocampal alterations associated with the model. It may be speculated that a component of blood, such as a vasoconstrictor, is

responsible for the resultant ischaemic cortical damage; and indeed, several peptides found in the blood have been postulated to perform such a function (for review see Uddman & Edvinsson, 1989). In conclusion, these results suggest that hippocampal activation in this model stems from ischaemic processes originating in the cortex due to injection of blood.

Increased intracranial pressure may, however, be an important secondary factor in ischaemia-induced damage of the hippocampus. In non-pathologically affected tissue, glucose metabolism and cerebral bloodflow are tightly coupled (Kuschinski et al. 1987). Thus increases in glucose use are usually associated with concomitant increases in local bloodflow, within a discrete homogeneous region of brain. Following subdural haematoma, as glucose metabolism increases in response to greater neuronal function, so will the build-up of waste-products continue within the tissue. However, an increased demand for perfusion may be confounded by the raised intracranial pressure; if the energy demand cannot be met by increased perfusion, the result will be acidosis and consequent cellular damage (for review see Hakim & Shoubridge, 1989). As discussed previously, recent evidence suggests that NMDA antagonists may exert some therapeutic effect by increasing cerebral perfusion to ischaemic areas, thus facilitating clearance of substances present in toxic amounts. This effect is of obvious importance in situations where the cerebral perfusion is compromised, either by vasoconstriction, or by an increase in intracranial pressure.

Non-Limbic Structures

Following acute subdural haematoma, glucose utilisation was reduced in the dorsolateral and medial geniculate bodies, and there was evidence of functional depression in other subcortical auditory and visual areas. These are probably reflective of the extent of cortical damage induced by the haematoma, and are further evidence of the

importance of glutamatergic transmission in cortical and subcortical neurotransmission.

Effect of D-CPP-ene on Cerebral Glucose Utilisation in Rats with Acute Subdural Haematoma

The cerebral metabolic effects of D-CPP-ene have been discussed previously in detail. However, in the present series of data, several differences emerged, which may be attributed to either the anaesthetic state of the animal, or the presence of the haematoma, at the time of administration of D-CPP-ene. Because of the trauma involved in the production of the subdural haematoma, the procedure was performed in anaesthetised animals, and these were therefore anaesthetised at the time of drug administration, prior to the induction of the haematoma. Most notable of these were the increased rates of glucose utilisation in the posterior cingulate cortex and anteroventral thalamic nucleus following D-CPP-ene administration. While other NMDA antagonists have been shown to induce large metabolic activations in certain Papez structures (see Discussion Section 1), D-CPP-ene had far less marked effects, and did not alter glucose utilisation in either structure in the conscious rat. Initially this may be thought to be due to the interaction of D-CPP-ene and halothane. However, halothane anaesthesia has been shown to ameliorate activation of the posterior cingulate cortex and anteroventral thalamic nucleus by MK-801 (Kurumaji et al., 1989), and therefore the reason for the discrepancy between the present two studies is unclear. However, it is possible that the effects of the haematoma and consequently the increased extracellular glutamate in cortical regions act synergistically with D-CPP-ene to compromise glutamatergic feedback mechanisms in these regions. D-CPP-ene was also observed to increase glucose utilisation in the entorhinal cortex and lateral olfactory tract and decrease glucose use in the parietal cortex contralateral, but not ipsilateral, to the haematoma; the lack of ipsilateral functional

alteration is possibly due to mechanisms resulting from the presence of the haematoma.

In rats with acute subdural haematoma glucose utilisation was decreased in auditory and visual areas; these decreases were found to be partly diminished in D-CPP-ene pretreated animals; however, D-CPP-ene has been observed to decrease glucose utilisation in sensory regions (Results Section 1.2.1.), an effect attributed to its anaesthetic action, and therefore it is difficult to discern between functional alterations produced by D-CPP-ene and by the presence of the haematoma itself. Whether or not these areas benefit from D-CPP-ene pretreatment, therefore, would require further study, possibly involving detailed histological analysis.

In summary, acute subdural haematoma induced widespread metabolic alterations in the rat brain, of which the most striking were the massive functional activation in the hippocampus, and the profound loss of deoxyglucose uptake in the cortex directly below the haematoma. Pretreatment with D-CPP-ene was found to reduce functional disturbances, particularly in the hippocampus, thus providing evidence that this class of drug may be beneficial in the treatment of ischaemic damage in the clinic.

3.2. COMMENT ON THE APPLICATION OF THE DEOXYGLUCOSE METHOD TO THE ISCHAEMIC BRAIN

Given that ischaemic damage is a dynamic, pathological process, it is important to consider certain aspects underlying the validity of the mathematical model (Sokoloff et al., 1977). In a subsequent series of measurements, it has been shown that the alterations in hippocampal glucose utilisation described here are transient, and are not present at four hours (Kuroda et al., 1992), and thus strictly speaking, glucose metabolism within regions of the brain cannot be assumed to be in steady state. While it is useful to quantify rates of deoxyglucose uptake as rates of local cerebral glucose utilisation in order to make statistical comparisons, it should be noted that these rates may not represent the exact rates of glucose utilisation within the cerebral tissue.

In focal cerebral ischaemia, marked reductions of bloodflow, and hence glucose supply, may interfere with the quantitative estimation of cerebral metabolism in several ways. A severe decrease in bloodflow to a particular region of brain would be expected to limit the rate of glucose utilisation within that region. Tanaka et al. (1985) have shown that when bloodflow is reduced to less than 25% of normal values and hence supply of glucose and deoxyglucose is critically limited, local glucose utilisation is significantly underestimated.

Secondly, although measurement of glucose utilisation tends to be relatively insensitive to changes in the rate constants for uptake and phosphorylation of glucose and deoxyglucose, it is conceivable that in severely ischaemic tissue these constants will become inaccurate. Using fluorodeoxyglucose in order to make repeated measurements of metabolic rate, Nakai et al. (1988) demonstrated that k_1^* and k_3^* were decreased significantly in ischaemic tissue, while large variations in k_2^* also occurred. Additionally the time at which the model would become insensitive to alterations in the rate constants increased, resulting in an

underestimation of glucose use had the normal rate constants been used.

A number of studies have shown that the lumped constant is changed in ischaemic tissue. Ginsberg and Reivich (1979) observed a two-fold increase in the value of the lumped constant: in such a case, the use of the conventional value of the lumped constant would result in a two-fold overestimation of cerebral glucose use.

The lumped constant might become altered for the following reasons: the tissue damage which accompanies cerebral ischaemia will disrupt cellular compartmentalisation, and hence it can no longer be assumed that λ , the distribution ratio of glucose and deoxyglucose is equal to that of normal tissue. Secondly, Sokoloff (1979) postulated that lysosomal acid hydrolases released during ischaemia would result in the hydrolysis of glucose-6-phosphate; the value of ϕ , the fraction of phosphorylated glucose which continues to be metabolised in glycolysis, would therefore be altered, and the lumped constant would no longer be accurate. This is especially important when calculating the rates of glucose utilisation in the penumbral region: by definition this represents a region in which bloodflow is compromised; Nedergaard et al. (1986) have shown an increase in lumped constant in areas bordering the infarct, and therefore the use of the conventional lumped constant to measure glucose utilisation leads to a potential overestimation of glucose utilisation within this area.

When this model is used to study changes in cerebral metabolism in response to ischaemia, these limitations must be borne in mind; in severely ischaemic tissue it is not possible to measure accurately cerebral glucose utilisation with the rate and lumped constants defined by Sokoloff et al. (1977), and hence values for the region of infarct have not been calculated.

4. OVERVIEW: COMMENT ON TECHNIQUES FOR ANALYSIS OF HIPPOCAMPAL FUNCTION

The deoxyglucose technique has proved to be an extremely potent tool in neuroscience research (for review see McCulloch 1982). The coupling which has been demonstrated to exist between rates of energy consumption and CNS activity, combined with the capacity to localise and quantify changes in metabolic demand autoradiographically has provided the basis for expanded research into the CNS metabolic demands created by pathological, pharmacological and physiological challenge. Furthermore, deoxyglucose autoradiography provides a rare opportunity to investigate these effects in the conscious brain. However, while deoxyglucose autoradiographic techniques have proved to be particularly successful in mapping global distributions of dynamic functional alterations (McCulloch, 1982) such as the effects of acute drug administration, or the massive functional disturbances which accompany ischaemia (Ginsberg, 1990 and the present study), their worth has to date been limited in the study of the hippocampal function. Indeed, the complexity of the hippocampus and limbic system have restricted both the application of deoxyglucose autoradiography and the interpretation of results gained from such studies: in the present study, administration of the pharmacologically active cholinergic and glutamatergic agents has been shown to produce only slight alterations in glucose use in the hippocampus, despite the high numbers of hippocampal cholinergic and glutamatergic receptors within the hippocampal formation. Lack of functional alterations in response to cholinergic agents has been reported previously: the failure of the muscarinic agonist oxotremorine to alter significantly glucose utilisation within the hippocampus (Dam & London, 1984) has been suggested to reflect the ability of muscarinic receptor stimulation to modify membrane excitability without producing adequate depolarisation to alter glucose utilisation notably.

Alternatively, given the complexity of hippocampal circuitry, it is possible that alterations in response to muscarinic stimulation represent an immeasurably small fraction of the total synaptic activity within the hippocampus. However, as discussed (Section 1.2.), the diversity of functional response within the hippocampus, in particular to different cholinomimetic agents, has done little to advance the current understanding of functional activity in relation to cholinergic transmission, and reflects the generally poor perception of the mechanisms which underlie muscarinic transmission in the hippocampus.

Nevertheless, several investigators have employed deoxyglucose autoradiography to investigate hippocampal function with relative success. For example, local cerebral glucose utilisation has been shown to increase in specific hippocampal layers in response to cognitive challenge in the behaving monkey (Friedman & Goldman-Rakic, 1988): in a series of behavioural paradigms designed to test working memory, glucose utilisation was found to increase in the CA1, CA3 and the dentate gyrus, while glucose use in the amygdala was unaltered, demonstrating that cognitive processes can be seen to produce specific hippocampal alterations in function.

The complex relationship between firing of hippocampal neurones and local cerebral glucose utilisation has been highlighted in a study by Ackermann and colleagues (1984) who demonstrated that activation of recurrent inhibitory interneurons in the hippocampus results in an increased metabolic demand; the authors suggested that the energy savings produced by the apparent inhibition of hippocampal firing are offset by the energy requirements of the inhibitory neurones; thus a net energy demand is observed. In polysynaptic pathways such as the hippocampus, therefore, studies of function are limited by the inability of the deoxyglucose technique to distinguish between the metabolic demands of different transmitter systems. Instead, the ability of the

deoxyglucose technique to reveal brain function maybe increased significantly by simultaneous measurements of neurophysiological variables such as electrophysiological activity. Thus, while the deoxyglucose technique is indeed a powerful tool in neuroscience, and is able to provide novel *in vivo* insights into CNS function, its greatest limitation is perhaps the dependence on other techniques in parallel which provide information on the status of specific neurotransmitter systems in the CNS.

The availability of receptor-specific radio-labelled ligands, and the development of quantitative *in vitro* ligand binding autoradiography (Kuhar, 1981; Rainbow et al., 1982) has been instrumental in mapping populations of receptors and receptor sub-types within specific pathways of the CNS (Chang et al., 1980; Quirion et al., 1985; Wenk & Englisch, 1986). However, despite the enormous potential of these techniques, little success has been achieved in the attempt to elucidate the locus of synaptic change in denervation studies and degenerative diseases such as Alzheimer's Disease.

The discovery that Alzheimer's Disease is associated with the loss of cholinergic neurones in the basal forebrain has fuelled expanded research into the functions of cholinergic transmitter systems (Bartus et al., 1982; Perry et al., 1978). However, despite the demonstration of consistently reduced presynaptic cholinergic markers in the cortex and hippocampus, and the profound loss of cells from the cholinergic basal forebrain nuclei, cholinergic receptors have not been shown to be convincingly and reproducibly diminished (Perry et al., 1978). As a result, experimental lesions of the cholinergic pathways have been employed in order to investigate the plastic response of cholinergic receptors to denervation; however, the diversity of lesion methods is perhaps responsible for the array of conflicting reports of increased, decreased or unaltered cholinergic receptors following denervation (Court et al., 1990;

Joyce et al., 1989; Kamiya et al., 1981; Mash et al., 1985; McKinney & Coyle, 1982; Norman et al., 1986; Overstreet et al., 1980; Smith et al., 1989; Watson et al., 1985; Westlind et al., 1981; Yamamura & Snyder, 1974).

While excitotoxins such as ibotenic acid have been employed as specific neurotoxins for cholinergic cells, it has recently become apparent that these also destroy non-cholinergic cells; thus the specificity of lesions produced by these neurotoxins has been questioned. The first suggestion that some of the learning and memory deficits produced by ibotenic acid lesions may not be due primarily to damage of cholinergic neurones was provided by Dunnett et al. (1987). The investigators compared the effects of four neurotoxins in terms of their ability to produce behavioural, biochemical and histological alterations when injected into the nucleus basalis. While ibotenate produced large deficits in behavioural memory tasks, ibotenate-induced depletions in choline acetyltransferase (ChAT) activity were much smaller than those produced by quisqualate. In contrast, quisqualate produced much smaller deficits in behavioural memory tasks than ibotenate; the dissociation between cognitive deficits and ChAT depletion would suggest that ibotenate-induced disruption of learning and memory was not due to destruction solely of cholinergic neurones. Since this report, several subsequent studies have confirmed the dissociation of ChAT depletion and cognitive deficits (Robbins et al., 1989a,b; Wenk et al., 1989), meriting caution in the interpretation of results based on studies which employ neurotoxins.

There is convincing evidence for the existence of non-cholinergic cells in the septohippocampal pathway (Köhler et al., 1984); thus, denervation of non-cholinergic hippocampal inputs may be responsible for many of the behavioural and neurochemical deficits produced in the process of excitotoxic lesions of the septohippocampal pathway, and may provide some explanation for discrepancies between studies of ligand binding to receptors following denervation of the hippocampus. While denervation techniques, combined with the high degree of anatomical

resolution afforded by ligand binding provide a powerful investigatory tool in neuroscience research, therefore, before plastic mechanisms in response to excitotoxic lesion can be evaluated fully, it is important that these excitotoxins are characterised further in terms of their specificity. Such an approach could be conceived to play a major role in elucidation of the mechanisms underlying denervation-induced plasticity, and ultimately, degenerative diseases such as Alzheimer's Disease.

APPENDIX I

THE CEREBRAL METABOLIC EFFECTS OF THE COMPETITIVE NMDA ANTAGONIST D-CPP-ENE IN THE RAT.

Glucose utilisation was measured in conscious, lightly restrained rats using deoxyglucose autoradiography, following intravenous administration of D-CPP-ene (0.3, 3 or 30mg kg⁻¹) or saline. The data presented in Tables 2-7 represent mean glucose utilisation ($\mu\text{mol } 100\text{g}^{-1} \text{ min}^{-1}$) \pm SEM of 76 anatomically distinct regions of brain. Data in Table 1 represent physiological parameters following D-CPP-ene administration. * $p < 0.05$, ** $p < 0.01$ for statistical comparison of drug-treated groups with saline-treated controls (unpaired Student's t-test, two-tailed, with Bonferroni correction).

APPENDIX I - TABLE 1
PHYSIOLOGICAL PARAMETERS

PHYSIOLOGICAL PARAMETER	D-CPP-ENE (mgkg ⁻¹)			
	CONTROL	0.3	3	30
Mean Arterial Blood Pressure (mmHg)	128 ± 3	128 ± 9	142 ± 6	149 ± 9
Δ Mean Arterial Blood Pressure (mmHg)	4.3 ± 2.8	-5.0 ± 2.0	11.4 ± 7.0	21.0 ± 6.2
Arterial Plasma Glucose (mM)	8.5 ± 0.3	7.6 ± 0.8	7.4 ± 0.6	8.2 ± 0.1
Arterial pH	7.44 ± 0.01	7.41 ± 0.01	7.40 ± 0.01	7.37 ± 0.01**
PaCO ₂ (mmHg)	42.5 ± 0.37	40.3 ± 2.9	42.2 ± 1.5	43.6 ± 0.84
PaO ₂ (mmHg)	83.5 ± 3.0	86.8 ± 3.2	92.8 ± 2.8	92.8 ± 3.0
Rectal Temperature (°C)	36.9 ± 0.14	36.2 ± 0.64	36.2 ± 0.37	36.7 ± 0.54
Number of Animals	9	5	5	5

Values are presented as mean ± SEM. **P<0.01 for statistical comparison between each drug-treated group and saline-treated controls. Number in each group are 9 (saline-treated controls) or 5 (drug-treated). Arterial blood gases and rectal temperature were measured 35 minutes after [¹⁴C]-deoxyglucose administration. Absolute values for mean arterial blood pressure are those measured two hours after drug or saline administration. Δ Mean arterial blood pressure represents the change in blood pressure two hours after drug or saline administration relative to the value prior to injection.

APPENDIX I - TABLE 2

GLUCOSE UTILISATION FOLLOWING D-CPP-ENE ADMINISTRATION: HIPPOCAMPAL FORMATION

STRUCTURE	CONTROL	D-CPP-ENE (mgkg ⁻¹)		
		0.3	3	30
<u>Ammon's Horn</u>				
CA1 Str. Oriens/ Pyramidale	51 ± 2	54 ± 5	42 ± 4	50 ± 2
CA1 Str. Radiatum	55 ± 2	56 ± 5	46 ± 4	53 ± 2
CA1 Str. Lacunosum Moleculare	73 ± 2	76 ± 6	63 ± 6	85 ± 7
CA2 Str. Oriens/ Pyramidale	69 ± 3	67 ± 4	58 ± 5	67 ± 3
CA2 Str. Radiatum	71 ± 3	72 ± 4	60 ± 6	69 ± 3
CA2/3 Str. Lacunosum Molecular	80 ± 3	81 ± 5	68 ± 7	82 ± 3
CA3 Str. Oriens/ Pyramidale	69 ± 2	66 ± 4	60 ± 9	69 ± 3
CA3 Str. Radiatum	67 ± 2	70 ± 4	58 ± 8	67 ± 3
CA4 Str. Pyramidale	62 ± 2	64 ± 5	47 ± 3*	61 ± 3
<u>Dentate Gyrus</u>				
Molecular Layer (Superior Blade)	61 ± 3	65 ± 6	48 ± 8	59 ± 9
Molecular Layer (Inferior Blade)	54 ± 2	56 ± 5	50 ± 7	58 ± 4
Polymorphic Layer	51 ± 2	54 ± 5	41 ± 4	52 ± 3
Pre Subiculum	87 ± 5	84 ± 4	74 ± 8	108 ± 6
Subiculum	73 ± 2	72 ± 5	57 ± 5*	77 ± 7

Data are presented as mean ± S.E.M. of 9 (control) or 5 (drug-treated) animals. Glucose utilisation is expressed in $\mu\text{mol}\cdot 100\text{g}^{-1}\cdot \text{min}^{-1}$. * $P < 0.05$, for statistical comparison between drug-treated group and saline-treated controls.

APPENDIX I - TABLE 3
GLUCOSE UTILISATION FOLLOWING D-CPP-ENE ADMINISTRATION:
AREAS ASSOCIATED WITH LIMBIC FUNCTION

STRUCTURE	CONTROL	D-CPP-ENE (mgkg ⁻¹)		
		0.3	3	30
Dorsal Tegmental Nucleus	102 ± 5	94 ± 10	76 ± 6*	92 ± 4
Dorsal Raphe	79 ± 4	76 ± 5	71 ± 5	77 ± 7
Median Raphe	86 ± 4	82 ± 6	72 ± 5	81 ± 5
Mamillary Body (Medial)	101 ± 3	98 ± 10	77 ± 7**	97 ± 7
Mamillary Body (Lateral)	97 ± 3	91 ± 10	79 ± 5*	104 ± 10
Habenular Nucleus (Medial)	72 ± 4	87 ± 6	63 ± 5	68 ± 3
Habenular Nucleus (Lateral)	109 ± 6	117 ± 11	90 ± 7	104 ± 5
Thalamus:-				
Mediodorsal	94 ± 6	98 ± 10	82 ± 5	106 ± 7
Laterodorsal	85 ± 4	78 ± 6	70 ± 6	81 ± 3
Anteromedial	102 ± 4	97 ± 5	91 ± 8	102 ± 4
Anteroventral	95 ± 4	88 ± 13	84 ± 8	112 ± 5
Hypothalamus	56 ± 3	58 ± 4	47 ± 4	49 ± 2
Amygdala:-				
Medial Nucleus	50 ± 3	44 ± 3	39 ± 4	41 ± 2
Lateral Nucleus	69 ± 3	65 ± 4	55 ± 4	50 ± 2*
Basolateral Nucleus	76 ± 6	75 ± 6	68 ± 7	77 ± 4
Medial Septum	66 ± 3	70 ± 5	63 ± 7	84 ± 6
Lateral Septum	48 ± 2	50 ± 5	41 ± 4	46 ± 2
Vertical Diagonal Band	71 ± 4	68 ± 5	59 ± 6	70 ± 6
Horizontal Diagonal Band	86 ± 4	82 ± 3	75 ± 7	90 ± 5
Medial Forebrain Bundle	89 ± 4	86 ± 6	76 ± 6	90 ± 6
Nucleus Accumbens	65 ± 2	60 ± 6	47 ± 5*	63 ± 5
Cortex:-				
Posterior Cingulate Cortex	91 ± 3	86 ± 7	72 ± 7	101 ± 8
Anterior Cingulate Cortex	112 ± 2	96 ± 6	83 ± 11*	81 ± 6**
Parietal Cortex	111 ± 4	103 ± 6	81 ± 7**	63 ± 4**
Frontal Cortex	109 ± 4	106 ± 4	82 ± 9*	67 ± 6**

Data are presented as mean ± S.E.M. of 9 (control) or 5 (drug-treated) animals. Glucose utilisation is expressed in $\mu\text{mol} \cdot 100\text{g}^{-1} \cdot \text{min}^{-1}$. *P<0.05, **P<0.01 for statistical comparison between drug-treated group and saline-treated controls.

APPENDIX I - TABLE 4
GLUCOSE UTILISATION FOLLOWING D-CPP-ENE ADMINISTRATION:
OLFACTORY AREAS

STRUCTURE	CONTROL	D-CPP-ENE (mgkg ⁻¹)		
		0.3	3	30
Lateral Olfactory Cortex	120 ± 7	122 ± 11	102 ± 7	102 ± 9
Lateral Olfactory Tract	110 ± 5	121 ± 11	131 ± 17	179 ± 12**
Anterior Olfactory Nucleus	74 ± 4	84 ± 9	76 ± 7	106 ± 7**
Primary Olfactory Cortex	122 ± 4	116 ± 6	123 ± 12	141 ± 7
Posterior Piriform Cortex	73 ± 5	77 ± 5	82 ± 9	104 ± 9*
Amygdalar Nucleus	72 ± 3	73 ± 3	71 ± 7	103 ± 7**

Data are presented as mean ± S.E.M. of 9 (control) or 5 (drug-treated) animals. Glucose utilisation is expressed in $\mu\text{mol}\cdot 100\text{g}^{-1}\cdot \text{min}^{-1}$. *P<0.05, **P<0.01 for statistical comparison between drug-treated group and saline-treated controls.

APPENDIX I - TABLE 5
GLUCOSE UTILISATION FOLLOWING D-CPP-ENE ADMINISTRATION:
AUDITORY AND VISUAL STRUCTURES

STRUCTURE	CONTROL	D-CPP-ENE (mgkg ⁻¹)		
		0.3	3	30
<u>Auditory System</u>				
Auditory Cortex II	112 ± 7	109 ± 11	80 ± 8	67 ± 3**
Auditory Cortex IV	133 ± 9	128 ± 9	93 ± 9	68 ± 5**
Medial Geniculate Body	114 ± 4	100 ± 5	79 ± 5**	69 ± 3**
Inferior Colliculus	166 ± 9	141 ± 7	118 ± 8**	107 ± 6**
Lateral Lemniscus	88 ± 3	87 ± 6	83 ± 7	86 ± 5
Cochlear Nucleus	133 ± 7	124 ± 9	102 ± 8	110 ± 7
Superior Olivary Nucleus	118 ± 6	104 ± 10	109 ± 11	117 ± 5
<u>Visual System</u>				
Visual Cortex IV	105 ± 6	89 ± 5	75 ± 7**	62 ± 2**
Dorsolateral Geniculate Body	88 ± 2	85 ± 5	71 ± 5*	71 ± 3**
Ventrolateral Geniculate Body	70 ± 3	69 ± 3	57 ± 6	58 ± 2
Anterior Pretectal Nucleus	88 ± 2	83 ± 4	66 ± 6**	70 ± 6*
Lateral Post-Thalamic Nucleus	92 ± 4	86 ± 6	74 ± 5	83 ± 7
Superior Colliculus (Super)	76 ± 4	70 ± 4	57 ± 3*	54 ± 2**
Superior Colliculus (Deep)	75 ± 3	73 ± 3	65 ± 4	64 ± 4

Data are presented as mean ± S.E.M. of 9 (control) or 5 (drug-treated) animals. Glucose utilisation is expressed in $\mu\text{mol}\cdot 100\text{g}^{-1}\cdot \text{min}^{-1}$. *P<0.05, **P<0.01 for statistical comparison between drug-treated group and saline-treated controls.

APPENDIX I - TABLE 6
GLUCOSE UTILISATION FOLLOWING D-CPP-ENE ADMINISTRATION:
EXTRAPYRAMIDAL AND SENSORIMOTOR AREAS

STRUCTURE	CONTROL	D-CPP-ENE (mgkg ⁻¹)		
		0.3	3	30
Cerebellar Nucleus	91 ± 3	90 ± 4	83 ± 6	79 ± 5
Cerebellar Hemisphere	57 ± 2	54 ± 2	46 ± 3*	55 ± 2
Vestibular Nucleus	113 ± 4	110 ± 5	108 ± 8	101 ± 4
Inferior Olive	73 ± 3	69 ± 4	55 ± 4*	59 ± 2
Pontine Grey	52 ± 3	54 ± 4	45 ± 4	51 ± 3
Red Nucleus	65 ± 3	64 ± 4	59 ± 4	66 ± 5
Sustantia Nigra: Pars Compacta	54 ± 5	54 ± 2	47 ± 5	55 ± 4
Pars Reticulata	54 ± 2	53 ± 3	46 ± 6	58 ± 7
Caudate Nucleus	104 ± 3	104 ± 6	88 ± 8	96 ± 8
Globus Pallidus	56 ± 6	54 ± 4	44 ± 3	47 ± 4
Thalamus (Ventrolateral Nucleus)	78 ± 3	82 ± 4	65 ± 5	61 ± 4
Subthalamic Nucleus	84 ± 2	82 ± 5	71 ± 4	73 ± 5

Data are presented as mean ± S.E.M. of 9 (control) or 5 (drug-treated) animals. Glucose utilisation is expressed in $\mu\text{mol}\cdot 100\text{g}^{-1}\cdot \text{min}^{-1}$. *P<0.05 for statistical comparison between drug-treated group and saline-treated controls.

APPENDIX I - TABLE 7
GLUCOSE UTILISATION FOLLOWING D-CPP-ENE ADMINISTRATION:
MYELINATED FIBRE TRACTS

STRUCTURE	CONTROL	D-CPP-ENE (mgkg ⁻¹)		
		0.3	3	30
Cerebellar White Matter	34 ± 1	34 ± 2	30 ± 2	32 ± 1
Internal Capsule	32 ± 2	32 ± 2	27 ± 2	27 ± 2
Fimbria Fornix	28 ± 3	24 ± 2	23 ± 2	25 ± 2
Corpus Callosum	38 ± 2	40 ± 3	33 ± 2	34 ± 3
Genu of Corpus Callosum	32 ± 1	34 ± 2	27 ± 3	28 ± 3

Data are presented as mean ± S.E.M. of 9 (control) or 5 (drug-treated) animals. Glucose utilisation is expressed in $\mu\text{mol}\cdot 100\text{g}^{-1}\cdot \text{min}^{-1}$.

APPENDIX II

THE CEREBRAL METABOLIC EFFECTS OF A NOVEL MUSCARINIC AGONIST, L-679-512, IN THE RAT

Glucose utilisation was measured in conscious, lightly restrained rats using deoxyglucose autoradiography, following intravenous administration of L-679-512 (3, 10 or 30 μgkg^{-1}) or saline. The data presented in Tables 2-7 represent mean glucose utilisation ($\mu\text{mol } 100\text{g}^{-1} \text{ min}^{-1}$) \pm SEM of 76 anatomically distinct regions of brain. Data in Table 1 represent physiological parameters following L-679-512 administration. * $p < 0.05$, ** $p < 0.01$ for statistical comparison of drug-treated groups with saline-treated controls (unpaired Student's t-test, two-tailed, with Bonferroni correction).

APPENDIX II - TABLE 1
PHYSIOLOGICAL PARAMETERS

PHYSIOLOGICAL PARAMETER	L-679-512 (μgkg^{-1})			
	CONTROL	3	10	30
Mean Arterial Blood Pressure (mmHg)	128 \pm 3	127 \pm 9	128 \pm 4	146 \pm 6
Δ Mean Arterial Blood Pressure (mmHg)	3.0 \pm 1.6	-2.6 \pm 4.4	-5.4 \pm 7.4	8.0 \pm 3.6
Arterial Plasma Glucose (mM)	8.3 \pm 0.3	8.6 \pm 0.6	10.1 \pm 0.7*	14.7 \pm 0.7**
Arterial pH	7.442 \pm 0.01	7.443 \pm 0.01	7.438 \pm 0.01	7.420 \pm 0.01
PaCO ₂ (mmHg)	42.4 \pm 0.34	38.5 \pm 1.4*	43.0 \pm 1.8	40.0 \pm 0.88**
PaO ₂ (mmHg)	84.8 \pm 2.3	87.5 \pm 1.5	87.3 \pm 2.5	86.3 \pm 1.4
Rectal Temperature ($^{\circ}\text{C}$)	36.9 \pm 0.14	37.4 \pm 0.31	36.4 \pm 0.49	36.1 \pm 0.37
Number of Animals	9	5	5	5

Values are presented as mean \pm SEM. Glucose values were measured at the time of administration of [¹⁴C]-2-deoxyglucose. Arterial blood gases and rectal temperature were measured 35 minutes post-deoxyglucose administration. Absolute values for mean arterial blood pressure are those measured 15 minutes after saline or drug administration, prior to [¹⁴C]-deoxyglucose administration. Δ Mean arterial blood pressure represents the change in blood pressure 15 minutes after drug or saline injection relative to the value prior to injection.

APPENDIX II - TABLE 2

GLUCOSE UTILISATION FOLLOWING L-679-512 ADMINISTRATION: HIPPOCAMPAL FORMATION

STRUCTURE	CONTROL	L-679-512 (μgkg^{-1})		
		3	10	30
<u>Ammon's Horn</u>				
CA1 Str. Oriens/ Pyramidale	51 ± 2	54 ± 5	44 ± 4	48 ± 3
CA1 Str. Radiatum	54 ± 2	58 ± 4	48 ± 3	52 ± 4
CA1 Str. Lacunosum Moleculare	72 ± 2	73 ± 4	63 ± 2*	64 ± 5
CA2 Str. Oriens/ Pyramidale	70 ± 3	70 ± 6	58 ± 2*	60 ± 4
CA2 Str. Radiatum	72 ± 3	73 ± 5	62 ± 2	64 ± 4
CA2/3 Str. Lacunosum Molecular	80 ± 3	82 ± 5	67 ± 1*	68 ± 4
CA3 Str. Oriens/ Pyramidale	69 ± 2	67 ± 5	60 ± 3	62 ± 3
CA3 Str. Radiatum	66 ± 2	71 ± 6	58 ± 3	62 ± 4
CA4 Str. Pyramidale	60 ± 2	66 ± 4	55 ± 2	60 ± 4
<u>Dentate Gyrus</u>				
Molecular Layer (Superior Blade)	61 ± 3	66 ± 4	57 ± 2	59 ± 5
Molecular Layer (Inferior Blade)	53 ± 2	59 ± 5	49 ± 2	56 ± 4
Polymorphic Layer	50 ± 2	55 ± 4	48 ± 3	49 ± 4
Pre Subiculum	83 ± 3	80 ± 2	85 ± 7	73 ± 2
Subiculum	71 ± 2	71 ± 3	70 ± 6	64 ± 2

Data are presented as mean ± S.E.M. of 9 (control) or 5 (drug-treated) animals. Glucose utilisation is expressed in $\mu\text{mol}\cdot 100\text{g}^{-1}\cdot \text{min}^{-1}$. * $p < 0.05$, for statistical comparison between drug-treated group and saline-treated controls.

APPENDIX II - TABLE 3:
GLUCOSE UTILISATION FOLLOWING L-679-512 ADMINISTRATION:
AREAS ASSOCIATED WITH LIMBIC FUNCTION

STRUCTURE	CONTROL	L-679-512 (μgkg^{-1})		
		3	10	30
Dorsal Tegmental Nucleus	99 ± 5	108 ± 7	98 ± 9	91 ± 2
Dorsal Raphe	76 ± 3	75 ± 4	75 ± 5	69 ± 2
Median Raphe	84 ± 3	86 ± 5	82 ± 4	73 ± 2
Mamillary Body (Medial)	100 ± 2	83 ± 7*	91 ± 4	83 ± 4*
Mamillary Body (Lateral)	96 ± 3	78 ± 5*	81 ± 4*	76 ± 5*
Habenular Nucleus (Medial)	73 ± 4	85 ± 8	74 ± 4	65 ± 2
Habenular Nucleus (Lateral)	108 ± 6	107 ± 4	108 ± 6	107 ± 4
Thalamus:-				
Mediodorsal	93 ± 6	104 ± 6	96 ± 4	89 ± 4
Laterodorsal	81 ± 3	89 ± 5	84 ± 6	76 ± 6
Anteromedial	101 ± 4	102 ± 2	104 ± 4	95 ± 8
Anteroventral	93 ± 4	102 ± 9	100 ± 4	105 ± 6
Hypothalamus	55 ± 3	57 ± 4	51 ± 3	50 ± 3
Amygdala:-				
Medial Nucleus	47 ± 3	47 ± 4	42 ± 2	40 ± 2
Lateral Nucleus	68 ± 3	68 ± 3	60 ± 2	56 ± 4
Basolateral Nucleus	74 ± 6	74 ± 4	70 ± 6	59 ± 3
Medial Septum	66 ± 3	64 ± 6	58 ± 3	56 ± 1
Lateral Septum	48 ± 2	49 ± 3	41 ± 2	44 ± 2
Vertical Diagonal Band	70 ± 4	71 ± 7	65 ± 4	63 ± 3
Horizontal Diagonal Band	86 ± 4	82 ± 5	74 ± 5	64 ± 5*
Medial Forebrain Bundle	89 ± 4	85 ± 6	78 ± 6	66 ± 4*
Nucleus Accumbens	64 ± 2	73 ± 4	66 ± 7	64 ± 1
Cortex:-				
Posterior Cingulate Cortex	89 ± 3	87 ± 6	89 ± 8	78 ± 2
Anterior Cingulate Cortex	105 ± 8	109 ± 7	96 ± 4	88 ± 3
Parietal Cortex	108 ± 4	102 ± 7	100 ± 6	89 ± 4*
Frontal Cortex	108 ± 4	107 ± 8	104 ± 4	91 ± 2

Data are presented as mean ± S.E.M. of 9 (control) or 5 (drug-treated) animals. Glucose utilisation is expressed in $\mu\text{mol}\cdot 100\text{g}^{-1}\cdot \text{min}^{-1}$. * $p < 0.05$ for statistical comparison between drug-treated group and saline-treated controls.

APPENDIX II - TABLE 4
GLUCOSE UTILISATION FOLLOWING L-679-512 ADMINISTRATION: OLFACTORY AREAS

STRUCTURE	CONTROL	L-679-512 (μgkg^{-1})		
		3	10	30
Lateral Olfactory Cortex	118 \pm 8	122 \pm 5	123 \pm 7	96 \pm 9
Lateral Olfactory Tract	107 \pm 5	107 \pm 7	105 \pm 4	82 \pm 5*
Anterior Olfactory Nucleus	73 \pm 5	85 \pm 12	72 \pm 6	67 \pm 8
Primary Olfactory Cortex	119 \pm 4	112 \pm 8	108 \pm 5	89 \pm 3*
Posterior Piriform Cortex	73 \pm 5	72 \pm 7	79 \pm 9	64 \pm 2
Entorhinal Cortex (Layers I-II)	70 \pm 3	72 \pm 4	63 \pm 6	56 \pm 1*

Data are presented as mean \pm S.E.M. of 9 (control) or 5 (drug-treated) animals. Glucose utilisation is expressed in $\mu\text{mol}\cdot 100\text{g}^{-1}\cdot\text{min}^{-1}$. * $p < 0.05$ for statistical comparison between drug-treated group and saline-treated controls.

APPENDIX II - TABLE 5
GLUCOSE UTILISATION FOLLOWING L-679-512 ADMINISTRATION:
AUDITORY AND VISUAL STRUCTURES

STRUCTURE	CONTROL	L-679-512 (μgkg^{-1})		
		3	10	30
<u>Auditory System</u>				
Auditory Cortex II	111 \pm 7	122 \pm 9	116 \pm 9	97 \pm 3
Auditory Cortex IV	133 \pm 9	131 \pm 9	132 \pm 9	107 \pm 4
Medial Geniculate Body	113 \pm 4	106 \pm 5	103 \pm 6	87 \pm 5*
Inferior Colliculus	161 \pm 8	158 \pm 12	151 \pm 15	134 \pm 2
Lateral Lemniscus	89 \pm 4	88 \pm 6	84 \pm 8	80 \pm 2
Cochlear Nucleus	127 \pm 6	130 \pm 11	134 \pm 9	112 \pm 8
Superior Olivary Nucleus	118 \pm 6	130 \pm 8	116 \pm 10	100 \pm 4
<u>Visual System</u>				
Auditory Cortex IV	102 \pm 6	102 \pm 7	99 \pm 7	74 \pm 6*
Dorsolateral Geniculate Body	99 \pm 5	108 \pm 7	98 \pm 9	91 \pm 2
Ventrolateral Geniculate Body	69 \pm 3	71 \pm 3	70 \pm 3	69 \pm 4
Anterior Pretectal Nucleus	87 \pm 2	93 \pm 4	95 \pm 6	87 \pm 5
Lateral Post-Thalamic Nucleus	89 \pm 3	94 \pm 5	90 \pm 5	80 \pm 4
Superior Colliculus (Super)	74 \pm 3	76 \pm 3	85 \pm 7	68 \pm 3
Superior Colliculus (Deep)	74 \pm 2	74 \pm 4	82 \pm 5	70 \pm 2

Data are presented as mean \pm S.E.M. of 9 (control) or 5 (drug-treated) animals. Glucose utilisation is expressed in $\mu\text{mol}\cdot 100\text{g}^{-1}\cdot \text{min}^{-1}$. * $P < 0.05$ for statistical comparison between drug-treated group and saline-treated controls.

APPENDIX II - TABLE 6
GLUCOSE UTILISATION FOLLOWING L-679-512 ADMINISTRATION:
EXTRAPYRAMIDAL AND SENSORIMOTOR AREAS

STRUCTURE	CONTROL	L-679-512 (μgkg^{-1})		
		3	10	30
Cerebellar Nucleus	89 ± 3	94 ± 4	91 ± 5	83 ± 2
Cerebellar Hemisphere	56 ± 1	58 ± 2	64 ± 6	60 ± 3
Vestibular Nucleus	110 ± 3	109 ± 3	117 ± 6	106 ± 4
Inferior Olive	74 ± 4	71 ± 6	66 ± 4	60 ± 3
Pontine Grey	50 ± 2	53 ± 3	52 ± 4	53 ± 2
Red Nucleus	65 ± 3	68 ± 2	69 ± 2	69 ± 4
Sustantia Nigra: Pars Compacta	58 ± 3	65 ± 10	58 ± 4	49 ± 2
Pars Reticulata	52 ± 2	62 ± 8	52 ± 4	50 ± 2
Caudate Nucleus	102 ± 4	93 ± 4	89 ± 4	80 ± 3*
Globus Pallidus	56 ± 6	59 ± 7	49 ± 3	48 ± 3
Thalamus (Ventrolateral Nucleus)	78 ± 3	85 ± 5	77 ± 5	75 ± 2
Subthalamic Nucleus	84 ± 2	86 ± 3	88 ± 4	84 ± 2

Data are presented as mean ± S.E.M. of 9 (control) or 5 (drug-treated) animals. Glucose utilisation is expressed in $\mu\text{mol}\cdot 100\text{g}^{-1}\cdot \text{min}^{-1}$. * $p < 0.05$ for statistical comparison between drug-treated group and saline-treated controls.

APPENDIX II - TABLE 7
GLUCOSE UTILISATION FOLLOWING L-679-512 ADMINISTRATION:
MYELINATED FIBRE TRACTS

STRUCTURE	CONTROL	L-679-512 (μgkg^{-1})		
		3	10	30
Cerebellar White Matter	34 \pm 1	36 \pm 2	35 \pm 3	36 \pm 1
Internal Capsule	32 \pm 2	37 \pm 3	31 \pm 2	31 \pm 1
Fimbria Fornix	28 \pm 3	30 \pm 4	24 \pm 2	28 \pm 1
Corpus Callosum	38 \pm 2	40 \pm 4	36 \pm 2	35 \pm 2
Genu of Corpus Callosum	30 \pm 1	31 \pm 3	29 \pm 2	29 \pm 1

Data are presented as mean \pm S.E.M. of 9 (control) or 5 (drug-treated) animals. Glucose utilisation is expressed in $\mu\text{mol}\cdot 100\text{g}^{-1}\text{min}^{-1}$. Glucose utilisation is expressed in $\mu\text{mol}\cdot 100\text{g}^{-1}\text{min}^{-1}$.

APPENDIX III

THE CEREBRAL METABOLIC EFFECTS OF 9-AMINO-1,2,3,4-TETRA-HYDROACRIDINE (THA), A COMPOUND OF POTENTIALLY MIXED CHOLINERGIC AND GLUTAMATERGIC ACTION

Glucose utilisation was measured in conscious, lightly restrained rats using deoxyglucose autoradiography, following intravenous administration of THA (2.5mg kg^{-1}) or saline. The data presented in Tables 2-7 represent mean glucose utilisation ($\mu\text{mol } 100\text{g}^{-1} \text{min}^{-1}$) \pm SEM of 76 anatomically distinct regions of brain. Data in Table 1 represent physiological parameters measured in response to drug or saline administration. * $p < 0.05$, ** $p < 0.01$ for statistical comparison of drug-treated groups with saline-treated controls (unpaired Student's t-test, two-tailed).

APPENDIX III - TABLE 1
PHYSIOLOGICAL PARAMETERS

PHYSIOLOGICAL PARAMETERS	CONTROL	THA (2.5mgkg ⁻¹)
Mean Arterial Blood Pressure (mmHg)	120 ± 2	129 ± 5
ΔMean Arterial Blood Pressure (mmHg)	1.2 ± 2.4†	11.4 ± 1.5**
Arterial Plasma Glucose (mM)	8.0 ± 4.7	12.3 ± 0.61**
Arterial pH	7.331 ± 0.01	7.303 ± 0.02
PaCO ₂ (mmHg)	40.7 ± 0.49	42.0 ± 1.9
PaO ₂ (mmHg)	91.2 ± 2.3	90.8 ± 3.4
Rectal Temperature (°C)	36.7 ± 0.2	36.0 ± 0.3
Number of Animals	6	5

Values are presented as mean ± SEM. Plasma glucose concentration was estimated at the time of administration of [¹⁴C]-2-deoxyglucose. Arterial blood gases and rectal temperatures were measured 35 minutes post-deoxyglucose administration. Absolute values for mean arterial blood pressure represent those measured 15 minutes after injection of THA or saline, prior to injection of [¹⁴C]-deoxyglucose. ΔMean arterial blood pressure represents the change in blood pressure 15 minutes after THA or saline administration, relative to the value prior to injection.

mean of 5 animals: no data was available for the 6th animal.

*P<0.01 for statistical comparison between drug-treated group and saline-treated animals.

APPENDIX III - TABLE 2
GLUCOSE UTILISATION FOLLOWING THA ADMINISTRATION:
HIPPOCAMPAL FORMATION

STRUCTURE	CONTROL	THA (2.5mgkg ⁻¹)
<u>Ammon's Horn</u>		
CA1 Str. Oriens/Pyramidale	45 ± 3	51 ± 4
CA1 Str. Radiatum	50 ± 4	54 ± 3
CA1 Str. Lacunosum Moleculare	68 ± 5	71 ± 3
CA2 Str. Oriens/Pyramidale	62 ± 5	61 ± 3
CA2 Str. Radiatum	65 ± 5	64 ± 2
CA2/3 Str. Lacunosum Molecular	72 ± 8	70 ± 4
CA3 Str. Oriens/Pyramidale	58 ± 4	60 ± 2
CA3 Str. Radiatum	59 ± 4	60 ± 2
CA4 Str. Pyramidale	57 ± 4	61 ± 5
<u>Dentate Gyrus</u>		
Molecular Layer/(Superior Blade)	53 ± 7	56 ± 4
Molecular Layer/(Inferior Blade)	54 ± 3	62 ± 3
Polymorphic Layer	46 ± 3	51 ± 2
Pre Subiculum	83 ± 3	87 ± 8
Subiculum	69 ± 3	81 ± 3*

Data are presented as mean ± S.E.M. of 6 (control) or 5 (drug-treated) animals. Glucose utilisation is expressed in $\mu\text{mol} \cdot 100\text{g}^{-1} \cdot \text{min}^{-1}$.
 *P<0.05, for statistical comparison between drug-treated group and saline-treated controls.

APPENDIX III - TABLE 3
GLUCOSE UTILISATION FOLLOWING THA ADMINISTRATION:
AREAS ASSOCIATED WITH LIMBIC FUNCTION

STRUCTURE	CONTROL	THA (2.5mgkg ⁻¹)
Dorsal Tegmental Nucleus	86 ± 5	84 ± 5
Dorsal Raphé	78 ± 3	66 ± 5*
Median Raphé	83 ± 3	76 ± 5
Mamillary Body (Medial)	97 ± 4	102 ± 7
Mamillary Body (Lateral)	91 ± 4	100 ± 4
Habenular Nucleus (Medial)	62 ± 2	69 ± 3
Habenular Nucleus (Lateral)	101 ± 3	104 ± 4
Thalamus:-		
Mediodorsal	99 ± 6	103 ± 6
Laterodorsal	79 ± 5	88 ± 3
Anteromedial	97 ± 6	101 ± 5
Anteroventral	108 ± 5	135 ± 10*
Hypothalamus	51 ± 3	52 ± 3
Amygdala:-		
Medial Nucleus	43 ± 2	46 ± 2
Lateral Nucleus	62 ± 3	61 ± 3
Basolateral Nucleus	54 ± 3	57 ± 3
Medial Septum	61 ± 4	63 ± 4
Lateral Septum	42 ± 3	43 ± 2
Vertical Diagonal Band	65 ± 3	63 ± 2
Horizontal Diagonal Band	62 ± 9	62 ± 8
Medial Forebrain Bundle	75 ± 10	78 ± 11
Nucleus Accumbens	61 ± 5	58 ± 4
Cortex:-		
Posterior Cingulate Cortex	92 ± 3	92 ± 4
Anterior Cingulate Cortex	104 ± 6	98 ± 5
Parietal Cortex	109 ± 5	111 ± 6
Frontal Cortex	99 ± 2	109 ± 7

Data are presented as mean ± S.E.M. of 6 (control) or 5 (drug-treated) animals. Glucose utilisation is expressed in $\mu\text{mol} \cdot 100\text{g}^{-1} \cdot \text{min}^{-1}$.

*P<0.05 for statistical comparison between drug-treated group and saline-treated controls.

APPENDIX III - TABLE 4
GLUCOSE UTILISATION FOLLOWING THA ADMINISTRATION:
OLFACTORY AREAS

STRUCTURE	CONTROL	THA (2.5mgkg ⁻¹)
Lateral Olfactory Cortex †	116 ± 7	127 ± 9
Lateral Olfactory Tract †	115 ± 7	100 ± 6
Anterior Olfactory Nucleus †	72 ± 7	79 ± 4
Primary Olfactory Cortex	96 ± 5	99 ± 3
Post Piriform Cortex	84 ± 7	82 ± 6
Entorhinal Cortex	61 ± 2	61 ± 4

Data are presented as mean ± S.E.M. of 6 (control) or 5 (drug-treated) animals. Glucose utilisation is expressed in $\mu\text{mol} \cdot 100^{-1} \text{min}^{-1}$.

† Data comprised of comparisons between 3 control and 3 drug-treated animals; no tissue available for autoradiographic measurement within other animals.

APPENDIX III - TABLE 5
GLUCOSE UTILISATION FOLLOWING THA ADMINISTRATION:
AUDITORY AND VISUAL STRUCTURES

STRUCTURE	CONTROL	THA (2.5mgkg ⁻¹)
<u>Auditory System</u>		
Auditory Cortex II	109 ± 6	110 ± 7
Auditory Cortex IV	122 ± 8	126 ± 8
Medial Geniculate Body	95 ± 5	98 ± 7
Inferior Colliculus	149 ± 8	146 ± 7
Lateral Lemniscus	85 ± 4	84 ± 4
Cochlear Nucleus	103 ± 11	110 ± 5
Superior Olivary Nucleus	111 ± 5	105 ± 7
<u>Visual System</u>		
Visual Cortex IV	95 ± 2	94 ± 7
Dorsolateral Geniculate Body	74 ± 3	95 ± 2**
Ventrolateral Geniculate Body	63 ± 4	79 ± 4*
Anterior Pretectal Nucleus	88 ± 5	102 ± 4
Lateral Postthalamic Nucleus	83 ± 4	92 ± 5
Superior Colliculus (Superficial)	75 ± 2	105 ± 4**
Superior Colliculus (Deep)	72 ± 2	79 ± 5

Data are presented as mean ± S.E.M. of 6 (control) or 5 (drug-treated) animals. Glucose utilisation is expressed in $\mu\text{mol}\cdot 100\text{g}^{-1}\text{min}^{-1}$.
 *P<0.05, **P<0.01 statistical comparison between drug-treated group and saline-treated controls.

APPENDIX III - TABLE 6
GLUCOSE UTILISATION FOLLOWING THA ADMINISTRATION:
EXTRAPYRAMIDAL AND SENSORIMOTOR AREAS

STRUCTURE	CONTROL	THA (2.5mgkg ⁻¹)
Cerebellar Nucleus	81 ± 5	86 ± 5
Cerebellar Hemisphere	49 ± 1	56 ± 2*
Vestibular Nucleus	92 ± 2	106 ± 7
Inferior Olive	65 ± 2	67 ± 4
Pontine Grey	51 ± 2	49 ± 4
Red Nucleus	58 ± 3	63 ± 4
Substantia Nigra:		
Pars Compacta	57 ± 4	66 ± 5
Pars Reticulata	46 ± 2	44 ± 5
Caudate Nucleus	91 ± 4	86 ± 4
Globus Pallidus	47 ± 2	49 ± 3
Thalamus (Ventrolateral Nucleus)	79 ± 5	91 ± 4
Subthalamic Nucleus	70 ± 4	74 ± 2

Data are presented as mean ± S.E.M. of 6 (control) or 5 (drug-treated) animals. Glucose utilisation is expressed in $\mu\text{mol}\cdot 100\text{g}^{-1}\cdot \text{min}^{-1}$. *P<0.05 for statistical comparison between drug-treated group and saline-treated controls.

APPENDIX III - TABLE 7
GLUCOSE UTILISATION FOLLOWING THA ADMINISTRATION:
MYELINATED FIBRE TRACTS

STRUCTURE	CONTROL	THA (2.5mgkg ⁻¹)
Cerebellar White Matter	26 ± 2	32 ± 2
Internal Capsule	28 ± 1	34 ± 3
Fimbria Fornix	20 ± 2	26 ± 2
Corpus Callosum	32 ± 2	36 ± 2
Genu of Corpus Callosum	25 ± 1	30 ± 1*

Data are presented as mean ± S.E.M. of 6 (control) or 5 (drug-treated) animals. Glucose utilisation is expressed in $\mu\text{mol}\cdot 100\text{g}^{-1}\cdot \text{min}^{-1}$.
 * $p < 0.05$ for statistical comparison between drug-treated group and saline-treated controls.

APPENDIX IV

LOCAL CEREBRAL GLUCOSE UTILISATION IN RESPONSE TO LESIONS OF THE MEDIAL SEPTUM

Glucose utilisation was measured in conscious, lightly restrained rats using deoxyglucose autoradiography, three weeks after lesions of the medial septum or sham operation. The data presented in Tables 2 - 4 represent mean glucose utilisation ($\mu\text{mol } 100^{-1} \text{min}^{-1}$) \pm S.E.M. of 57 anatomically defined regions of brain. Data in Table 1 represent physiological parameters following lesion or sham operation. Statistical comparisons were made using unpaired Student's t-test, (two-tailed).

APPENDIX IV - TABLE 1
PHYSIOLOGICAL PARAMETERS FOLLOWING MEDIAL SEPTAL LESIONS

PHYSIOLOGICAL PARAMETER	SHAM (n=7)	LESION (n=6)
Body Weight (g)	370 ± 8	381 ± 11
Mean Arterial Blood Pressure (mmHg)	136 ± 1	129 ± 3
Arterial Plasma Glucose (mM)	7.5 ± 0.4	7.9 ± 0.4
Arterial pH	7.44 ± 0.01	7.46 ± 0.01
PaCO ₂ (mmHg)	41.4 ± 1	40.1 ± 1
PaO ₂ (mmHg)	83.9 ± 2	85.1 ± 4
Rectal Temperature (°C)	36.7 ± 0.3	37.0 ± 0.3

an arterial blood pressure was measured immediately prior to administration of [¹⁴C]-deoxyglucose. Arterial plasma glucose values are those measured 1 minute post-injection of [¹⁴C]-deoxyglucose. Rectal temperature and blood gases were measured 35 minutes after deoxyglucose administration.

APPENDIX IV - TABLE 2
LOCAL CEREBRAL GLUCOSE UTILISATION FOLLOWING MEDIAL SEPTAL LESIONS:
HIPPOCAMPAL FORMATION

STRUCTURE	LCGU ($\mu\text{mol}/100\text{g}/\text{min}$)	
	SHAM (N=7)	LESION (N=6)
<u>Ammon's Horn</u>		
CA1 Str. Oriens	47 \pm 3	50 \pm 3
Str. Pyramidale	51 \pm 3	53 \pm 3
Str. Radiatum	59 \pm 7	54 \pm 2
Str. Lacunosum Moleculare	66 \pm 4	70 \pm 3
CA2 Str. Oriens	64 \pm 3	67 \pm 4
Str. Pyramidale	74 \pm 4	78 \pm 5
Str. Radiatum	68 \pm 4	72 \pm 4
Str. Lacunosum Moleculare	77 \pm 5	83 \pm 5
CA3 Str. Oriens	62 \pm 4	63 \pm 4
Str. Pyramidale	68 \pm 5	72 \pm 5
Str. Radiatum/Lacunosum Mol.	66 \pm 5	71 \pm 5
CA4 Str. Pyramidale	56 \pm 4	64 \pm 5
<u>Dentate Gyrus</u>		
Superior Blade:		
Molecular Layer (outer)	64 \pm 3	64 \pm 3
Molecular Layer (inner)	57 \pm 3	57 \pm 3
Granular Layer	53 \pm 3	53 \pm 3
Infragranular Layer	52 \pm 3	55 \pm 3
Inferior Blade:		
Molecular Layer (outer)	47 \pm 2	46 \pm 2
Molecular Layer (inner)	47 \pm 2	48 \pm 2
Granular Layer	46 \pm 2	47 \pm 3
Subiculum	86 \pm 4	84 \pm 6
Presubiculum	100 \pm 6	97 \pm 5
<u>Entorhinal Cortex :</u>		
Lateral, Layers I-II	77 \pm 5	71 \pm 3
Lateral, Layers III-VI	86 \pm 7	84 \pm 4
Medial, Layers I-II	81 \pm 5	74 \pm 4
Medial, Layers III-VI	84 \pm 7	83 \pm 5

Data are presented as mean \pm S.E.M. of 7 (control) or 6 (lesioned) animals. Glucose utilisation is expressed in $\mu\text{mol } 100\text{g}^{-1}\text{min}^{-1}$.

APPENDIX IV - TABLE 3
LOCAL CEREBRAL GLUCOSE UTILISATION FOLLOWING MEDIAL SEPTAL LESIONS:
AREAS ASSOCIATED WITH LIMBIC FUNCTION

STRUCTURE	LCGU ($\mu\text{mol}/100\text{g}/\text{min}$)	
	SHAM (N=7)	LESION (N=6)
Dorsal Raphé	100 \pm 4	100 \pm 6
Median Raphé	99 \pm 6	108 \pm 6
Mamillary Body	111 \pm 6	113 \pm 8
Thalamus:-		
Anterodorsal Nucleus	80 \pm 6	89 \pm 4
Anteroventral Nucleus	121 \pm 10	134 \pm 3
Laterodorsal Nucleus	95 \pm 7	96 \pm 8
Habenular Nucleus (Medial)	83 \pm 6	78 \pm 3
Habenular Nucleus (Lateral)	130 \pm 12	132 \pm 5
Amygdala (Basolateral Nucleus)	87 \pm 7	83 \pm 4
Hypothalamus	55 \pm 5	53 \pm 3
Medial Septum	71 \pm 4	67 \pm 3
Lateral Septum	52 \pm 4	53 \pm 1
Diagonal Band, Vertical Limb	79 \pm 5	76 \pm 4
Diagonal Band, Horizontal Limb	98 \pm 10	96 \pm 8
Nucleus Accumbens	65 \pm 5	65 \pm 3
Cortex (Layer IV):		
Posterior Cingulate Cortex	107 \pm 8	101 \pm 6
Anterior Cingulate Cortex	111 \pm 6	111 \pm 6
Parietal Cortex	114 \pm 12	119 \pm 6
Frontal Cortex	125 \pm 9	125 \pm 4
Primary Olfactory Cortex	131 \pm 7	127 \pm 6

Data are presented as mean \pm S.E.M. of 7 (control) or 6 (lesioned) animals. Glucose utilisation is expressed in $\mu\text{mol}\cdot 100\text{g}^{-1}\cdot \text{min}^{-1}$.

APPENDIX IV - TABLE 4
LOCAL CEREBRAL GLUCOSE UTILISATION FOLLOWING MEDIAL SEPTAL LESIONS:
OTHER AREAS

STRUCTURE	LCGU ($\mu\text{mol}/100\text{g}/\text{min}$)	
	SHAM (N=7)	LESION (N=6)
Auditory and Visual Regions:-		
Auditory Cortex, Layer IV	156 \pm 11	140 \pm 5
Medial Geniculate Body	115 \pm 9	117 \pm 6
Inferior Colliculus	162 \pm 15	159 \pm 8
Visual Cortex, Layer IV	114 \pm 9	111 \pm 6
Dorsolateral Geniculate Body	86 \pm 6	92 \pm 3
Superior Colliculus (Superficial)	83 \pm 5	82 \pm 5
Superior Colliculus (Deep)	86 \pm 6	82 \pm 5
Extrapyramidal & Sensorimotor Areas:		
Cerebellar Hemisphere	51 \pm 4	51 \pm 3
Vestibular Nucleus	118 \pm 6	117 \pm 7
Caudate Nucleus	108 \pm 7	105 \pm 5
Myelinated Fibre Tracts:		
Cerebellar White	30 \pm 2	33 \pm 2
Fimbria Fornix	26 \pm 3	29 \pm 1

Data are presented as mean \pm S.E.M. of 7 (control) or 6 (lesioned) animals. Glucose utilisation is expressed in $\mu\text{mol}\cdot 100\text{g}^{-1}\cdot \text{min}^{-1}$.

APPENDIX V

QUANTITATIVE LIGAND BINDING TO GLUTAMATERGIC AND MUSCARINIC RECEPTORS IN HIPPOCAMPAL AND ASSOCIATED STRUCTURES FOLLOWING MEDIAL SEPTAL LESIONS

[³H]-QNB, [³H]-AMPA, [³H]-kainate and NMDA-sensitive [³H]-glutamate binding were measured at single ligand concentrations in hippocampal and septal regions in sham-operated rats and rats with lesions of the medial septum. Data are presented as mean ligand bound (pmol/g tissue) ± S.E.M. *P<0.05, **P<0.01 for statistical comparisons (unpaired Student's t-test, two-tailed).

APPENDIX V - TABLE 1
[³H]-QNB BINDING IN HIPPOCAMPAL AND
ASSOCIATED STRUCTURES FOLLOWING MEDIAL SEPTAL LESIONS

STRUCTURE	[³ H]-QNB BINDING	
	SHAM (N=7)	LESION (N=7)
1. <u>Ammon's Horn</u>		
CA1 Str. Oriens	293 ± 15	302 ± 17
Str. Pyramidale	362 ± 17	354 ± 22
Str. Radiatum	360 ± 17	354 ± 20
Str. Lacunosum Moleculare	280 ± 17	274 ± 11
CA2 Str. Oriens	203 ± 12	209 ± 10
Str. Pyramidale	259 ± 26	249 ± 7
Str. Radiatum	243 ± 16	231 ± 7
Str. Lacunosum Moleculare	231 ± 15	218 ± 3
CA3 Str. Oriens	208 ± 8	204 ± 14
Str. Pyramidale	237 ± 10	229 ± 7
Str. Radiatum/ Lacunosum Mol.	236 ± 10	223 ± 4
CA4 Str. Pyramidale	282 ± 18	281 ± 9
2. <u>Dentate Gyrus</u>		
Superior Blade:		
Molecular Layer (outer)	298 ± 16	293 ± 11
Molecular Layer (inner)	312 ± 13	305 ± 12
Granular Layer	272 ± 14	260 ± 4
Infragranular Layer	253 ± 17	261 ± 7
Inferior Blade:		
Molecular Layer (outer)	324 ± 16	308 ± 13
Molecular Layer (inner)	346 ± 17	346 ± 24
Granular Layer	274 ± 17	286 ± 17
3. <u>Subicular Complex:</u>		
Subiculum	271 ± 13	233 ± 12*
Presubiculum	181 ± 8	184 ± 7
4. <u>Entorhinal Cortex:</u>		
Medial Portion, Layers I-II	279 ± 15	255 ± 12
Layers III-VI	286 ± 18	283 ± 9
Lateral Portion, Layers I-II	267 ± 9	274 ± 10
Layers III-VI	263 ± 11	253 ± 9
5. <u>Septal Nuclei:</u>		
Medial Septum	170 ± 7	115 ± 13**
Lateral Septum	202 ± 5	176 ± 5**
Diagonal Band (Vertical Line)	158 ± 8	163 ± 8

Data are presented as [³H]-QNB binding, pmol g⁻¹ tissue in 7 sham or 7 lesioned animals. *P<0.05, **P<0.01 for statistical comparison between sham and lesioned animals.

APPENDIX V - TABLE 2
[³H]-AMPA BINDING IN HIPPOCAMPAL AND ASSOCIATED STRUCTURES
FOLLOWING MEDIAL SEPTAL LESIONS

STRUCTURE	[³ H]-AMPA BINDING	
	SHAM (N=7)	LESION (N=7)
1. <u>Ammon's Horn</u>		
CA1 Str. Oriens	379 ± 11	345 ± 12
Str. Pyramidale	442 ± 14	394 ± 10*
Str. Radiatum	501 ± 14	458 ± 11*
Str. Lacunosum Moleculare	448 ± 16	403 ± 16
CA2 Str. Oriens	297 ± 10	252 ± 14*
Str. Pyramidale	341 ± 10	280 ± 10**
Str. Radiatum	380 ± 15	335 ± 15
Str. Lacunosum Moleculare	413 ± 11	354 ± 22*
CA3 Str. Oriens	272 ± 16	231 ± 18
Str. Pyramidale	311 ± 3	272 ± 12*
Str. Radiatum/ Lacunosum Mol.	340 ± 6	306 ± 18
CA4 Str. Pyramidale	346 ± 11	312 ± 11
2. <u>Dentate Gyrus</u>		
Superior Blade:		
Molecular Layer (outer)	437 ± 14	409 ± 14
Molecular Layer (inner)	393 ± 20	362 ± 13
Granular Layer	330 ± 16	289 ± 13
Infragranular Layer	334 ± 10	309 ± 13
Inferior Blade:		
Molecular Layer (outer)	433 ± 23	374 ± 21
Molecular Layer (inner)	425 ± 17	379 ± 19
Granular Layer	329 ± 8	295 ± 17
3. <u>Subicular Complex:</u>		
Subiculum	368 ± 20	301 ± 35
Presubiculum	187 ± 22	158 ± 23
4. <u>Entorhinal Cortex:</u>		
Medial Portion, Layers I-II	237 ± 21	213 ± 16
Layers III-VI	272 ± 19	215 ± 16*
Lateral Portion, Layers I-II	270 ± 13	208 ± 16**
Layers III-VI	267 ± 10	238 ± 19
5. <u>Septal Nuclei:</u>		
Medial Septum	103 ± 20	53 ± 9*
Lateral Septum	341 ± 27	277 ± 22
Diagonal Band (Vertical Line)	97 ± 7	84 ± 10

Data are presented as [³H]-AMPA binding, pmol g⁻¹ tissue in 7 sham or 7 lesioned animals. *P<0.05 **P<0.01 for statistical comparison between shams and lesioned animals.

APPENDIX V - TABLE 3
[³H]-KAINATE BINDING IN HIPPOCAMPAL AND ASSOCIATED STRUCTURES
FOLLOWING MEDIAL SEPTAL LESIONS

STRUCTURE	[³ H]-KAINATE BINDING	
	SHAM (N=6)	LESION (N=7)
1. <u>Ammon's Horn</u>		
CA1 Str. Oriens	36 ± 4	37 ± 2
Str. Pyramidale	34 ± 4	35 ± 2
Str. Radiatum	40 ± 4	43 ± 1
Str. Lacunosum Moleculare	42 ± 5	49 ± 1
CA2 Str. Oriens	37 ± 4	41 ± 1
Str. Pyramidale	61 ± 7	63 ± 6
Str. Radiatum	47 ± 4	51 ± 5
Str. Lacunosum Moleculare	38 ± 3	44 ± 2
CA3 Str. Oriens	34 ± 2	35 ± 2
Str. Pyramidale	73 ± 5	83 ± 4
Str. Radiatum/ Lacunosum Mol.	47 ± 3	49 ± 2
CA4 Str. Pyramidale	100 ± 8	114 ± 4
Str. Lucidum	187 ± 6	187 ± 6
2. <u>Dentate Gyrus</u>		
Superior Blade:		
Molecular Layer (outer)	49 ± 4	55 ± 1
Molecular Layer (inner)	63 ± 5	72 ± 1
Granular Layer	51 ± 4	58 ± 2
Infragranular Layer	65 ± 4	72 ± 1
Inferior Blade:		
Molecular Layer (outer)	52 ± 4	58 ± 2
Molecular Layer (inner)	70 ± 5	79 ± 2
Granular Layer	57 ± 3	62 ± 2
3. <u>Subicular Complex:</u>		
Subiculum	62 ± 6	66 ± 5
Presubiculum	74 ± 6	84 ± 6
4. <u>Entorhinal Cortex:</u>		
Medial Portion, Layers I-II	86 ± 4	87 ± 7
Layers III-VI	62 ± 6	65 ± 8
Lateral Portion, Layers I-II	94 ± 8	98 ± 9
Layers III-VI	45 ± 7	46 ± 5
5. <u>Septal Nuclei:</u>		
Medial Septum	39 ± 2	37 ± 2
Lateral Septum	53 ± 4	60 ± 4
Diagonal Band (Vertical Line)	44 ± 4	49 ± 3

Data are presented as [³H]-kainate binding, pmol g⁻¹ tissue in 6 sham or 7 lesioned animals.

APPENDIX V - TABLE 4
NMDA-DISPLACEABLE [³H]-GLUTAMATE BINDING IN HIPPOCAMPAL AND
ASSOCIATED STRUCTURES FOLLOWING MEDIAL SEPTAL LESIONS

STRUCTURE	<u>[³H]-NMDA DISPLACEABLE GLUTAMATE BINDING</u>	
	SHAM (N=6)	LESION (N=6)
1. <u>Ammon's Horn</u>		
CA1 Str. Oriens	56 ± 10	66 ± 12
Str. Pyramidale	54 ± 12	63 ± 11
Str. Radiatum	67 ± 10	78 ± 14
Str. Lacunosum Moleculare	45 ± 9	48 ± 4
CA2 Str. Oriens	35 ± 9	30 ± 4
Str. Pyramidale	32 ± 8	32 ± 9
Str. Radiatum	38 ± 8	40 ± 7
Str. Lacunosum Moleculare	41 ± 8	35 ± 7
CA3 Str. Oriens	29 ± 7	30 ± 6
Str. Pyramidale	22 ± 5	17 ± 4
Str. Radiatum/ Lacunosum Mol.	31 ± 6	32 ± 7
CA4 Str. Pyramidale	32 ± 8	32 ± 5
2. <u>Dentate Gyrus</u>		
Superior Blade:		
Molecular Layer (outer)	51 ± 9	54 ± 7
Molecular Layer (inner)	53 ± 8	56 ± 8
Granular Layer	40 ± 8	41 ± 9
Infragranular Layer	26 ± 8	25 ± 6
Inferior Blade:		
Molecular Layer (outer)	49 ± 7	48 ± 6
Molecular Layer (inner)	51 ± 8	56 ± 8
Granular Layer	38 ± 8	39 ± 7
3. <u>Subicular Complex:</u>		
Subiculum	40 ± 7	54 ± 11
Presubiculum	19 ± 3	32 ± 6
4. <u>Entorhinal Cortex:</u>		
Medial Portion, Layers I-II	62 ± 7	76 ± 19
Layers III-VI	57 ± 3	70 ± 18
Lateral Portion, Layers I-II	74 ± 9	84 ± 11
Layers III-VI	53 ± 6	69 ± 17
5. <u>Septal Nuclei:</u>		
Medial Septum	13 ± 2(a)	10 ± 3
Lateral Septum	22 ± 6	30 ± 6
Diagonal Band (Vertical Line)	13 ± 2(b)	25 ± 5

Data are presented as [³H]-L-glutamate binding, pmol g⁻¹ tissue in 6 sham or 6 lesioned animals. (a) n=5 (b) n=4.

APPENDIX VI

LOCAL CEREBRAL GLUCOSE UTILISATION IN RESPONSE TO ACUTE SUBDURAL HAEMATOMA

Glucose utilisation was measured in conscious, lightly restrained rats two hours following acute subdural haematoma, acute subdural haematoma with D-CPP-ene pre-treatment or sham operation. The data in Tables 2-7 represent mean glucose utilisation ($\mu\text{mol } 100\text{g}^{-1}\text{min}^{-1}$) \pm S.E.M. of 41 anatomically defined regions of the brain. Data presented in Table 1 represents physiological parameters in response to experimental procedures. Statistical comparison was made using unpaired Student's t-test, two-tailed, with Bonferroni correction. * $P < 0.05$, ** $P < 0.01$ for statistical comparison between sham operation and acute subdural haematoma; † $P < 0.05$, †† $P < 0.01$ for statistical comparison between acute subdural haematoma and D-CPP-ene pre-treatment.

APPENDIX VI - TABLE 1
PHYSIOLOGICAL PARAMETERS FOLLOWING ACUTE SUBDURAL HAEMATOMA IN THE RAT

PHYSIOLOGICAL PARAMETER	SHAM (n=5)	ASDH (n=5)	+ D-CPP-ene 15mg kg ⁻¹ (n=5)
Body Weight (g)	440 ± 43	398 ± 22	449 ± 9
Mean Arterial Blood Pressure (mmHg)	114 ± 6	131 ± 16	121 ± 11
Arterial Plasma Glucose (mM)	7.7 ± 0.5	8.6 ± 0.7	7.6 ± 0.7
Arterial pH	7.43 ± 0.03	7.43 ± 0.01	7.38 ± 0.02
PaCO ₂ (mmHg)	43 ± 4	41 ± 3	47 ± 2
PaO ₂ (mmHg)	96 ± 9	109 ± 6	84 ± 10
Rectal Temperature (°C)	36.1 ± 0.3	34.9 ± 0.8	36.0 ± 0.5

Mean arterial blood pressure was measured prior to administration of [¹⁴C]-2-deoxyglucose. Arterial plasma glucose values are those measured 1 minute post-injection of [¹⁴C]-deoxyglucose. Rectal temperature and blood gases were measured 35 minutes after deoxyglucose administration.

D-CPP-ene (15mg kg⁻¹) was administered 15 minutes prior to induction of ASDH.

APPENDIX VI - TABLE 2

LOCAL CEREBRAL GLUCOSE UTILISATION FOLLOWING ACUTE SUBDURAL HAEMATOMA:
HIPPOCAMPAL AREA

STRUCTURE	LCGU ($\mu\text{mol} \cdot 100\text{g}^{-1} \text{min}^{-1}$)					
	SHAM		ASDH		ASDH + D-CPP-ENE	
	IPSI.	CONTRA.	IPSI.	CONTRA.	IPSI.	CONTRA.
<u>Ammon's Horn:</u>						
CA1 Str. Oriens/ Pyramidale	42 ± 2	42 ± 3	88 ± 11*	74 ± 15	54 ± 7	47 ± 2
CA1 Str. Radiatum	43 ± 3	43 ± 3	104 ± 11 **	88 ± 15	61 ± 10 †	49 ± 3
CA1 Str. Lacunosum Moleculare	62 ± 4	63 ± 3	116 ± 10 **	111 ± 14*	102 ± 14	88 ± 3
CA2 Str. Oriens/ Pyramidale	61 ± 3	60 ± 3	111 ± 16*	80 ± 12	81 ± 3	71 ± 4
CA2 Str. Radiatum	55 ± 2	59 ± 3	121 ± 17*	97 ± 16	74 ± 7	64 ± 2
CA2/3 Str. Lacunosum Molecular	71 ± 2	73 ± 4	141 ± 12 **	122 ± 17	110 ± 16	91 ± 2
CA3 Str. Oriens/ Pyramidale	57 ± 4	56 ± 3	114 ± 12 **	98 ± 13 *	73 ± 5†	68 ± 4
CA3 Str. Radiatum	56 ± 4	56 ± 4	119 ± 13 **	99 ± 17	67 ± 8†	63 ± 4
<u>Dentate Gyrus:</u>						
Molecular Layer (Superior Blade)	53 ± 3	52 ± 4	97 ± 15*	89 ± 11 *	62 ± 7	58 ± 2
Polymorphic Layer	42 ± 2	41 ± 3	89 ± 11*	75 ± 13	53 ± 6	48 ± 2
Pre Subiculum	70 ± 4	73 ± 4	69 ± 11	62 ± 10	98 ± 17	120 ± 9†
Subiculum	60 ± 3	64 ± 5	84 ± 8	72 ± 9	76 ± 5	71 ± 4

Data are presented as mean ± S.E.M. of 5 control, ASDH or ASDH + D-CPP-ene-treated animals. Glucose utilisation is expressed in $\mu\text{mol} \cdot 100\text{g}^{-1} \text{min}^{-1}$.

*P<0.05, **P<0.01 for statistical comparison of ASDH with controls.

†P<0.05 for statistical comparison of ASDH + D-CPP-ene with ASDH.

APPENDIX VI - TABLE 3
LOCAL CEREBRAL GLUCOSE UTILISATION FOLLOWING ACUTE SUBDURAL HAEMATOMA:
AREAS ASSOCIATED WITH LIMBIC FUNCTION

STRUCTURE	LCGU ($\mu\text{mol} \cdot 100\text{g}^{-1} \cdot \text{min}^{-1}$)					
	SHAM		ASDH		ASDH + D-CPP-ENE	
	IPSI.	CONTRA.	IPSI.	CONTRA.	IPSI.	CONTRA.
Mamillary Body	83 ± 3	84 ± 3	81 ± 8	81 ± 7	88 ± 4	88 ± 6
Thalamus:						
Anterodorsal Nucleus	67 ± 5	71 ± 4	57 ± 4	68 ± 2	76 ± 9 (a)	85 ± 11 (a)
Anteroventral Nucleus	90 ± 11	96 ± 3	64 ± 10	81 ± 5	108 ± 12 (a)	112 ± 10 †(a)
Laterodorsal Nucleus	71 ± 4	70 ± 4	40 ± 8*	68 ± 2	65 ± 12 (b)	92 ± 9 (b)
Habenular Nucleus:						
Medial	59 ± 4	72 ± 5	74 ± 8	78 ± 8	53 ± 3 (b)	56 ± 4 (b)
Lateral	105 ± 7	106 ± 7	97 ± 8	101 ± 9	63 ± 10 (b)	62 ± 10 (b)
Amygdala (Basolateral Nuc.)	60 ± 6	61 ± 6	55 ± 4	57 ± 6	70 ± 4	74 ± 6
Hypothalamus	38 ± 4	39 ± 4	39 ± 3	41 ± 4	37 ± 3	36 ± 3
Medial Septum	52 ± 4	53 ± 4	51 ± 4	57 ± 5	60 ± 6	64 ± 6
Lateral Septum	36 ± 2	36 ± 2	64 ± 13	59 ± 11	35 ± 3	35 ± 3
Diagonal Band, Vertical Limb	57 ± 3	53 ± 4	55 ± 6	57 ± 5	57 ± 3	58 ± 4
Diagonal Band, Horizontal Limb	71 ± 3	74 ± 2	66 ± 8	77 ± 9	72 ± 5	75 ± 4
Nucleus Accumbens	49 ± 4	49 ± 4	49 ± 4	54 ± 4	56 ± 8 (b)	56 ± 8 (b)
Cortex:						
Post.Cing. cortex (Layer IV)	69 ± 5	75 ± 3	61 ± 6	70 ± 4	90 ± 8 †	104 ± 4 ††
Ant. Cing. Cortex (Layer IV)	82 ± 6	80 ± 5	89 ± 13	74 ± 7	85 ± 6	84 ± 7
Parietal Cortex (Layer IV)	55 ± 8	81 ± 5	- (c)	71 ± 5	- (c)	61 ± 5
Parietal Cortex (Ischaemic Penumbra) (a)	67 ± 3	81 ± 4	102 ± 11*	70 ± 8	83 ± 3	69 ± 6
Frontal Cortex (Layer IV)	79 ± 8	88 ± 6	82 ± 11	82 ± 5	55 ± 4	62 ± 4†
Entorhinal Cortex (Layers I-II)	60 ± 4	63 ± 3	74 ± 12	64 ± 4	80 ± 4	86 ± 5†
Lat. Olf. Tract. (Layers I-II)	77 ± 6	81 ± 1	111 ± 12	96 ± 8	133 ± 8	143 ± 8†

Data are presented as mean ± S.E.M. of 5 control, ASDH or ASDH + D-CPP-ene-treated animals. Glucose utilisation is expressed in $\mu\text{mol} \cdot 100\text{g}^{-1} \cdot \text{min}^{-1}$. * $P < 0.05$ for statistical comparison of ASDH with controls † $P < 0.05$, †† $P < 0.01$ for statistical comparison between ASDH + D-CPP-ene and ASDH alone (Student's unpaired t-test, two-tailed with Bonferroni correction). (a) $n=3$ (b) $n=4$ (c) infarcted area below ASDH; (d) parietal cortex.

APPENDIX VI - TABLE 4
LOCAL CEREBRAL GLUCOSE UTILISATION FOLLOWING ACUTE SUBDURAL HAEMATOMA:
OTHER AREAS

STRUCTURE	LCGU ($\mu\text{mol} \cdot 100\text{g}^{-1}\text{min}^{-1}$)					
	SHAM		ASDH		ASDH + D-CPP-ENE	
	IPSI.	CONTRA.	IPSI.	CONTRA.	IPSI.	CONTRA.
<u>Auditory & Visual Regions:</u>						
Auditory Cortex Layer IV	99 ± 5	119 ± 6	62 ± 13	84 ± 11	66 ± 6	68 ± 5
Medial Geniculate Body	92 ± 3	99 ± 1	48 ± 5 **	73 ± 12	69 ± 7	63 ± 5
Visual Cortex Layer IV	75 ± 5	81 ± 4	85 ± 18 **	77 ± 8	59 ± 13	71 ± 6
Dorsolateral Geniculate Body	72 ± 4	73 ± 4	41 ± 5 **	70 ± 6	61 ± 9	72 ± 7
Superior Colliculus (Superficial)	70 ± 5	71 ± 3	72 ± 9	74 ± 7	56 ± 4	54 ± 4
Superior Colliculus (Deep)	63 ± 2	68 ± 2	61 ± 3	69 ± 5	56 ± 3	63 ± 6
<u>Extrapyramidal and Sensorimotor Areas:</u>						
Caudate Nucleus	73 ± 5	80 ± 5	52 ± 6	77 ± 6	63 ± 2	72 ± 7
<u>Myelinated Fibre Tracts:</u>						
Corpus Callosum	29 ± 1	28 ± 2	49 ± 10	31 ± 6	35 ± 3	31 ± 2
Lateral Septum	20 ± 2	21 ± 2	27 ± 4	26 ± 1	24 ± 2	25 ± 2

Data are presented as mean ± S.E.M. of 5 control, ASDH or ASDH + D-CPP-ene-treated animals. Glucose utilisation is expressed in $\mu\text{mol} \cdot 100\text{g}^{-1}\text{min}^{-1}$. ** $P < 0.01$ for statistical comparison of ASDH with controls. (Student's unpaired t-test, two-tailed with Bonferroni correction).

REFERENCES

- ACKERMANN, R. F., FINCH, D. M., BABB, T. L. & ENGEL, J. (1984) Increased glucose metabolism during long-duration recurrent inhibition of hippocampal pyramidal cells. *J. Neurosci.* **4**, 251-264.
- AEBISCHER, B., FREY, P., HAERTEL, H.-P., HERRLING, P. L., MUELLER, W., OLVERMAN, H. J. & WATKINS, J. C. (1989) Synthesis and NMDA antagonistic properties of the enantiomers of 4-(3-phosphonopropyl)piperazine-2-carboxylic acid (CPP) and of the unsaturated analogue (E)-4-(3-phosphonoprop-2-enyl)piperazine-2-carboxylic acid (CPP-ene). *Helvet. Chim. Acta* **72**, 1043-1051.
- ALBIN, R. L., YOUNG, A. B. & PENNEY, J. B. (1988) Tetrahydro-9-aminoacridine (THA) interacts with the phencyclidine (PCP) receptor site. *Neurosci. Lett.* **88**, 303-307.
- AMARAL, D. G. & KURZ, J. (1985) An analysis of the origins of the cholinergic and non-cholinergic septal projections to the hippocampus in the rat. *J. Comp. Neurol.* **240**, 37-59.
- ANDERSEN, P., ECCLES, J. C. & LØYNING, Y. (1964a) Localization of postsynaptic inhibitory synapses of hippocampal pyramids. *J. Neurophysiol.* **27**, 592-607.
- ANDERSEN, P., ECCLES, J. C. & LØYNING, Y. (1964b) Pathway of postsynaptic inhibition in the hippocampus. *J. Neurophysiol.* **27**, 592-607.
- ARSENIO-NUNEZ, M. L., HOSSMANN, K. A. & FARKAS-BARGETON, E. (1973) Ultrastructural and histochemical investigation of the cerebral cortex of cat during and after complete ischaemia. *Acta Neuropathol. (Berl.)* **26**, 329-344.
- ARTOLA, A. & SINGER, W. (1987) Long-term potentiation and NMDA receptors in rat visual cortex. *Nature (Lond)* **330**, 649-652.

- ASCHER, P. & NOWAK, L. (1987) Electrophysiological studies of NMDA receptors. *Trends Neurosci.* **10**, 284-288.
- ASHKENAZI, A., WINSLOW, J. W., PERALTA, E. G., PETERSEN, G. L., SCHIMERLIK, M. I., CAPON, D. J. & RAMACHANDRAN, J. (1987) An M2 muscarinic receptor subtype coupled to both adenylyl cyclase and phosphoinositide turnover. *Science* **238**, 672-672.
- ASTRUP, J., SYMON, L., BRANSTON, N. M. & LASSEN, N. A. (1977) Cortical evoked potential and extracellular K⁺ and H⁺ at critical levels of brain ischemia. *Stroke* **8**, 51-67.
- ASTRUP, J., SIESJO, B. K. & SYMON, L. (1981) Thresholds in cerebral ischemia- the ischemic penumbra. *Stroke* **12**, 723-725.
- BARABAN, J. M., SNYDER, S. H. & ALGER, B. E. (1985) Protein kinase C regulates ionic conductance in hippocampal pyramidal neurons: Electrophysiological effects of phorbol esters. *Proc. Natl. Acad. Sci. USA* **82**, 2538-2542.
- BARTUS, R. T., DEAN, R. L. III, BEER, B. & LIPPA, A. S. (1982) The cholinergic hypothesis of learning and memory. *Science* **217**, 408-417.
- BAUGHMAN, R. W. & GILBERT, C. D. (1981) Aspartate and glutamate as possible neurotransmitters in the visual cortex. *J. Neurosci.* **1**, 427-439.
- BAUMGOLD, J., MERRIL, C. & GERSHON, E. S. (1987) Loss of pirenzepine regional selectivity following solubilization and partial purification of the putative M1 and M2 muscarinic receptor sub-types. *Molec. Brain Res.* **2**, 7-14.

- BEAL., M. F., MAZUREK, M. F., TRAN, V. T., CHATTA, G., BIRD, E. D. & MARTIN, J. B. (1985) Reduced numbers of somatostatin receptors in cerebral cortex of Alzheimer's Disease. *Science* **217**, 408-417.
- BECK, T., WREE, A. & SCHLEICHER, A. (1990) Glucose utilization in rat hippocampus after long-term recovery from ischemia. *J. Cereb. Blood Flow Metab.* **10**, 542-549.
- BECK, T., WREE, A. & SCHLEICHER, A. (1989) Postischemic glucose utilization in rat hippocampal layers. *Brain Res.* **510**, 74-83.
- BEN-BARAK, J. & DUDAI, Y. (1980) Early septal lesion: effect on the development of the cholinergic system in rat hippocampus. *Brain Res.* **185**, 323-334.
- BENVENISTE, H., DREJER, J., SCHOUSBOE, A. & DIEMER, N. H. (1984) Elevation of the extracellular concentrations of glutamate and aspartate in rat hippocampus during transient cerebral ischemia monitored by intracerebral microdialysis. *J. Neurochem.* **43**, 1369-1374.
- BERRIDGE, M. J., DAWSON, R. M. C., DOWNES, C. P., HESLOP, J. P. & IRVINE, R. F. (1983) Changes in the levels of inositol phosphates after agonist-dependent hydrolysis of membrane phosphoinositides. *Biochem. J.* **212**, 473-482.
- BERTHOLF, R. L. (1987) Aluminium and Alzheimer's Disease: Perspectives for a Cytoskeletal Mechanism. *CRC Crit. Rev. Clin. Lab Sci.* **25**, 195-210.
- BLACKSTAD, T. W. & KJAERHEIM, A. (1961) Special axo-dendritic synapses in the hippocampal cortex. Electron and light microscopic studies on the layer of mossy fibres. *J. Comp. Neurol.* **117**, 133-159.

- BLESSED, G., TOMLINSON, B. E. & ROTH, M. (1968) The association between quantitative measures of dementia and of senile change in the cerebral gray matter of elderly subjects. *Br. J. Psychiatry* **114**, 797-811.
- BLISS, T. V. P., DOUGLAS, R. M., ERRINGTON, M. L. & LYNCH, M. A. (1986) Correlation between long-term potentiation and release of endogenous amino acids from dentate gyrus of anaesthetised rats. *J. Physiol. (Lond.)* **377**, 391-408.
- BLISS, T. V. P. & LOMO, T. (1973) long-lasting potentiation of synaptic transmission in the dentate area of the anaesthetised rabbit following stimulation of the perforant path. *J. Physiol. (Lond.)* **232**, 331-356.
- BLOMQUIST, P., MABE, H., INGVAR, M. & SIESJO, B. K. (1984) Models for studying long-term recovery following forebrain ischemia in the rat. 1. Circulatory and functional effects of 4-vessel occlusion. *Acta Neurol. Scand.* **69**, 376-384.
- BOAST, C. A., GERHARDT, S. C., PASTOR, G., LEHMANN, J., ETIENNE, P. E. & LIEBMAN, J. M. (1988) The N-methyl-D-aspartate antagonists CGS 19755 and CPP reduce ischemic brain damage in gerbils. *Brain Res.* **442**, 345-348.
- BONNER, T. I. (1989) The molecular basis of muscarinic receptor diversity. *Trends Neurosci.* **12**, 148-151.
- BOWERY, N. G., WONG, E. H. F. & HUDSON, A. L. (1988) Quantitative autoradiography of [³H]-MK-801 binding sites in mammalian brain. *Br. J. Pharmacol.* **93**, 944-954.
- BRIDGES, R. J., KESSLAK, J. P., NIETO-SAMPEDRO, M., BRODERICK, J. T., YU, J. & COTMAN, C. W. (1987) A L-[³H]glutamate binding site on glia: an autoradiographic study on implanted astrocytes. *Brain Res.* **415**, 163-168.

- BROWN, A. W. & BRIERLY, J. B. (1972) Anoxic-ischemic cell change in rat brain: light microscopic and fine structural observations. *J. Neurol. Sci.* **16**, 59-84.
- BROWN, D. A., FORWARD, A. & MASH, S. (1980) Antagonist discrimination between ganglionic and ileal muscarinic receptors. *Br. J. Pharmacol.* **71**, 362-364.
- BROWN, J. H. & GOLDSTEIN, D. (1986) Analysis of cardiac muscarinic receptors recognized selectively by non-quaternary ligands. *J. Pharmacol. Exp. Ther.* **238**, 580-586.
- BROWN, J. H., GOLDSTEIN, D. & MASTERS, S. B. (1985) The putative M1 muscarinic receptor does not regulate phosphoinositide hydrolysis. *Molec. Pharmacol.* **27**, 525-531.
- BROWN, E., KENDALL, D. A. & NAHORSKY, S. R. (1984) Inositol phospholipid hydrolysis in rat cerebral cortical slices: I. Receptor characterization. *J. Neurochem.* **42**, 1379-1387.
- BRUN, A. (1983) An overview of light and electron microscope changes. In *Alzheimer's Disease, the Standard Reference*, B. Reisberg (Ed.), Free Press, New York, pp 37-47.
- BUCHAN, A. M. & PULSINELLI, W. A. (1990) Septo-hippocampal deafferentation protects CA1 neurons against ischemic injury. *Brain Res.* **512**, 7-14.
- BULLOCK, R., GRAHAM, D. I., CHEN, M.-H., LOWE, D. & McCULLOCH, J. (1990) Focal cerebral ischaemia in the cat: pretreatment with a competitive NMDA receptor antagonist, D-CPP-ene. *J. Cereb. Blood Flow Metab.* **10**, 668-674.
- BULLOCK, R., BUTCHER, S. P., CHEN, M.-H., KENDALL, L. & McCULLOCK, J. (1991a) Correlation of the extracellular glutamate concentration with extent of blood flow reduction after subdural haematoma in the rat. *J. Neurosurg.* **74**, 794-802.

- BULLOCK, R., INGLIS, F. M., KURODA, Y., BUTCHER, S., McCULLOCH, J. & MAXWELL, W. (1991b) Transient hippocampal hypermetabolism associated with glutamate release after subdural haematoma in the rat: a potentially neurotoxic mechanism? *J. Cereb. Blood Flow Metab.* **11** (Suppl. 2), S109.
- BULLOCK, R., BUTCHER, S. P., CHEN, M.-H., KENDALL, L. & McCULLOCH, J. (1991) Correlation of the extracellular glutamate concentration with extent of bloodflow reduction after subdural hematoma in the rat. *J. Neurosurg.* **74**, 794-802.
- CARLSEN, J., DE OLMOS, J. & HEIMER, L. (1982) Tracing of two-neuron pathways in the olfactory system by the aid of transneuronal degeneration: projections to the amygdaloid body and hippocampal formation. *J. Comp. Neurol.* **208**, 196-208.
- CHALMERS, D. T., DEWAR, D., GRAHAM, D. I., BROOKS, D. N. & McCULLOCH, J. (1990) Differential alterations of cortical glutamatergic binding sites in senile dementia of the Alzheimer type. *Proc. Natl. Acad. Sci. USA* **87**, 1352-1356.
- CHALMERS, D. T. & McCULLOCH, J. (1989) Reduction in [³H]glutamate binding in the visual cortex after unilateral orbital enucleation. *Neurosci. Lett.* **97**, 298-304.
- CHANG, R. S. L., TRAN, V. T. & SNYDER, S. H. (1980) Neurotransmitter receptor localizations: brain lesion induced alterations in benzodiazepine, GABA, β -adrenergic and histamine H1-receptor binding. *Brain Res.* **190**, 95-110.
- CHAPMAN, A. G. & BOWKER, H. M. (1987) Inhibition of hippocampal ³H-D-aspartate release by 2-APB, 2-APV, and 2-APH. In *Excitatory Amino Acid Transmission, Neurology and Neurobiology*, Vol. 24, Hicks, T. P. et al. (eds.), Liss, New York, pp 165-168.

- CHAPMAN, A. G., GRAHAM, J. & MELDRUM, B. S. (1990) Potent oral anticonvulsant action of CPP and CPPene in DBA/2 mice. *Eur. J. Pharmacol.* **178**, 97-99.
- CHAPMAN, A. G., GRAHAM, J. L., SWAN, J. H. & MELDRUM, B. S. (1991) Regional cerebral glucose utilization in rat brain following the administration of CGP 39551, a competitive NMDA antagonist. *J. Cereb. Blood Flow Metab.* **11 (Suppl. 2)**, S226.
- CHAPMAN, A. G., SWAN, J. H. & MELDRUM, B. S. (1989) Enhanced glucose utilization in pyriform cortex of rats induced by the competitive NMDA antagonist AP7. *J. Cereb. Blood Flow Metab.* **9 (Suppl. 1)**, S310.
- CHEN, M., BULLOCK, R., GRAHAM, D. I., FREY, P., LOWE, D. & McCULLOCH, J. (1991) Evaluation of a competitive NMDA antagonist D-CPP-ene in feline focal cerebral ischemia. *Ann. Neurol.* in press.
- CHOI, D. W., MAULUCCI-GEDDE, M. A. & KRIEGLSTEIN, A. R. (1987) Glutamate neurotoxicity in cortical cell culture. *J. Neurosci.* **7**, 357-368.
- CHOI, D. W., KOH, J. & PETERS, S. (1988) Pharmacology of glutamate neurotoxicity in cortical cell culture: attenuation by NMDA antagonists. *J. Neurosci.* **8**, 185-196.
- CLARKE, P. B. S., PERT, C. B. & PERT, A. (1984) Autoradiographic distribution of nicotine receptors in rat brain. *Brain Res.* **323**, 390-395.
- CLIFFORD, D. B., OLNEY, J. W., MANIOTIS, A., COLLINS, R. C. & ZORUMSKI, C. F. (1987) The functional anatomy and pathology of lithium-pilocarpine and high dose pilocarpine seizures. *Neuroscience* **23**, 953-968.

- CLINESCHMIDT, B. V., MARTIN, G. E. & BUNTING, P. R. (1982) Anticonvulsant activity of (+)-5-methyl-10, 11, dihydro-5H-dibenzo [a, d] cyclohepten-5, 10-imine (MK-801), a substance with potent anticonvulsant, central sympathomimetic, and apparent anxiolytic properties. *Drug Dev. Res.* **2**, 123-134.
- COAN, E. J. & COLLINGRIDGE, G. L. (1987) Characterization of an N-methyl-D-aspartate receptor component of synaptic transmission in rat hippocampal slices. *Neuroscience*. **22**, 1-8.
- COLE, A. E. & NICOLL, R. A. (1984a) Characterization of a slow cholinergic post-synaptic potential recorded *in vitro* from rat hippocampal pyramidal cells. *J. Physiol. (Lond.)* **352**, 173-188.
- COLE, A. E. & NICOLL, R. A. (1984b) The pharmacology of cholinergic excitatory responses in hippocampal pyramidal cells. *Brain Res.* **305**, 283-290.
- COLLERTON, D. (1986) Cholinergic function and intellectual decline in Alzheimer's Disease. *Neuroscience* **19**, 1-28.
- COLLINGRIDGE, G. L. (1985) Long term potentiation in the hippocampus: mechanisms of initiation and modulation by neurotransmitters. *Trends Pharmacol.* **6**, 407-411.
- COLLINGRIDGE, G. L. & BLISS, T. V. P. (1987) NMDA receptors – their role in long-term potentiation. *Trends Neurosci.* **10**, 288-293.
- COLLINGRIDGE ; G.L., HERRON, C. E. & LESTER, R. A. J. (1988) Synaptic activation of N-methyl-D-aspartate receptors in the Schaffer collateral-commissural pathway of rat hippocampus. *J. Physiol. (Lond.)* **399**, 283-300.
- COLLINGRIDGE, G. L., KEHL, S. J., McLENNAN, H. (1983) Excitatory amino acids in synaptic transmission in the Schaffer ollateral-commissural pathway of the rat hippocampus. *J. Physiol. (Lond.)* **334**, 33-46.

- COLLINGRIDGE, G. S., REYMANN, K. G. & DAVIES, S. N. (1989) Involvement of protein kinases in two phases of long-term potentiation in rat hippocampal slices. *Soc. Neurosci. Abstr.* **15**.
- COLLINGRIDGE, G. L. & SINGER, W. (1990) Excitatory amino acid receptors and synaptic plasticity. *Trends. Pharmacol. Sci.* **11**, 290-296.
- COLLINS, G. G. S. & HOWLETT, S. J. (1988) The pharmacology of excitatory transmission in the rat olfactory cortex slice. *Neuropharmacology* **27**, 697-705.
- CONNICK, J. H. & STONE, T. W. (1988) Excitatory amino acid antagonists and endogenous aspartate release from rat hippocampal slices. *Br. J. Pharmacol.* **93**, 863-867.
- CONNOR, D. J. & HARRELL, L. E. (1989) Chronic septal lesions cause upregulation of cholinergic but not noradrenergic hippocampal phosphoinositide hydrolysis. *Brain Res.* **488**, 387-389.
- COTMAN, C. W., MONAGHAN, D. T., OTTERSEN, O. P. & STORM-MATHISEN, J. (1987) Anatomical organization of excitatory amino acid receptors and their pathways. *Trends Neurosci.* **10**, 273-279.
- COURT, J. A., KEITH, A. B., KERWIN, J. M & PERRY, E. K. (1990) Fimbria-fornix lesions in aged rats cause increased carbachol-stimulated phosphoinositide hydrolysis in the hippocampus, but no change in muscarinic receptor binding. *Brain Res.* **532**, 333-335.
- COWBURN, R., HARDY, J., ROBERTS, P. & BRIGGS, R. (1988a) Presynaptic and postsynaptic glutamate function in Alzheimer's disease. *Neurosci. Lett.* **86**, 109-113.

- COWBURN, R., HARDY, J., ROBERTS, P. & BRIGGS, R. (1988b) Regional distribution of pre-and postsynaptic glutamatergic function in Alzheimer's Disease. *Brain Res.* **452**, 403-407.
- CROSBY, G., CRANE, A. M. & SOKOLOFF, L. (1982) Local changes in cerebral glucose utilization during ketamine anesthesia. *Anesthesiology*, **56**, 437-443.
- CROSS, A. J., CROW, T. J., FERRIER, I. N., JOHNSON, J. A., BLOOM, S. R. & CORSELIS, J. A. N. (1984) Serotonergic receptor changes in dementia of the Alzheimer-type. *J. Neurochem.* **43**, 1574-1581.
- CROSS, A. J., SLATER, P., PERRY, E. K. & PERRY, R. H. (1988) An autoradiographic analysis of Serotonin receptors in human temporal cortex: changes in Alzheimer-type dementia. *Neurochemistry* **13**, 89-96.
- CROWDER, J. M., CROUCHER, M. J., BRADFORD, H. F. & COLLINS, J. F. (1987) Excitatory amino acid receptors and depolarization-induced Ca²⁺ influx into hippocampal slices. *J. Neurochem.* **48**, 1917-1924.
- CRUNELLI, V., KELLY, J. S., LERESCHE, N. & PIRCHIO, M. (1987) On the excitatory post-synaptic potential evoked by stimulation of the optic tract in the rat lateral geniculate nucleus. *J. Physiol.* **384**, 603-618.
- CRUTCHER, K. A., BROTHERS, L. & DAVIS, J. N. (1981) Sympathetic noradrenergic sprouting in response to central cholinergic denervation: a histochemical study of neuronal sprouting in the rat hippocampal formation. *Brain Res.* **210**, 115-128.
- CRUTCHER, K. A. & DAVIS, J. N. (1980) Hippocampal alpha- and beta-adrenergic receptors; comparison of [³H]-dihydroalprenolol and [³H]-WB 4101 binding with noradrenergic innervation in the rat. *Brain Res.* **182**, 107-117.
- CUELLO, A. C. & SOFRONIEW, M. V. (1984) The anatomy of CNS cholinergic neurons. *Trends Neurosci.* **7**, 74-78.

- CULL-CANDY, S. G. & USOWICZ, M. M. (1987) Multiple conductance channels activated by excitatory amino acids in cerebellar neurons. *Nature* **325**, 525-528.
- CUMMINGS, J. L., TOMIYASU, U., READ, S. & BENSON, D. F. (1984) Amnesia with hippocampal lesions after cardiopulmonary arrest. *Neurology* **34**, 679-681.
- CURTIS, D. R., PHILLIS, J. W. & WATKINS, J. C. (1959) Chemical excitation of spinal neurons. *Nature* **183**, 611-612.
- DAFNY, N. & QIAO, J.-T. (1990) Habenular neuron responses to noxious input are modified by dorsal raphe stimulation. *Neurol. Res.* **12**, 117-121.
- DAM, M., WAMSLEY, J. K., RAPOPORT, S. I. & LONDON, E. D. (1982) Effects of oxotremorine on local glucose utilization in the rat cerebral cortex. *J. Neurosci.* **2**, 1072-1078.
- DAM, M. & LONDON, E. D. (1983) Effects of cholinomimetics on glucose utilization in rat brain optic systems. *Eur. J. Pharmacol.* **87**, 137-140.
- DAM, M. & LONDON, E. D. (1984) Glucose utilization in the Papez circuit: effects of oxotremorine and scopolamine. *Brain Res.* **295**, 137-144.
- DANYSZ, W. & WROBLEWSKI, J. T. (1989) Amnesic properties of glutamate receptor antagonists. *Neurosci. Res. Comm.* **5**, 9-18.
- DAVENPORT, C. J., MONYER, H. & CHOI, D. W. (1988) Tetrahydroaminoacridine selectively attenuates NMDA receptor-mediated neurotoxicity. *Eur J. Pharmacol.* **154**, 73-78.
- DAVIES, C. H., STARKEY, S. J., POZZA, M. F. & COLLINGRIDGE, G. L. (1991) GABA_B autoreceptors regulate the induction of LTP. *Nature* **349**, 609-611.

- DAVIES, J., EVANS, R. H., HERRLING, P. L., JONES, A. W., OLVERMAN, H. J., POOK, P. & WATKINS, J. C. (1986) CPP, a new potent and selective NMDA antagonist. Depression of central neuron responses, affinity for [³H]D-AP5 binding sites on brain membranes and anticonvulsant activity. *Brain Res.* **382**, 169-173.
- DAVIES, J., EVANS, R. H., JONES, A. W., SMITH, D. A. S. & WATKINS, J. C. (1982) Differential activation and blockade of excitatory amino acid receptors in the mammalian and amphibian central nervous system. *Comp. Biochem. Physiol.* **72C**, 211-224
- DAVIES, S. N., LESTER, R. A. J., REYMAN, K. G. & COLLINGRIDGE, G. L. (1989) Temporally distinct pre- and post-synaptic mechanisms maintain long-term potentiation. *Nature* **338**, 500-503.
- DAVIES, P. & TERRY, R. D. (1981) Cortical somatostatin like immunoreactivity in cases of Alzheimer's Disease and senile dementia of Alzheimer type. *Neurobiol. Aging* **2**, 9-14.
- DAVIES, P. & VERTH, A. H. (1978) Regional distribution of muscarinic acetylcholine receptor in normal and Alzheimer's type dementia brains. *Brain Res.* **138**, 385-392.
- DAWSON, V. L. & WAMSLEY, J. K. (1990) Hippocampal muscarinic supersensitivity after AF64A medial septal lesion excludes M₁ receptors. *Brain Res. Bull.* **25**, 311-317.
- DEARY, I. J. & WHALLEY, L. J. (1988) Recent research on the causes of Alzheimer's Disease. *Brit. Med. J.* **297**, 807-10.
- DE BONI, U. & CRAPPER-McLACHLAN, D. R. (1985) Controlled induction of paired helical filaments of the Alzheimer type in cultured human neurons, by glutamate and aspartate. *J. Neurol. Sci.* **68**, 105-118.
- DELLA PUPPA, A. & LONDON, E. (1989) Cerebral metabolic effects of σ ligands in the rat. *Brain Res.* **505**, 283-290.

- DE SOUZA, E. B., WHITEHOUSE, P. J., KUCHAR, M. J., PRICE, D. L. & VALE, W. W. (1986) Reciprocal changes in corticotrophin releasing factor (CRF) -like immuno-reactivity and CRF receptors in cerebral cortex of Alzheimer's disease. *Nature* **319**, 593-595.
- DEWAR, D., CHALMERS, D. T., GRAHAM, D. I. & McCULLOCH, J. (1991) Glutamate metabotropic and AMPA binding sites are reduced in Alzheimer's Disease: an autoradiographic study of the hippocampus. *Brain Res.* **553**, 58-64.
- DEWAR, D., WALLACE, M. C., KURUMAJI, A. & McCULLOCH, J. (1989) Alterations in the N-methyl-D-aspartate receptor complex following cerebral ischemia. *J. Cereb. Blood Flow Metab.* **9**, 709-712.
- DIEMER, N. H. & SIEMKOWICZ, E. (1980) Increased 2-deoxyglucose uptake in the hippocampus, globus pallidus and substantia nigra after cerebral ischemia. *Acta Neurol. Scand.* **61**, 56-63.
- DOMINO, E. F., CHODOFF, P. & CORSSSEN, G. (1965) Pharmacological effects of CI-581, a new dissociative anesthetic, in man. *J. Clin. Pharmacol. Ther.* **6**, 279-281.
- DUNNETT, S. B., WISHAW, I. Q., JONES, G.H. & BUNCH, S. T. (1987) Behavioural, biochemical and histochemical effects of different neurotoxic amino acids injected into nucleus basalis magnocellularis of rats. *Neuroscience* **20**, 653-669.

- DUTAR, P. & NICOLL, R. A. (1988) Classification of muscarinic responses in hippocampus in terms of receptor subtypes and second-messenger systems: electrophysiological studies *in vitro*. *J. Neurosci.* **8**, 4214-4224.
- DUVERGER, D., BENAVIDES, J., CUDENNEC, A. et al., (1987) A glutamate antagonist reduces infarction following focal cerebral ischaemia independently of vascular and metabolic changes. *J. Cereb. Blood Flow Metab.* **7 (Suppl. 1)**, S144.
- DYKENS, J. A., STERN, A. & TRENKNER, E. (1987) Mechanism of kainate toxicity to cerebellar neurons *in vitro* is analogous to reperfusion tissue injury. *J. Neurochem.* **49**, 1222-1228.
- EHLERT, F. J., KOKA, N. & FAIRHURST, A. S. (1980) Altered [³H]quinuclidinyl benzilate binding in the striatum of rats following chronic cholinesterase inhibition with diisopropylfluorophosphate. *Mol. Pharmacol.* **17**, 24-30.
- ERRINGTON, M. L., LYNCH, M. A. & BLISS, T. V. P. (1987) Long-term potentiation in the dentate gyrus: induction and increased glutamate release are blocked by D(-)aminophosphonovalerate. *Neuroscience* **20**, 279-284.
- EVERITT, B. J., ROBBINS, T. W., EVENDEN, J. L., MARSTON, H. M., JONES, G. H. & SIRKIA, T. (1987) The effects of excitotoxic lesions of the substantia innominata, ventral and dorsal globus pallidus on the acquisition and retention of a conditional discrimination: implications for cholinergic hypotheses of learning and memory. *Neuroscience* **22**, 441-469.
- FAGG, G. E., FOSTER, A. C., MENA, E. E. & COTMAN, C. W. (1983) Chloride and calcium ions separate L-glutamate receptor populations in synaptic membranes. *Eur. J. Pharmacol.* **88**, 105-110.

- FISHER, S. K. & AGRANOFF, B. W. (1987) Receptor activation and inositol lipid hydrolysis in neural tissues. *J. Neurochem.* **48**, 999-1017.
- FISHER, S. K. & BARTUS, R. T. (1985) Regional differences in the coupling of muscarinic receptors to inositol phospholipid hydrolysis in guinea pig brain. *J. Neurochem.* **45**, 1085-1095.
- FISHER, S. K., BOAST, C. A. & AGRANOFF, B. W. (1980) The muscarinic stimulation of phospholipid labeling in hippocampus is independent of its cholinergic input. *Brain Res.* **189**, 284-288.
- FISHER, A. & HANIN, I. (1986) Potential animal models for senile dementia of the Alzheimer's type, with emphasis on AF64A-induced cholinotoxicity. *Ann Rev. Pharm. Toxicol.* **26**, 161-181.
- FISHER, S. K., KLINGER, P. D. & AGRANOFF, B. W. (1983) Muscarinic agonist binding and phospholipid turnover in brain. *J. Biol. Chem.* **258**, 7358-7363.
- FISHER, S. K. & SNIDER, R. M. (1987) Differential receptor occupancy requirements for muscarinic cholinergic receptor stimulation of inositol lipid hydrolysis in brain and in neuroblastomas. *Molec. Pharmacol.* **32**, 81-90.
- FLOOD, J. F. (1988) Effect of acute arecoline, tacrine, and arecoline + tacrine post-training administration on retention in late middle-aged mice. *J. Gerontol.* **43**, B54-B56.
- FLYNN, D. D., WEINSTEIN, D. A. & MASH, D. C. (1991) Loss of high-affinity agonist binding to Alzheimer's Disease: implications for the failure of cholinergic replacement therapies. *Ann. Neurol.* **29**, 256-262.
- FONNUM, F. (1975) A rapid radiochemical method for the determination of choline acetyltransferase. *J. Neurochem.* **24**, 407-409.

- FONNUM, F. (1984) Glutamate: a neurotransmitter in mammalian brain. *J. Neurochem.* **42**, 1-11.
- FONNUM, F., LUND-KARLSEN R. L., MALTHER-SORENSEN, D., SKREDE, K. K. & WALAAS, I. (1979) Localization of neurotransmitters, particularly glutamate, in hippocampus, septum, nucleus accumbens and superior colliculus. *Prog. Brain Res.* **51**, 167-191.
- FONNUM, F. & WALAAS, I. (1978) The effect of intrahippocampal kainic acid injections and surgical lesions on neurotransmitters in hippocampus and septum. *J. Neurochem.* **31**, 1173-1181.
- FOSSE, V. M. & FONNUM, F. (1987) Biochemical evidence for glutamate and-or aspartate as neurotransmitters in fibres from the visual cortex to the lateral posterior thalamic nucleus (pulvinar) in rats. *Brain Res.* **400**, 219-224.
- FOSTER, A. C. & FAGG, G. E. (1984) Acidic amino acid binding sites in mammalian neuronal membranes: their characteristics and relationship to synaptic receptors. *Brain Res. Rev.* **7**, 103-164.
- FOSTER, A. C. & FAGG, G. E. (1987) Comparison of L-[³H]glutamate, D-[³H] aspartate, DL-[³H]AP5 and [³H]NMDA as ligands for NMDA receptors in crude postsynaptic densities from rat brain. *Eur. J. Pharmacol.* **133**, 291-300.
- FOSTER, A. C., GILL, R., KEMP, J. A. & WOODRUFF, G. N. (1987) Systemic administration of MK-801 prevents N-methyl-D-aspartate-induced neuronal degeneration in rat brain. *Neurosci. Lett.* **76**, 307-311.

- FOWLER, C. J., MAGNUSON, O., MOHAMMED, A. K., DANYSZ, W. & ARCHER, T. (1986) The effect of selective noradrenergic lesions upon stimulation by nordrenaline of inositol phospholipid breakdown in rat hippocampal miniprisms. *Eur. J. Pharmacol.*, **123**, 401-407.
- FRANCE, C. P., WINGER, G. D. & WOODS, J. H. (1990) Analgesic, anaesthetic, and respiratory effects of the competitive N-methyl-D-aspartate (NMDA) antagonist CGS 19755 in rhesus monkeys. *Brain Res.* **526**, 335-358.
- FRANSEN A., DREJER, J. & SCHOUSBOE (1989) Direct evidence that excitotoxicity in cultured neurons is mediated via N-methyl-D-aspartate (NMDA) as well as non-NMDA receptors. *J. Neurochem.*, **53**, 297-299.
- FREEDMAN, S. B., HARLEY, E. A. & IVERSEN, L. L. (1988) Relative affinities of drugs acting at cholinergic receptors in displacing agonist and antagonist radioligands: the NMS/Oxo-M ratio as an index of efficacy at cortical muscarinic receptors. *Br. J. Pharmacol.* **93**, 437-445.
- FREEDMAN, S. B., HARLEY, E. A., PATEL, S., NEWBERRY, N. R., GILBERT, M. J., McKNIGHT, A. T., TANG, J. T., MAGUIRE, J. J., MUDUNKOTUWA, N. T., BAKER, R., STREET, L. J., MacLEOD, A. M., SAUNDERS, J. & IVERSEN, L. L. (1990) A novel series of non-quaternary oxadiazoles acting as full agonists at muscarinic receptors. *Br. J. Pharmacol.* **101**, 575-580.
- FRIEDMAN, H. R. & GOLDMAN-RAKIC, P. S. (1988) Activation of the hippocampus and dentate gyrus by working memory: a 2-deoxyglucose study of behaving rhesus monkeys. *J. Neurosci.* **8**, 4693-4706.
- GAGE, F. H., BJORKLUND, A. & STENEVI, U. (1984) Cells of origin of the ventral cholinergic septo-hippocampal pathway. *Neurosci. Lett.* **44**, 211-216.

- GAZIT, H., SILMAN, I. & DUDAI, Y. (1979) Administration of an organophosphate causes a decrease in muscarinic receptor levels in rat brain. *Brain Res.* **174**, 351-356.
- GEDDES, J. W., CHANG-CHUI, H., COOPER, S. M., LOTT, I. T. & COTMAN, C. W. (1986) Density and distribution of NMDA receptors in the human hippocampus in Alzheimer's disease. *Brain Res.* **399**, 156-161.
- GEDDES, J. W., MONAGHAN, D. T., COTMAN, C. W., LOTT, I. T., KIM, R. C. & CHANG CHUI, H. (1985) Plasticity of hippocampal circuitry in Alzheimer's Disease. *Science* **230**, 1179-1181.
- GIBSON, G. E., PELMAS, C. J. & PETERSON, C. (1983) Cholinergic drugs and 4-aminopyridine alter hypoxic-induced behavioural deficits. *Pharmacol. Biochem. Behav.* **18**, 909-916.
- GIL, D. W. & WOLFE, B. B. (1985) Pirenzepine distinguishes between muscarinic receptor-mediated phosphoinositide breakdown and inhibition of adenylate cyclase. *J. Pharmacol. Exp. Ther.* **232**, 608-616.
- GILL, R., FOSTER, A. C. & WOODRUFF, G. N. (1987) Systemic administration of MK-801 protects against ischemia-induced hippocampal neuro-degeneration in the gerbil. *J. Neurosci.* **7**, 3343-3349.
- GINSBERG, M. (1990) Local metabolic responses to cerebral ischemia. *Cerebrovasc. Brain Metab. Rev.* **2**, 58-93.
- GINSBERG, M. D. & BUSTO, R. (1989) Rodent models of cerebral ischemia. *Stroke* **20**, 1627-1642.
- GINSBERG, M. D. & REIVICH, M. (1979) Use of the 2-deoxyglucose method of local cerebral glucose utilisation in the abnormal brain: evaluation of the lumped constant during ischemia. *Acta Neurol. Scand.* **60 (S72)**, 226-7.

- GINSBERG, M. D., REIVICH, M. & GIANDOMENICO, A. (1977a) Regional brain glucose metabolism during recovery from transient cerebral ischemia. *Acta Neurol. Scand.* **56 (S64)**, 6.6-6.7.
- GINSBERG, M. D., REIVICH, M., GIANDOMENICO, A. & GREENBERG, J. H. (1977b) Local glucose utilisation in acute focal cerebral ischemia: local dysmetabolism and diaschisis. *Neurology*, **27**, 1042-1048.
- GOLDBERG, M. P., VISESKUL, V. & CHOI, D. W. (1988) Phencyclidine receptor ligands attenuate cortical neuronal injury after N-methyl-D-aspartate exposure or hypoxia. *J. Pharmacol. Exp. Ther.* **245**, 1081-1087.
- GOMEZ-RAMOS, P., NELSON, S., WALTER, D., CROSS, R. & SAMSON, F. E. (1982) Kainic acid alters cholinergic responses in the rat retina: a 2-deoxyglucose study. *J. Neurosci. Res.* **7**, 297-303.
- GONZALES, R. A. & CREWS, F. T. (1984) Characterization of the cholinergic stimulation of phosphoinositide hydrolysis in rat brain slices. *J. Neurosci.* **12**, 3120-3127.
- GOTTLIEB, D. I. & COWAN, W. M. (1973) Autoradiographic studies of the commissural and ipsilateral association connections of the hippocampus and dentate gyrus of the rat. I. The commissural connections. *J. Comp. Neurol.* **149**, 393-422.
- GOYAL, R. K. & RATTAN, S. (1978) Neurohumoral, hormonal and drug receptors for the lower esophageal sphincter. *Gastroenterol.* **74**, 598-619.
- GRAHAM, S. H., SHIRAISHI, K., PANTER, S. S., SIMON, R. P. & FADEN, A. I. (1990) Changes in extracellular amino acid neurotransmitters produced by focal cerebral ischemia. *Neurosci Lett.* **110**, 124-130.
- GREENAMYRE, J. T. (1986) The role of glutamate in neurotransmission and neurologic disease. *Science* **230**, 1179-1181.

- GREENAMYRE, J. T., PENNEY, J. B., D'AMATO, C. J., YOUNG, A. B. (1987) Dementia of the Alzheimer's type: changes in hippocampal L-[³H]-glutamate binding. *J. Neurochem.* **48**, 543-551.
- GREENAMYRE, J. T. & YOUNG, A. B. (1989) Excitatory amino acids and Alzheimer's Disease. *Neurobiol. Aging* **10**, 593-602.
- GROTTA, J. C. (1987) Medical progress: Current medical and surgical therapy for cerebrovascular disease. *New Eng. J. Med.* **317**, 1505-1516.
- HABERLY, L. B. & PRICE, J. L. (1978) Association and commissural fiber systems of the olfactory cortex of the rat. I. Systems originating in the piriform cortex and adjacent areas. *J. Comp. Neurol.* **178**, 711-740.
- HAGAN, J. J. & MORRIS, R. G. M. (1988) The cholinergic hypothesis of learning and memory: a review of animal experiments. In *Handbook of Psychopharmacology, Vol. 20*. Iversen, L. L. et al. (eds) Plenum Press pp 237-323.
- HAKIM, A. & SHOUBRIDGE, E. A. (1989) Cerebral acidosis in focal ischemia. *Cerebrovasc. Brain Metab. Rev.* **1**, 115-132.
- HAMMER, R., BERRIE, C. P., BIRDSALL, N. M. J., BURGEN, A. S. V. & HULME, E. C. (1980) Pirenzepine distinguishes between different subclasses of muscarinic receptors. *Nature* **283**, 90-92.
- HAMMER, R. P., HERKENHAM, M., PERT, C. B. & QUIRION, R. (1982) Correlation of regional brain metabolism with receptor localization during ketamine anesthesia: combined autoradiographic 2-[³H]deoxy-D-glucose receptor binding technique. *Proc. Natl. Acad. Sci. USA* **79**, 3067-3070.

- HAMMER, R. P. & HERKENHAM, M. (1983) Altered metabolic activity in the cerebral cortex of rats exposed to ketamine. *J. Comp. Neurol.* **220**, 396-404.
- HARA, H., ONODERA, H., YOSHIDOMI, M., MATSUDA, Y. & KOGURE, K. (1990) Staurosporine, a novel protein kinase C inhibitor, prevents postischemic neuronal damage in the gerbil and rat. *J. Cereb. Blood Flow Metab.* **10**, 646-653.
- HARDY, J., COWBURN, R., BARTON, A., REYNOLDS, G., LOFDAHL, E., O'CARROLL, A. M., WESTER, D. & WINBLAD, B. (1987) Region-specific loss of glutamate innervation in Alzheimer's Disease. *Neurosci. Lett.* **73**, 77-80.
- HARRELL, L. E. & DAVIS, J. N. (1984) Cholinergic denervation of the hippocampal formation does not produce long-term changes in glucose metabolism. *Exp. Neurol.* **85**, 128-138.
- HARVEY, A. L. & ROWAN, E. G. (1990) Effects of tacrine, aminopyridines, and physostigmine on acetylcholinesterase, acetylcholine release, and potassium currents. In *Advances in Neurology Vol. 51: Alzheimer's Disease*. Eds. Wurtman, J. et al., pp 227-233, Raven Press, New York.
- HAWKINS, R. A. & MILLER, A. L. (1978) Loss of radioactive 2-deoxy-d-glucose-6-phosphate from brains of conscious rats: implications for quantitative autoradiographic determination of regional glucose utilization. *Neuroscience* **3**, 251-258.
- HJORTH-SIMONSEN, A. (1972) Projection of the lateral part of the entorhinal area to the fascia dentata. *J. Comp. Neurol.* **147**, 219-232.

- HJORTH-SIMONSEN, A. & JEUNE, B. (1972) Origin and termination of the hippocampal perforant path in the rat studied by silver impregnation. *J. Comp. Neurol.* **144**, 215-232.
- HONORE, T., DAVIES, S. N., DREJER, J., FLETCHER, E. J., JACOBSEN, P., LODGE, D. & NIELSEN, F. E. (1988) Quinoxalinediones: potent competitive non-NMDA glutamate receptor antagonists. *Science* **241**, 701-703.
- HONORE, T., LAURIDSEN, J. & KROGSGAARD-LARSEN, P. (1982) The binding of [³H]-AMPA, a structural analogue of glutamic acid, to rat brain membranes. *J. Neurochem.* **38**, 173-178.
- HONORE, T. & NIELSEN, M. (1985) Complex structure of quisqualate-sensitive glutamate receptors in rat cortex. *Neurosci. Lett.* **54**, 27-32.
- HOPKINS, W. F. & JOHNSTON, D. (1984) Frequency-dependent noradrenergic modulation of long-term potentiation in the hippocampus. *Science* **226**, 350-352.
- HORSBURGH, K., DEWAR, D., GRAHAM, D. I. & McCULLOCH, J. (1991) Autoradiographic imaging of [³H]-phorbol 12,13 dibutyrate binding to protein kinase C in Alzheimer's Disease. *J. Neurochem.* **56**, 1121-1129.
- HORSBURGH, K., INGLIS, F. M. & McCULLOCH, J. (1991b) Increased [³H]-forskolin and [³H]-phorbol 12,13 dibutyrate binding in the hippocampus following excitotoxic lesions of the rat medial septum. *Soc. Neurosci. Abstr.* **17**, 240.2.
- HUME ADAMS, J. & GRAHAM, D. I. (1988) *An introduction to neuropathology*. Churchill Livingstone, Edinburgh, p 40.
- HUPPERT, F. A. & TYM, E. (1986) Clinical and neuropathological assessment of dementia. *Brit. Med. Bull.* **42**, 11-18.

- HYMAN, B. T., VAN HOESEN, G. W., DAMASIO, A. R. & BARNES, C. L. (1984) Alzheimer's disease: cell specific pathology isolates the hippocampal formation. *Science*, **225**, 1168-1170.
- INGLIS, F. M., KURODA, Y., MILLER, J., McCULLOCH, J., GRAHAM, D. I. & BULLOCK, R. (1991) The competitive NMDA antagonist D-CPP-ene reduces glucose hypermetabolism and infarct size after acute subdural haematoma. *J. Cereb. Blood Flow Metab.* **11**, Suppl. 2, S225.
- ISHIMORI, A. & YAMAGATA, S. (1982) Therapeutic effect of pirenzepine dihydrochloride on gastric ulcer evaluated by a double-blind controlled study. *Arzneimittelforsch/ Drugs Res.* **32**, 556-565.
- IZUMIYAMA, K., KOGURE, K., KATAOKA, S. & NAGATA, T. (1987) Quantitative analysis of glucose after transient ischemia in the gerbil hippocampus by light and electron microscope radioautography. *Brain Res.*, **416**, 175-179.
- JAHN, C. E. & STEVENS, C. F. (1987) Glutamate activates multiple single channel conductances in hippocampal neurons. *Nature* **325**, 522-525.
- JAMIESON, K. G. & YELLAND, J. D. N. (1972) Surgically treated traumatic subdural hematomas. *J. Neurosurg.* **37**, 137-149.
- JANOWSKY, A. LABARCA, R. & PAUL, S. M. (1984) Characterization of neurotransmitter receptor-mediated phosphatidylinositol hydrolysis in the rat hippocampus. *Life Sci.* **35**, 1953-1961.
- JOYCE, J. N., GIBBS, R. W., COTMAN, C. W. & MARSHALL, J. F. (1989) Regulation of muscarinic receptors in hippocampus following cholinergic denervation and reinnervation by septal and striatal transplants. *J. Neurosci.* **9**, 2776-2791.
- KAMIYA, H.-O., ROTTER, A. & JACOBOWITZ, D. M. (1981) Muscarinic receptor binding following cholinergic nerve lesions of the cingulate cortex and hippocampus of the rat brain. *Brain Res.* **209**, 432-439.

- KAUER, J. A., MALENKA, R. C. & NICOLL, R. A. (1988) A persistent post-synaptic modification mediates long-term potentiation in the hippocampus. *Neuron* **1**, 911-917.
- KELLY, E., ROONEY, T. A. & NAHORSKY, S. R. (1985a) Pertussis toxin separates two muscarinic receptor-effector mechanisms in the striatum. *Eur. J. Pharmacol.* **119**, 129-130.
- KELLY, P.A.T., GAGE, F. H., INGVAR, M., LINDVALL, O., STENEVI, U. & BJORKLUND, A. (1985b) Functional reactivation of the deafferentated hippocampus by embryonic septal grafts as assessed by measurements of local glucose utilization. *Exp. Brain Res.* **58**, 570-579.
- KELLY, P. A. T. & McCULLOCH, J. (1987) Cerebral glucose utilization following striatal lesions: the effects of the GABA agonist, muscimol, and the dopaminergic agonist, apomorphine. *Brain Res.* **425**, 290-300.
- KEMP, J. A., FOSTER, A. C. & WONG, E. H. F. (1987) Non-competitive antagonists of excitatory amino acid receptors. *Trends Neurosci.* **10**, 294-298.
- KHACHATURIAN, Z. S. (1985) Diagnosis of Alzheimer's Disease. *Arch. Neurol.* **42**, 1097-1104.
- KIDD, M. (1963) Paired helical filaments in electron microscopy of Alzheimer's disease. *Nature* **197**, 192-193.
- KIRINO, T. (1982) Delayed neuronal death in the gerbil hippocampus following ischemia. *Brain Res.* **239**, 57-69.
- KIYOSAWA, M., BARON, J.-C., HAMEL, E., PAPPATA, S., DUVERGER, D., RICHE, D., MAZOYER, B., NAQUET, R. & MacKENZIE, E. T. (1989) Time course of effects of unilateral lesions of the nucleus basalis of Meynert on glucose utilization by the cerebral cortex: positron tomography in baboons. *Brain* **112**, 435-455.

- KLEINSCHMIDT, A., BEAR, M. F. & SINGER, W. (1986) Blockade of "NMDA" receptors disrupts experience-dependent plasticity of kitten striate cortex. *Science* **238**, 355-358.
- KOHLER, C., SHIPLEY, M. T., SREBRO, B. & HARKMARK, W. (1978) Some retrohippocampal afferents to the entorhinal cortex. Cells of origin as studied by the HRP method in the rat and mouse. *Neurosci. Lett.* **10**, 115-120.
- KOHLER, C. (1986) Intrinsic connections of the retrohippocampal region in the rat brain. II. The medial entorhinal area. *J. Comp. Neurol.* **246**, 149-169.
- KOHLER, C., CHAN-PALAY, V. & WU, J.-W. (1984) Septal neurons containing glutamic acid decarboxylase immunoreactivity project to the hippocampal region in the rat brain. *Anat. Embryol.* **169**, 41-44.
- KOZLOWSKI, M. R. (1986) Effects of σ agonist compounds on local cerebral glucose utilization: relationship to psychotomimetic properties. *Brain Res.* **376**, 190-193.
- KOZUKA, M., SMITH, M.-L. & SIESJO, B. K. (1989), Preischemic hyperglycemia enhances postischemic depression of metabolic rate. *J. Cereb. Blood Flow Metab.* **9**, 478-490.
- KRNJEVIC, K. & ROPERT, N. (1982) Electrophysiological and pharmacological characteristics of facilitation of hippocampal population spikes by stimulation of the medial septum. *Neurosci.* **7**, 2165-2183.
- KUHAR, M. J. (1981) Autoradiographic localisation of drug and neurotransmitter receptors in the brain. *Trends Neurosci.* **4**, 60-64.

- KURODA, Y., INGLIS, F. M., MILLER, J. D., McCULLOCH, J., GRAHAM, D. I. & BULLOCK, R. (1992) Transient glucose hypermetabolism after acute subdural haematoma in the rat. *J. Neurosurg.* **76**, 471-477.
- KURUMAJI, A., NEHLS, D. G., PARK, C. K. & McCULLOCH, J. (1989) Effects of NMDA antagonists, MK-801 and CPP, upon local cerebral glucose use. *Brain Res.* **496**, 268-284.
- KURUMAJI, A. & McCULLOCH, J. (1989) Effects of MK-801 upon local cerebral glucose utilisation in conscious rats and in rats anaesthetised with halothane. *J. Cereb. Blood Flow Metab.* **9**, 786-794.
- KURUMAJI, A. & McCULLOCH, J. (1990a) Effects of unilateral intrahippocampal injection of MK-801 upon local cerebral glucose utilisation in conscious rats. *Brain Res.* **518**, 342-346.
- KURUMAJI, A. & McCULLOCH, J. (1990b) Effects of MK-801 upon local cerebral glucose utilisation in conscious rats following unilateral lesion of caudal entorhinal cortex. *Brain Res.* **531**, 72-82.
- KUSCHINSKI, W., SUDA, S. & SOKOLOFF, L. (1987) Local cerebral glucose utilization and blood flow during metabolic acidosis. *Am. J. Physiol.* **241**, H772-H777.
- LAMARCA, M. V. & FIBIGER, H. C. (1984) Deoxyglucose uptake and choline acetyltransferase activity in cerebral cortex following lesions of the nucleus basalis magnocellularis. *Brain Res.* **307**, 366-369.
- LAZARENO, S., KENDALL, D. A. & NAHORSKY, S. R. (1985) Pirenzepine indicates heterogeneity of muscarinic receptors linked to cerebral inositol phospholipid metabolism. *Neuropharmacology* **24**, 593-595.
- LEE, T. W. T., SOLE, M. J. & WELLS, J. W. (1986) Assessment of a ternary model for the binding of agonists to neurohumoral receptors. *Biochemistry* **25**, 7009-7020.

- LEHMANN, J., SCHNEIDER, J., MCPHERSON, S., MURPHY, D. E., BERNARD, P., TSAI, C., BENNET, D. A., PASTOR, G., STEEL, D. J., BOEHM, C., LIEBMAN, J. M., WILLIAMS, M. & WOOD, P. L. (1987) CPP, a selective N-methyl-D-aspartate (NMDA)-type receptor antagonist: characterization *in vitro* and *in vivo*. *J. Pharmacol. Exp. Ther.* **240**, 737-746.
- LEWIS, P. R., SHUTE, C. C. D. & SILVER, A. (1967) Confirmation from choline acetylase analyses of a massive cholinergic innervation to the rat hippocampus. *J. Physiol. (Lond.)* **191**, 215-224.
- LINDEN, D. J., WONG, K. L., SHEU, F.-S. & ROUTTENBERG, A. (1988) NMDA receptor blockade prevents the increase in protein kinase C substrate (protein F1) phosphorylation produced by long-term potentiation. *Brain Res.* **175**, 142-146.
- LONDON, E. D., CONNOLLY, R. J., SZIKSZAY, M., WAMSLEY, J. K. & DAM, M. (1988) Effects of nicotine on local cerebral glucose utilization in the rat. *J. Neurosci.* **8**, 3920-3928.
- LORENTE DE NO (1934) Studies on the structure of the cerebral cortex. II. Continuation of the ammonic system. *J. Psychol. Neurol.* **46**, 113-117.
- LOSCHER, W., HONACK, D. & FASBENDER, C.-P. (1991) Regional alterations in brain amino acids after administration of the N-methyl-D-aspartate receptor antagonists MK-801 and CGP 39551. *Neurosci. Lett.* **124**, 115-118
- LOWE, S. L., FRANCIS, P. T., PROCTER, A. W., PALMER, A. M., DAVISON, A. N. & BOWEN, D. M. (1988) Gamma-aminobutyric acid concentration in brain tissue at two stages of Alzheimer's Disease. *Brain* **111**, 789-799.

- LOWE, D. A., NEIJT, H. C. & AEBISCHER, B. (1990) D-CPP-ene (SDZ EAA 494), a potent and competitive N-methyl-D-aspartate (NMDA) antagonist: effect on spontaneous activity and NMDA-induced depolarizations in the rat neocortical slice preparation, compared with other CPP derivatives and MK-801. *Neurosci. Lett.* **113**, 315-321.
- LUCAS, D. R. & NEWHOUSE, J. P. (1957) The toxic effect of sodium L-glutamate on the inner layers of the retina. *Arch. Ophthalmol.* **58**, 193-201.
- LUND, J. P., MILLER, J. J. & COURVILLE, J. (1981) [³H]2-deoxy-D-glucose capture in the hippocampus and dentate gyrus of ketamine anesthetized rat. *Neurosci. Lett.* **24**, 149-153.
- LUTHIN, G. R. & WOLFE, B. B. (1984) [³H]-Pirenzepine and [³H]-quinuclidinyl benzilate binding to rat brain muscarinic cholinergic receptors. *Molec. Pharmacol.* **26**, 164-169.
- LYNCH, G. & BAUDRY, M. (1984) The biochemistry of memory: a new and specific hypothesis. *Science* **224**, 1057-1063.
- LYNCH M. A., CLEMENTS, M. P., ERRINGTON, M. L. & BLISS, T. V. P. (1988) Increased hydrolysis of phosphatidyl-4,5-biphosphate in long-term potentiation. *Neurosci. Lett.* **84**, 291-296.
- LYZAKOWSKI, A., WAINER, B. H., BRUCE, G. & HERSH, L. B. (1989) An atlas of the regional and laminar distribution of choline acetyltransferase immunoreactivity in rat cerebral cortex. *Neuroscience* **28**, 291-336.
- MacDERMOTT, A. & DALE, N. (1987) Receptors, ion channels and synaptic potentials underlying the integrative actions of excitatory amino acids. *Trends Neurosci.* **10**, 280-284.
- MALENKA, R. C., KAUER, J. A., ZUCKER, R. S. & NICOLL, R. A. (1988) Postsynaptic calcium is sufficient for potentiation of hippocampal synaptic transmission. *Science* **242**, 81-84.

- MANN, D. M. A. (1988) Neuropathological and neurochemical aspects of Alzheimer's Disease. In *Handbook of Psychopharmacology, Vol. 20*, Iversen, L. L. et al. (Eds.) Plenum Press, pp 1-67.
- MANN, D. M. A., YATES, P. O. & MARCYNIUK, B. (1985) Some morphometric observations on the cerebral cortex and hippocampus in presenile Alzheimer's disease, senile dementia of the Alzheimer type and Down's syndrome in middle age. *J. Neurol. Sci.* **69**, 139-159.
- MALINOW, R., MADISON, D. V. & TSIEN, R. W. (1988) Persistent protein kinase activity underlying long-term potentiation. *Nature* **335**, 820-824.
- MARAGOS, W. F., CHU, D. C. M., YOUNG, A. B., D'AMATO, C. J. & PENNEY, J. B. (1987) Loss of hippocampal [³H]-TCP binding in Alzheimer's Disease. *Neurosci. Lett.* **74**, 371-376.
- MASH, D. C., FLYNNE, D. D. & POTTER, L. T. (1985) Loss of M2 muscarinic receptors in the cerebral cortex in Alzheimer's Disease and experimental cholinergic denervation. *Science* **228**, 1115-1117.
- MASH, D. C. & POTTER, L. T. (1986) Autoradiographic localization of M1 and M2 muscarine receptors in the rat brain. *Neuroscience* **19**, 551-564.
- MATTHEWS, D. A., COTMAN, C. & LYNCH, G. (1976) An electron microscopic study of lesion-induced synaptogenesis in the dentate gyrus of the adult rat. I. Magnitude and time-course of degeneration. *Brain Res.* **115**, 1-21.
- MASLIAH, E., COLE, G., SHIMOHAMA, S., HANSEN, L., DeTERESA, R., TERRY, R. & SAITOH, T. (1990) Differential involvement of protein kinase C isozymes in Alzheimer's Disease. *J. Neurosci.* **10**, 2113-2124.

- McCULLOCH, J. (1982) Mapping functional alterations in the CNS with [¹⁴C]deoxyglucose. In *Handbook of Psychopharmacology, Vol. 15*, Iversen, L. L. et al. (eds.), Plenum Press, pp 321-410.
- McCULLOCH, J. & IVERSEN, L. L. (1991) Autoradiographic assessment of the effects of N-methyl-D-aspartate (NMDA) receptor antagonists in vivo. *Neurochemical Research* **16**, 951-963.
- McDONALD, J. W., SILVERSTEIN, F. S. & JOHNSTON, M. V. (1987) MK-801 protects the neonatal brain from hypoxic-ischemic damage. *Eur. J. Pharmacol.*, **140**, 359-361.
- McGEER, P. L., McGEER, E. G., SUZUKI, J., DOLMAN, C. E. & NAGAI, T. (1984) Aging, Alzheimer's Disease and the cholinergic system of the basal forebrain. *Neurology* **34**, 741-745.
- McKINNEY, M. & COYLE, J. T. (1982) Regulation of neocortical muscarinic receptors: effects of drug treatment and lesions. *J. Neurosci.* **2**, 97-105.
- McLENNAN, H. & LODGE, D. (1979) The antagonism of amino acid-induced excitation of spinal neurones in the cat. *Brain Res.* **169**, 83-90.
- McNAUGHTON, B. L. (1980) Evidence for two physiologically distinct perforant pathways to the fascia dentata. *Brain Res.* **199**, 1-19.
- MEIBACH, R. C. & SIEGEL, A. (1977) Efferent connections of the septal area in the rat: an analysis utilizing retrograde and anterograde transport methods. *Brain Res.* **119**, 1-20.
- MELLGREN, S. I. & SREBRO, B. (1973) Changes in acetylcholinesterase and distribution of degenerating fibres in the hippocampal region after septal lesions in the rat. *Brain Res.* **52**, 19-36.
- MESULAM, M.-M., MUFSON, E. J., WINER, B. H. & LEVEY, A. I. (1983) Central cholinergic pathways in the rat: an overview based on an alternative nomenclature. *Neuroscience* **10**, 1185-1201.

- MEYER, E. M. & OTERO, D. H. (1985) Pharmacological and ionic characterizations of the muscarinic receptors modulating acetylcholine release from rat cortical synaptosomes. *J. Neurosci.* **5**, 1202-1207.
- MILLAN, M. H., PATEL, S. & MELDRUM, B. S. (1988) The involvement of excitatory amino acid receptors within the prepiriform cortex in pilocarpine-induced limbic seizures in rats. *Exp. Brain Res.* **72**, 517-522.
- MILLER, J. D., BULLOCK, R., GRAHAM, D. I., CHEN, M.-H. & TEASDALE, G. M. (1990) Ischemic brain damage in a model of acute subdural hematoma. *Neurosurgery* **27**, 433-439.
- MILNER, T. A. & AMARAL, D. G. (1984) Evidence for a ventral septal projection to the hippocampal formation of the rat. *Exp. Brain Res.* **55**, 579-585.
- MILNER, T. A., LOY, R. & AMARAL, D. G. (1983) An anatomical study of the development of the septohippocampal projection in the rat. *Dev. Brain Res.* **8**, 343-371.
- MISHKIN, M. (1978) Memory in monkeys severely impaired by combined but not by separate removal of amygdala and hippocampus. *Nature* **273**, 297-298.
- MODY, I. & HEINEMANN, U. (1987) NMDA receptors of dentate gyrus granule cells participate in synaptic transmission following kindling. *Nature* **326**, 701-704.
- MODY, I., SALTER, M. W. & MacDONALD, J. F. (1988) Requirement of NMDA receptor/channels for intracellular high-energy phosphates and the extent of intraneuronal calcium buffering in cultured mouse hippocampal neurons. *Neurosci. Lett.* **93**, 73-78.

- MONAGHAN, D. T. (1991) Differential stimulation of [³H]MK-801 binding to subpopulations of NMDA receptors. *Neurosci. Lett.* **122**, 21-24.
- MONAGHAN, D. T. & COTMAN, C. W. (1985) Distribution of N-methyl-D-aspartate-sensitive L-[³H] glutamate-binding sites in rat brain. *J. Neurosci.* **5**, 2909-2919.
- MONAGHAN, D. T., GEDDES, J. W., YAO, D., CHUNG, C. & COTMAN, C. W. (1987) [³H]TCP binding in Alzheimer's Disease. *Neurosci. Lett.* **73**, 197-200.
- MONAGHAN, D. T., HOLETS, V. R., TOY, D. W. & COTMAN, C. W. (1983) Anatomical distributions of four pharmacologically distinct ³H-L-glutamate binding sites. *Nature* **306**, 176-179.
- MONAGHAN, D. T., YAO, D. & COTMAN, C. W. (1984) Distribution of [³H]AMPA binding sites in rat brain as determined by quantitative autoradiography. *Brain Res.* **324**, 160-164.
- MONAGHAN, D. T., MENA, E. & COTMAN, C. W. (1982) The effect of entorhinal cortical ablation on the distribution of muscarinic cholinergic receptors in the rat hippocampus. *Brain Res.* **234**, 480-485.
- MONSMA, F. J., ABOOD, L. G. & HOSS, W. (1988) Inhibition of phosphoinositide turnover by selective muscarinic antagonists in the rat striatum. *Biochemical Pharmacology* **37**, 2437-2443.
- MOORE, R. Y. & BLOOM, F. E. (1978) Central catecholamine neuron systems: anatomy and physiology of the dopamine systems. *Ann. Rev. Neurosci.* **1**, 129-169.
- MORRIS, R. G. M. (1989) Synaptic plasticity and learning: selective impairment of learning in rats and blockade of long-term potentiation *in vivo* by the N-methyl-D-aspartate receptor antagonist AP5. *J. Neurosci.* **9**, 3040-3057.

- MORRIS, R. G. M., ANDERSON, E., LYNCH, G. S. & BAUDRY, M. (1986) Selective impairment of learning and blockade of long-term potentiation by an N-methyl-D-aspartate receptor antagonist, AP5. *Nature*, **319**, 774-776.
- MOSKO, S., LYNCH, G. & COTMAN, C. W. (1973) The distribution of septal projections to the hippocampus of the rat. *J. Comp. Neurol.* **152**, 163-174.
- MOUNTJOY, C. Q., ROSSOR, M. N., IVERSEN, L. L. & ROTH, M. (1984) Correlation of cortical cholinergic and GABA deficits with quantitative neuropathological findings of senile dementia. *Brain* **107**, 507-518.
- MOUNTJOY, C. Q. (1986) Correlations between neuropathological and neurochemical changes. *Brit. Med. Bull.* **42**, 81-85.
- MOUNTJOY, C. Q., ROTH, M., EVANS, N. J. R. & EVANS, H. M. (1983) Cortical neuronal counts in normal elderly controls and demented patients. *Neurobiol. Aging* **4**, 1-11.
- MULLER, D., JOLY, M. & LYNCH, G. (1988a) Contributions of quisqualate and NMDA receptors to the induction and expression of LTP. *Science* **242**, 1694-1697.
- MULLER, D. & LYNCH, G. (1988) Long-term potentiation differentially affects two components of synaptic responses in hippocampus. *Proc. Natl. Acad. Sci. USA* **85**, 9346-9350.
- MULLER, D., TURNBULL, J., BAUDRY, M. & LYNCH, G. (1988b) Phorbol ester-induced synaptic facilitation is different than long-term potentiation. *Proc. Natl. Acad. Sci. USA* **85**, 6997-7000.

- NADLER, J. V., MARTIN, D., BUSTOS, G. A., BURKE, S. P. & BOWE, M. A. (1990) Regulation of glutamate and aspartate release from the Schaffer collaterals and other projections of CA3 hippocampal pyramidal cells. In *Progress in Brain Research*, Vol 83, Storm-Mathisen et al. (Eds.), Elsevier, Amsterdam pp 115-130.
- NADLER, J. V., VACA, K. W., WHITE, W. F., LYNCH, G. S. & COTMAN, C. W. (1976) Aspartate and glutamate as possible transmitters of excitatory hippocampal afferents. *Nature* **260**, 538-540.
- NAKAI, H., MATSUDA, H., TAKARA, E., DIKSIC, M., YAMAMOTO, Y. L., MEYER, E. & REDIES, C. (1988) Changes in lumped and rate constants in experimental cerebral ischemia – intra-animal comparison before and after middle cerebral artery occlusion. *Neurol. Med. Chir. (Tokyo)* **28**, 11-17.
- NEARY, D., SNOWDEN, J. S., MANN, D. M. A., BOWEN, D. M., SIMS, N. W., NORTHEN, B., YATES, P. O. & DAVISON, A. N. (1986) Alzheimer's Disease: a correlative study. *J. Neurol. Neurosurg. Psychiat.* **49**, 229-237.
- NEDERGAARD, M., GJEDDE, A. & DIEMER, N. H. (1986) Focal ischemia of the rat brain: autoradiographic determination of cerebral glucose utilization, glucose content, and blood flow. *J. Cereb. Blood Flow Metab.* **6**, 414-424.
- NELSON, S. R., DOULL, J., TOCKMAN, B. A., CHRISTIANO, P. J. & SAMSON, F. E. (1978) Regional brain metabolism changes induced by acetylcholinesterase inhibitors. *Brain Res.* **157**, 186-190.
- NEWMAN, M. E., KLEIN, E., BIRMAKER, B., FEINSOD, M. & BELMAKER, R. H. (1983) Lithium at therapeutic concentrations inhibits human brain adrenaline-sensitive cAMP accumulation. *Brain Res.* **278**, 380-381.

- NICOLETTI, F., MEEK, J. L., IADAROLA, M. J., CHUANG, D. M., ROTH, B. L. & COSTA, E. (1986) Coupling of inositol phospholipid metabolism with excitatory amino acid recognition sites in rat hippocampus. *J. Neurochem.* **46**, 40-46.
- NICOLETTI, F., VALERIO, C., PELLEGRINO, C., DRAGO, F., SCAPAGNINI, U. & CANONICO, P. L. (1988) Spatial learning potentiates the stimulation of phosphoinositide hydrolysis by excitatory amino acids in rat hippocampal slices. *J. Neurochem.* **51**, 725-729.
- NICOLL, R. A. (1985) The septohippocampal projection: a model cholinergic pathway. *Trends Neurosci.* **8**, 533-536.
- NICHOLLS, D. & ATTWELL, D. (1990) The release and uptake of excitatory amino acids. *Trends Pharmacol. Sci.* **11**, 462-468.
- NILSSON, L., ADEM, A., HARDY, J., WINBLAD, B. & NORDBERG, A. (1987) Do tetrahydroaminoacridine (THA) and physostigmine restore acetylcholine release in Alzheimer brains via nicotinic receptors? *J. Neural Transm.* **70**, 357-368.
- NORDBERG, A. & WINBLAD, B. (1986) Reduced number of [³H]nicotine and [³H]acetylcholine binding sites in the frontal cortex of Alzheimer brains. *Neurosci. Lett.* **72**, 115-119.
- NORMAN, A. B., BLAKER, S. N., THAL, L. & CREESE, I. (1986) Effects of aging and cholinergic deafferentation on putative muscarinic cholinergic receptor sub-types in rat cerebral cortex. *Neurosci. Lett.* **70**, 289-294.
- NOWAK, L., BREGESTROVSKI, P., ASCHER, P., HERBERT, A. & PROCHIANTZ, Z. (1984) Magnesium gates glutamate-activated channels in mouse central neurones. *Nature* **307**, 462-465.
- NYAKAS, C., LUITEN, P. G. M., SPENCER, D. G. & TRABER, J. (1987) Detailed projection patterns of septal and diagonal band efferents to the hippocampus in the rat with emphasis on innervation of CA1 and dentate gyrus. *Brain Res. Bull.* **18**, 533-545.

- OGUCHI, K., ARAKAWA, K., NELSON, S. R. & SAMSON, F. (1982) The influence of droperidol, diazepam, and physostigmine on ketamine-induced behavior and brain regional glucose utilization in rat. *Anesthesiology* **57**, 353-358.
- O'KEEFE, J. & NADEL, L. (1978) *The hippocampus as a cognitive map*. Clarendon Press, Oxford.
- OLNEY, J. W., HO, O. L. & RHEE, V. (1971) Cytotoxic effects of acidic and sulphur-containing amino acids on the infant mouse central nervous system. *Exp. Brain Res.* **14**, 61-76.
- OLNEY, J. W., LABRUYERE, J. & PRICE, M. T. (1989) Pathological changes induced in cerebrocortical neurons by phencyclidine and related drugs. *Science* **244**, 1360-1362.
- OLNEY, J., PRICE, M., SALLES, K. S., LABRUYERE, J. & FRIERDICH, G. (1987) MK-801 powerfully protects against N-methyl aspartate neurotoxicity. *Eur. J. Pharmacol.*, **141**, 357-361.
- OLNEY, J. W. & SHARPE, L. G. (1969) Brain lesions in an infant rhesus monkey treated with monosodium glutamate. *Science* **166**, 386-388.
- OLVERMAN, H. J., MONAGHAN, D. T., COTMAN, C. W. & WATKINS, J. (1986) [³H] CPP, a new competitive ligand for NMDA receptors. *Eur. J. Pharmacol.* **131**, 161-162.
- ONALI, P., OLIANAS, M. C., SCHWARTZ, J. P. & COSTA, E. (1983) Involvement of a high-affinity GTPase in the inhibitory coupling of striatal muscarinic receptors to adenylate cyclase. *Molec. Pharmacol.* **24**, 380-386.

- ONODERA, H., ARAKI, T. & KOGURE, K. (1989) Protein kinase C activity in the rat hippocampus after forebrain ischaemia: autoradiographic analysis by [³H]-phorbol 12,13 dibutyrate. *Brain Res.* **487**, 343-347.
- ONODERA, H. & KOGURE, K. (1989) Mapping second messenger systems in the rat hippocampus after transient forebrain ischemia: in vitro [³H]forskolin and [³H]inositol 1,4,5 trisphosphate binding. *Brain Res.* **487**, 343-347.
- ORRENIUS, S., McCONKEY, D. J., BELLOMO, G. & NICOTERA, P. (1989) Role of Ca²⁺ in toxic cell killing. *Trends Neurosci.* **10**, 281-285.
- OSTERRIEDER, W. (1987) 9-Amino-1,2,3,4-tetrahydroacridine (THA) is a potent blocker of cardiac potassium channels. *Br. J. Pharmacol.* **92**, 521-525.
- OTTE, A. P., van RUN, P., HELDEVELD, M., van DRIEL, R. & DURSTON, A. T. (1989) Neural induction is mediated by cross-talk between the protein kinase C and cyclic AMP pathways. *Cell* **58**, 641-648.
- OTTERSEN, O. P. (1982) Connections of the amygdala of the rat. IV. Corticoamygdaloid and intraamygdaloid connections as studied with axonal transport of horseradish peroxidase. *J. Comp. Neurol.* **205**, 30-48.
- OTTERSEN, O. P. & STORM-MATHISEN, J. (1984) Neurons containing or accumulating transmitter amino acids. In *Handbook of Chemical Neuroanatomy*, A. Bjorklund et al., (Eds.), Elsevier Amsterdam. pp 141-246.
- OVERSTREET, D. H., SPETH, R. C., HRUSKA, R. E., EHLERT, E., DUMONT, Y. & YAMAMURA, H. I. (1980) Failure of septal lesions to alter muscarinic cholinergic or benzodiazepine binding sites in hippocampus of rat brain. *Brain Res.* **195**, 203-207.

- OZYURT, E., GRAHAM, D. I., WOODRUFF, G. N. & McCULLOCH, J. (1988) Protective effect of the glutamate antagonist, MK-801 in focal cerebral ischemia in the cat. *J. Cereb. Blood Flow Metab.* **8**, 138-143.
- PANETTA, J. A., PHILLIPS, M. L. & CLEMENS, J. A. (1989) Effects of various pharmacological treatments on brain damage in rats subjected to cerebral ischemia. *J. Cereb. Blood Flow Metab.* **9 (Suppl. 1)**, S635.
- PARDRIDGE, W. M., TRIGUERO, D., YANG, J. & CANCELLA, P. A. (1990) Comparison of in vitro and in vivo models of drug transcytosis through the blood-brain barrier. *J. Pharmacol. Exp. Ther.* **253**, 884-889.
- PARK, C. K., NEHLS, D. G., GRAHAM, D. I., TEASDALE, G. M. & McCULLOCH, (1988a) The glutamate antagonist MK-801 reduces focal ischemic brain damage in the rat. *Ann. Neurol.* **24**, 543-551.
- PARK, C. K., NEHLS, D. G., GRAHAM, D. I., TEASDALE, G. M. & McCULLOCH, (1988b) Focal cerebral ischaemia in the cat: treatment with the glutamate antagonist MK-801 after induction of ischaemia. *J. Cereb. Blood Flow Metab.* **8**, 757-762.
- PAXINOS, G. & WATSON, C. (1986) *The rat brain in stereotaxic coordinates* (2nd edition) Academic Press, Australia.
- PEARSON, R. C. A., ESIRI, M. M., HIORNS, R. W., WILCOCK, G. K. & POWELL, T. P. S. (1985) Anatomical correlates of the distribution of the pathological changes in the neocortex in Alzheimer disease. *Proc. Natl. Acad. Sci. USA* **82**, 4531-4534.
- PEARSON, R. C. A., GATTER, K. C. & POWELL, T. P. S. (1983) Retrograde degeneration in the basal nucleus in monkey and man. *Brain Res.* **261**, 321-326.
- PEINADO, J. M. & MORA, F. (1986) Glutamic acid as a putative transmitter of the interhemispheric corticocortical connections in the rat. *J. Neurochem.* **47**, 1598-1603.

- PENG, C. T. (1977) Sample preparation in liquid scintillation. *Radiochem. Centre Rev.* **17**.
- PERRY, E. K., PERRY, R. H., BLESSED, G. & TOMLINSON, B. E. (1977) Necropsy evidence of cerebral cholinergic deficits in senile dementia. *Lancet* (i) 189.
- PERRY, E. K., PERRY, R. H., SMITH, C. J., PUROHIT, D., DICK, D. J., CANDY, J. M., EDWARDSON, J. A. & FAIRBAIRN, A. (1986) Cholinergic receptors in cognitive disorders. *Can. J. Neurol. Sci.* **13**, 521-527.
- PERRY, E. K., TOMLINSON, B. E., BLESSED, G., BERGMANN, K., GIBSON, P. & PERRY, R. H. (1978) Correlation of cholinergic abnormalities with senile plaques and mental test scores in senile dementia. *Brit. Med. J.* (ii) 1457-1459.
- PERRY, R. H. (1986) Recent advances in neuropathology. *Brit. Med. Bull.* **42**, 34-41.
- PERSSON, L., HARDEMARK, H. G., BOLANDER, H. G., HILLERED, L. & OLSSON, Y. (1989) Neurologic and neuropathologic outcome after middle cerebral artery occlusion in rats. *Stroke* **20**, 641-645.
- PETERSEN, D. W., COLLINS, J. F. & BRADFORD, H. F. (1983) The kindled amygdala model of epilepsy: anticonvulsant action of amino acid antagonists. *Brain Res.* **275**, 169-172.
- PHAN, D. V., DODA, M., BILE, A. & GYORGY, L. (1973) Antinociceptive activity of nicotine. *Acta Physiol. Acad. Sci. Hung.* **1**, 85-93.
- PIREDDA, S. & GALE, K. (1986) Role of excitatory amino acid transmission in the genesis of seizures elicited from the deep prepiriform cortex. *Brain Res.* **377**, 205-210.

- PORRINO, L. J., HUSTON-LYONS, D., BAIN, G., SOKOLOFF, L. & KORNITSKY, C. (1990) The distribution of changes in local energy metabolism associated with brain stimulation reward to the medial forebrain bundle of the rat. *Brain Res.* **511**, 1-6.
- POTTER, L. T. & FERRENDELLI, C. A. (1989) Affinities of different cholinergic agonists for the high and low affinity states of hippocampal M1 muscarine receptors. *J. Pharmacol. Exp. Ther.* **248**, 974-978.
- PULSINELLI, W. A., BRIERLEY, J. B. & PLUM, F. (1982a) Temporal profile of neuronal damage in a model of transient forebrain ischemia. *Ann Neurol.* **11**, 491-498.
- PULSINELLI, W. A., LEVY, D. E. & DUFFY, T. E. (1982b) Regional cerebral bloodflow and glucose metabolism following transient forebrain ischemia. *Ann Neurol.* **11**, 499-509.
- QUIRION, R., CHIUEH, C. C., EVERIST, H. D. & PERT, A. (1985) Comparative localization of neurotensin receptors on nigrostriatal and mesolimbic dopaminergic terminals. *Brain Res.* **327**, 385-389.
- QUIRION, R., MARTEL, J. C., ROBITAILLE, Y., ETTIENNE, P., WOOD, P., NAIR, N. P. V. & GAUTHIER, S. (1986) Neurotransmitter and receptor deficits in senile dementia of the Alzheimer type. *Can. J. Neurol. Sci.* **13**, 503-510.
- RAINBOW, T. C., WIECZOREK, C. M. & HALPAIN, S. (1984) Quantitative autoradiography of binding sites for [³H]AMPA, a structural analogue of glutamic acid. *Brain Res.* **309**, 173-177.
- RAMON Y CAJAL, S. (1911) *Histologie du Système Nerveux de l'Homme et des Vertébrés*. Norbert Maloine, Paris.
- RAPOPORT, S. I., OHNO, K. & PETTIGREW, K. D. (1979) Drug entry into the brain. *Brain Res.* **172**, 354-359.

- RAULLI, R. E., AENDISH, G. & CREWS, F. (1989) Effects of nBM lesions on muscarinic-stimulation of phosphoinositide hydrolysis. *Neurobiol. Aging*, **10**, 191-197.
- REED, L. J. & de BELLEROCHE, J. (1988) Elevated polyphosphoinositide responsiveness and increased ornithine decarboxylase activity in the cerebral cortex induced by cholinergic denervation. *J. Neurochem.* **50**, 1566-1571.
- REGENOLD, W., ARAUJO, D. M. & QUIRION, R. (1989) Quantitative autoradiographic distribution of [³H]AF-DX 116 muscarinic M₂ receptor binding sites in rat brain. *Synapse* **4**, 115-125.
- REPRESA, A., DUYCKAERTS, C., TREMBLAY, E., HAUW, J. J. & BEN-ARI, Y. (1988) Is senile dementia of the Alzheimer type associated with hippocampal plasticity? *Brain Res.* **457**, 355-359.
- RICHTER, J. A., PERRY, E. K. & TOMLINSON, B. E. (1980) Acetylcholine and choline levels in postmortem brain tissue: preliminary observations in Alzheimer's Disease. *Life Sci.* **26**, 1683-1689.
- RINNE, J. O., RINNE, J. K., LAASKO, K., PAIJARVI, L. & RINNE, U. K. (1984) Reduction in muscarinic receptor binding in limbic areas of Alzheimer brain. *J. Neurol. Neurosurg. Psychiat.* **47**, 651-653.
- RISCHKE, R. & KREIGLSTEIN, J. (1991) Postischemic neuronal damage causes astroglial activation and increase in local cerebral glucose utilization of rat hippocampus. *J. Cereb. Blood Flow Metab.* **11**, 106-113.
- ROBBINS, T. W., EVERITT, B. J., MARSTON, H. M., WILKINSON, J., JONES, G. H. & PAGE, K. J. (1989) Comparative effects of ibotenic acid- and quisqualic acid-induced lesions of the substantia innominata on the attentional function in the rat: further implications for the role of the nucleus basalis in cognitive processes. *Behav. Brain Res.* **35**, 221-240.

- ROBBINS, T. W., EVERITT, B. J., MARSTON, H. M., JONES, G. H. & PAGE, K. J. (1989) Comparative effects of quisqualic and ibotenic acid-induced lesions of the substantia innominata and globus pallidus on the acquisition of a conditional visual discrimination: differential effects on cholinergic mechanisms. *Neuroscience* **28**, 337-352.
- ROD, M. R. & AUER, R. N. (1989) Pre- and post-ischemic administration of dizocilpine (MK-801) reduces cerebral necrosis in the rat. *Can. J. Neurol. Sci.* **16**, 340-344.
- ROOM, P. & TIELEMANS, A. J. P. C. (1989) Circadian variations in local cerebral glucose utilization in freely moving rats. *Brain Res.* **505**, 321-325.
- ROSSOR, M. & IVERSEN, L. L. (1986) Non-cholinergic neurotransmitter abnormalities in Alzheimer's Disease. *Brit. Med. Bull.* **42**, 70-74.
- ROWELL, P. W. & WINKLER, D. L. (1984) Nicotinic stimulation of [³H]-acetylcholine release from mouse cerebral cortical synaptosomes. *J. Neurochem.* **43**, 1593-1598.
- RYLETT, R. J., BALL, M. J. & COLHOUN, E. M. (1983) Evidence for high affinity choline transport in synaptosome prepared from hippocampus and neocortex of patients with Alzheimer's Disease. *Brain Res.* **284**, 169-175.
- SAITOH, T., MASLIAH, E., JIN, L. W., COLE, G. M., WEILOCH, T. & SHAPIRO, I. P. (1991) Protein kinases and phosphorylation in neurologic disorders and cell death. *Laboratory Investigation* **64**, 596-616.

- SANFELIU, C., HUNT, A. & PATEL, A. J. (1990) Death of subcortical cholinergic neurons in certain neurodegenerative disorders may not be due to an overstimulation of N-methyl-D-aspartate receptors. *Brain Res.* **506**, 319-322.
- SAPER, C. B. (1984) Organisation of cerebral cortical afferent systems in the rat. II. Magnocellular basal nucleus. *J. Comp. Neurol.* **222**, 313-342.
- SAPER, C. B., GERMAN, D. C. & WHITE, C. L. (1985) Neuronal pathology in nucleus basalis and associated cell groups in senile dementia of Alzheimer type: possible role in cell loss. *Neurology* **35**, 1089-1095.
- SAUER, D., NUGLISCH, J., ROSSBERG, C., MENNEL, H.-D., BECK, T., BIELENBERG, G. W. & KREIGLSTEIN, J. (1988) Phencyclidine reduces postischemic neuronal necrosis in rat hippocampus without changing bloodflow. *Neurosci. Lett.* **91**, 327-332.
- SAUNDERS, J. & FREEDMAN, S. B. (1989) The design of full agonists for the cortical muscarinic receptor. *Trends Pharmacol. Sci.* **10 (Suppl.)**, 70-75.
- SCARTH, B. J., JHAMANDAS, K., BOEGMAN, R. J., BENINGER, R. J. & REYNOLDS, J. N. (1989) Cortical Muscarinic receptor function following quinolinic acid-induced lesion of the nucleus basalis, magnocellularis. *Exp. Neurol.* **103**, 158-164.
- SCATCHARD, G. (1949) The attractions of protein for small molecules and ions. *Ann. NY Acad. Sci.* **51**, 660-672.
- SCHMUTZ, M., KLEBS, K., OLPE, H. R., OLPE, H.-R., ALLGEIER, H., HECKENDORN, R., ANGST, C., BRUNDISH, D., DINGWALL, J. G. & FAGG, G. E. (1989) CGP 37849/CGP 39551: Competitive NMDA receptor antagonists with potent oral anticonvulsant activity. *Br. J. Pharmacol.* **97**, 581P.

- SCHOEPP, D. D. & JOHNSON, B. G. (1988) Excitatory amino acid agonist-antagonist interactions at 2-amino-4-phosphonobutyric acid-sensitive quisqualate receptors coupled to phosphoinositide hydrolysis in slices of rat hippocampus. *J. Neurochem.* **50**, 1605-1613.
- SCHWARCZ, R., HOKFELT, T., FUXE, K., JONSSON, G., GOLDSTEIN, M. & TERENIUS, L. (1979) *Exp. Brain Res.* **37**, 199-216.
- SCHWARTZ, R. D., LEHMANN, J. & KELLAR, K. J. (1984) Presynaptic nicotinic cholinergic receptors labeled by [³H]acetylcholine on catecholamine and serotonin axons in the brain. *J. Neurochem.* **42**, 1495-1498.
- SCHWOB, J. E., FULLER, T., PRICE, J. L. & OLNEY, J. W. (1980) Widespread patterns of neuronal damage following systemic or intracerebral injections of kainic acid: a histological study. *Neuroscience* **5**, 991-1014.
- SELKOE, D. J. (1987) Deciphering Alzheimer's Disease: the pace quickens. *Trends Neurosci.* **10**, 181-184.
- SEUBERT, P., LEE, K. & LYNCH, G. (1989) Ischemia triggers NMDA receptor-linked cytoskeletal proteolysis in hippocampus. *Brain Res.* **492**, 366-370.
- SHEARDOWN, M. J., NIELSEN, E. O., HANSEN, A. J., JACOBSEN, P. & HONORE, T. (1990) 2,3-dihydro-6-nitro-7-sulphamoylbenzo(f)quinoxaline: a neuroprotectant for cerebral ischaemia. *Science* **247**, 571-574.
- SHERIDAN, R. D. & SUTOR, B. (1990) Presynaptic M₁ muscarinic cholinergic receptors mediate inhibition of excitatory synaptic transmission in the hippocampus in vitro. *Neurosci. Lett.* **108**, 273-278.
- SHIMOHAMA, S., TANIGUCHI, T., FUJIWARA, M. & KAMEYAMA, M. (1985) Biochemical characterization of the nicotinic cholinergic receptors in human brain: binding of (-)-[³H]nicotine. *J. Neurochem.* **45**, 604-610.

- SHIMOHAMA, S., TANIGUCHI, T., FUJIWARA, M. & KAMEYAMA, M. (1986a) Biochemical characterization of α -adrenergic receptors in human brain and changes in Alzheimer-type dementia. *J. Neurochem.* **47**, 1294-1301.
- SHIMOHAMA, S., TANIGUCHI, T., FUJIWARA, M. & KAMEYAMA, M. (1986b) Changes in nicotinic and muscarinic cholinergic receptors in Alzheimer-type dementia. *J. Neurochem.* **46**, 288-293.
- SHIMOHAMA, S., TANIGUCHI, T., FUJIWARA, M. & KAMEYAMA, M. (1987) Changes in β -adrenergic receptor sub-types in Alzheimer-type dementia. *J. Neurochem.* **48**, 1215-1221.
- SHIMOHAMA, S., TANIGUCHI, T., FUJIWARA, M. & KAMEYAMA, M. (1988) Changes in benzodiazepine receptors in Alzheimer-type dementia. *Ann. Neurol.* **23**, 404-406.
- SHIRAISHI, K., SHARP, F. & SIMON, R. P. (1989) Sequential metabolic changes in rat brain following middle cerebral artery occlusion: a 2-deoxyglucose study. *J. Cereb. Blood Flow Metab.* **9**, 765-773.
- SIMAN, R., NOSZEK, J. C. & KEGERISE, C. (1989) Calpain activation is specifically related to excitatory amino acid induction of hippocampal damage. *J. Neurosci.* **9**, 1579-1590.
- SIMON, R. P., SWAN, J. H., GRIFFITHS, T. & MELDRUM, B. S. (1984) Blockade of N-methyl-D-aspartate receptors may protect against ischemic damage in the brain. *Science* **226**, 850-852.
- SIMON, R. P. & SHIRAISHI, K. (1990) N-methyl-D-aspartate antagonist reduces stroke size and regional glucose metabolism. *Ann. Neurol.* **27**, 606-611.

- SIMPSON, M. D. C., ROYSTON, M. C., DEAKIN, J. F. W., CROSS, A. J., MANN, D. M. A. & SLATER, P. (1988) Regional changes in [³H] D-aspartate and [³H]TCP binding in Alzheimer's Disease brains. *Brain Res.* **462**, 76-82.
- SMITH, G. (1988) Animal models of Alzheimer's Disease: experimental cholinergic denervation. *Brain Res. Rev.* **13**, 103-118.
- SMITH, C. J., COURT, J. A., KEITH, A. B. & PERRY, E. K. (1989) Increases in muscarinic stimulated hydrolysis of inositol phospholipids in rat hippocampus following cholinergic deafferentation are not paralleled by alterations in cholinergic receptor density. *Brain Res.* **485**, 317-324.
- SNELL, L. D., YI, S.-J. & JOHNSON, K. M. (1988) Comparison of the effects of MK-801 and phencyclidine on catecholamine uptake and NMDA-induced norepinephrine release. *Eur. J. Pharmacol.* **145**, 223-226.
- SOFRONIEW, M. V. & PEARSON, R. C. A. (1985) Degeneration of cholinergic neurons in the basal nucleus following kainic or N-methyl-D-aspartic acid application to the cerebral cortex in the rat. *Brain Res.* **339**, 186-190.
- SONCRANT, T. T., HOLLOWAY, H. W. & RAPOPORT, S. I. (1985) Arecoline-induced elevations of regional cerebral metabolism in the conscious rat. *Brain Res.* **347**, 205-216.
- SOKOLOFF, L., REIVICH, M., KENNEDY, C., DES ROSIERS, M. H., PATLAK, C. S., PETTIGREW, K. D., SAKURADA, O. & SHINOHARA, M. (1977). The [¹⁴C]deoxyglucose method for the measurement of local cerebral glucose utilisation: theory, procedure, and normal values in the conscious and anesthetised albino rat. *J. Neurochem.* **28**, 897-916.
- SOKOLOFF, L. (1979) The [¹⁴C]deoxyglucose method: four years later. *Acta Neurol. Scand.* **60** (Suppl. 2), 640-649.

- SOKOLOFF, L. (1981) Localization of functional activity in the central nervous system by measurement of glucose utilization with radioactive deoxyglucose. *J. Cereb. Blood Flow Metab.* **1**, 7-36.
- SPENCER, D. G. Jr, HORVATH, E. & TRABER, J. (1986) Direct autoradiographic determination of M1 and M2 muscarinic acetylcholine receptor distribution in the rat brain: relation to cholinergic nuclei and projections. *Brain Res.* **380**, 59-86.
- SQUIRE, L. R. & ZOLA-MORGAN, S. (1983) The neurology of memory: the case for correspondence between the findings for man and non-human primate. In *The Physiological Basis of Memory*. Ed. Deutsch, J. A. pp 199-267. Academic Press, New York.
- STANTON, P. K. & SARVEY, J. M. (1985) depletion of norepinephrine, but not serotonin, reduces long-term potentiation in the dentate gyrus of rat hippocampal slices. *J. Neurosci.* **5**, 2169-2176.
- STEVENS, D. R. & COTMAN, C. W. (1987) Excitatory actions of tetrahydro-9-aminoacridine (THA) on hippocampal pyramidal neurons. *Neurosci. Lett.* **79**, 301-305.
- STONE, J. L., RIFAI, M. H. S., SUGAR, O., LANG, R. G. A., OLDERSHAW, J. B. & MOODY, R. A. (1983) Subdural hematomas. Acute subdural hematoma: progress in definition, clinical pathology and therapy. *Surg. Neurol.* **19**, 216-231.
- STORM-MATHISEN, J. (1970) Quantitative histochemistry of acetylcholinesterase in rat hippocampal region correlated to histochemical staining. *J. Neurochem.* **17**, 739-750.
- STORM-MATHISEN, J. (1977) Glutamic acid and excitatory nerve endings: reduction of glutamic acid uptake after axotomy. *Brain Res.* **120**, 379-386.

- STORM-MATHISEN, J. & IVERSEN, L. L. (1979) Uptake of (³H)-glutamic acid in excitatory nerve endings: light and electron-microscopic observations in the hippocampal formation of the rat. *Neuroscience*, **4**, 1237-1253.
- STORM-MATHISEN, J., LEKNES, A. K., BORE, A. T., VAALAND, J. L., EDMINSON, P., HAUG, F.-M. S. & OTTERSEN, O. P. (1983) First visualisation of glutamate and GABA in neurones by immunocytochemistry. *Nature* **301**, 517-520.
- SUGIYAMA, H., ITO, I. & HIRINO, C. (1987) A new type of glutamate receptor linked to inositol phospholipid metabolism. *Nature* **325**, 531-533.
- SUMMERS, W. K., MAJOVSKI, L. V., MARSH, G. M., TACHIKI, K. & KLING, A. (1986) Oral tetrahydroaminoacridine in long-term treatment of senile dementia, Alzheimer type. *N. Engl. J. Med.* **315**, 1241-1245.
- SUMPTER, P. Q., MANN, D. M. A., DAVIES, C. A., YATES, P. O., SNOWDEN, J. S. A. & NEARY, D. (1986) An ultrastructural analysis of the effects of accumulation of neurofibrillary tangles in pyramidal cells of the cerebral cortex in Alzheimer's disease. *Neuropathol. Appl. Neurobiol.* **12**, 321-329.
- SUZUKI, R., YAMAGUCHI, T., KIRINO, T., ORZI, F. & KLATZO, I. (1983) The effects of 50-minute ischemia in mongolian gerbils: I. Blood-brain barrier, cerebral blood flow, and local cerebral glucose utilization changes. *Acta Neuropathol.* **60**, 207-216.
- SWANSON, L. W. & COWAN, W. M. (1977) An autoradiographic study of the organization of the efferent connections of the hippocampal formation in the rat. *J. Comp. Neurol.* **172**, 49-84.
- SWANSON, L. W. & COWAN, W. M. (1979) The connections of the septal region of the rat. *J. Comp. Neurol.* **186**, 621-655.

- SWANSON, L. W., KOHLER, C. & BJORKLUND, A. (1987) The limbic region. I The septohippocampal system. In *Handbook of Chemical Neuroanatomy Vol. 5: Integrated systems of the CNS, part I, hypothalamus, hippocampus, amygdala, retina*. Eds. Björklund, A. et al., Elsevier, Amsterdam, pp 125-277.
- SWANSON, L. W., WYSS, J. M. & COWAN, W. M. (1978) An autoradiographic study of the organization of intrahippocampal association pathways in the rat. *J. Comp. Neurol.* **181**, 681-716.
- TAKIZAWA, S., HOGAN M. & HAKIM, A. M. (1991) The effects of a competitive NMDA receptor antagonist (CGS-19755) on cerebral bloodflow and pH in focal ischaemia. *J. Cereb. Blood Flow Metab.* **11**, 786-793.
- TAMURA, A., GRAHAM, D. I., McCULLOCH, J. & TEASDALE, G. M. (1981) Focal cerebral ischaemia in the rat. 1. Description of technique and early neuropathological consequences following middle cerebral artery occlusion. *J. Cereb Blood Flow Metab.* **1**, 53-80.
- TANAKA, K., GREENBERG, J. H., GONATAS, N. K. & REIVICH, M. K. (1985) Regional flow-metabolism couple following middle cerebral artery occlusion in cats. *J. Cereb. Blood Flow Metab.* **5**, 241-252.

- TEITELBAUM, J. S., ZATORRE, R. J., CARPENTER, S., GENDRON, D., EVANS, A. C., GJEDDE, A. & CASHMAN, N. R. (1990) Neurologic sequelae of domoic acid intoxication due to ingestion of contaminated mussels. *N. Engl. J. Med.* **322**, 1781-1787.
- TERRY, R. D., PECK, A., DETERESA, R., SCHECHTER, R. & HOROUPIAN, D. S. (1981) Some morphometric aspects of the brain in senile dementia of the Alzheimer type. *Ann. Neurol.* **10**, 184-192.
- TONNAER, J. A. D. M., ERNSTE, B. H. W., WESTER, J. & KELDER, K. (1988) Cholinergic innervation and topographical organization of muscarinic binding sites in rat brain: a comparative autoradiographic study. *J. Chem. Neuroanat.* **1**, 95-110.
- UDDMANN, R. & EDVINSSON, L. (1989) Neuropeptides in the cerebral circulation. *Cerebrovasc. Brain Metab. Rev.* **1**, 230-252.
- ULAS, J., MONAGHAN, D. T. & COTMAN, C. W. (1990 a) Plastic response of hippocampal excitatory amino acid receptors to deafferentation and reinnervation. *Neuroscience* **34**, 9-17.
- ULAS, J., MONAGHAN, D. T. & COTMAN, C. W. (1990 b) Kainate receptors in the hippocampus: a distribution and time course of changes in response to unilateral lesions of the entorhinal cortex. *J. Neurosci.* **10**, 2352-2362.
- UNGERSTEDT, U. (1971) Stereotaxic mapping of the monoaminergic pathways of the brain. *Acta Physiol. Scand. Suppl.* **267**, 1-48.
- VACCARINO, F., GUIDOTTI, A. & COSTA, E. (1987) Ganglioside inhibition of glutamate-mediated protein kinase C translocation in primary cultures of cerebellar neurons. *Proc. Natl. Acad. Sci. USA* **84**, 8707-8711.

- VAN HARREVELD, A. (1959) Compounds in brain extracts causing spreading depression of cerebral cortical activity and contraction of crustacean muscle. *J. Neurochem.* **3**, 300-315.
- VOLPE, B. T. & HIRST, W. (1983) The characterization of an amnesic syndrome following hypoxic ischemic injury. *Arch. Neurol.* **40**, 436-440.
- WACHTEL, H. (1988) Defective second-messenger function in the etiology of endogenous depression: novel therapeutic approaches. In *New Concepts in Depression*, Briley M. et al. (eds.), MacMillan Press, pp 277-293.
- WACHTEL, H. (1989) Dysbalance of neuronal second messenger function in the aetiology of affective disorders: a pathophysiological concept hypothesizing defects beyond first messenger receptors, *J. Neural Transmission* **75**, 21-29.
- WALAAS, I. & FONNUM, F. (1980) Biochemical evidence for glutamate as a transmitter in hippocampal efferents to the basal forebrain and hypothalamus in the rat brain. *Neurosci.* **5**, 1691-1698.
- WALKER, L. C., KITT, C. A., CORK, L. C., STRUBLE, R. G., DELLOVADE, T. L. & PRICE, D. L. (1988) Multiple transmitter systems contribute neurites to individual senile plaques. *J. Neuropath. Exp. Neurol.* **47**, 134-144.
- WALLENSTEIN, S., ZUCKER, C. L. & FLEISS, J. (1980) Some special statistical methods useful in circulation research. *Circ. Res.* **47**, 1-9.
- WAMSLEY, J. K., GEHLERT, D. R., ROESKE, W. R. & YAMAMURA, H. I. (1984) Muscarinic antagonist binding site heterogeneity as evidenced by autoradiography after direct labeling with [³H]QNB and [³H]pirenzepine. *Life Sci.* **34**, 1395-1402.

- WAMSLEY, J. K., ZARBIN, M. A., BIRDSALL, N. M. J. & KUHAR, H. J. (1980) Muscarinic cholinergic receptors: autoradiographic localisation of high and low affinity agonist binding sites. *Brain Res.* **200**, 1-12.
- WARBURTON, D. M. & WESNES, K. (1984) drugs as research tools in psychology: cholinergic drugs and information processing. *Neuropsychology* **11**, 121-132.
- WASTERLAIN, C. (1989) Epileptic seizures. In *Basic Neurochemistry*, Siegel, G. et al. (eds.), 4th Edition, Raven Press, New York, pp 797-810.
- WASTERLAIN, C. G. & DWYER, B. E. (1983) Brain metabolism during prolonged seizures in neonates. In *Status Epilepticus, Advances in Neurology Vol. 4*, Delgado-Escveta, A. V. et al. (eds.), 4th Edition, Raven Press, New York, pp 797-810.
- WATKINS, J. C. & EVANS, R. H. (1981) Excitatory amino acid transmitters. *Ann. Rev. Pharmacol. Toxicol.* **21**, 165-204.
- WATSON, M., VICKROY, T. W., FIBIGER, H. C., ROESKE, W. R. & YAMAMURA, H. I. (1985) Effects of bilateral ibotenate-induced lesions of the nucleus basalis magnocellularis upon selective cholinergic biochemical markers in the rat anterior cerebral cortex. *Brain Res.* **346**, 387-391.
- WEINBERGER, J., GREENBERG, J. H., WALDMAN, M. T. G., SYLVESTRO, A. & REIVICH, M. (1979) The effects of scopolamine on local cerebral glucose metabolism in rat brain. *Brain Res.* **177**, 337-345.
- WEISSMAN, A. D., DAM, M. & LONDON, E. D. (1987) Alterations in local cerebral glucose utilization induced by phencyclidine. *Brain Res.* **435**, 29-40.
- WENK, G. L., CRIBBS, B. & McCALL, L. (1984) Nucleus basalis magnocellularis: optimal coordinates for selective reduction of choline acetyltransferase in frontal neocortex by ibotenic acid injections. *Exp. Brain Res.* **56**, 335-340.

- WENK, G. L. & ENGLISCH, K. L. (1986) [³H]Ketanserin (serotonin type 2) binding increases in rat cortex following basal forebrain lesions with ibotenic acid. *J. Neurochem.* **47**, 845-850.
- WENK, G. L., MARKOWSKA, A. L. & OLTON, D. S. (1989) Basal forebrain lesions and memory: alterations in neurotensin, not acetylcholine, may cause amnesia. *Behav Neurosci.* **103**, 765-769.
- WENK, G. L. & OLTON, D. S. (1984) Recovery of neocortical choline acetyltransferase activity following ibotenic acid injection into the nucleus basalis of Meynert. *Brain Res.* **293**, 184-186.
- WERNIS, S. T. & LUCCHESI, B. R. (1990) Free radicals and ischemic tissue injury. *Trends Pharmacol. Sci.* **11**, 161-166.
- WESTERBERG, E., MONAGHAN, D. T., COTMAN, C. W. & WIELOCH, T. (1987) Excitatory amino acid receptors and ischaemic brain damage in the rat. *Neurosci. Lett.* **73**, 119-124.
- WESTERBERG, E., MONAGHAN, D. T., KALIMO, H., COTMAN, C. W. & WIELOCH, T. W. (1989) Dynamic changes of excitatory amino acid receptors in the rat hippocampus following transient cerebral ischemia. *J. Neurosci.* **9**, 798-805.
- WESTLIND, A., GRYNFARB, M., HEDLUND, B., BARTFAI, T. & FUXE, K. (1981) muscarinic supersensitivity induced by septal lesion or chronic atropine treatment. *Brain Res.* **225**, 131-141.
- WHITE, P., GOODHART, M. J., KEET, J. P., HILEY, C. R., CARRASCO, L. H., WILLIAMS, I. E. I. & BOWEN, D. M. (1977) Neocortical cholinergic neurones in elderly people. *Lancet* (i), 668-671.
- WHITEHOUSE, P. J., MARTINO, A. M., ANTUONO, P. G., LOWENSTEIN, P. R., COYLE, J. T., PRICE, D. L. & KELLAR, K. J. (1986) Nicotinic acetylcholine binding in Alzheimer's disease. *Brain Res.* **37**, 146-151.

- WHITEHOUSE, P. J., PRICE, D. L., CLARK, A. W., COYLE, J. T. & DELONG, M. R. (1981) Alzheimer Disease: evidence for selective loss of cholinergic neurons in the nucleus basalis. *Ann. Neurol.* **10**, 122-126.
- WHITEHOUSE, P. J., PRICE, D. L., STRUBEL, R. G., CLARK, A. W., COYLE, J. T. AND DELONG, M. R. (1982) Alzheimer's Disease and senile dementia. Loss of neurones in the basal forebrain. *Science* **215**, 1237-1239.
- WIELOCH, T., LINDVALL, O., BLOMQUIST, P. & GAGE, F. H. (1985) Evidence for amelioration of ischemic neuronal damage in the hippocampal formation by lesions of the perforant path. *Neurol. Res.* **7**, 24-26.
- WILCOCK, G. K. & ESIRI, M. M. (1982) Plaques, tangles and dementia: a quantitative study. *J. Neurol. Sci.* **57**, 402-417.
- WILLIAMS, J. H. & BLISS, T. V. P. (1988) Induction but not maintenance of calcium-induced long-term potentiation in dentate gyrus and area CA1 of the hippocampal slice is blocked by nordihydroguaiaretic acid. *Neurosci. Lett.* **88**, 81-85.
- WILLIAMS, J. H. & BLISS, T. V. P. (1989) An in vitro study of the effect of lipoxygenase and cyclooxygenase inhibitors of arachidonic acid on the induction and maintenance of long-term potentiation in the hippocampus. *Neurosci. Lett.* **107**, 301-306.
- WISNIEWSKI, H. M. & TERRY, R. D. (1973) Re-examination of the pathogenesis of the senile plaque. In *Progress in Neuropathology*, Vol. 2, H. M. Zimmerman (Ed.), Grune & Stratton, New York, pp 1-26.
- WONG, E. H. F. & NIELSEN, M. (1989) The N-methyl-D-aspartate receptor channel complex and the σ site have different target sizes. *Eur. J. Pharmacol.* **172**, 493-496.

- WOUTERLOOD, F. G., MUGNANI, E. & NEDERLOF, J. (1985) Projection of the olfactory bulb efferents to layer I GABAergic neurons in the entorhinal area. Combination of anterograde degeneration and immunoelectron microscopy in the rat. *Brain Res.* **343**, 283-296.
- YAMAGUCHI, T., KUNIMOTO, M., PAPPATA, S., CHAVOIX, C., BROUILLET, E., RICHE, D., MAZIERE, M., NAQUET, R., MacKENZIE, E. T. & BARON, J. C. (1990) Effects of unilateral lesion of the nucleus basalis of Meynert on brain glucose utilization in callotomized baboons: a PET study. (1990) *J. Cereb. blood Flow Metab.* **10**, 618-623.
- YAMAMURA, H. I. & SNYDER, S. H. (1974) Postsynaptic localization of muscarinic receptor binding in rat hippocampus. *Brain Res.* **78**, 320-326.
- ZOLA-MORGAN, S., SQUIRE, L. R. & AMARAL, D. G. (1986) Human amnesia and the medial temporal region: enduring memory impairment following a bilateral lesion limited to field CA1 of the hippocampus. *J. Neurosci.* **6**, 2950-2967.

LIST OF PUBLICATIONS

Definitive Papers:

INGLIS F.M., BULLOCK R., CHEN M.H., GRAHAM D.I., MILLER J.D., McCULLOCH J., TEASDALE G.M. (1990) Ischaemic brain damage associated with tissue hypermetabolism in acute subdural haematoma. Reduction by a glutamate antagonist. *Proceedings of Brain Edema 1990; Acta Neurochirurgica, Suppl. 51*, 277-279.

KURODA Y., INGLIS F.M., MILLER J.D., McCULLOCH J., GRAHAM D.I., BULLOCK R. (1992) Transient glucose hypermetabolism after acute subdural haematoma in the rat. *J. Neurosurg.* **76**, 471-477.

HORSBURGH K., INGLIS F.M., McCULLOCH, J. (1992) Selective increases in [³H]-forskolin and [³H]-phorbol 12,13 dibutyrate binding after cholinergic denervation of the hippocampus. *Neurosci. Lett.* (In submission).

INGLIS F.M., KURODA, Y., BULLOCK, R. (1992) Glucose hypermetabolism after acute subdural haematoma is prevented by a competitive NMDA antagonist *J. Neurotrauma* (In submission).

Abstracts:

INGLIS F.M., DEWAR D., McCULLOCH J. (1989) Effects on local cerebral glucose utilisation of 9-Amino-1,2,3,4-tetrahydroacridine (THA) in the rat brain. *J. Cereb. Blood Flow Metab.* **9**, S497.

BULLOCK R., McCULLOCH J., TEASDALE G.M., GRAHAM D.I., INGLIS F.M. Competitive NMDA antagonists: A valuable treatment for preventing ischaemic neuronal death. Proceedings of the Society of British Neurological Surgeons, September 1989 meeting; *J. Neurol. Neurosurg. Psychiat.* **53**, 446 (1990).

INGLIS F.M., MACRAE I.M., BULLOCK R., McCULLOCH J. (1991) The effects of the competitive NMDA antagonist, D-CPP-ene, on cerebral glucose use in the rat. *J. Cereb. Blood Flow Metab.* **11, Suppl. 2**, S307.

INGLIS F.M., KURODA Y., MILLER J.D., McCULLOCH J., GRAHAM D.I., BULLOCK, R. (1991) The competitive NMDA antagonist D-CPP-ene reduces glucose hypermetabolism and infarct size after acute subdural haematoma. *J. Cereb. Blood Flow Metab.* **11, Suppl. 2**, S225.

BULLOCK R., INGLIS F.M., BUTCHER S.P., McCULLOCH J., MAXWELL W. (1991) Transient hippocampal hypermetabolism associated with glutamate release after acute subdural haematoma in the rat: a potentially neurotoxic mechanism? *J. Cereb. Blood Flow Metab.* **11, Suppl. 2**, S109.

KURODA Y., BULLOCK R., INGLIS F.M., McCULLOCH J. (1991) High intracranial pressure exacerbates disrupted flow-metabolism coupling: a double-label autoradiographic study in two ischaemia models. *J. Cereb. Blood Flow Metab.* **11, Suppl. 2**, S74.

MACRAE I.M., INGLIS F.M., VILA E., REID J.L., McCULLOCH J. (1991) Central effects of competitive NMDA antagonist D-CPP-ene on brainstem cerebral glucose use and blood pressure control in the conscious rat. *J. Cereb. Blood Flow Metab.* **11, Suppl. 2**, S309.

HORSBURGH K., INGLIS F.M., McCULLOCH, J. (1991) Increased [³H]-forskolin and [³H]-phorbol 12,13 dibutyrate binding in the hippocampus following excitotoxic lesion of the rat medial septum. *Soc. Neuroscience Abstr.* **17**, 240.2

